Study of bacterial conjugation from a practical and fundamental perspective

Audrey Reuter

N° d'ordre NNT :
2021LYSE1257

THESE de DOCTORAT DE L'UNIVERSITE DE LYON
opérée au sein de
l'Université Claude Bernard Lyon 1

École Doctorale ED341
(Évolution Écosystèmes Microbiologie Modélisation)

Spécialité de doctorat :
Discipline : Microbiologie

Soutenue publiquement le 29/11/2021, par :
Audrey Reuter

Study of bacterial conjugation from a practical and fundamental perspective

---

Devant le jury composé de :

Doublet Patricia	Professeur	CIRI-Lyon 1	Présidente
Baharoglu Zeynep	Chercheuse	Institut Pasteur Paris	Rapportrice
Bikard David	Chercheur	Institut Pasteur Paris	Rapporteur
Barnich Nicolas	Professeur	M2ISH-Clermont-ferrand	Examinateur
Bigot Sarah	Chargée de recherche	MMSB-Lyon1	Directrice de thèse
Lesterlin Christian	Directeur de recherches	MMSB-Lyon1	Co-directeur de thèse

Université Claude Bernard – LYON 1

Président de l'Université	M. Frédéric FLEURY
Président du Conseil Académique	M. Hamda BEN HADID
Vice-Président du Conseil d'Administration	M. Didier REVEL
Vice-Président du Conseil des Etudes et de la Vie Universitaire	M. Philippe CHEVALLIER
Vice-Président de la Commission de Recherche	M. Jean-François MORNEX
Directeur Général des Services	M. Pierre ROLLAND

COMPOSANTES SANTE

Département de Formation et Centre de Recherche en Biologie Humaine	Directrice : Mme Anne-Marie SCHOTT
Faculté d'Odontologie	Doyenne : Mme Dominique SEUX
Faculté de Médecine et Maïeutique Lyon Sud - Charles Mérieux	Doyenne : Mme Carole BURILLON
Faculté de Médecine Lyon-Est	Doyen : M. Gilles RODE
Institut des Sciences et Techniques de la Réadaptation (ISTR)	Directeur : M. Xavier PERROT
Institut des Sciences Pharmaceutiques et Biologiques (ISBP)	Directrice : Mme Christine VINCIGUERRA

COMPOSANTES & DEPARTEMENTS DE SCIENCES & TECHNOLOGIE

Département Génie Electrique et des Procédés (GEP)	Directrice : Mme Rosaria FERRIGNO
Département Informatique	Directeur : M. Behzad SHARIAT
Département Mécanique	Directeur M. Marc BUFFAT
Ecole Supérieure de Chimie, Physique, Electronique (CPE Lyon)	Directeur : Gérard PIGNAULT
Institut de Science Financière et d'Assurances (ISFA)	Directeur : M. Nicolas LEBOISNE
Institut National du Professorat et de l'Education	Administrateur Provisoire : M. Pierre CHAREYRON
Institut Universitaire de Technologie de Lyon 1	Directeur : M. Christophe VITON
Observatoire de Lyon	Directrice : Mme Isabelle DANIEL
Polytechnique Lyon	Directeur : Emmanuel PERRIN
UFR Biosciences	Administratrice provisoire : Mme Kathrin GIESELER
UFR des Sciences et Techniques des Activités Physiques et Sportives (STAPS)	Directeur : M. Yannick VANPOULLE
UFR Faculté des Sciences	Directeur : M. Bruno ANDRIOLETTI

Remerciements

Tout d'abord je souhaiterais remercier les membres de mon jury Zeynep Baharoglu, Patricia Doublet, Nicolas Barnich et David Bikard pour avoir accepté de donner de leur temps afin de juger mes travaux de thèse.

J'aimerais aussi remercier les membres de mon comité de suivi de thèse Claire Prigent-Combaret, Yoshiharu Yamaichi, Gregory Jubelin et Erwan Gueguen pour leurs conseils avisés et le regard qu'ils ont porté sur mes travaux. Particulièrement, je remercie grandement Gregory Jubelin et Erwan Gueguen qui ont collaboré à mes travaux de thèse par la réalisation d'expérimentations *in vivo* pour Gregory et par la conception du web-service CSTB pour Erwan.

Je reviendrais plus tard sur l'aide toute particulière qu'ont pu m'apporter Erwan Gueguen et Patricia Doublet lors de mon parcours.

Pour l'heure, je remercie Jean-Michel Jault et Christophe Grangeasse qui se sont succédé à la direction du MMSB et qui ont permis que je réalise ma thèse au sein de l'équipe TacC. Je remercie également Dorothée Bernard et Souad Boukoum, nos secrétaires qui sont toujours d'une grande aide et d'une grande patience.

Au sein de l'IBCP je veux particulièrement remercier Patricia Morales, responsable de la laverie. Patricia tu as toujours été présente pour m'écouter que je sois dans la peine ou la joie. De plus, tu as toujours eu des attentions bienveillantes à mon égard. J'espère avoir pu être là pour toi aussi lorsque tu en avais besoin.

Parmi les personnes du MMSB et de l'IBCP, je souhaite remercier toutes les personnes avec qui j'ai pu interagir, doctorants ou non : Benjamin, Morgane, Agathe, Margot, Julie, Léa, Mathieu, Camille, Alexia, Jorag, Altan, Marine, Marine, Cédric, Patrice, Lionel, Basma, Nicolas, Samuel, Alexis, Frédéric et certainement d'autres que j'ai oubliés avec qui j'ai pu échanger parfois une phrase et parfois un verre ou des délires permettant d'illuminer mes journées.

Tout spécialement, j'adresse un grand merci à Chantal Tessa qui prépare les milieux pour tout le MMSB. Je crois que sans toi je n'aurais pas pu faire le quart des manips que j'ai réalisées, tu es tellement efficace !! D'ailleurs je pense que la plupart des personnes du MMSB savent que tu es notre clé de voute. Chantal tu as été ma confidente pendant ces trois années, toi qui étais constamment à mes côtés (au propre et au figuré puisque ton bureau était collé au mien !). J'ai été ravie d'échanger avec toi, tu m'as toujours donné ton avis sans détours et tu es toujours de bon conseil.

Passons maintenant aux personnes de l'équipe TacC. Tout d'abord je souhaite remercier les trois étudiantes que j'ai encadrées : Lisa Rubio, Lola Bosc et Avril Rovira-Cartro. Encadrer des étudiantes m'a beaucoup appris et m'a permis de me poser des questions sur des détails que je ne questionnais même plus ! C'était une expérience formidable qui m'a poussée aussi à m'affirmer plus et à être plus sûre de moi, même si nous ne sommes pas encore au bout du chemin.

Je remercie également Sophie Nolivos qui m'a appris à faire de la microscopie en microfluidique ainsi qu'à analyser mes images. Même partie j'ai pu te demander ton aide quand j'en ai eu besoin et j'ai toujours aimé la façon claire et précise que tu as d'exprimer ton point de vue.

Je remercie Annick Dedieu, notre Lab Manager toujours présente si on a la moindre question et qui en fait souvent un peu trop. Grâce à toi le laboratoire fonctionne à plein régime car nous ne manquons jamais de rien et tu prends toujours soin de nous.

Je remercie les étudiants qui ont été présents dans l'équipe lors de ma thèse : Julien Cayron, Agathe Couturier, Chloé Virolle, Kelly Goldlust et Sarah Djermoun. Vous avez apporté au laboratoire cette petite étincelle qui fait qu'il n'est pas seulement un lieu de travail mais surtout un lieu convivial. Chloé, Kelly et Sarah nous avons vécu cette période COVID ensemble également et j'ai l'impression que ça nous a rapprochées. Toutes les trois vous avez été un pilier pour moi, mon roc, lorsque j'avais de mauvaises phases. Nos délires au laboratoire ont permis de relâcher la tension qui régnait lorsque nous étions contraintes à sortir uniquement pour travailler. Julien, Agathe, Chloé, Kelly et Sarah je vous remercie sincèrement d'avoir été présent(es), pour tous nos échanges scientifiques ou personnels qui m'ont grandement enrichie. Je chérirais à jamais ces instants heureux que nous avons passés, surtout grâce aux clichés pris par nos photographes Kelly et Chloé.

Je souhaite remercier mes deux encadrants Christian Lesterlin et Sarah Bigot. J'espère avoir pu atteindre les exigences que vous avez pour vos étudiants.

Christian, j'aime beaucoup ta façon posée d'expliquer les choses et surtout de tirer le positif de chaque situation. Tu as un talent certain pour faire passer des messages clairs et directs et j'espère avoir appris ne serait-ce qu'un tout petit peu à faire de même. Tu as toujours été d'excellent conseil, en terme de manip ou bien lecture, série, … J'espère que je ne te désole pas trop car je ne fais rien pour aimer la bière ni l'alcool en général ni pour exercer mon palais, je pense que ce ne sera jamais pour moi !

Sarah, j'espère que je ne t'en ai pas trop fait baver… J'ai été ravie que tu sois mon encadrante pendant ces trois ans, tu me pousses toujours à donner le meilleur de moi-même et le plus fou c'est que ça fonctionne ! Je crois que de nous deux tu es celle qui a le plus confiance en moi ! J'espère que tu ne regrettes pas de m'avoir encadrée et je ferais tout pour que ce ne soit pas le cas. Pendant ces trois ans tu m'as sans cesse encouragée à m'affirmer. Sache que j'admire grandement ta confiance en toi, ta bienveillance ainsi que ton énergie et ton enthousiasme qui ont été mon moteur pendant ces trois années et demie (avec le M2). Te rencontrer lors de mon stage de M1 est certainement ce qui m'est arrivé de mieux, surtout que c'est grâce à toi que j'ai pu continuer ma route avec toi en M2.

J'éprouve une grande reconnaissance envers Patricia Doublet et Erwan Gueguen qui m'ont également permis de réaliser le M2 Infectiologie Fondamentale et sans qui je ne sais pas où j'en serais aujourd'hui.

J'aimerais maintenant remercier ma famille pour leur soutien indéfectible malgré le manque de compréhension dans ce que je pouvais bien faire. Maman, Papa, merci de m'avoir laissé faire des études et de ne pas voir jugé mes changements d'orientations parfois. Grâce à vous j'ai pu entreprendre sereinement ma vie étudiante et vous étiez toujours là derrière moi si j'avais une quelconque incertitude.

Je remercie également mes amis : Séverine, Matthias, Hugo, Quentin, Rebecca Mathilde et bien sûr Océane qui m'ont vu entreprendre ma thèse et malgré mon absence notoire à certains rendez-vous ont à chaque fois répondu présent pour moi !

Finalement, je remercie Mehdi que j'ai rencontré pendant ma thèse (merci Chloé), qui est devenu mon amoureux et m'a soutenue pendant toute ma dernière année de thèse et a été aux premières loges durant mes moments de doute. Promis Mehdi je ferais aussi la cuisine et la vaisselle pour toi durant ta rédaction !

RESUME :

Les communautés microbiennes sont composées d'espèces bactériennes variées capables d'échanger des informations génétiques par transfert horizontal de gènes. Parmi ceux-là, la conjugaison bactérienne permet le transfert de larges fragments d'ADN, la plupart du temps des plasmides, entre une bactérie donneuse et une receveuse en contact direct. L'acquisition du plasmide et l'expression des gènes portés par celui-ci convertissent la receveuse en transconjugant. Le produit des gènes peut conférer un mode de vie symbiotique, des facteurs de virulence ou des résistances aux métaux lourds ainsi qu'aux antibiotiques. On estime que la conjugaison est responsable de 80% de l'acquisition de la résistance aux antibiotiques chez les bactéries, lesquelles constituent un enjeu de santé publique majeur dans le monde entier. Dans ce contexte, deux objectifs majeurs sont de développer de nouvelles stratégies antibactériennes alternatives aux antibiotiques ainsi que de mieux comprendre le mécanisme fondamental de dissémination de la résistance par conjugaison.

L'équipe « Cell-to-Cell DNA transfer » dans laquelle j'ai réalisé mon doctorat combine analyses microscopiques et microbiologiques à l'échelle de la cellule unique et populationnelle pour comprendre le processus et la dynamique de la conjugaison. Mon projet de thèse visait à explorer les aspects pratiques et fondamentaux de ce mécanisme.

J'ai tout d'abord développé une stratégie antibactérienne innovante basée sur des plasmides délivrés par conjugaison et portant des systèmes CRISPR-Cas (Clustered Regularly Interspaced Short Palindromic Repeats-CRISPR associated protein). Le système CRISPR-Cas est capable de reconnaître et de cibler des séquences d'ADN spécifiques et d'introduire des cassures double-brin létales pour les bactéries. Nous avons donc créé des plasmides appelés TAPs (Targeted-Antibacterial-Plasmids) mobilisables par conjugaison, capables de tuer spécifiquement des bactéries au sein d'une population. Par des techniques de dénombrements, de cytométrie en flux et de microscopie à fluorescence j'ai pu montrer la capacité des TAPs à être transférés et à tuer spécifiquement la souche ciblée. Nous avons également montré que les TAPs pouvaient re-sensibiliser une population bactérienne à un antibiotique.

Outre cette application biotechnologique, j'ai également étudié la dynamique de la conjugaison bactérienne à l'échelle cellulaire, en utilisant comme modèle le plasmide F. J'ai exploré le timing d'expression des gènes plasmidiques une fois le plasmide transféré dans la bactérie receveuse ainsi que l'établissement de la résistance aux antibiotiques après l'acquisition du plasmide. Je me suis intéressée aux gènes se situant sur la première partie du plasmide à entrer dans la receveuse, appelée « *leading region* ». J'ai pu montrer que contrairement aux autres gènes plasmidiques, ceux-ci sont exprimés transitoirement uniquement dans le transconjugant et non chez la donneuse. Ces premiers résultats ont suggéré une stratégie d'expression qui permettrait d'abord l'établissement du plasmide transféré, sa maintenance dans la nouvelle cellule hôte, puis finalement son transfert à une nouvelle bactérie receveuse.

J'ai également étudié l'acquisition de la résistance à la tétracycline conférée par le plasmide F portant un gène codant pour une pompe à efflux spécifique, TetA, qui permet d'effluer la tétracycline hors de la cellule. Grâce à l'utilisation de la microscopie à fluorescence, nous avons pu observer et analyser la dynamique de production de TetA et l'efflux de la tétracycline en temps réel. Notre étude montre que la résistance à la tétracycline dépend d'un équilibre entre la production de TetA et la capacité de la tétracycline à bloquer cette production. De plus, nous avons pu corréler l'augmentation de la quantité intracellulaire de TetA avec la capacité des cellules à résister à des concentrations croissantes de tétracycline.

ABSTRACT :

Microbial communities are composed of various bacterial species capable of exchanging genetic information through horizontal gene transfer mechanisms. Among these, bacterial conjugation allows the transfer of large DNA fragments, mostly plasmids, between a donor and a recipient bacterium in direct contact. The acquisition of the plasmid and the expression of the carried genes converts the recipient cell into a transconjugant cell. The product of the genes can confer a symbiotic lifestyle, virulence factors or resistance to heavy metals and antibiotics. It is estimated that conjugation is responsible for 80% of the acquisition of antibiotic resistance in bacteria, which is a major public health problem worldwide. In this context, two major objectives are to develop new antibacterial strategies alternative to antibiotics and to better understand the fundamental mechanism of dissemination of resistance by conjugation.

Our team combines microscopic and microbiological analyses at the single-cell and population scales to understand the process and dynamics of conjugation. My thesis project aimed at exploring practical and fundamental aspects of this mechanism.

First, I developed a novel antibacterial strategy based on conjugation-delivered plasmids carrying CRISPR-Cas (Clustered Regularly Interspaced Short Palindromic Repeats-CRISPR associated protein) systems. The CRISPR-Cas system is able to recognize and target specific DNA sequences, and introduce lethal double-strand breaks into the DNA of bacteria. We have therefore created plasmids mobilized by conjugation, called TAPs (Targeted-Antibacterial-Plasmids), able to specifically kill bacteria in a population. By platting assays, flow cytometry and fluorescence microscopy techniques, I was able to show the ability of TAPs to be transferred and to kill targeted strains. We also showed that TAPs can be used to re-sensitize a bacterial strain to an antibiotic.

In addition to this biotechnological application, I studied the dynamics of bacterial conjugation at the cellular level, using the F plasmid as a model. I explored the timing of expression of plasmid genes once transferred into the recipient bacterium as well as the establishment of antibiotic resistance after plasmid acquisition. I was interested in the genes located on the first part of the plasmid to enter in the recipient, called the "leading region". I was able to show that, unlike other plasmid genes, these are transiently expressed only in the transconjugant and not in the donor. This first result suggested an expression strategy that would first allow the establishment of the transferred plasmid, then its maintenance and eventually its transfer to another recipient cell.

I also studied the acquisition of tetracycline resistance conferred by the F plasmid encoding a specific TetA efflux pump that confers resistance to tetracycline. Using fluorescence microscopy, we were able to observe and analyze the dynamics of TetA production and tetracycline efflux in real-time. Our study shows that tetracycline resistance depends on a balance between TetA production and the ability of the tetracycline to block this production. Furthermore, we were able to correlate the increase in the intracellular amount of TetA with the ability of the cells to resist increasing amounts of tetracycline.

Résumé substantiel

Les communautés microbiennes sont composées d'espèces bactériennes variées capables d'échanger des informations génétiques ainsi que les propriétés métaboliques associées par des mécanismes de transfert horizontal de gènes. Parmi ceux-là, la conjugaison bactérienne permet le transfert de larges fragments d'ADN entre une bactérie donneuse et une receveuse en contact direct. L'acquisition du plasmide et l'expression des gènes le composant changent la receveuse en transconjugant. Il a été montré que la conjugaison est un mécanisme ubiquitaire et qu'il peut aussi avoir lieu entre une bactérie donneuse et une cellule eucaryote receveuse, telles que les cellules de plantes, levures et mammifères. Différents éléments peuvent être transférés par conjugaison comme les plasmides, les transposons conjugatifs et les éléments conjugatifs intégratifs. Ils portent des gènes permettant de conférer des propriétés diverses telles que le mode de vie symbiotique, des facteurs de virulence ou une résistance aux métaux lourds. Plus important encore, on estime que la conjugaison est responsable de 80% de l'acquisition de la résistance aux antibiotiques chez les bactéries, ce qui constitue un problème de santé publique majeur dans le monde entier.

L'utilisation accrue des antibiotiques a engendré une sélection des microorganismes résistants. En effet, en raison de leur capacité à cibler des fonctions essentielles dans un large éventail d'espèces bactériennes, les antibiotiques manquent de spécificité et leur utilisation provoque la sélection de souches résistantes. Ces souches sont souvent capables de diffuser la résistance aux antibiotiques à d'autres bactéries par conjugaison, ce qui peut entraîner l'émergence de microbes multi-résistants. C'est pourquoi, il est nécessaire de trouver des alternatives aux antibiotiques afin de lutter contre les infections bactériennes.

Notre équipe combine des analyses microscopiques et microbiologiques sur les populations bactériennes et à l'échelle de la cellule unique pour comprendre le processus de conjugaison, au niveau de la population jusqu'à celui de la cellule unique. Mon projet de thèse visait à explorer des aspects pratiques et fondamentaux de la conjugaison.

Le premier objectif de ma thèse était de développer un outil basé sur la conjugaison pour délivrer un antimicrobien spécifique d'une souche bactérienne. Le but est de créer un antimicrobien n'ayant pas un effet délétère sur un large spectre d'hôte pour éviter l'apparition de résistance dans des bactéries spectatrices qui ne sont pas responsable d'une pathologie. Pour ce faire, nous avons utilisé le système CRISPR-Cas9 (Clustered Regularly Interspaced Short Palindromic Repeats-CRISPR associated protein) issu de *Streptococcus pyogenes*.

Chez les bactéries, le système CRISPR-Cas permet l'éradication d'infections par des bactériophages (phages), virus infectant uniquement les bactéries, ou ADN exogènes tels que des plasmides. Pour ce faire, trois étapes sont essentielles : l'adaptation, l'expression et l'interférence qui vont être très brièvement résumées ci-dessous. Lors de l'entrée du phage, celui-ci injecte son ADN dans la cellule infectée. Parfois, cet ADN viral est dégradé par une machinerie bactérienne, libérant des *protospacer*. Dans ce cas, les protéines d'adaptation du système CRISPR-Cas, les protéines Cas, vont intégrer un *protospacer* dans leur propre génome, sous la forme de *spacer*, ce qui permettra de garder une trace de l'infection passée. Suite à cela, le *spacer* est exprimé en un ARN CRISPR (crRNA) et en association avec des protéines Cas va permettre de sonder l'ADN. Finalement, lorsque le *spacer* repère une séquence complémentaire à la sienne par homologie, ce qui indique qu'il repère la séquence de l'ADN exogène, alors le complexe protéique Cas associé au *spacer* introduit une cassure double brin dans cet ADN exogène, cela constitue l'étape d'interférence. Notre intérêt pour le système

CRISPR-Cas réside dans l'interférence. En effet, il a été montré qu'utiliser un tel système pour cibler une séquence d'un génome bactérien permet de tuer spécifiquement la bactérie visée.

Les système CRISPR-Cas sont divers et ont été répertoriés dans 42% et 85% des génomes bactériens et archées connus aujourd'hui. Ils sont classés dans deux classes différentes, six types et trente-trois sous-types.

Streptococcus pyogenes possède plusieurs systèmes CRISPR-Cas et nous avons utilisé son système de Type II-A. Ce système comporte trois acteurs pour performer l'étape d'interférence. Tout d'abord, le crRNA qui comporte le *spacer* d'une taille de ~20 nt, la protéine Cas9 qui est responsable de l'introduction des cassures double brin dans l'ADN ciblé et l'ARN transactivateur du crRNA (tracrRNA). Ce dernier se lie au crRNA et recrute la protéine Cas9, permettant la formation d'un complexe ARN-Cas9 qui cherche la séquence ciblée par le *spacer*. En liant le crRNA et le tracrRNA, il a été créé l'ARN guide (gRNA) qui comporte à la fois le *spacer* et recrute la Cas9 pour former le complexe Cas9-RNA.

La protéine Cas9 est une large protéine possédant de multiples domaines dont un qui reconnait une séquence adjacente au *protospacer*, appelée séquence PAM. Cette séquence doit être directement reconnue par la Cas9 pour que celle-ci s'active et induise le clivage de l'ADN. Elle est très spécifique du système CRISPR-Cas et chez *S. pyogenes* notamment cette séquence est 3'-NGG-5'. De plus, elle possède deux domaines, HNH et RuvC, chacun permettant de cliver un brin d'ADN ciblé.

Des recherches ont permis d'identifier des mutants de chacun de ces domaines et de créer une Cas9 incapable d'induire une cassure double brin, nommée *dead* Cas9 (dCas9). Cette protéine est tout de même capable de former un complexe dCas9-RNA permettant de reconnaitre la séquence ciblée mais reste ancrée à la séquence reconnue. La dCas9 est aussi large que la Cas9 et son ancrage à la séquence cible génère un encombrement stérique. Si la séquence ciblée se trouve être le promoteur d'un gène ou bien le début de la séquence codante, l'encombrement stérique créé par la dCas9 empêche le recrutement de la machinerie de transcription et entrave l'expression du gène ciblé. Cette utilisation du système CRISPR-Cas avec la dCas9 est appelée CRISPR interférence (CRISPRi).

Comme évoqué précédemment, lorsque l'on utilise un *spacer* ciblant une séquence d'un génome bactérien, cela est létal pour la bactérie. En effet, l'utilisation de ce système permet de viser toutes les séquences présentes à la fois, ce qui indique que si l'on cible le génome d'une bactérie, toutes les copies de la séquence seront clivées. Pour réparer les cassures double brin, les bactéries utilisent un système de réparation de l'ADN qui se base sur une séquence homologue. Or, si toutes les copies des séquences clivées sont ciblées, il n'y a aucune séquence homologue disponible afin d'effectuer la réparation et la bactérie incapable de réparer son ADN meurt. Il est aussi possible d'utiliser la fonction CRISPRi de la dCas9 afin de réprimer des gènes essentiels pour tuer les bactéries. De plus, afin de combattre les infections bactériennes, il est possible d'utiliser le CRISPRi pour réprimer les gènes de virulence ou bien les gènes de résistance des pathogènes.

Au laboratoire ont été créés les *Targeted-Antibacterial-Plasmids* (TAPs) qui sont des plasmides comportant le système CRISPR-Cas9 ou CRISPR-dCas9 de *S. pyogenes* avec un gRNA. Ces plasmides sont mobilisables par conjugaison car ils portent une origine de transfert (*oriT*) et peuvent ainsi être transférés dans la bactérie cible. Notre stratégie consiste à utiliser une bactérie donneuse comportant un plasmide *helper* ainsi que le TAP. Le plasmide *helper* contient les gènes permettant de produire la machinerie de conjugaison afin de pouvoir mobiliser et transférer par conjugaison le TAP dans la bactérie receveuse. Si cette dernière contient une séquence ciblée par le système CRISPR-Cas porté par le TAP, alors le système

CRISPR-Cas9 exercera son activité conduisant à la mort cellulaire ou à la répression du gène ciblé. Dans le cas où la receveuse ne contient aucune séquence ciblée, le système CRISPR-Cas9 sera incapable d'agir et la receveuse continuera à croitre.

Notre but est d'utiliser les TAPs afin de tuer une espèce bactérienne cible dans une communauté. Pour ce faire, il faut être capable de connaitre une séquence *spacer* de 20 nt présente dans le génome de la bactérie cible et absente des autres bactéries composant la communauté bactérienne. Dans ce but, un algorithme a été développé avant mon arrivée au laboratoire qui permet de trouver des séquences *spacer* spécifiques d'une bactérie. Il est nommé CRISPR Search Tool for Bacteria (CSTB). Cet outil permet de comparer le génome d'une ou plusieurs bactéries ciblées avec le génome d'autres bactéries non-ciblées, pour sélectionner celles uniquement présentes chez les bactéries ciblées.

La plus grande partie de mon travail de thèse a été de montrer l'efficacité de cette stratégie TAP. Pour ce faire, j'ai construit plusieurs TAPs avec différents *spacers* et j'ai testé leur activité face aux bactéries visées. Dans un premier temps, j'ai validé cette stratégie dans le modèle bactérien *Escherichia coli* en montrant par des approches de cytométrie que le TAP est bien transféré dans cette espèce et par des approches de microscopie que le fait de cibler une séquence génomique de cette bactérie induit des cassures à l'ADN qui sont létales.

Suite à cela, j'ai utilisé le CSTB afin de trouver des spacers pour cibler différentes bactéries pathogènes telles que *Citrobacter rodentium*, *Escherichia coli* enteropathogène, *Enterobacter cloacae*, *Salmonella enterica* serovar Typhimurium, *Vibrio cholerae* et *Klebsiella penumoniae*.

J'ai pu montrer que toutes les bactéries ciblées sont tuées par les TAPs. De plus, en utilisant le CSTB j'ai été capable de montrer qu'il est possible de trouver des séquences permettant de cibler plusieurs loci du génome bactérien, notamment j'ai utilisé un spacer qui touchait 22 loci du génome de *C. rodentium*. J'ai également pu montrer qu'il est possible d'utiliser la stratégie TAP dans un mix composé de différentes espèces. Seule la bactérie ciblée est tuée dans un tel mix. De plus, j'ai pu montrer qu'il est possible de trouver des séquences permettant de cibler plusieurs souches bactériennes à la fois tout en excluant d'autres.

De plus nous avons montré que les TAPs sont capables de cibler la résistance aux antibiotiques portée par un plasmide conjugatif. En effet, nous avons construit un TAP permettant de cibler le gène bla_{OXA-48} porté par le plasmide pOXA-48a et conférant une résistance aux carbapénèmes et notamment à l'ampicilline. Ce TAP a permis de réduire de 90% la quantité des bactéries receveuse résistantes à l'ampicilline.

Cette étude m'a également permis de sonder les limites de notre stratégie TAP. Tout d'abord, certaines bactéries sont capables d'échapper à la mort induite par les TAPs. L'analyse de ces résistants a montré que les bactéries ont deux moyens d'échapper aux TAPs. Tout d'abord, nous avons vu qu'il est possible que la bactérie ait muté la séquence ciblée dans son génome, ce qui la rend non reconnaissable par le système CRISPR-Cas9. Cependant, il est possible de réduire cette proportion de mutants. En effet, aucun résistant *C. rodentium* analysé n'avait pu changer sa cible génomique lorsque le *spacer* cible 22 loci sur son génome. La seconde façon de résister aux TAPs est de perturber leur systèmes CRISPR-Cas9. Le séquençage des TAPs des résistants a révélé l'insertion de transposases dans la séquence codante du gène de la Cas9. Cela empêche l'expression de la Cas9 et donc l'activité de clivage de l'ADN par celle-ci.

De plus, nous avons vu que pour avoir une influence significative des TAPs sur les bactéries ciblées, l'efficacité de conjugaison doit être haute, ~90 % des receveuses doivent recevoir le plasmide. Or, notre machinerie de conjugaison fournie par le plasmide F ou bien le

plasmide RP4 ne permet pas d'atteindre une telle efficacité. En effet, nous avons tout d'abord utilisé la machinerie de conjugaison du plasmide F qui est transféré à une efficacité de 100 % de *E. coli* à *E. coli* et a un spectre d'hôtes restreint aux entérobactéries. L'utilisation de cette machinerie a révélé que l'efficacité de transfert est plus basse pour *C. rodentium* (3,66 %), *E. cloacae* (0,092 %) et *E. coli* entéropathogène (12,2 %). De plus, nous n'avions pas été capable de transférer les TAPs dans *K. pneumoniae* et *V. cholerae*. Nous avons donc utilisé la machinerie de transfert du plasmide RP4 qui a un spectre d'hôte plus large et a permis d'atteindre ces espèces mais toujours avec une efficacité faible. Les TAPs sont très polyvalents et il est possible de changer très facilement l'*oriT* afin d'utiliser un autre plasmide *helper* dans le but de les mobiliser. La future amélioration des TAPs sera certainement d'utiliser un nouveau plasmide *helper*.

Enfin, une autre limite des TAPs est le transfert du plasmide *helper*. En effet, nous utilisons un plasmide *helper* capable de s'auto-transférer. Ceci est un problème dans notre cas tout d'abord car le plasmide *helper* peut porter des gènes de résistances aux antibiotiques qui pourraient être disséminés dans les communautés bactériennes. De plus, les plasmides conjugatifs portent des gènes d'exclusion qui sont exprimés chez le transconjugant. Ces gènes permettent d'éviter que le même plasmide soit transféré deux fois à une cellule l'ayant déjà reçu. Or, il arrive que notre plasmide *helper* soit transféré seul dans la bactérie cible et que cela résulte en l'expression des gènes d'exclusion, rendant la bactérie cible immunisée contre le transfert du TAP. C'est notamment ce qui a été observé lors de notre expérience visant à réduire l'antibio-résistance induite par le plasmide pOXA-48a, les 10 % de cellules receveuses toujours résistantes à l'ampicilline avaient acquis le plasmide F *helper* mais pas le TAP. C'est pourquoi j'ai construit une version du plasmide F délétée de son *oriT* et montré que cette construction permettait de réduire la quantité de receveuses résistantes à l'ampicilline à 3 %.

Finalement, j'ai montré que cette stratégie TAP permettait bien de tuer les bactéries ciblées de manière très spécifique grâce au CSTB qui permet de choisir les spacers.

Outre cette application biotechnologique, j'ai également étudié la dynamique de conjugaison bactérienne à l'échelle cellulaire, en utilisant comme modèle le plasmide F. J'ai exploré le timing d'expression des gènes plasmidiques une fois transférés dans la bactérie receveuse ainsi que l'établissement de la résistance aux antibiotiques après l'acquisition du plasmide.

Tout d'abord, je me suis intéressée aux gènes se situant sur la première partie du plasmide à entrer dans la receveuse, appelée « *leading region* ». Durant la conjugaison le plasmide est transféré de façon simple brin dans la receveuse, est re-circularisé puis le brin complémentaire est synthétisé pour former la version double brin du plasmide. Une fois le plasmide complet, les gènes qu'il porte sont exprimés dans le transconjugant. Cependant, avant mon arrivée au laboratoire, il avait été montré par des approches de microscopie que le gène *ssb* faisant partie de la *leading region* était exprimé de manière transitoire avant la conversion du plasmide sous forme double brin chez le transconjugant. De plus, *ssb* ne semblait pas s'exprimer dans la cellule donneuse. Par les mêmes approches de microscopie, j'ai pu prouver que les gènes de la *leading region yfjA, yfjB, psiB* et *ygeA* sont également exprimés de manière transitoire uniquement chez le transconjugant avant l'acquisition de la forme double brin du plasmide. Parmi ces gènes, *ssb* et *psiB* encodent pour des protéines de fonctions connues. En effet, SSB est l'homologue de la protéine éponyme chez *E. coli* et permet de protéger les intermédiaires simple brin de l'ADN lors de la réplication. PsiB, quant-à-elle, est une protéine permettant de contenir la réponse SOS induite lors de la formation d'intermédiaires simples brins suite à la cassure d'ADN. La réponse SOS déclenche l'expression

de nombreux gènes et peut résulter en la dégradation du plasmide conjugatif arrivé dans la receveuse sous forme simple brin. Ces deux protéines pourraient être impliquées dans un processus de protection de l'ADN simple brin qui permettrait un meilleur établissement de ce plasmide. Les autres protéines n'ayant pas de fonction connue pourraient être impliquées dans un processus similaire. Ces premiers résultats ont suggéré une stratégie d'expression qui permettrait d'abord l'établissement du plasmide transféré, sa maintenance puis son transfert à une autre receveuse. Ce projet que j'ai initié a ensuite été poursuivi au laboratoire pour déterminer la dynamique d'expression des protéines du plasmide F.

J'ai également étudié l'acquisition de la résistance à la tétracycline conférée par le plasmide F portant une pompe à efflux spécifique TetA qui permet d'éjecter la tétracycline hors de la cellule. La tétracycline est un antibiotique bactériostatique empêchant la croissance des bactéries mais ne les tuant pas. Il agit sur le ribosome bactérien et empêche la production de protéines par la bactérie. Grâce à l'utilisation de la microscopie à fluorescence, nous avons pu observer et analyser la dynamique de production de TetA en temps réel et l'efflux de tétracycline dans les cellules portant le plasmide F. Notre étude montre que la résistance à la tétracycline dépend d'un équilibre entre la production de TetA et la capacité de la tétracycline à bloquer cette production. De plus, nous avons pu corréler l'augmentation de la quantité intracellulaire de TetA avec la capacité des cellules à résister à des concentrations croissantes de tétracycline.

Pendant mes trois années au laboratoire, j'ai prouvé que la stratégie TAP est un moyen innovant de tuer spécifiquement les agents pathogènes ou d'inhiber la résistance aux antibiotiques *in vitro*, ce qui constitue une preuve de concept du développement d'alternatives aux antibiotiques originales basées sur la conjugaison. De plus, l'étude fondamentale de la dynamique de l'expression des gènes plasmidiques a permis d'amorcer d'autres projets afin de mieux comprendre le phénomène de conjugaison.

Table of contents

Preamble

Bacterial DNA conjugation is an horizontal gene transfer mechanism allowing the transfer of large plasmid or chromosome DNA between bacterial cell in direct contact. Conjugation is a common mechanism in bacterial species and decades of studies revealed its fundamental biological importance in the evolution of bacterial genomes and the dissemination of bacterial metabolic properties. In particular, conjugation is known to play a major role in the dissemination of antibiotic resistance among bacteria within natural and clinical environments. Since the discovery of bacterial conjugation in 1946, extensive genetic, biochemical, and genomic studies have revealed the wide diversity of conjugative plasmids and allowed to describe the reaction steps required for their transfer from one bacterium to another. These studies also provided an abundant literature showing that conjugation is a highly conserved mechanism among bacterial species and ubiquitous in a wide range of bacterial ecosystems. Moreover, on the practical point of view, conjugation systems allowed the development of a range of tools to perform genetic modification of various bacterial species or allowing the delivery of antibacterial genes.

During my thesis, I worked on both the practical and fundamental aspects of conjugation. First, I developed an antibacterial approach that uses conjugation to deliver strain-specific CRISPR-Cas systems. I also studied the mechanism of conjugation at the cellular scale, with particular interest in the pattern of plasmid gene expression in the recipient cell during plasmid establishment and the dynamics of plasmid-born drug resistance in live-cells.

In the first part of the introduction, I will draw a bird's eye overview on conjugation by describing several properties including its ubiquity, conservation, general mechanism, highlighting its role in environmental adaptation of bacteria. I will also mention the main limitations to the success of plasmid transfer by conjugation between bacterial species. To do so, I will discuss the examples of the F, the R64 and the RP4 plasmids as paradigmatic model systems.

Next, I will review non-antibiotic antibacterial approaches based on phages, conjugation and/or on CRISPR-Cas systems. I will specifically focus on the Type II CRISPR-Cas9 system of *Streptococcus pyogenes* that I used during my thesis, detailing its ability to kill specifically chosen bacterial species as well as its limitations.

Finally, I will go further into the mechanistic details of conjugation using the F plasmid as a study model. I will describe the key steps of plasmid transfer and the subsequent establishment of the plasmid in the new host cell, and highlight our current gap in knowledge regarding the timing, chronology, coordination and intracellular organisation of plasmid conjugation.

Introduction

I. Overview on DNA transfer by bacterial conjugation

Environmental niches are colonized by diverse microorganisms including bacteria that interact via multiple processes. Notably, bacteria are able to acquire DNA from other bacteria or from the environment, mainly through three types of Horizontal Gene Transfer (HGT) mechanisms: transduction, natural transformation and conjugation.

Transduction is a phenomenon enabling the transfer of bacterial genes through bacteriophage particles. Bacteriophages are viruses infecting specifically bacteria, basically composed of DNA contained into a capsid composed of proteins. During the infection cycle, phage and/or bacterial DNA can be encapsidated within the phage particles and subsequently delivered to another bacteria, thus allowing the acquisition of new genes and associated metabolic properties such as virulence. Famous examples are the cholerae toxin carried by the CTXϕ phage and responsible for *Vibrio cholerae* virulence (Waldor and Mekalanos 1996) or the shiga-toxins genes (*stx1* and *stx2)* from the VT1-sakai and VT2-sakai prophages found in *E. coli* (STEC) O157:H7 from the Sakai outbreak in 1996 in Japan (Makino *et al.* 1999; Yokoyama *et al.* 2000).

Natural transformation is an active DNA uptake mechanism used by bacteria to acquire DNA from the environment. Transformation was first discovered in the bacterial pathogen *Streptococcus pneumoniae* (Griffith 1928) and was proven to contribute to its virulence and the acquisition of resistance determinants (Croucher *et al.* 2013). Moreover, Domingues *et al*. revealed that transformation ability enables highly efficient HGT of transposable elements like Tn*21* between unrelated bacterial species (Domingues *et al.* 2012).

Conjugation is a contact-dependent gene transfer process between a donor and a recipient bacterial cell. Conjugation supports the transfer of varied DNA elements, including plasmids, transposons or even chromosomes, and is a widespread phenomenon among bacterial communities.

HGT have been preponderant actors in the plasticity of bacterial genomes allowing for their adaptation in different ecological niches. Notably, it was estimated that Mobile Genetic Elements (MGE) contribute to 18% of the genome of *Escherichia coli* MG1655 strain and to 2 to 6 % of the genome of *Pseudomonas fluorescens* group (Lawrence and Ochman 1998; Loper *et al.* 2012). The percentage of horizontally acquired genes in diverse bacterial genomes can vary from 1.5 to 14.5 % depending on the bacterial or archaeal genome considered (Garcia-Vallve 2000). Using different techniques, it is possible to track HGT events, notably to identify MGE in sequenced genomes or metagenomics studies using sequence comparison and identifying related regions or HGT-related marker genes. Other techniques allow to link MGE with their hosts using culture-dependent genome sequencing, culture-independent single-cell sequencing, reporter genes or proximity ligation of environmental DNA. Metagenomics approaches enable to see the HGT abundance of a bacterial community at a precise time point. Whereas studies on HGT using a reporter gene allow to follow the direction of HGT. However, no technique is yet able to clearly associate the HGT mechanism with its direction in a complex environment (Brito 2021).

I.1. Conjugation is an ubiquitous process conserved among bacteria

Conjugation is an ubiquitous mechanism as where bacteria are found, conjugation can be observed. In nature, bacteria are able to colonize liquid and solid surfaces, and to perform

conjugation in both cases. Indeed, conjugative plasmids equipped with reporter systems combined with microscopy enabled to observe conjugation between *Pseudomonas putida* and seawater bacteria both on seawater and in sediment (Dahlberg, Bergström and Hermansson 1998). Moreover, survey on groundwater revealed the presence of conjugative plasmids in this niche. Plant-associated bacteria in the rhizosphere or the phylloplane were also reported to achieve conjugation (Lilley *et al.* 1994; Normander *et al.* 1998) as well as animal and human-related bacteria (Rang *et al.* 1996; García-Quintanilla, Ramos-Morales and Casadesús 2008; Jones, Sun and Marchesi 2010). Moreover, conjugation has been shown to happen between bacteria colonizing man-shaped environments, for instance in activated sludge and dust (Soda *et al.* 2008; Ben Maamar *et al.* 2020). As conjugative plasmids can be vector of numerous antibiotic resistance determinants, they were monitored in hospital environment for instance, which revealed that abiotic surfaces and evacuation pipes were an ecological niche for many pathogen bacteria to exchange conjugative elements (Weingarten *et al.* 2018).

Bacterial conjugation is a universally conserved mechanism that can occur among and between gram-negative and gram-positive bacteria. Conjugational transfer can even happen in both directions, for instance between the gram-positive *Enterococcus faecalis* and the gram-negative *E. coli* (Abajy *et al.* 2007; Arends *et al.* 2012).

Conjugation generally involves a machinery composed of three essential components: (i) the relaxosome protein complex processing the plasmid DNA before transfer, (ii) a coupling protein connecting the conjugation substrate to the mating pair channel and (iii) a mating pair channel to serve as a conduit for the DNA through the bacterial membranes. The establishment of the mating pair between the donor and the recipient cell requires an extracellular appendage called the conjugative pilus. The role of these systems and their function in the key steps of conjugation will be extensively developed in the section III. Yet, here we can stress that gram-positive bacteria, including but not limited to *Staphylococcus*, *Lactococcus*, *Enterococcus* and *Bacillus* genus, have evolved an additional mechanism of plasmid transfer by conjugation. In this case, they do not produce a conjugative pilus but adhesins to mediate donor-recipient contact (Grohmann, Muth and Espinosa 2003; Kohler, Keller and Grohmann 2019). Moreover, multicellular gram-positive bacteria of the *Streptomyces* genus use a transfer machinery, similar to division and sporulation mechanisms, composed of a DNA-binding protein forming pores into the cell membrane and wall to contact neighbour mycelium and transfer double-stranded DNA plasmid (Goessweiner-Mohr *et al.*; Thoma and Muth 2015; Thoma *et al.* 2019). This particular conjugative mechanism is limited to mycelium forming *Streptomyces*, while most bacteria have a unicellular lifestyle and use more canonical conjugation machineries.

Conjugation is a highly versatile mechanism that is not limited to bacteria-bacteria exchanges only, but that can also happen between bacteria and eukaryotic cells or organelles. The most famous example is the transfer of the *Agrobacterium tumefaciens* Ti plasmid into plant cells, but other cases have been reported. Notably, it was shown that the Ti plasmid was able to be transferred in several fungi species, yeasts and HeLa cells (Bundock *et al.* 1995; de Groot *et al.* 1998; Kunik *et al.* 2001). F, R751 and ColE1 plasmids were also proven to transfer into the *Saccharomyces cerevisiae* yeast (Heinemann and Sprague 1989). Moreover, conjugative tools based on the RP4 conjugative machinery have been developed to transfer DNA from bacteria to mammalian mitochondria (Yoon and Koob 2005).

Particular interest was accorded to the study of gene flux within the gut microbiota, considering its impact on the host health and in the development of the immune system, as a

protective barrier against pathogens and as an helper for digestive function (Sekirov *et al.* 2010; Brooks *et al.* 2021). Researches informed on the actual correlation between perturbed composition of the microbiota (dysbiosis) and host diseases, among which diabetes and obesity (Turnbaugh *et al.* 2006; Sekirov *et al.* 2010; Stecher, Maier and Hardt 2013; Fan and Pedersen 2020). Studies conducted *in vitro* tended to reproduce a microbiota-like environment and reported the influence of different factors on conjugation rates of different plasmids (pH, temperature, anaerobic conditions) (Rang *et al.* 1996; García-Quintanilla, Ramos-Morales and Casadesús 2008; Aviv, Rahav and Gal-Mor 2016; Neil, Allard and Rodrigue 2021). For instance, the transfer of the *Salmonella enterica* serovar Typhimurium virulence plasmid pSLT in the mouse gut was addressed (García-Quintanilla, Ramos-Morales and Casadesús 2008). The objective was to discover the gut part favouring the transfer of this virulence plasmid. Sodium deoxychlorate, mimicking bile found in the duodenum, and propionate, simulating the large intestine, were proven to prevent conjugation. *In vivo* assays in ileal loops demonstrated that conjugation occurs in the ileum of mouse. Moreover, *in vivo* experiment in mouse without antibiotic pre-treatment showed that conjugation occurs even in the presence of microbiota competitors (García-Quintanilla, Ramos-Morales and Casadesús 2008). However, other studies showed that laboratory conditions do not necessarily reflect the real transfer efficiency in the microbiota. Indeed, laboratory broth is not a suitable media to mimic *in vivo* conditions in contrast to intestinal extracts or caecal contents (Rang *et al.* 1996). It was demonstrated that despite low conjugation rates *in vitro*, $IncI_2$ Tp114 plasmid was highly transferred in the microbiota of mice (Neil *et al.* 2020). It was further determined that mating pair stabilisation is a key factor to promote conjugation in the gut environment (Neil, Allard and Rodrigue 2021). Metagenomic investigation of the conjugative plasmids in human faecal samples was conducted using an "*E. coli* recording" strain (Munck *et al.* 2020). This strain was equipped with overexpressed CRISPR adaptation system in order to record the acquisition of foreign DNA in the spacer memory. Analysis of the spacer sequences and their quantity allowed to infer the relative transfer of different plasmids in the recording strain. Notably, IncX plasmids were shown to transfer at higher rates than IncI plasmids.

Besides, administration of antibiotics in the microbiota was reported to trigger microbiota dysbiosis by modifying the relative abundance of resident bacteria species and sometimes favour the colonization with opportunistic pathogens (De La Cochetière *et al.* 2008). For instance, *S. enterica* serovar Typhimurium persisters can colonize the mouse gut following antibiotic treatment. They were observed to mediate efficient conjugative transfer of plasmid-encoded antibiotic resistance to commensal *E. coli* (Bakkeren *et al.* 2019). Various studies further report that resistant determinants are present and active in the microbiota, constituting a resistome available for pathogenic strains (van Schaik 2015; Francino 2016).

It became obvious from these studies that the gut microbiota is a complex environment where physiology, pH, nutrients and O_2 availability variations shapes the interactions between bacterial strains, including the extent of DNA transfer by conjugation.

I.2. Importance of conjugation in bacterial adaptation

Autonomous conjugative plasmids generally carry transfer, maintenance and potential additional cargo genes. Cargo genes are not required for the conjugation process *per se*, but might confer advantageous adaptive metabolic functions that compensate for the fitness cost induced by their acquisition, thus improving the survival of the recipient cell in a given ecological niche. For example, in the rumen microbiota, function provided by plasmids were related to carbohydrate metabolization or cell-wall and capsule formation, which is an

advantage for bacteria considering that carbohydrates are abundant in the rumen environment and that cell-wall and capsule are key determinants to escape host immune system (Kav *et al.* 2012). Other studies showed that the mobile gene pool of gut microbiota depends on the diet of their host (Hehemann *et al.* 2010; Brito *et al.* 2016). A variety of biological functions that might confer selective advantage to the new host cell can be found on conjugative plasmids. In the next part, I will briefly mention a few examples such as symbiosis, virulence, metal and antibiotic resistance.

I.2.1. Symbiosis

As for the gut microbiota, bacteria are important actors in the soil and in the rhizosphere. The plant rhizosphere is composed of various bacterial species predominantly from α and β-*Proteobacteria*, *Actinobacteria*, *Firmicutes*, *Bacteroidetes*, *Planctomycetes*, *Verrucomicrobia* and *Acidobacteria* (Turner, James and Poole 2013). *Leguminosae* developed symbiotic relationship with bacteria, called rhizobia, from diverse genera encompassing notably : *Azorhizobium*, *Allorhizobium*, *Bradyrhizobium*, *Mesorhizobium*, *Rhizobium* and *Sinorhizobium* (Ferguson *et al.* 2010).

In several rhizobia, symbiotic genes are found on conjugative plasmids, for example in pSymA of *Sinorhizobium meliloti,* which encodes for *nod* and *nif* genes (Lagares, Sanjuán and Pistorio). Indeed, thanks to plasmid-encoded *nod* genes, rhizobia develop symbiosis with the plant host, growing new organs named nodules (Redmond *et al.* 1986). Nodules are specialized structures formed with plant cells infected by differentiated rhizobia to perform symbiotic nitrogen fixation. In the nodule, rhizobia express *nif* genes to produce a nitrogenase reducing atmospheric nitrogen (N_2) into ammonia (NH_3) and favour plant growth (Chen *et al.* 2003). In exchange, the plant promotes the multiplication of symbiotic bacteria by providing carbon nutrients (Lindström and Mousavi 2020). Furthermore, it was shown that conjugative transfer of symbiotic islands was encouraged by the flavonoid plant production. The narningenin flavonone was reported to increase conjugative transfer of the symbiotic island on the ICE of *Azorhizobium caulinodans* (Ling *et al.* 2016). Moreover, *Rhizobium elti* pSym can be transferred in endophytic recipient strains inside nodules (Bañuelos-Vazquez *et al.* 2020). In this study, four out of nine endophytic transconjugant strains were then able to form nodules and fix nitrogen, proving that conjugative transfer allows the dissemination of the symbiotic lifestyle.

I.2.2. Virulence

Pathogenic bacteria encode virulence genes that are often contained in pathogenicity islands encoding proteins implicated in pathogenicity. Function associated with pathogenicity are diverse and include host-cell adhesion, cytotoxicity, immunoevasion, immunosuppression, entry and/or exit of the infected cell and host-encoded nutrient uptake (Casadevall and Pirofski 2009).

The human-related pathogen *S. enterica* serovar Typhimurium can carry the pSLT conjugative plasmid. It contains *Salmonella* plasmid virulence (*spv*) locus notably composed of *spvB* and *spvC*. SpvB and SpvC are effectors translocated into the infected cell by the Type III Secretion System and interfere with the actin cytoskeleton of eukaryotic cells (Guiney and Fierer 2011).

In the rhizosphere, *A. tumefaciens* uses the conjugative Ti plasmid to induce tumor in the plant. A specific portion of the Ti plasmid, called T-DNA, is transferred in the plant cell and induces expression of oncogenes to generate a tumor. Notably, *iaaM*, *iaaH* and *ipt* genes

enable the production of phytohormones promoting the plant growth and thus inducing the tumor (Barry *et al.* 1984; Klee *et al.* 1984; Astot *et al.* 2000). Moreover T-DNA contains genes encoding opine-related proteins leading to opine secretion by the plant, which favours the growth of Ti-carrying *A. tumefaciens.* In addition, the Ti plasmid contains genes coding proteins implicated in opine uptake and catabolism (Escobar and Dandekar 2003).

I.2.3. Metal resistance

Metals are naturally present in the environment and acquisition of a metal-resistance carrying plasmid considerably improve the survival of environmental bacteria. The overuse of metals in medical and agriculture fields added to pollution due to industries and urbanization led to increased concentration of metals in the environment (Nicholson *et al.* 2003; Men *et al.* 2018; Carver 2019). Notably, it was reported that conjugative plasmids of environmental bacteria such as pigs-associated *E. coli* and *Enterococcus* harbour copper-resistance genes on pRJ1004 plasmid and an unnamed plasmid respectively (Tetaz and Luke 1983; Hasman and Aarestrup 2002). Moreover, medically relevant bacteria were associated with plasmid-encoded heavy-metal resistance. For instance, the pUPI199 conjugative plasmid of *Acinetobacter baumannii* contains silver resistance genes and pUM505 plasmid of *Pseudomonas aeruginosa* contains both mercury and chromate resistance genes (Deshpande and Chopade 1994; Hernández-Ramírez *et al.* 2018).

A genomic analysis in 2015 done on referenced bacterial genomes and plasmids in PubMed revealed that metal ion resistance are reported in bacteria from diverse environment, in clinical and agricultural field, in domestic and wild animals and from human sources (Pal *et al.* 2015). Several metal resistance genes were revealed to be found on the same 'multi-metal resistance' plasmids. For instance, copper resistance was co-occurring with nickel and cobalt resistance genes, while arsenic, copper and silver resistance tend to cluster together. Interestingly, the investigation of metal and antibiotic resistance co-selection showed that bacteria isolated from human and domestic animals generally held plasmids with co-selection. Overall, 57% of plasmids co-selecting for both metal and antibiotic resistance were conjugative. This study highlights the co-selection with MGE markers like transposases. For example, cadmium and zinc resistance were mostly associated with aminoglycoside and macrolide resistance. Mercury resistance was associated with two clusters related to different transposases. Mercury resistance associated with ISCR2 transposases clustered with sulphonamides, amphenicol and tetracycline resistance whereas its association with ISCR1 transposases correlate with sulphonamides and aminoglycosides resistance. Moreover, co-selection is preferentially found in large conjugative plasmids and that it is particularly found in clinical relevant bacteria like *Escherichia*, *Staphylococcus*, *Salmonella* and *Klebsiella* genera. It was indeed observed that R100 plasmid containing resistance to tetracyclines, chloramphenicol, sulphonamides and aminoglycosides also carry the Tn*21* mercury resistance transposon (Liebert, Hall and Summers 1999). Moreover, Tn*21* containing mercury determinants has evolved and acquired the In2 integron containing several antibiotic resistances (Kholodii *et al.* 2003). Although medical practices are changing to prevent or ban the use of mercury dental amalgams, notably in European countries (UNEP 2016), the environmental pollution by metals can select for metal ion resistance and thus for antibiotic resistance in environmental and human-related bacteria.

I.2.4. Antibiotic resistance

Antibiotics are naturally produced by soil bacteria, in particular by Actinobacteria of the *Streptomyces* genus and fungi, and are involved in competition interactions between bacteria (Laskaris *et al.* 2010; Hutchings, Truman and Wilkinson 2019). If it is clear that antibiotic resistance genes can originate from natural evolution, there is not further doubt that the anthropization of the environment (mainly the heavy use of antibiotics) triggers the emergence, dissemination and accumulation of drug-resistant strains in a variety of environmental settings. Analysis of drug-resistant strains has revealed a multitude of conjugative resistance-plasmids carrying genes conferring resistance to most, if not all classes of antibiotics currently used in clinical treatments. It has been estimated that conjugation accounts for 80% of acquired resistances in bacteria (Barlow 2009).

Conjugative plasmids carry a single or multiple resistance genes. For example, the pKpQIL plasmid carrying Tn*4401* transposon played a role in the dissemination of bla_{KPC} genes responsible for carbapenem resistance outbreak since 2010 in the North-West England in *Klebsiella pneumoniae*, *E. coli* and *Enterobacter* species (Doumith *et al.* 2017). Resistance genes can be mobilized by Insertion Sequences able to locate on transposons which are themselves sometimes held by conjugative or mobilizable plasmids. This Russian doll organization of resistance determinants can lead to accumulation of resistance in plasmids and in bacterial strains leading to multi drug resistant (MDR) bacterial strains. An illustration of this feature is provided by the previously evoked Tn*21* transposon carried by the R100 plasmid of *Shigella flexneri* conferring resistance to mercury and has been shown to contain a class 1 integron conferring resistance to sulfonamides and streptomycin thanks to *sul* and *aad* genes (Liebert, Hall and Summers 1999).

A number of antibiotic resistance determinants were found on conjugative plasmids and ICEs of hospital wastewater bacteria or in soil environments (Forsberg *et al.* 2012; Weingarten *et al.* 2018). Besides, various studies reported the emergence of resistance by bystanders microbes following antibiotic treatments (Sjlund *et al.* 2003; Tedijanto *et al.* 2018). This is thought to result from HGT events and further selection by antibiotics found in the environment under minimum inhibitory concentrations (Gullberg *et al.* 2014). In hospital environment especially, the emergence of MDR pathogens is a global concern regarding nosocomial infections. In 2017, WHO published a list of antibiotic resistant "priority pathogens" designating as a critical priority to develop new treatments against carbapenem-resistant *A. baumannii*, *P. aeruginosa* and Extended Spectrum β-Lactamase (ESBL)-producing *Enterobacteriaceae* (Monteiro et al. 2019). Conjugation plays a prevalent role in the dissemination of these resistance as carbapenem resistance and ESBL genes are found on several families of conjugative plasmids (Cantón *et al.* 2012; Brolund and Sandegren 2016; De Oliveira *et al.* 2020) that disseminate resistance determinants among *Enterobacteriaceae*, *P. aeruginosa* or *A. baumannii*.

I.3. General mechanism of conjugation

Conjugation allows the transfer of diverse genetic elements including plasmids, Integrative Conjugative Elements (ICEs), chromosomes or transposons, among and between a wide range of Gram-negative and Gram-positive bacteria. ICEs are conjugative elements that integrate to the chromosome of bacteria and are replicated with it. These elements conserve the ability to be excised and transferred into a new host. These different conjugative elements carry specific set of conjugation genes and use various strategies to complete the conjugation process. Despite these significant discrepancies, it is possible to build a model describing the main

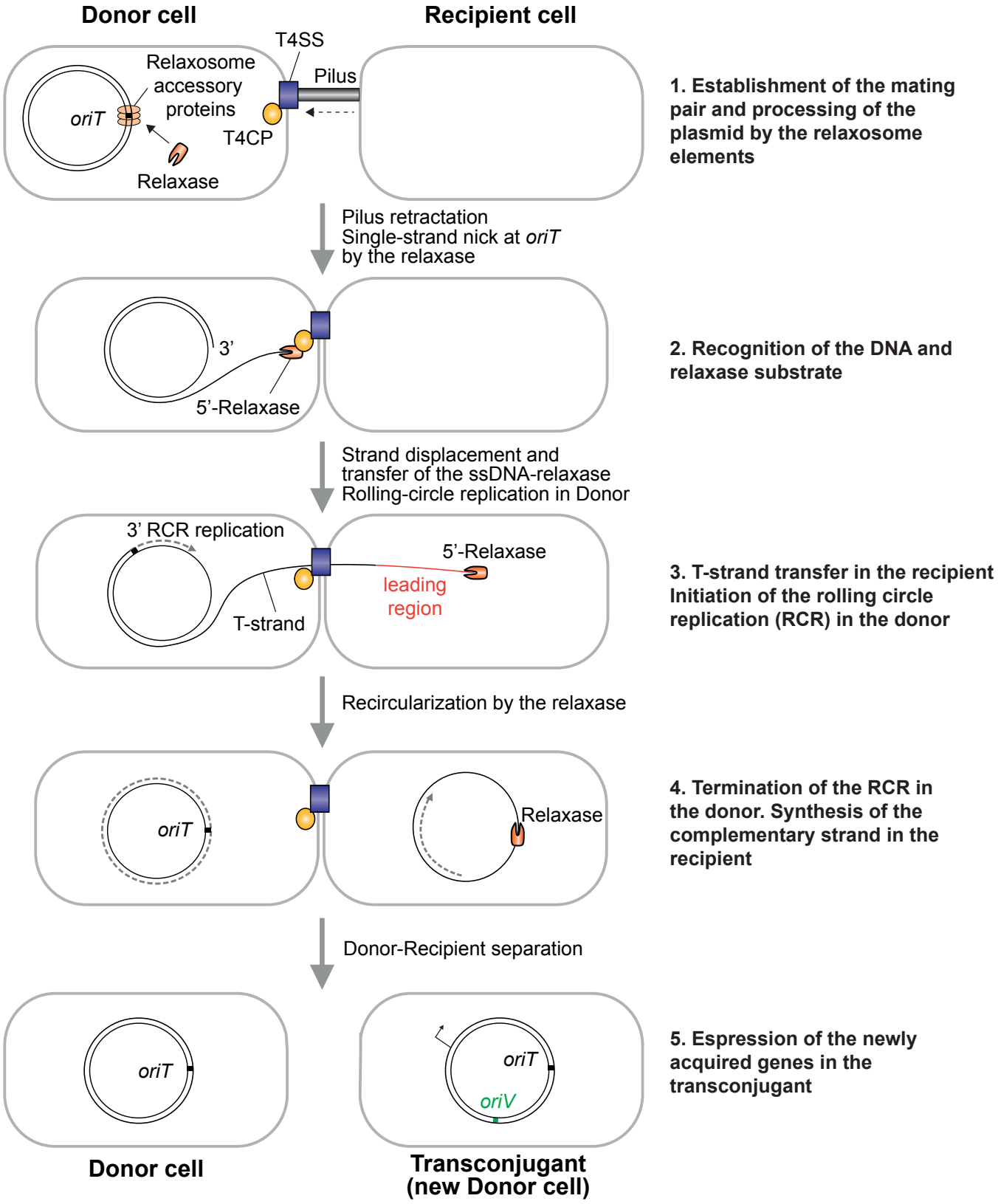

Figure 1 : Key steps of DNA transfer by conjugation
Scheme to visualize the different conserved steps of DNA transfer during the conjugation mechanism. 1. First the donor cell contacts the recipient cell while the plasmid is processed for the transfer. 2. The processed plasmid strand is recognized to be transferred in the recipient. 3. The transferred (T-strand) enters the recipient cell while the rolling circle replication (RCR) occurs in the donor. 4. The T-strand is recircularized and the complementary strand is synthetized. 5. The newly acquired plasmidic genes can be expressed in the transconjugant cell.

sequence of reactions that is common to the majority of conjugation systems. In the following section, I will present a general step-by-step model for the conjugation process of plasmid in Gram-negative bacteria, which is the primary focus of my work (Figure 1). The genetic and mechanistic details regarding the factors involved in the different reactions will be described in more details in the section III.

The first step of the conjugation mechanism is the establishment of the mating pair between the donor and the recipient cell. To do so, donors produce a plasmid-encoded external appendage called conjugative pilus, which is assembled by and linked to the Type IV secretion system (T4SS) (Hospenthal, Costa and Waksman 2017). The T4SS is a membrane apparatus forming a channel through the donor membrane and allows the passage of the transferred DNA to the recipient (Lawley *et al.* 2003). The conjugative pilus has the ability to retract to establish the mating pair between the donor and recipient cells (Figure 1 step 1) (Clarke *et al.* 2008).

In the donor strain, the plasmid is processed prior to the transfer by the relaxosome. The relaxosome is a protein complex assembling at a specific region of the plasmid called the origin of transfer (*oriT*). It is composed of plasmid or host-encoded proteins which recognize the *oriT* and recruit the key relaxase protein (Wong, Lu and Glover 2012). The relaxase is a multifunctional protein composed of two distinct domains : trans-esterase and helicase (Ilangovan *et al.* 2017). The relaxase introduces a nick at the *nic* site in the *oriT* by trans-esterification. Consequently, a tyrosine residue of the trans-esterase domain remains covalently bound to the 5' end of the cleaved DNA. Then, the helicase domain of the relaxase unwinds the plasmid DNA to extrude the ssDNA molecule called the transferred strand (T-strand), which will be transferred into the recipient cell (Draper *et al.* 2005).

The T-strand linked to the relaxase will next be recognized and addressed to the T4SS by the Type IV Coupling Protein (T4CP). The T4CP is a T4SS component mediating the substrate specificity by specific recognition of the relaxase-T-strand nucleoprotein complex (Álvarez-Rodríguez *et al.* 2020). To do so, the T4CP interacts with both the relaxosome components and the T4SS, thus performing the coupling function (Figure 1 step 2). This leads to the energized transfer of the T-strand into the recipient through the T4SS. The first T-strand region entering the recipient cell is called the leading region (Figure 1 step 3). While the T-strand is transferred by the 5'-relaxase end, the 3' end generated by the cleavage reaction serves to initiate the rolling-circle-replication (RCR) reaction that converts the remaining ssDNA plasmid into dsDNA in the donor strain (Wawrzyniak, Płucienniczak and Bartosik 2017). This allows the maintenance of the double stranded copy of the plasmid in the donor, making conjugation a conservative transfer mechanism (Figure 1 step 3).

After the entry of the ssDNA into the recipient, the co-transferred relaxase re-circularizes the T-strand, which is subsequently converted into dsDNA by complementary strand synthesis reaction (Figure 1 Step 4). Once the recipient cell contains the dsDNA plasmid, expression of the plasmid genes results in the establishment of new metabolic properties, a step referred to as the phenotypic conversion of the recipient into a transconjugant cell (Figure 1 Step 5). The maintenance and stable inheritance of the newly acquired dsDNA plasmid during cell divisions will then depend on the presence of a functional origin of replication (*oriV*), and a partition system that are compatible with the host cell machineries (Lilly and Camps 2015; Brooks and Hwang 2017). The *oriV* and replication system ensure plasmid duplication and the control of the plasmid copy-number. Indeed, conjugation plasmids are generally maintained at low-copy number, most probably to limit the metabolic burden associated with the numerous metabolic functions their confer to the cell. The stable

inheritance of low-copy number replicons cannot be ensured by random segregation and rely on the active partition systems (see sections III.3.2. and III.3.3). Importantly, two plasmids harbouring the same replication and/or partition mechanisms cannot be maintained in the same bacterial cell. This is why the first classification of plasmids into incompatibility groups is based on the compatibility of replication and partition systems (I.4.2). Besides, the transconjugant becomes a new plasmid donor by the production of the transfer machineries, and is unable to receive a new copy of the already acquired plasmid by conjugation through the production of exclusion (or immunity to self-transfer) systems. In addition, the transconjugant cells might also gain new properties that are not directly related to conjugation, such as drug or metal resistance, virulence and symbiotic lifestyle as previously evoked.

I.4. Restriction of conjugation efficiency

Not all conjugative plasmids can transfer efficiently and/or be maintained into any bacterial species (Figure 2). I will first describe the bottlenecks of the conjugation transfer regarding factors specific to the donor and recipient cells. Then I will describe incompatibility and fertility inhibition factors, which are related to the co-occurrence of another conjugative plasmid in the recipient or the donor strain, respectively.

I.4.1. Donor and recipient factors

The ability of a plasmid to be transferred and maintained in a given bacterial host is defined as the plasmid host-range. Conjugation host-range can be restricted by several processes:

- Plasmid transfer can be limited by the inability to form and maintain a stable mating pair between donor and recipient cells (Figure 2A).
- The recipient cell might carry gene systems to protect against the acquisition of foreign DNA (Figure 2A). Plasmid acquisition is also prevented in a recipient cell that already carries identical or closely related conjugation plasmid through the mechanism of exclusion against self-transfer (Figure 2B).

The contact between the donor and the recipient is mediated by the conjugative pilus. Plasmids encode different pilus types adapted to various conditions, like the F plasmid thick flexible pilus adapted for conjugation in liquid and solid media whereas RP4 short rigid pilus allow mating in solid media only (Bradley 1980). It was also shown that the F-pilus is able to retract to form conjugative junctions whereas the RP4-pilus does not, but enables donor and recipient aggregation thanks to their adhesive properties (Novotny and Fives-Taylor 1974). Plasmids of the IncI family, like the R64 plasmid, were shown to encode two types of pili: thin flexible (classified as type IVb pili) and thick flexible which allow conjugation in liquid and solid media. These conjugative plasmids have been shown to produce adhesins localized potentially at the tip of the thin flexible pilus. The 3’ of the adhesin gene contains a shufflon construct enabling C-terminal switching of the adhesin thus changing specificity in adhesion (Yoshida, Kim and Komano 1999; Gyohda *et al.* 2002). Indeed, the shufflon encodes a shufflase (or recombinase for clustered inversion), which is able to re-organize the coding DNA locus and promote the recombination by inversion between two facing *sfx* sequences (Komano 1999). This allows a genetic variability of the produced adhesins that are thought to mediate contact with the lipopolysaccharide (LPS) of different recipient cells (Ishiwa and Komano 2000). By contrast, the broad host-range RP4 plasmid was not shown to depend on any kind of recipient receptor for the conjugation process (Moriguchi *et al.* 2020), as was already demonstrated for

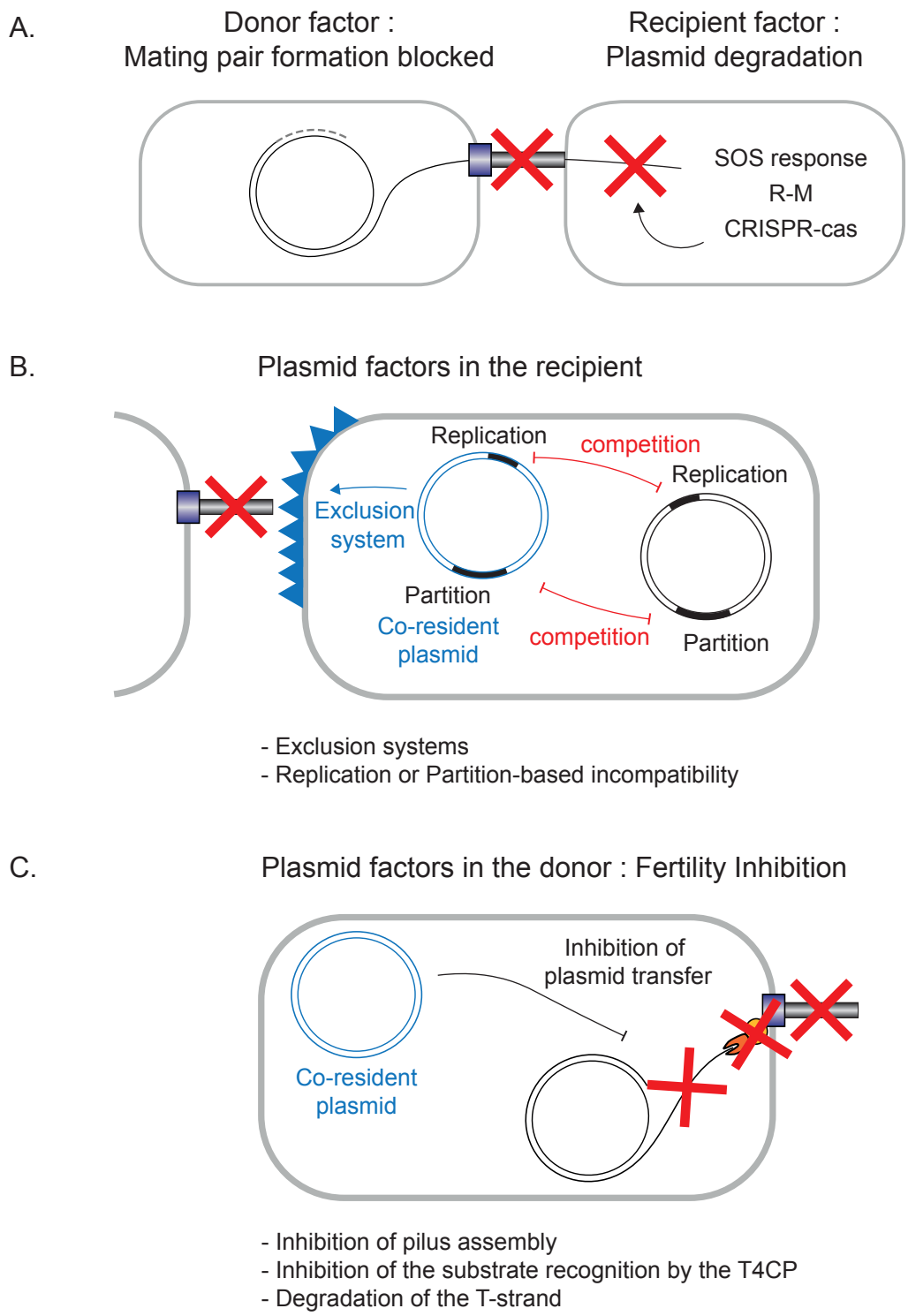

Figure 2 : Bottlenecks of conjugation. Schematic view of the different bottleneck of conjugation in the donor and the recipient. A. The donor can be unable to maintain a stable mating pair or the recipient can degrade the plasmid DNA after the induction of SOS response expressing degradation mechanisms, Restriction Modification (R-M) or CRISPR-Cas systems. B. In the recipient co-resident plasmid can express exclusion systems similar to the transferred plasmid, inhibiting mating pair formation. Moreover, co-resident plasmid can possess similar replication or partition system which compete with those of the transferred plasmid impeding the maintenance of the newly acquired plasmid. C. Mechansims of fertility inhbition. Inhibition exerced by co-resident plasmid acts on the formation of the pilus, on inhibition of the T4CP function or allows the degradation of the transferred strand (T-strand).

the R388 plasmid (Pérez-Mendoza and de la Cruz 2009). In the same manner, it was shown that pilin protein of the F plasmid do not recognize any recipient factor (Anthony *et al.* 1994).

However, after formation, the mating pair needs to be stabilized, at least during the DNA transfer period. The TraN protein of the F plasmid is a T4SS protein localized in the outer-membrane that interacts with the outer membrane protein OmpA and the LPS of the recipient bacteria. It was shown that this interaction is central for F conjugation (Klimke *et al.* 2005).

In bacteria, the presence of ssDNA can be interpreted as DNA damage intermediate and trigger the induction of the SOS response in bacteria. It was shown to be the case during conjugation, as the entry of the ssDNA plasmid triggers the induction of the SOS response in the recipient cell (Baharoglu, Bikard and Mazel 2010). The ssDNA plasmid interacts with the homologous-pairing RecA protein to form a nucleoprotein filament that activates the auto-proteolysis of the LexA repressor, resulting in the derepression of several genes involved in DNA repair, recombination and mutagenesis (Courcelle *et al.* 2001). The SOS response enables the repair of double stranded DNA breaks (explained in part II.2.4.2), but can also lead to the degradation of the incoming plasmid ssDNA or its unwanted processing as a DNA repair intermediate. Interestingly, it has been shown that some conjugative plasmids carry genes which function is to inhibit the onset of the SOS response. For instance, the PsiB protein (psi for plasmid SOS Interference/Inhibition) whose encoding gene is located in the leading region of the F, R64 and ColIb-P9 plasmids suppresses the SOS response by binding to RecA, thus preventing the auto-proteolysis of LexA and the triggering of the SOS response (Dutreix *et al.* 1988; Sampei *et al.* 2010).

Recipient bacteria also harbour specific genetic systems to protect themselves against foreign DNA, including restriction/modification (RM) systems and adaptive immunity mediated by CRISPR-Cas systems. RM systems are generally based on two enzymes. The restriction endonuclease (RE) that cleaves non-methylated DNA by recognizing 4 or 6 bp sites. The methyltransferase enzymes (MT) that methylates the DNA of the recipient bacteria at defined adenine or cytosine residue, to protect the self-DNA from restriction by the RE (Oliveira, Touchon and Rocha 2014). These systems are thus able to recognize self- from non-self-DNA and eliminate incoming foreign DNA such as conjugative plasmids. Several anti-restriction/modification systems are found on conjugative plasmids as *ard* genes, found for instance in the R64 plasmid leading region (Sampei *et al.* 2010). For instance, *ardA* gene of the ColIb-P9 plasmid encodes a protein which mimic ssDNA to bind Type I RE and block its function (McMahon *et al.* 2009). Another example is the *ardC* gene found on the pSa plasmid which produces a protein binding to the ssDNA to protect it (Belogurov *et al.* 2000). Moreover, it seems that some conjugative plasmids like the broad-host range RP4 select for sequences that do not encompass restriction sites, thus allowing evasion from certain RM systems (Wilkins *et al.* 1996).

CRISPR-Cas systems (discussed in detail in the section II) are also used by bacteria to prevent invasion by both plasmids and phages. They hold the capacity to keep in memory fragments of foreign DNA upon a first invasion. During second invasion, CRISPR-Cas systems use RNA-guided endonucleases to cleave the recognized foreign DNA and impede DNA entry. Examples were found of conjugative plasmids that encode anti-CRISPR-Cas proteins (Acr), thus impeding immunity by several mechanisms: inhibition of DNA binding or cleavage, oligomerization of the nuclease and inhibition of RNA guide binding (Davidson *et al.* 2020; Marino *et al.* 2020).

Plasmid acquisition would also be inhibited into a recipient cell that already carries identical or closely related conjugation plasmids (Figure 2B). Indeed, most conjugation

plasmids encode exclusion (or immunity) systems. The exclusion mechanism (detailed in section III.4.2) has two main functions. First, it inhibits competition between identical plasmids for the same host and ensure stable replication and segregation of the resident plasmid (Garcillán-Barcia and de la Cruz 2008). Second, exclusion also prevent excessive metabolic burden or even the recipient death (termed lethal zygosis) due to repeated rounds of plasmid acquisition (Skurray and Reeves 1974).

I.4.2. Incompatibility

The maintenance of a newly acquired plasmid can be impeded by the presence of another plasmid into the recipient by a mechanism named plasmid incompatibility (Figure 2B). Table 1 summarizes the different incompatibility groups with a representative conjugative plasmid. Two incompatible plasmids are unable to be maintained within the same bacterial cell (Novick and Hoppensteadt 1978). Historically, even non-conjugative plasmids have been classified according their incompatibility groups (Couturier *et al.* 1988). Our current view is that the incompatibility phenomenon is attributable to plasmid interference or competition for the machineries involved in plasmid replication or partition. We then refer to replication-based or partition-based incompatibility mechanisms.

Replication-based incompatibility occurs when two plasmids with isologue origins of replication cannot be maintained stably in a bacterial cell. Competition of the plasmids for the replication machinery triggers the deregulation of the plasmid copy number and the loss of one of the two plasmids over the bacterial cell divisions (Coetzee, Datta and Hedges 1972; Datta and Hedges 1973). Replication-based incompatibility mainly rely on the replication initiator protein Rep and is evaluated by PCR (Carattoli *et al.* 2005; Villa and Carattoli 2020). Moreover, regulation of replication systems (discussed in part III.3.2) can also lead to incompatibility by impeding the replication of a co-resident plasmid resulting in plasmid instability phenotype.

Partition-based incompatibility occurs when two conjugative plasmids encode similar partition systems (detailed in section III.3.3). Indeed, conjugative plasmids are generally maintained at low copy number, most probably to limit the metabolic burden associated with the numerous metabolic functions they encode. Therefore, the stable inheritance of the plasmids during cell division requires active partition systems. Two plasmids encoding the same partition machinery will be randomly associated with the partition machinery, leading the unstable maintenance of one or the other plasmid over cell divisions (Nordström, Molin and Aagaard-Hansen 1980; Austin and Nordström 1990).

Incompatibility between two plasmids should not be mistaken with surface exclusion. For instance, IncA plasmids were demonstrated to be compatible with IncC plasmid (Datta and Hedges 1973; Ambrose, Harmer and Hall 2018). However, it was proven that the presence of the RA1 IncA plasmid in a recipient host impedes the acquisition of R57b IncC plasmid thanks to exclusion systems (Datta and Hedges 1973). The “A-C complex” which encompass the IncA and IncC plasmids was created and then transformed in the literature in the IncA/C incompatibility group (Hedges 1974; Harmer and Hall 2015). It was later found that IncA and IncC plasmids share mechanisms of exclusion that prevent the acquisition of a plasmid by conjugation, but does not mediate incompatibility between these plasmids (Humbert *et al.* 2019).

Noteworthy, plasmid evolution tends to extend the Inc classification, like in the case of IncL/M plasmids family. According to Carattoli and colleagues, IncL/M plasmids probably emerged from strictly incompatible plasmids due to their identical replication machineries and

exclusion entry systems. However, mutations disturbing the regulation of replication meditated by antisense RNA, lead to a first differentiation of these two incompatibility groups, while exclusion entry systems remained the same. Then, acquisition of different exclusion system lead to clearly identifiable compatibility between IncL and IncM plasmids (Carattoli *et al.* 2015).

I.4.3. Fertility Inhibition

Fertility inhibition systems carried by plasmids can specifically inhibit the conjugational transfer of a second plasmid co-resident in the donor cell (Figure 2C). The first identified fertility inhibition system was actually related to the regulation of the transfer (*tra*) genes of the F plasmid. Transfer of the F plasmid is regulated by the product of the *traJ* gene. Indeed, TraJ activates the *tra* genes expression (Willetts 1977). To prevent the constitutive expression of *tra* genes, the *finP* gene encodes an antisense mRNA recognizing and binding to *traJ* mRNA, which hides the ribosome binding site of *traJ* mRNA and impedes its translation (Frost *et al.* 1989; Koraimann *et al.* 1996). Moreover, FinO RNA chaperon serves to stabilize the FinP-*traJ* RNA duplex and allows the protection of FinP RNA degradation by RNAse E (van Biesen and Frost 1992, 1994; Jerome, van Biesen and Frost 1999). The F plasmid naturally carry an insertion of the IS3 insertion sequence into the *finO* gene, leading to decreased levels of FinP RNA and derepressed expression of the *tra* genes (Frost, Ippen-Ihler and Skurray 1994). It is the only IncF plasmid carrying this insertion, thus other F-like plasmids expressing the *finO* gene were found to inhibit the transfer of the F plasmid.

It was also discovered that a plasmid can impede the conjugative transfer of another plasmid if they share the same donor host. This phenomenon named fertility inhibition has been discovered and described for numerous plasmids (Getino and de la Cruz 2018). Plasmids encode specific proteins able to impede a fundamental step in the conjugation mechanism of other conjugative plasmids.

One mechanism of fertility inhibition relies on targeting the mating pair formation. For example, FinU, FinV and FiwB were shown to interfere with the pilus assembly. The ability of the *finU* and *finV* gene products of $IncI_1$ JR66a and IncX R485 plasmids respectively to inhibit pilus assembly of IncF plasmid was demonstrated by phage sensitivity test (Gasson and Willetts 1975). Indeed, several bacteriophages uses pilin as a receptor to infect bacteria and thus bacteria which do not assemble a pilus are resistant to such phages. Using the same principle, it was observed that RP1 plasmid *fiwB* gene product also interfere with pilus assembly of IncW R388 plasmid (Yusoff and Stanisich 1984). It was further demonstrated that FinU is able to impede entry exclusion in addition to its interference with the pilus assembly. Mechanisms of transfer inhibition mediated by *finU*, *finV* and *fiwB* gene products are not fully understood yet.

Some other mechanisms impede the recognition and transfer of the DNA substrate. For instance, *finC*, *pifC*, *fipA* and *osa* products mostly target the T4CP to inhibit transfer of diverse incompatibility plasmids. The FinC protein of CloDF13 ColE plasmid was shown to interfere in the T4CP function of IncF plasmids. Both the PifC and FipA proteins of the F plasmid and pKM101 IncN plasmid, respectively, were shown to inhibit IncP plasmids transfer by acting on their T4CPs (Miller, Lanka and Malamy 1985; Santini and Stanisich 1998). Indeed, PifC and FipA inhibit the transfer of the mobilizable RSF1010 plasmid which uses machineries of IncP plasmids. RSF1010 does not encode its own T4CP, whereas CloDF13 mobilizable plasmid encoding its own T4CP was not impaired in its transferability (Santini and Stanisich 1998). It was observed that the Osa protein found in IncW pSA and R388 plasmids prevents the transfer

Incompatibility group	Host range*	Host organism	Representative plasmid	MOB classification	MPF classification	Reference
	Broad	*Agrobacterium tumefaciens*, Plants, *Saccharomyces cerevisiae, Streptomyces lividans*	Ti	MOB_P/MOB_Q	MPF_T	(Zupan and Zambryski 1995; Bundock and Hooykaas 1996; Kado 1998)
IncF	Narrow	*Enterobacteriaceae* : *Escherichia*, *Salmonella*, *Shigella* Proteus group *Rhizobium lupini*	F	MOB_F	MPF_F	(Datta and Hedges 1972; Heinemann and Sprague 1989; Pansegrau and Lanka 1996)
IncP	Broad	*Enterobacteriaceae*: *Escherichia, Salmonella, Shigella* Proteus group Rhizobia *Agrobacterium Vibrio cholerae, Thiobacillus novellus*	RP4	MOB_P	MPF_T	(Datta and Hedges 1972; Davidson and Summers 1983; Demarre *et al.* 2005)
IncQ	Broad	*E. coli, P. aeruginosa Streptomyces, Actinomyces, Synechococcus*, *Mycobacterium*	RSF1010	MOB_Q	N/A	(Rozwandowicz *et al.* 2018)
IncW	Broad	*E. coli, V. cholerae, Thiobacillus novellus*	R388	MOB_F	MPF_T	(Davidson and Summers 1983; Demarre *et al.* 2005)
IncI	Narrow	*Enterobacteriaceae* : *Escherichia, Salmonella, Shigella*	R64	MOB_P	MPF_I	(Datta and Hedges 1972; Foley *et al.* 2021)
IncH	Broad	*Enterobacteriaceae : Escherichia, Salmonella, Aeromonas slamoniciada, Vibrio anguillarum, Yersinia rucketi*	R27	MOB_H	MPF_F	(Lawley and Taylor 2003; Garcillán-Barcia, Francia and de La Cruz 2009; Shintani, Sanchez and Kimbara 2015; Rozwandowicz *et al.* 2018)
IncL	Broad	*Klebsiella pneumoniae, E. coli, E. cloacae*	pOXA-48a	MOB_P	MPF_I	(Potron, Poirel and Nordmann 2014; Yano *et al.* 2019)
IncM	Broad	*Klebsiella pneumoniae, E. coli, E. cloacae, Citrobacter freundii*	pCTX-M3	MOB_P	MPF_I	(Shintani, Sanchez and Kimbara 2015; Yano *et al.* 2019)
IncA/C	Narrow	*Klebsiella pneumoniae, E. coli, V. cholerae*	pNDM-KN	MOB_H	MPF_F	(Walsh *et al.* 2011; Yano *et al.* 2019)

Table 1 : Representative plasmids, host range and their MOB, MPF and Inc classifications. N/A for non-applicable.
*according to (Rozwandowicz *et al.* 2018).

of the Ti and IncP plasmids (Close and Kado 1991; Chen and Kado 1994). Osa blocks the translocation of virulence factors and DNA of the Ti plasmid by interacting with the T4CP (Chen and Kado 1996; Lee and Gelvin 2004; Cascales *et al.* 2005). In fact, Osa protein exerts ATP-dependent DNAse activity enabling the degradation of the T-stand prior to its transfer (Maindola *et al.* 2014).

Another fertility inhibition mechanism is acting on *tra* gene transcription. Transcriptional fusion assay showed that FinW produced by R455 IncF plasmid reduces the transcription of a relaxosome accessory protein of other IncF plasmids (Gaffney *et al.* 1983). FinQ protein produced by $IncI_1$ R62 plasmid (Willetts and Paranchych 1974; Gasson and Willetts 1975) interferes with the IncF *tra* genes with the Rho-independent transcription termination and induces the termination of the transcription of several *tra* genes, including the T4CP and genes implicated in pilus assembly and extension, mating pair stabilization, exclusion (Gasson and Willetts; Gaffney *et al.* 1983).

Several other plasmids were described to exert fertility inhibition against other co-resident plasmids, however the protein and action mechanisms are not identified yet (Datta *et al.* 1971; Coetzee, Datta and Hedges 1972; Pinney and Smith 1974; Olsen and Shipley 1975). It can be imagined that each step of the conjugation process in the donor strain is a target for fertility inhibition systems. All those fertility inhibition proteins play a role in the plasmid competition for the dissemination within bacterial communities.

I.5. Classification and structure of conjugative plasmids

To perform conjugation and be maintained, plasmids need (i) a T4SS to form the mating pair between the donor and recipient bacteria and a T4CP to connect the processed DNA to the T4SS channel, (ii) an origin of transfer enabling the plasmids processing by the relaxase and (iii) a replication and partition system to be stably inherited along the recipient divisions. Three main types of plasmid classifications have been proposed based on the key features found on conjugative plasmids.

As already mentioned, **a first plasmid classification** is based on replication and partition systems that determine plasmid incompatibility groups (Inc) (Novick and Hoppensteadt 1978; Couturier *et al.* 1988).

The second classification is based on the highly conserved relaxase, which is a key enzyme for the conjugation process, and allows to classify autonomous and mobilizable plasmids into MOB families (Table 1) (Garcillán-Barcia, Francia and de La Cruz 2009). This classification encompasses nine families : MOB_F, MOB_H, MOB_Q, MOB_C, MOB_P, MOB_V, MOB_T, MOB_B and MOB_M (Garcillán-Barcia, Francia and de La Cruz 2009; Garcillán-Barcia *et al.* 2020). Relaxase are classified by homology with representatives of each relaxase family. The large majority of relaxases use a catalytic tyrosine residue to perform the nick and transfer the T-strand. However, the MobM relaxase of the pMV158 plasmid that belongs to the MOB_V family rather uses a histidine residue to perform this step (Pluta *et al.* 2017). Most MOB_F, MOB_P, MOB_Q, MOB_H, MOB_B and MOB_V relaxases belong to the HUH endonuclease superfamily (Chandler *et al.* 2013) with two histidine amino acids of the HUH motif allowing the coordination with the metal ion to perform the cleavage activity (Chandler *et al.* 2013). MOB_C relaxase rather possess a HTH DNA binding domain at their N-terminal and a C-terminal catalytic domain related to PD-(D/E)XK restriction endonuclease and thus need the three Aspartic acid, Glutamic acid and Glutamic acid (DEE) conserved amino acids to coordinate two metal ions (Mg^{2+}) and perform the catalytic activity (Francia *et al.* 2013). MOB_T relaxases possess rep-trans domain present in rolling-circle-replication (RCR) initiator. It was shown that

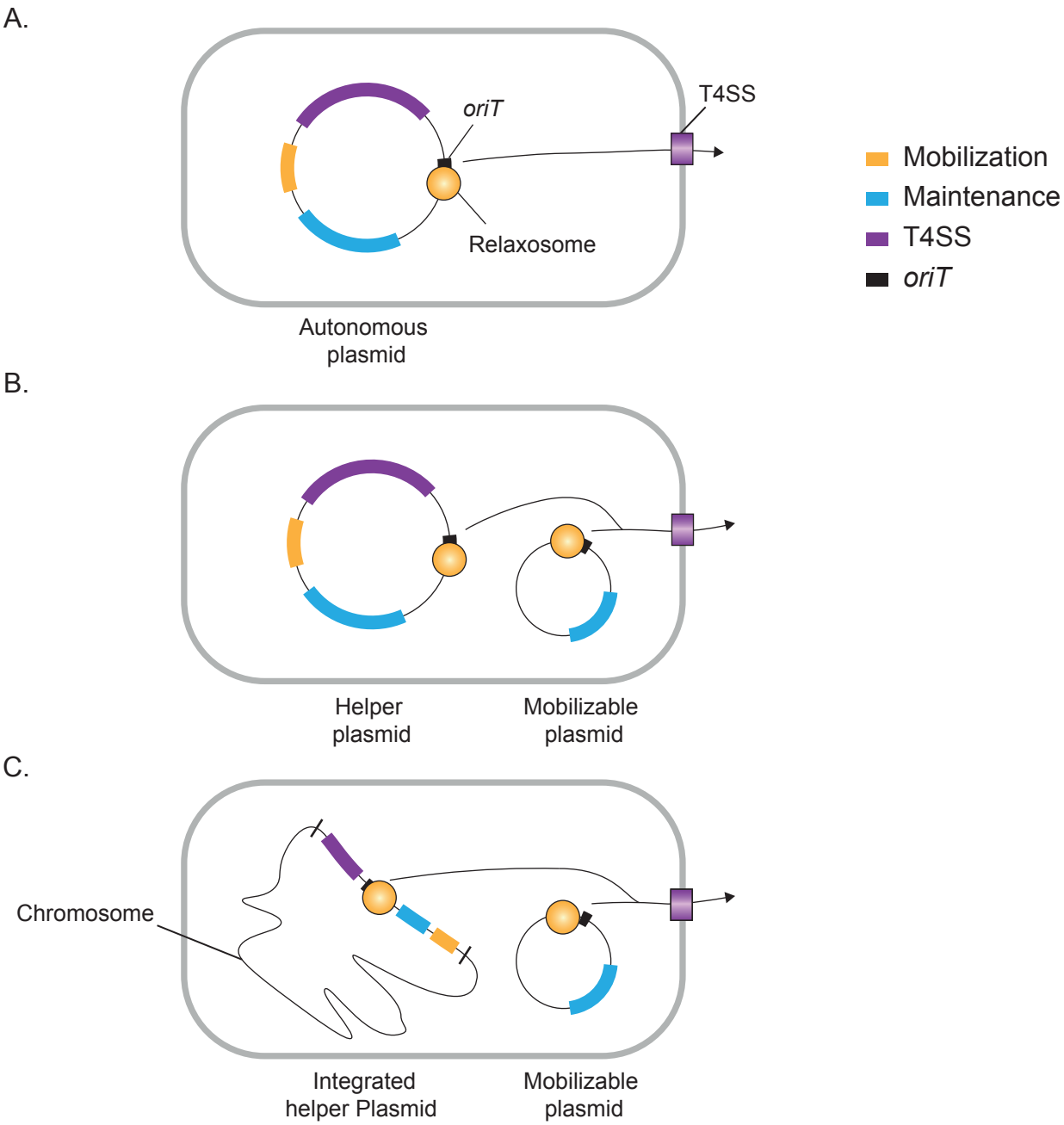

Figure 3 : Definition of three types of plasmids : autonomous, mobilizable and helper. Shematic view of the different organization that can be adopted by conjugative plasmids in the donor strain. Autonomous plasmids (A) encode T4SS, mobilization (relaxosome), maintenance genes and have an *oriT* to be transferred. Mobilizable plasmids (B and C) generally lack T4SS and a part or all the mobilization genes but encode maintenance and have an *oriT*. They are able to be transferred only if another conjugative plasmid encoding for the mobilization machinery is in the donnor cell. This plasmid is thus the Helper plasmid (B), it is generally autonomous or can be integrated into the donor chromosome (C).

relaxases of the Tn*916* and ICE*Bs1,* which are representatives of the MOB_T family, allow replication via the RCR mechanism (Wright, Johnson and Grossman 2015; Wright and Grossman 2016). It was also shown that MOB_V families of relaxase were mostly present on mobilizable plasmid whereas MOB_F and MOB_H are present on autonomous plasmids (Smillie *et al.* 2010).

Finally, **a third classification** of conjugative plasmids was proposed on the basis of categorizing the T4SS of autonomous plasmids into different Mating Pair Formation (MPF) class (Table 1) (Smillie *et al.* 2010). There are four families of MPF, each with a representative T4SS from model conjugative plasmids: MPF_F with F plasmid of *E. coli*, MPF_I with R64 plasmid of *S. enterica*, MPF_T with Ti plasmid of *A. tumefaciens* and MPF_G with ICE*HIN1056* of *Haemophilus influenzae* genome island-like. MPF classification allows to understand which genes are always conserved in T4SS conjugative systems, notably the T4CP granting the recognition and active transport of the relaxase-T-strand complex through the T4SS, and also the major ATPase responsible for the pilus biogenesis. Moreover, this classification allowed to differentiate between the most complex T4SS machineries of the MPF_F and MPF_I plasmids with 30 genes for the T4SS and the MPF_T family with around 12 genes for their T4SS. This can be related to their properties as, for example, T4SS of the MPF_F and MPF_I families are able to mediate conjugation on liquid media whereas MPF_T T4SS are not.

The MOB and MPF classifications are based on the fact that if plasmid maintenance is essential for conjugative plasmids, their conjugative transfer is as essential for their survival in an environmental niche. Moreover, even if conjugation is a relatively conserved phenomenon, it seems that conjugative machineries are diverse and their classification helps defining models to understand the implication of each part in mediating the transfer of DNA. The comparison of the different machineries also allows the tracking of their evolution, which can be related to both their hosts and their ecological niches.

Plasmids are also classified depending on their transfer ability. Plasmids carrying all the genes required for their self-transfer (mobilisation machinery and *oriT*) and maintenance are called “autonomous” plasmids (Figure 3). Autonomous plasmids can adopt two forms: circular or integrated into the bacterial chromosome; which is illustrated in the Figure 3. One example is ICE that relies on integration on the host DNA to be maintained. The F plasmid is also able to integrate into *E. coli* chromosome by homologous recombination using Insertion Sequences. Strains carrying integrated F (named Hfr for high frequency of recombination) can transfer their entire chromosome within 100 minutes, and the F plasmid retains the ability to excise from the chromosome to recover its form as an extra-chromosomal replicon. In contrast, non-autonomous plasmids lacking transfer machinery genes but carrying *oriT* are called mobilizable plasmids (Figure 3B and C). Their mobilization by conjugation require the presence in the donor cell of conjugative plasmid, called “helper”, which provides the conjugative machinery. The helper plasmid can be either autonomous or non-autonomous depending on whether it carries an *oriT*. The mobilizable plasmid generally possesses the maintenance genes (replication and partition). We can note that some mobilizable plasmids carry T4SS genes that do not encode the entire secretion system. For instance CloDF13 mobilizable plasmid was shown to encode for its own T4CP and relaxase (Escudero *et al.* 2003), but lacks the other T4SS genes.

Bacterial DNA conjugation is a mechanism of chief biological importance as it is ubiquitous, highly conversed and has a major impact on the evolution and adaptation of bacterial strains. Especially, the dissemination of metabolic properties such as virulence, resistance to metal and drugs within bacterial communities is often attributable to conjugative

plasmids. In addition to its biological role, conjugation is a highly versatile mechanism as conjugation elements use a variety of strategy to disseminate efficiently. This modularity offers valuable biotechnological tools for the delivery of gene system and the development of innovative antibacterial strategies for instance.

II. Using conjugation to deliver CRISPR systems with strain-specific antibacterial activity

Antibiotic resistance is a global health issue leading to infection treatment failure. Indeed, a recent report estimates that without any response to the antimicrobial resistance threat, by 2050 infections will cause 10 million deaths worldwide (O'Neill 2014).

In this context, it appears critical to develop strategies to fight against drug-resistant bacteria. A major challenge is to develop antibacterial strategies alternative to the use of antibiotics. Indeed, due to the targeting of essential cellular functions, antibiotics lack specificity and affect a broad spectrum of bacteria. As a consequence, antibiotic treatments lead to the disruption of bacteria present in the commensal flora of the patient, called microbiota. As the microbiota is related to human health, its alteration is correlated to several diseases like diabetes or obesity (Fan and Pedersen 2020). In addition, antibiotics selection leads to the accumulation of drug-resistant strains. Various studies reported the emergence of resistance by bystanders microbes following antibiotic treatments (Sjlund *et al.* 2003; Tedijanto *et al.* 2018). Overall, the abusive utilization of antimicrobials in the medical and husbandry fields provoke the emergence and dissemination of antibiotic resistant bacteria (Goossens 2009; Safari Sinegani and Younessi 2017; Wojkowska-Mach *et al.* 2018). For these reasons, it is necessary to develop innovative strategies able to specifically eradicate a targeted pathogen while sparing the host microbiota. In this section, I will review briefly the strategies delivering non-antibiotic antibacterial systems to date, and focus on the CRISPR-Cas systems activities and its delivery methods to exert strain-specific antibacterial activity.

II.1. Use of phages and conjugation to deliver antibacterial compounds

Diverse strategies use bacterial conjugation or phages to exert antibacterial effect by delivering antimicrobial compounds and fight against bacterial infections. The antibacterial systems based on conjugation without CRISPR-Cas systems are listed in the Table 2. In the next paragraphs I will discuss the antimicrobial systems delivered by phages and conjugation that do not exploit the CRISPR-Cas systems.

II.1.1. Phage-delivered antimicrobials

Bacteriophages, also called phages, are viruses infecting exclusively bacteria, hijacking cellular machinery to replicate. They are ubiquitous in the environment and regulate the bacterial population in environmental niches (Hanlon 2007). They are basically constituted of capsid proteins enveloping their genome. Phages can be divided in two categories: virulent phage with a lytic life cycle and temperate phages going through lysogenic life cycle which consists in integration in the bacterial genome as a prophage to be maintained along with bacterial divisions until the host is exposed to environmental stress. The temperate phage will then extract its genome from the bacterial chromosome and replicate as lytic phages.

Phage host-range is dictated by the interaction of the phage-binding proteins and the bacterial receptor involved in the adsorption step which is very specific for each phage. Notably, phage-binding proteins interact with one specific receptor located on the bacterial cell wall like teichoic acids, peptidoglycan for gram-positive bacteria or LPS and proteins of the outer membrane for gram-negative bacteria. Moreover, they can bind to external bacterial structures such as pili, flagella and capsules as the phages M13 and λ that use respectively the F pilin TraA and LamB outer membrane protein involved in maltose uptake as a receptor to infect bacteria (Randall-Hazelbauer and Schwartz 1973; Rasched and Oberer 1986).

Sometimes phages require interaction with two specific bacterial receptors to achieve adsorption (Bertozzi Silva, Storms and Sauvageau 2016).

As phages are strictly infecting bacterial cells with a narrow host range, it was proposed to use bacteriophages to fight bacterial infections but the discovery of penicillin by Fleming and the subsequent antibiotic era slowed down the research on this field (Fleming 1929). However, eastern Europe and especially Georgia continued the development of phage therapy, in the Eliava Institute (Kutter *et al.* 2010). Interestingly, in Georgia, phages are intended for the prophylactic and treatment purposes. Notably two phage cocktails which were developed in 1930's are still in use: *intestiphage* to treat gastrointestinal disorders like the traveller's diarrhea and *pyophage* to treat purulent infection. Generally, phages used to treat bacterial infections are virulent phages. Indeed, these phages only perform a lytic infection, leading to bacterial death whereas temperate phages can integrate and stay in the bacterial genome during a long time without harming the bacteria. Moreover, the extraction of the prophage to pursue the temperate life cycle has been shown to increase the risk of HGT between bacteria (Harrison and Brockhurst 2017), which is a major concern as it could lead to resistance determinants dissemination.

In the USA, it is only in 2006 that FDA approved the use of LISTEX P100 in food packaging as Generally Recognized as Safe (GRAS) to prevent *Listeria* colonization. This opened the food packaging industry to phage additives (USFDA 2006). Still, today no phage treatment has been approved for the use in human in the USA or the EU (João *et al.* 2021).

The limitations in the bacterial host-range lead to the utilization of phage cocktails and engineered phages. Indeed, *intestiphage* and *pyophage* mentioned above are phage cocktails which are, by law, evaluated every 6 months against current pathogenic bacterial strains and are upgraded if necessary (Kutter *et al.* 2010). Several reviews report different ways to obtain genetically modified phages to eradicate a bacterial infection (Łobocka, Dąbrowska and Górski 2021). The genetic engineering of phages can be realized to obtain new properties, for example to transform temperate phages into virulent, to increase the host-range or to modify the pharmaco-kinetic properties of phages. Sometimes phages properties are linked, as for ϕEf11 phage in which the suppression of the lysogenic genes lead to an extended host-range (Zhang *et al.* 2013). Engineering of phages could also be performed to target virulence properties of bacteria like the ability to form biofilm. Dispersin B (DspB) is an enzyme enabling the hydrolysis of β-1,6-N-acetyl-D-glucosamine, an adhesin crucial for biofilm formation in *E. coli* and *Staphylococcus* (Itoh *et al.* 2005). DspB-producing T7 phage were engineered and used to infect *E. coli* biofilm. Infection of *E. coli* cells with this phage allowed the production of DspB and its releasing in the media after the lysis of the infected cells. Hydrolysis activity of DspB lead to the destruction of the biofilm due to the degradation of the N-acetyl-D-glucosamine. This engineered phage successfully disrupted the biofilm, compared to the wild-type T7 phage (Lu and Collins 2007). Biofilm lifestyle is controlled at the community level through quorum sensing. Thus, it was also thought to disrupt this signalling pathway to prevent biofilm formation. The *aiiA* gene encodes a lactonase degrading acyl homoserine lactones which are quorum sensing autoinducers produced by *E. coli* and *P. aeruginosa* to control biofilm formation (Wang *et al.* 2004). These autoinducers are secreted in the media and bacteria detect the accumulation of autoinducers. When autoinducers concentration attains a threshold, bacteria regulate their gene expression, leading to different community behaviours, notably biofilm lifestyle (Waters and Bassler 2005). As *dspB*, *aiiA* gene was incorporated in the genome of the T7 phage to block biofilm formation of *P. aeruginosa* and *E. coli.* Induction of AiiA production in infected bacteria and then its release following the lyse

Delivery method	Death mechanism	Construct	Strain targeted	Pros	Cons	Reference
RP4 conjugation machinery	Over replication	Mobilizable plasmid with RP4 *oriT* and mutated replication *pir* gene enabling for hyper replicative phenotype. Donor is protected by a wt version of the *pir* gene on its chromosome.	*E. coli* O157:H7, *Serratia marcescens*, *Enterobacter nimipressuralis*, *Salmonella enterica* and *Erwinia carotovora*	Broad host range	non-specific of the targeted strain	(Peng, Rakowski, and Filutowicz 2006)
RP4 conjugation machinery	Colicin E3	Autonomous plasmid containing the *colE3* gene. Donor is protected by the immunity protein Im3	*Acinetobacter baumannii*	Broad host range	non-specific of the targeted strain	(Shankar et al. 2007)
pOX38 conjugation machinery	Colicin E7	Mobilizable plasmid with pOX38 *oriT* and *colE7* gene. Donor is protected by colE7 immunity gene.	*E. coli* K12 and Uropathogenic *E. coli* (UPEC) DL82		Narrow host-range, non-specific of the targeted strain	(Starčič Erjavec et al. 2015)
RP4 conjugation machinery	overexpressed protein aggregator lipophilic (OpaL)	Mobilizable plasmid with RP4 oriT and *opaL* gene under the T7 promoter. Donor protected by the absence of T7 RNA polymerase.	*E.coli* BL21	Broad host range, specific of the targeted strain thanks to the promoter used	Low modularity	(Collins et al. 2019)
RP4 conjugation machinery	Gyrase poison CcdB split by intein	Mobilizable plasmid with *ccdB* gene split by an intein under P_{BAD} and P_{ompU} promoters. Donor is protected by the intein construction and the absence of the ToxRS system regulating P_{ompU}.	Pathogenic *V. cholerae* (containing ToxRS system)	Broad host range, specific of the targeted strain thanks to the promoter used	Low modularity	(López-Igual et al. 2019)

Table 2 : List of non-antibiotic microbial delivered by conjugation

of the infected bacteria impaired the biofilm formation in *E. coli* and *P. aeruginosa* (Pei and Lamas-Samanamud 2014).

All the strategies mentioned above employ engineered phages to produce proteins with antimicrobial activity against a broad bacterial spectrum but do not allow specific targeting of a bacterial specie. To overcome this, engineered phages that produce CRISPR-Cas system were developed to exert antimicrobial activity in a species specific manner to target specific pathogen or antibiotic resistance determinants. These strategies are listed in Table 3 and the CRISPR-Cas systems detailed in section II.3.

II.1.2. Conjugation-delivered antimicrobials

Conjugation is a mechanism enabling bacteria to transfer genes encoding diverse metabolic pathways that enable bacterial adaptation in diverse environments. It is then possible to exploit this machinery against the bacterium itself. Studies using the conjugation as vehicle to transfer antimicrobial systems are reported in Table 2. Two main strategies have been developed : (i) using the replicative properties of the transferred plasmid or (ii) transferring a toxin-producing plasmid to kill the recipient bacteria.

First, it was proposed to use the replicative properties of the plasmid to kill the recipient bacteria. Indeed, it was shown that plasmid over replication is deleterious for the bacterial host (Haugan *et al.* 1995). In this context, an hyper-replicative plasmid was transferred by conjugation to kill the recipient cells (Peng, Rakowski and Filutowicz 2006). The transferred plasmid contains the γ origin of replication (γ*ori*) of the R6K plasmid which replication depends on the π protein, product of the *pir* gene. Double mutation or deletion of the F107 and P106 amino acids of the π protein lead to an increased copy number of plasmids. Mobilizable plasmid encompassing γ*ori*, mutated *pir* gene and RP4 origin of transfer was constructed and introduced into a donor strain encoding the wild-type (wt) π protein and the RP4 plasmid conjugative machinery. Once the mobilizable plasmid is transferred into a recipient strain lacking the wt π protein, only the mutated π protein from the plasmid is produced leading to an increase of the copy number that becomes deleterious for the bacteria and leads to its death. This method was used with success to kill the different pathogens *E. coli* O157:H7, *Serratia marcescens*, *Enterobacter nimipressuralis*, *S. enterica* and *Erwinia carotovora*.

Second strategies consists in the transfer of plasmids encoding toxins. Two studies used plasmids designed to encode colicins E3 and E7 (ColE3 and ColE7 respectively) (Shankar *et al.* 2007; Starčič Erjavec *et al.* 2015). ColE3 cleaves conserved regions of the 16S ribosomal RNA while ColE7 cleaves DNA non-specifically (Cascales *et al.* 2007). Those two colicins are thus able to kill a broad host range of bacteria. In this regard, to protect the donor strain of the bactericidal effect of the colicins, immunity genes were cloned in their genome. This way, only recipient bacteria that do not produce immunity proteins are killed by the colicin. The plasmid producing ColE7 was mobilized by the pOX38 machinery to kill laboratory *E. coli* strain K12 and uropathogenic *E. coli* strain DL82 *in vitro*. pOX38 is the larger fragment of the F plasmid after digestion with HindIII restriction enzyme (Guyer *et al.* 1981). It encompasses all the *tra* genes necessary for the conjugative machinery production and the replication and partition genes. The RP4 conjugative machinery was used as helper to mobilize the plasmid producing ColE3 and kill *A. baumannii* pathogen, in a sepsis burn mouse model. Both strategies were successfully applied and allowed to kill recipient bacteria. However, the three methods described above tend to indiscriminately kill recipient bacteria and do not allow the specific targeting of a bacterial pathogen.

While protection of the donor from the colicin activity implies the presence of immunity protein, the toxicity of the system in the donor can also be avoided by controlling the expression of the antibacterial system (Collins *et al.* 2019; López-Igual *et al.* 2019). An antibacterial strategy based on the CcdB toxin was used to specifically produce this toxin in virulent *V. cholerae* strains and kill them (López-Igual *et al.* 2019). CcdB is a toxin from the toxin-antitoxin (TA) system of *Vibrio fischeri* which inhibits the essential DNA gyrase by binding to its GyrA subunit (De Jonge *et al.* 2012; Guérout *et al.* 2013). The F plasmid also harbors a similar TA system evoked in the III.3.4 section. A mobilizable plasmid carrying *ccdB* gene split in two parts and the RP4 *oriT* was constructed to be transferred with the RP4 conjugative machinery encoded on the chromosome of the donor strain. To protect the donor strain and non-targeted recipient strain, C-terminal and N-terminal parts of the CcdB were used as exteins and each fused with a fragment of a split-intein. Inteins are proteins known for their role in the splicing post-transcriptional process. Typically, they are found in polypeptides which are composed of two exteins flanking the intein. During splicing, the intein will auto-catalyse its excision from the polypeptide and the ligation of the two flanking exteins to form the fully functional protein composed of the two exteins (Topilina and Mills 2014). Split-inteins have the same ability but are split in two polypeptides, each containing an extein. Both CcdB-intein fusions are under the control of two promoters. One under the P_{BAD} promoter inducible with arabinose in both donor and recipient bacteria. The second under the *ompU* promoter which is regulated by the *toxRS* operon found only in pathogenic *V. cholerae* (Crawford, Kaper and DiRita 1998). The CcdB is then entirely produced and reconstituted only in virulent *V. cholerae* strains, protecting the donor and non-targeted recipient from the antibacterial effect of the toxin (López-Igual *et al.* 2019).

Another study used an engineered toxin to specifically kill *E. coli* which expression is controlled by the T7 promoter (Collins *et al.* 2019). This toxin named OpaL (for overexpressed protein aggregator lipophilic) is a polypeptide designed to be highly hydrophobic and form intracellular aggregates lethal for bacteria. The antibacterial system relies on mobilizable plasmid carrying *opaL* under the T7 promoter and the RP4 *oriT* that is recognized by the RP4 helper plasmid machinery present in the donor. The T7 promoter is only activated in strains producing the T7 RNA polymerase generally induced with IPTG (Tabor and Richardson 1985; Studier and Moffatt 1986). Donor strain does not produce the T7 RNA polymerase and is then protected while the targeted strain carries it and undergoes OpaL aggregation phenotype that kill them (Collins *et al.* 2019).

Transferring plasmids which encode toxins under the control of specific promoters allowing expression only in the targeted recipient strain is a good strategy to protect the donor strain and other non-targeted recipients. However, some promoters can have leaky expression which could lead to the death of the bacteria if the toxin is produced. This was observed in the case of the T7 promoter (Collins *et al.* 2019). The double control of the toxin production using the split intein allows a better protection of the donor and non-targeted recipient (López-Igual *et al.* 2019). In these studies, the antibacterial activity is mediated by a toxin produced thanks to a promoter specific of the targeted bacterial strain. It is thus required to study the bacterial strain to know that this promoter is present only in the targeted strain. Moreover, it is not excluded that the chosen promoter could be expressed in a non-targeted bacteria. It is also possible to specifically target a bacterial strain using the CRISPR-Cas systems as it only requires to know the genome of the targeted bacteria. In the next paragraph, I will explain how CRISPR-Cas systems work, especially the Class II Type 2 of *S. pyogenes* and explain how it mediates antibacterial activity.

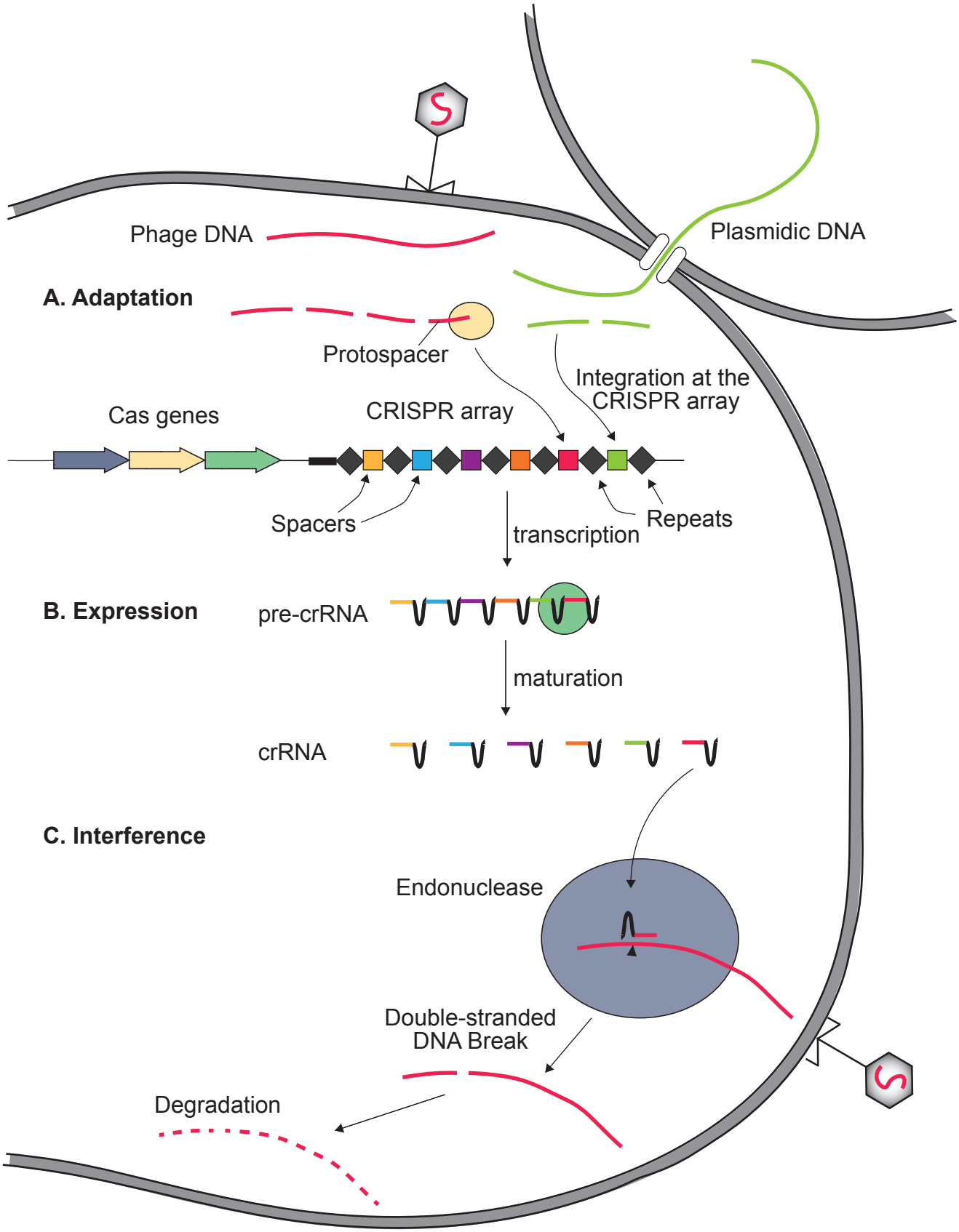

Figure 4 : General mechanism of CRISPR-Cas mediated adaptive immunity in bacteria or archaea.Cas genes encode the Adaptation (yellow), Expression (green) and Interference (violet) complexes. A. The adaptation machinery (yellow) cleaves foreign DNA in the bacteria (here phage DNA), liberating protospacers and inserting them as spacers in the CRISPR array to record past invaders. B. Expression of the CRISPR array produces a pre-CRISPR RNA (pre-crRNA) which is then matured in crRNAs by the expression complex (green). C. Following the injection of recognized foreign DNA, crRNA indentifies its complementary sequence and allows the recruitment of the Interference machinery (violet) to induce a double- stranded break. This allows the degradation of the foreign DNA and prevents phage infection in this example. Adapted from 2017 Jiang and Doudna.

II.2. CRISPR-Cas systems

II.2.1. History of CRISPR-Cas systems

The discovery of CRISPR-Cas started with the report of DNA repeats in *E. coli* genome in 1987 by Ishino *et al.* and their description in 1989 by Nakata *et al.* which compared them to similar repeats present in genomes of *S. enterica* serovar Typhimurium and *Shigella dysenteriae* (Ishino *et al.* 1987; Nakata, Amemura and Makino 1989). These regions were also identified in the genome of archaea (Mojica, Juez and Rodriguez-Valera 1993). Their function remained unknown but these repeats draw attention because they seemed ubiquitous in prokaryotes. Indeed, they were found in approximately 42% and 85% of bacteria and archaea genomes respectively (Makarova *et al.* 2020). In 2002, Jansen *et al.* named these repeats Clustered Regularly Interspaced Short Palindromic Repeats (CRISPR) and reported the existence of CRISPR associated (Cas) genes (Jansen *et al.* 2002). Spacer sequence separating the repeats were related to sequences found in bacteriophages and conjugative plasmids. All those discoveries lead to the identification of the adaptive immunity function of CRISPR-Cas systems towards invading DNA in bacteria. Moreover, due to the existence of chromosome-targeting spacers it was suggested that CRISPR-Cas systems could have various other functions in bacterial physiology related to interspecies competition, DNA repair, gene regulation, programmed cell death or biofilm formation (Faure, Makarova and Koonin 2019; Gong *et al.* 2020). Yet, the mechanism involving CRISPR-Cas systems in these biological processes is still not clear.

II.2.2. CRISPR-Cas systems: general mechanism

CRISPR-Cas role in the adaptive bacterial immunity has been well described and consists in three essential steps: adaptation, expression and interference (Figure 4) (Westra *et al.* 2012). First, when infected by foreign DNA from bacteriophages or conjugative plasmids, a complex of Cas proteins named the adaptive machinery binds and cleaves the foreign DNA. The DNA sections liberated are the protospacers, which compose the spacers once integrated into the CRISPR array between two repeat sequences. The specificity of the CRISPR-Cas systems is based on the spacers composing the CRISPR array which keep the memory of former invading DNA. Next, during the expression step, the CRISPR array is expressed as a long RNA transcript, the pre-CRISPR RNA (pre-crRNA) and then processed into mature CRISPR RNA (crRNA), each encompassing a spacer motif and a repeat able to recruit directly or not the Cas nuclease (Charpentier *et al.* 2015). Finally, the interference step occurs by the recognition of the foreign DNA by the spacer within the crRNA. This leads to the cleavage of the foreign DNA by the Cas nuclease thus eradicating the DNA invasion.

Several studies showed that CRISPR-Cas systems are able to reduce the MGE acquisition in bacterial species (O'Meara and Nunney 2019; Westra and Levin 2020). Notably, it would limit the acquisition of plasmids through conjugative process (Marraffini and Sontheimer 2008; Wheatley and MacLean 2021). As previously mentioned, it was shown that plasmids and MGE in general can carry anti-CRISPR genes (*acr*) (Davidson *et al.* 2020; Marino *et al.* 2020; Pinilla-Redondo *et al.* 2020b). These genes were shown to interfere with the interference step of the CRISPR-Cas machinery. Notably, it was shown that these proteins impede the binding of the nuclease to the targeted DNA or the nuclease activity (Marino *et al.* 2020).

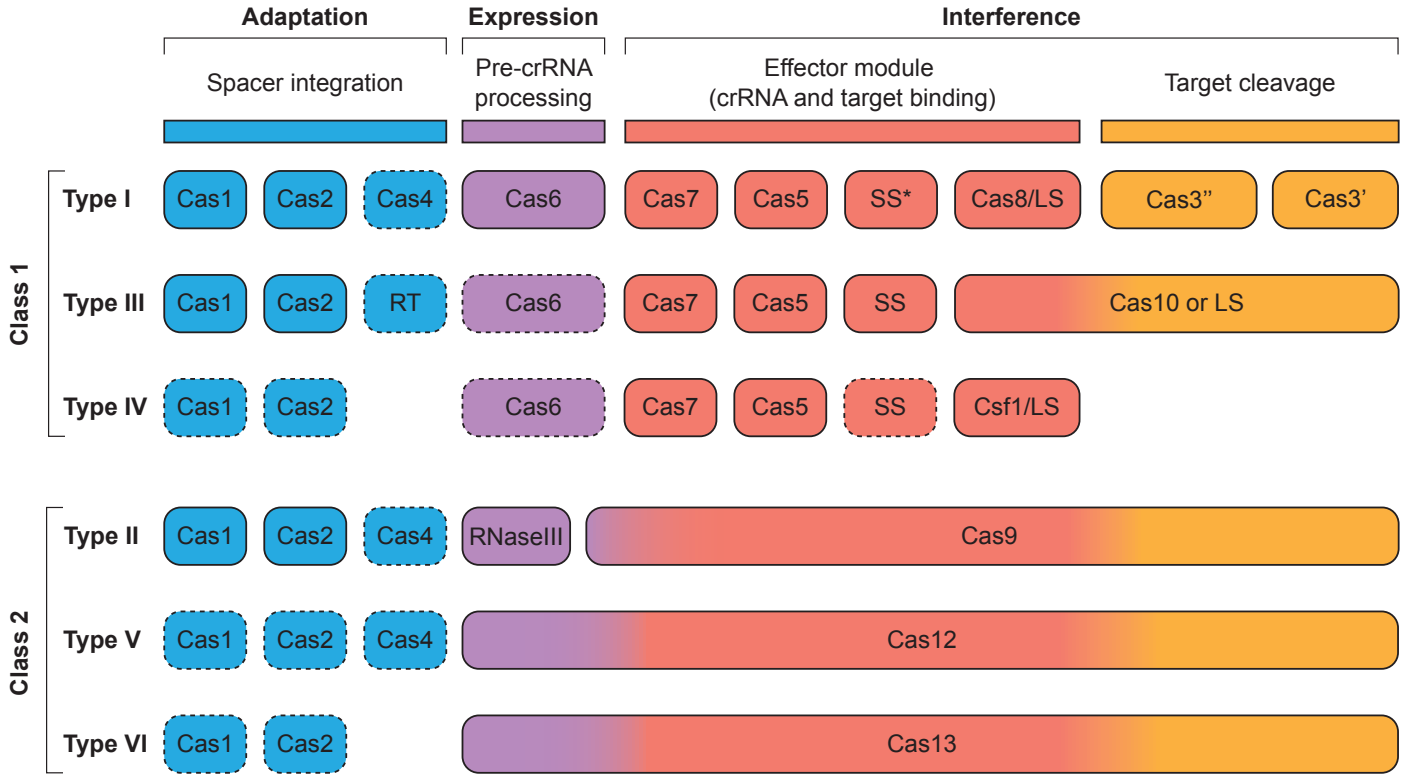

Figure 5 : Classification of the CRISPR-Cas systems.
Schematic view of the functional modules of the different CRISPR-Cas systems. Proteins are distributed depending on their role in the CRISPR-Cas mediated immunity. Proteins with dashed outlines represent absent or dispensible proteins in certain CRISPR-Cas subtypes. In most Type III systems the Cas6 protein is provided in trans by other CRISPR-Cas system. Asterix indicates that the small subunit (SS) can be fused to the large subtunit (LS) in certain Type I systems. Adapted from Makarova *et al.* 2020.

II.2.3. Classification of the CRISPR-Cas systems

CRISPR-Cas systems are diverse and do not share any ubiquitous genes. They have been classified in two main classes which are further divided into 6 types and 33 subtypes (Makarova et al. 2020, Figure 5).

Cas proteins can be classified based on their function in 3 modules: adaptation, expression and interference. The adaptation module encompasses the most conserved genes among CRISPR-Cas systems. The interference module is the most variable and the basis for the main classification. In Class 1 systems (type I, III and IV), the interference module consists of a multi-protein complex whereas class 2 systems (type II, V and VI) use a large multidomain protein to perform crRNA processing, binding, target recognition and interference. Types of CRISPR-Cas systems are based on the comparison of the gene composition and their conservation whereas subtypes rather rely on the locus structure.

CRISPR-Cas systems are mostly found on the chromosome but sometimes are present on MGE (Pinilla-Redondo *et al.* 2021). Indeed, it was found a Type I-B and I-F CRISPR-Cas system on the Tn*7* transposon (Peters *et al.* 2017). These transposons lack transposase element but use the CRISPR-Cas machinery to their advantage and repurposed it to act as a transposase and direct the transposition event. They encompass a CRISPR array targeting several plasmids which could be used to direct transposition.

In addition, the large majority of Type IV CRISPR-Cas systems are found on MGE, notably plasmids and typically lack the adaptation and target cleavage module (Makarova et al. 2020). For instance, IncFIB and IncH1B plasmids were shown to encode Type IV-A3 CRISPR-Cas systems (Newire *et al.* 2020). As reported in Table 1, these plasmids have narrow host range and found in *Enterobacteriaceae* bacteria. The adaptation and inhibition activity is thought to be mediated by the CRISPR-Cas systems found in their host, particularly the Type I systems that might explain that the presence of Type IV is correlated with Type I-E and I-F host-encoded CRISPR-Cas systems (Pinilla-Redondo *et al.* 2020a). Type IV CRISPR-Cas systems have been suggested to act in plasmid competition for the host, for instance the Type IV-A3 was shown to contain 25.5% of spacers targeting plasmids, which are more than spacers targeting phages (9%) (Newire *et al.* 2020). Interestingly, spacers targeting *traN* and *traL* genes of the IncFII conjugative machinery have been found and might prevent the conjugation and/or maintenance of the targeted IncFII plasmid. If a recipient strain harbors a conjugative plasmid carrying the Type IV-A3 and endogenous Type I CRISPR-Cas systems, conjugation and or stable maintenance of an IncFII plasmid will be impeded by the interference proteins of the Type I directed by the crRNA of the Type IV-A3 CRISPR-Cas system.

The effector module of Class 2 CRISPR-Cas systems consists only of a large multidomain protein and has been therefore suited for biotechnological application. Among them, the Type II-A CRISPR-Cas interference module system of *S. pyogenes* is the best studied and well described. Since I used this system during my thesis, I described it in more detail in the following section.

II.2.4. Class 2 Type II system of *Streptococcus pyogenes*

II.2.4.1. Mechanism of interference: natural and biotechnological aspect

As shown in figure 6, the *S. pyogenes* type II-A CRISPR-Cas system is composed of four genes, a trans-activating CRISPR RNA (tracrRNA) and the CRISPR array. Cas1, Cas2 and Csn2 proteins are involved in the adaptation process whereas the multidomain protein Cas9 in complex with tracrRNA and crRNA are sufficient to exert the interference process.

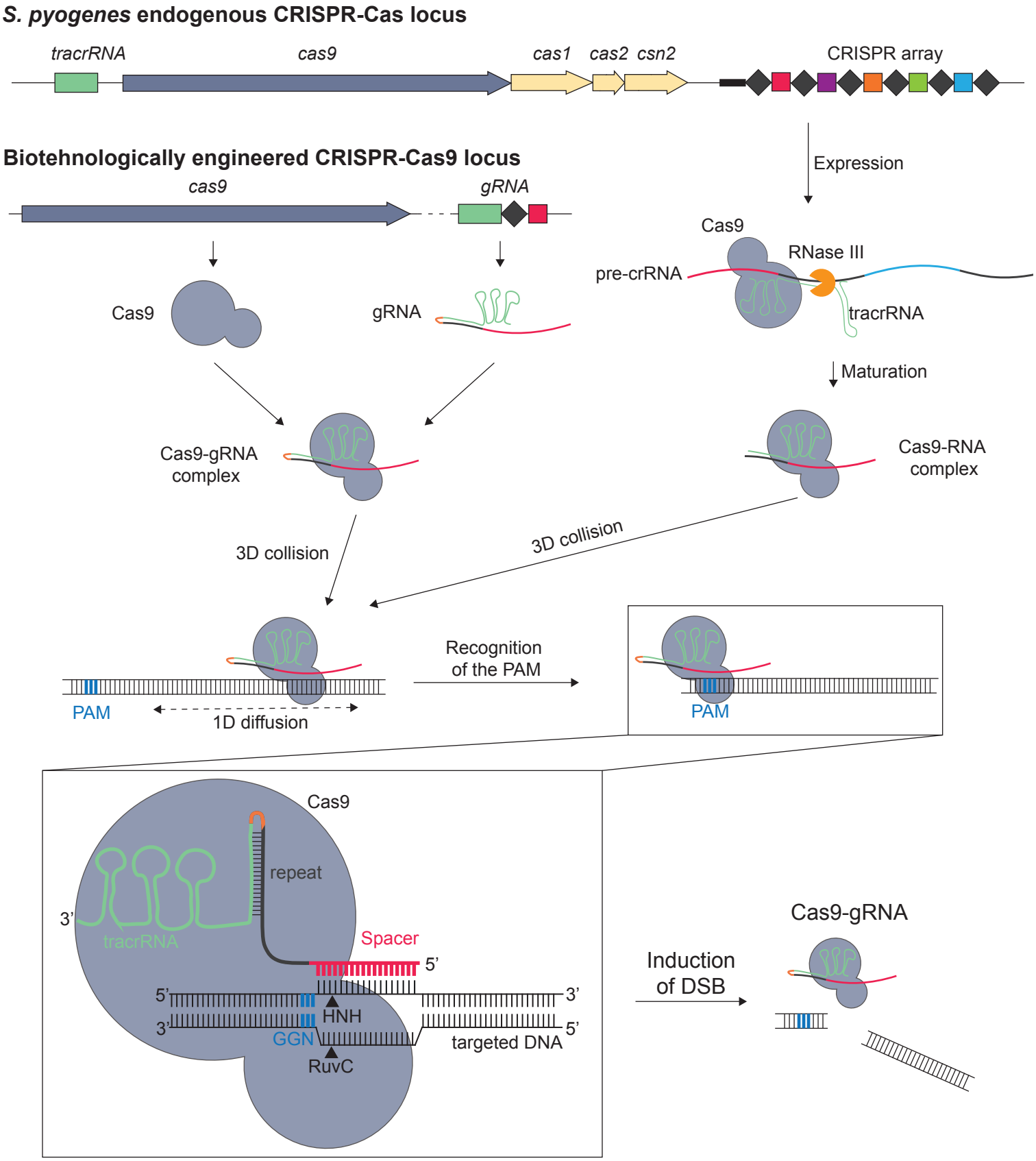

Figure 6 : Interference by Type II CRISPR-Cas system of *S. pyogenes* or engineered CRISPR-Cas system. During the expression phase, the pre-crRNA binds to the tracrRNA-Cas9 complex. The RNAse III binds and cleaves the pre-crRNA to form the crRNA-tracrRNA-Cas9 (or RNA-Cas9) complex. In the biotechnologically engineered system, the gRNA connects the tracrRNA and crRNA sequence by a loop depicted in orange. It does not need to be processed and assembles with the Cas9 directly. The RNA-Cas9 complex uses 3D collision to find DNA and 1D diffusion to recognize PAM sequences (5-NGG-3'). After the recognition of the PAM, the spacer allows the specific regognition of the targeted sequence and the HNH and RuvC domains of the Cas9 induce cleavage of both strands creating a DSB.

Once the CRISPR arrays is expressed as a pre-crRNA, it undergoes a maturation through the action of three main actors: the tracrRNA, the endoribonuclease RNase III and the Cas9 protein (Deltcheva *et al.* 2011). The tracrRNA is composed of two main parts: anti-repeats complementary to the repeats of the CRISPR array allowing binding to the pre-crRNA and three stem loop structures (Nishimasu *et al.* 2014). The first stem loop allows the formation of a complex with the Cas9 while the two others are required for the stabilization of this complex (Jinek *et al.* 2012; Nishimasu *et al.* 2014).

Evidence revealed that the pre-crRNA and tracrRNA are co-processed by the endoribonuclease RNase III to form a processed tracrRNA-crRNA duplex (Deltcheva *et al.* 2011). Indeed, *in vitro* incubation of both tracrRNA and pre-crRNA paired or alone with RNase III demonstrated that only paired tracrRNA and pre-crRNA were cleaved by the RNase III (Deltcheva *et al.* 2011). Then, this processed tracrRNA-crRNA duplex will require further maturation by additional unknown RNAse (Hille *et al.* 2018; Le Rhun *et al.* 2019). Furthermore, one by one deletion of each *cas* genes revealed that only the *cas9* gene (previously known as *csn1*) is essential to perform pre-crRNA maturation (Deltcheva *et al.* 2011).

The last actor, Cas9 protein, is composed of three different domains: (i) the REC lobe needed for interaction with the crRNA-tracrRNA duplex, (ii) the NUC lobe needed for the introduction of DSB and (iii) the C-terminal domain implicated in the recognition of a proto-spacer acquisition motif (PAM) sequence. The NUC and C-terminal domains will be evoked in more details in the following paragraphs. The REC lobe of the Cas9 encompasses three helical domains (REC1, REC2 and REC3) which interact with the tracrRNA-crRNA duplex able to recognize the targeted DNA. The proposed model suggests that Cas9 stabilizes the interaction between tracrRNA and crRNA, probably through its interaction with the stem loops formed by the tracrRNA. After the completion of the maturation process, mature tracrRNA-crRNA complex stays bound to the Cas9 to search for the DNA target (Deltcheva *et al.* 2011; Jinek *et al.* 2012).

A CRISPR-Cas system producing only crRNA, tracrRNA and Cas9 is active and can perform RNA-guided cleavage into a targeted DNA sequence. Biotechnological improvement engineered a gRNA consisting of the tracrRNA fused to the crRNA to avoid the maturation step and make the system even more convenient (Figure 6) (Jinek *et al.* 2012). The gRNA is directly recognized by the Cas9 through the three stem loops formed by the tracrRNA part (Jinek *et al.* 2012; Nishimasu *et al.* 2014). This allows the CRISPR-Cas9 system to be even more convenient for biotechnological applications as only two actors will be required to perform the interference step: the Cas9 and the gRNA. In the next paragraphs, the complex formed by the Cas9 with the tracrRNA-crRNA duplex or the gRNA will be called the “Cas9-RNA” complex.

The first step towards the target cleavage is its finding. To do so, the Cas9 protein uses its C-terminal domain to first identify PAM sequences in the foreign or targeted DNA. The PAM sequence is a 5’-NGG-3’ motif for *S. pyogenes* (Mojica *et al.* 2009) and is recognized during the adaptation phase to select spacers by the Cas9 in complex with the trans-activating CRISPR RNA (tracrRNA) (Heler *et al.* 2015). Indeed, PAM recognition is essential for the Cas9 to perform its nuclease activity, thus functional spacers are those flanking a PAM sequence. The Cas9-RNA complex use 3D collision and 1D diffusion to search for its cognate PAM. A model suggest that 3D collision allows Cas9-RNA binding to DNA whereas rapid and local 1D diffusion allows the recognition of the PAM by the Cas9 (Sternberg *et al.* 2014; Globyte *et al.* 2019). PAM recognition is a prerequisite for the interference activity even before the target recognition via the spacer (Sternberg *et al.* 2014). Structural studies of the Cas9 established that two arginine residues, the Arg1333 and Arg1335, perform specific hydrogen-binding

interactions with the two Gs of the 5'-NGG-3' PAM (Anders *et al.* 2014). PAM recognition by the Cas9 occurs on the non-targeted strand and single-protein fluorescence microscopy revealed that this step is quickly performed in *E. coli* (< to 30ms) (Jinek *et al.* 2012; Jones *et al.* 2017).

After PAM recognition, DNA melts to allow binding between the spacer and the targeted DNA. Binding originates at the PAM and continues along with sequential base pairing of the spacer with the targeted sequence, forming a R-loop (Sternberg *et al.* 2014). The minimum length of the spacer sequence required for efficient cleavage is 13 nt (Jinek *et al.* 2012) and the spacer sequence flanking the PAM is crucial for the recognition of the targeted DNA. Indeed, this sequence is named seed sequence and no mismatches between this seed and the targeted sequence are tolerated for the actual cleavage by Cas9. Point mutations introduced in the PAM-proximal 7 nt of the spacer sequence abolish the cleavage activity of the Cas9, thus these nucleotides are considered to constitute the seed sequence (Jinek *et al.* 2012). Moreover, the study of the Type I-E CRISPR-Cas system of *E. coli* revealed a similar seed sequence comprised into the 8 nt PAM-proximal sequence, showing that it is not restricted to the Type II (Semenova *et al.* 2011).

After the recognition of the targeted sequence by the Cas9-RNA complex, the Cas9 introduces double-strand breaks (DSB). The NUC lobe contains a HNH and three RuvC-like domains essential for the Cas9 activation and induction of DSB on foreign DNA. Cas9 mutants of HNH and RuvC catalytic domains demonstrated that each domain introduce a nick on a different DNA strand (Jinek *et al.* 2012). Radiolabelled dsDNA assays revealed that HNH domain cleaves the targeted strand whereas RuvC the non-targeted strand (Jinek *et al.* 2012). RuvC cleavage of the non-targeted DNA is allosterically controlled by HNH conformational state, meaning that RuvC cleavage of the non-targeted strand is always synchronized to HNH cleavage of the targeted strand (Sternberg *et al.* 2015). Moreover, the position of the non-targeted strand is essential for both the position of RuvC and HNH domains and to induce the transition between inactive and active Cas9 state (Jiang *et al.* 2016; Palermo *et al.* 2016). The synergy in the activation of the HNH and RuvC domains introduce a blunt end DSB.

II.2.4.2. How do Cas9-mediated double-strand breaks kill bacteria ?

Cas9-mediated DSB generate blunt DNA ends that are lethal to some bacteria but not others based on their ability to repair DSB (Bikard *et al.* 2012; Tong *et al.* 2015). To repair DSB, most bacteria use homologous recombination (HR) which consists in using homologous template DNA to correctly replicate cleaved DNA. Some bacteria use another DNA repair mechanism termed Non-Homologous End Joining (NHEJ). I will develop the reasons why HR is not efficient to repair DSB introduced by Cas9 into the bacterial genome whereas NHEJ is.

To explain the inability of HR to repair Cas9-induced DSB, I will first describe briefly the HR mechanism for any DSB. The RecBCD complex is recruited to process and degrade the DNA ends (Smith 2012). RecBCD ensure nuclease and helicase activity to unwind DNA ends and degrade them until it encounters a Chi hotspot recombination site of cleavage (Ponticelli *et al.* 1985). The Chi site modify the activity of RecBCD (Dixon and Kowalczykowski 1993; Singleton *et al.* 2004) that stop degrading both strands and will only degrade one strand generating formation of a ssDNA end (Dixon and Kowalczykowski 1993). The homologous-pairing RecA protein is then recruited to the ssDNA with the stimulation of RecBCD (Anderson and Kowalczykowski 1997; Spies and Kowalczykowski 2006). RecA binding to the ssDNA induces the auto-proteolysis of the SOS response LexA repressor, triggering the expression of many genes involved in HR and other mechanisms. RecA's role on the ssDNA is to search for

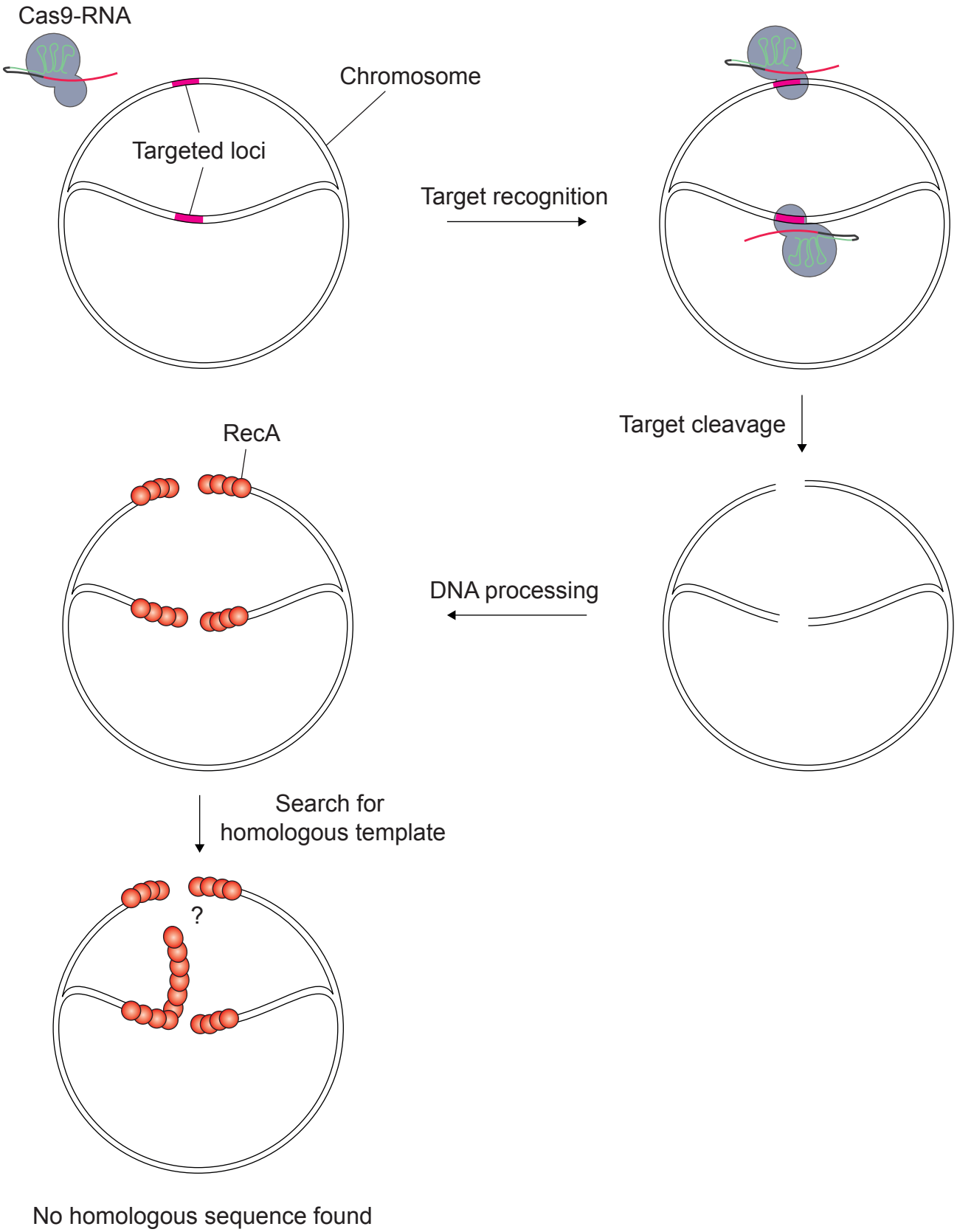

Figure 7 : Homologous recombination cannot repair Cas9-mediated double stranded breaks.
Schematic representing a model of the induction of double stranded break by the Cas9-RNA machinery into both sister chromatides of a chromosome undergoing replication. Both sequences are cleaved and processed by the HR repair machinery to be repaired. When RecA assembles in bundles to search for homologous sequence present on the sister chromatide, it is not found because it was cleaved by the Cas9-RNA complex.

homologous sequence, generally found on sister chromosome, by forming RecA bundles (Lesterlin *et al.* 2014). A displacement (D)-loop is then formed by the invasion of ssDNA-RecA complex into the homologous template. Synthesis of the DNA is realized using the homologous sequence as a template. After replication, RuvABC machinery allows the resolution of the replication intermediates to reconstitute each chromosome (Sharples *et al.* 1990; Takahagi *et al.* 1991; Wyatt and West 2014).

HR mechanism needs homologous template to repair DNA. During CRISPR-Cas9 interference, many Cas9-RNA complexes are produced, leading to the recognition and cleavage of all the targeted sequences (Figure 7). In this context, DSB introduced by RNA-guided Cas9 in a bacterial genome target all homologous sequences. Thus, no intact homologous sequence can serve as a template to repair the DSB induced by Cas9. This is why Cas9-mediated DSB are lethal, both sister chromatids are cleaved by Cas9-RNA complexes, leading to an absence of template DNA to mediate HR repair (Cui and Bikard 2016).

A study performed in *E. coli* evaluated the killing efficiency of the Cas9-mediated DSB on the chromosome (Cui and Bikard 2016). It was observed that Cas9-mediated DSB do not result in the same killing activity, depending on the targeted locus. Utilisation of *recA* mutant strain, which is unable to perform HR-mediated DNA repair, showed that Cas9 was able to introduce DSB in all targeted loci and all killing activity differences were abolished. Thus, the killing activity was shown to depend on the balance between the capacity of Cas9-RNA complexes to cleave all chromosomic loci and the capacity of the HR pathway to repair the damage. DSB caused by Cas9 induce bacterial SOS response (Cui and Bikard 2016) which enhances mutation rates through expression of error-prone *umuDC* polymerase (Smith and Walker 1998). These mechanisms favour the acquisition of mutations that can arise in the targeted sequence, in the PAM region or in the CRISPR-Cas9 genes. This can lead to the emergence of escape mutants that are no longer sensible to Cas9-mediated DSB due to mutations rendering the targeted sequence unrecognizable or damage in the CRISPR-Cas9 system. To avoid repair with the HR mechanism, it was shown that the introduction of Gam protein into the targeted bacteria can be a solution. Gam protein is able to bind linear DNA ends to protect it against nuclease activity (Akroyd and Symonds 1986). Its introduction in a bacteria suffering from Cas9-mediated DSB enhanced the killing efficiency due to inaccessibility of the DNA ends for the repair machinery (Cui and Bikard 2016).

Another system described in *E. coli* as Alternative-End Joining (A-EJ) could also allow bacteria to survive Cas9-mediated DSB. This system implies the same actors as homologous recombination, notably RecBCD exonuclease that degrade DNA ends. However, the joining of the DNA ends is thought to be mediated by the Ligase A using microhomology (Chayot *et al.* 2010). The use of microhomologies can lead to the insertion of errors into the repaired sequence which could make the targeted sequence unrecognizable for the Cas9-RNA complex. A-EJ has a low repair frequency of 0.35 to 3.9 $x10^{-5}$ (Chayot *et al.* 2010) which does not seem efficient enough to rescue bacteria in case of Cas9-mediated DSB. In comparison, the NHEJ mechanism was shown to have 1% efficiency to repair blunt ends DSB (Aniukwu, Glickman and Shuman 2008).

Bacteria resistant to Cas9-mediated DSB use the NHEJ mechanism to repair DNA (Figure 8). NHEJ is a two component repair pathway implying LigD and Ku proteins. Ku protein is a ligand protein forming a homodimer able to bind DNA end generated by a DSB to protect them from degradation. It recruits to the DNA break the LigD protein, an ATP-dependent DNA ligase sometimes fused with a polymerase domain or a nuclease domain. Once recruited, LigD processes the DNA and then ligates them thanks to its polymerase and/or nuclease and ligase

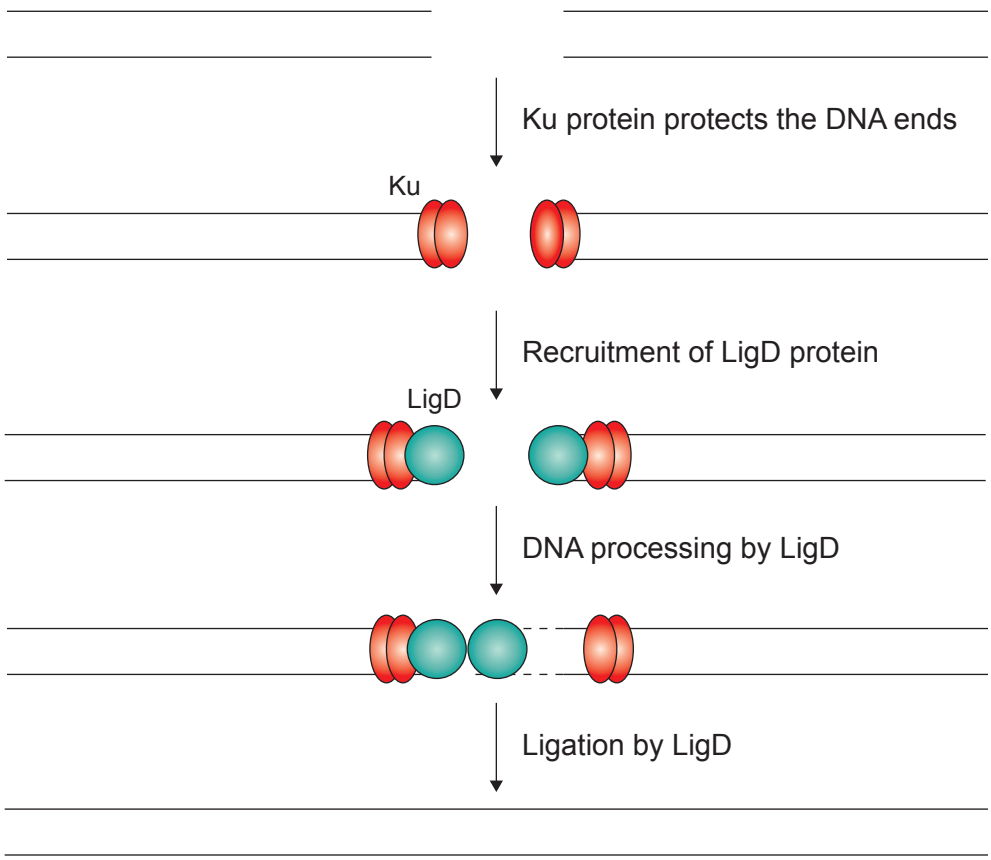

Figure 8 : Non-Homologous End Joining (NHEJ) repair mechanism.
When a DSB occurs on the DNA, the Ku protein is recruited to the DNA ends and protects them from degradation. This allows the recruitment of the LigD ligase to the DNA ends. LigD performs DNA processing and the ligation of the two DNA ends. After the LigD-mediated ligation, the DSB is repaired.

domain respectively (Weller 2002). Bacteria generally lack this repair mechanism, except for *Bacillus subtilis*, *Mycobacterium tuberculosis*, *Streptomyces ambofaciens, Sinorhizobium meliloti, Streptomyces coelicor* or *Clostridium cellulolyticum* (Bertrand *et al.* 2019). However, it has been observed that although *Clostridium cellulolyticum* harbours a NHEJ repair pathway, it is sensitive to Cas9-induced DSBs, probably due to the weak expression of the repair pathway (Xu *et al.* 2015). To verify the ability of the NHEJ system to repair Cas9-mediated DSB in *E. coli*, *ku* and *ligD* genes of *Mycobacterium tuberculosis* were introduced in a *recB* mutant strain, unable to use the HR repair pathway. No rescue of *E. coli* was observed after induction of the Cas9-mediated DSB. *M. tuberculosis* NHEJ system alone is then unable to rescue *E. coli*, suggesting the NHEJ system is not efficient enough to compete with Cas9-mediated DSB (Cui and Bikard 2016).

II.2.4.3. CRISPR interference with dCas9

The Cas9 is composed of the NUC lobe which encompass RuvC and HNH domains, each introducing a nick into the targeted DNA, producing a blunt end DSB. A catalytically inactive Cas9 called dead Cas9 (dCas9) has been engineered (Jinek *et al.* 2012). Single point mutations on RuvC and HNH domains (D10A and H840A respectively) allowed the complete inhibition of the cleavage activity of the dCas9 product (Jinek *et al.* 2012). dCas9 complexed to gRNA still recognizes and binds the target but does not cleave the DNA. Due to the impossibility of the dCas9 to perform DSB, the dCas9-RNA complex stays bound to the targeted sequence. If the complex targets a promoter region or an open reading frame, it can block the transcription machinery due to steric hindrance caused by the dCas9 binding and thus inhibits the gene transcription. Such mechanism relies on CRISPR interference or CRISPRi (Bikard *et al.* 2013; Qi *et al.* 2013). A study was conducted on *E. coli* MG1655 to explicit the rules for using this technique (Cui *et al.* 2018). First, targeted strand and localization of the targeted locus have an importance. Equal gene repression levels were observed by targeting any strand in the promoter region. However, targeting the coding strand in open reading frames was always the most efficient to silence gene expression. These results are in accordance with previous results obtained in *E. coli*, *S. pneumoniae* and *M. smegmatis* (Bikard *et al.* 2013; Qi *et al.* 2013; Choudhary *et al.* 2015). Targeting operon structures showed that genes downstream of the targeted sequence were repressed whereas genes upstream were not necessarily impacted by CRISPRi (Cui *et al.* 2018).

Such technology can be used to kill bacteria by inhibiting essential gene expression. Moreover, in order to fight against antibiotic resistance or bacterial infection, CRISPRi targeting resistance determinants or virulence genes can be imagined. However, to be able to use this technology it is crucial to know the limits of RNA-guided dCas9 gene silencing.

II.2.4.4. Limits of Cas9/dCas9

Type II CRISPR-Cas system is an excellent biotechnological tool to specifically kill bacteria or impede gene expression. However, it also has its limits. Notably, it was observed that the Cas9/dCas9 can introduce DSB or bind at non-targeted sites in the DNA, which is referred as off-target activity. As pairing with all the targeted sequence is not necessary for the cleavage (Jinek *et al.* 2012), it is possible that sequences similar to that targeted sequence are cleaved by error. For the dCas9, off-target activity was observed with a perfect match between the 6 to 15 nt proximal to the PAM. In particular, definition of the PAM-proximal 9 nt as the seed sequence was found to be the best indicator to predict off-target activity *in silico* (Cui *et al.* 2018). Moreover, it was revealed that dCas9 can have a toxic effect in *E. coli* related to specific

5 nt seed sequences in the spacer (Cui *et al.* 2018). This effect is called the "bad-seed" effect. To avoid the bad-seed effect, it is possible to decrease dCas9 expression resulting in a reduced concentration of dCas9 in the bacterial cell. This effect was observed in *E. coli* and it remains to be determined whether this is also the case for other bacterial species.

Off-targeting of CRISPR-Cas system prevents this system to be specific. Thus it is crucial to avoid the off-target to keep the specificity of the system. It was showed that expression of the dCas9 can be finely tuned to avoid bad-seed effect and to a lesser extent off-targeting while conserving the CRISPRi activity (Cui *et al.* 2018). In the case of DSB introduction, it was also proposed to decrease the Cas9 production to avoid off-target activity with the CRISPR-Cas9 system (Hsu *et al.* 2013).

In order to prevent off-targeting, high fidelity Cas9 were engineered (Kleinstiver *et al.* 2016; Chen *et al.* 2017; Hu *et al.* 2018; Vakulskas *et al.* 2018; Guo *et al.* 2019). To induce the DSB, its was shown that the conversion of the Cas9 from inactive to active state during the cleavage was also mediated by the positioning of the non-targeted DNA strand into the REC lobe of the Cas9 (Jiang *et al.* 2016; Palermo *et al.* 2016). The Cas9 possesses the REC lobe responsible for the binding with tracrRNA-crRNA duplex (or gRNA) composed of three domains REC1, REC2 and REC3. Structure of Cas9-gRNA complex with targeted DNA revealed that the REC lobe interacts with the repeat-anti-repeat sequences of the gRNA to form the Cas9-RNA duplex (Nishimasu *et al.* 2014). It was suggested that part of the REC lobe interacts with the gRNA-DNA heteroduplex during the DNA target recognition and notably that REC3 domain stabilize the targeted DNA distant from the PAM region (Jiang *et al.* 2016). Further studies showed that REC3 domain binding to the RNA-DNA heteroduplex triggers a conformational change in REC2 domain which allows the docking of HNH to the cleavage site (Chen *et al.* 2017). Thus, interaction of the REC3 domain with the RNA-DNA heteroduplex converts inactive Cas9 into cleavage active Cas9. Studies showed that this conformational change rendering the Cas9 active is possible even before the recognition of all the spacer, allowing off-target cleavage. Mutations in the REC3 domain were shown to impact the recognition and binding of the REC3 domain to the RNA-DNA duplex. Thus, it impacts the conversion between active and inactive state of the Cas9 when distal PAM mismatches are present on the spacer (Chen *et al.* 2017; Vakulskas *et al.* 2018). Engineering of the Cas9 HF1 (for High Fidelity) and Cas9 HiFi (for High Fidelity) were realized with the introduction of mutations in the REC3 domain which leads to decreased off-target activity (Kleinstiver *et al.* 2016; Vakulskas *et al.* 2018).

Other change was applied to the Cas9 protein to vary the PAM recognition sequence and make it more permissive in order not to be limited in the targeting (Hu *et al.* 2018). Indeed, to recognize the targeted sequence, Cas9 first needs to detect its cognate PAM. Spacers thus have to flank a 5'-NGG-3' sequence which limits the choice of spacers in a given genome. The idea is to engineer Cas9 which have more permissive PAM recognition, for example the xCas9 3.7 (xCas9 for expanded PAM Cas9) can recognize the divergent 5'-NG-3', 5'-GAA-3' and 5'-GAT-3' PAMs (Hu *et al.* 2018) which could extent the library of spacers that can be used and broaden the applications of this tool. As PAM is the key verification made by the Cas9 before the spacer recognition, it was hypothesized that permissive PAM would lead to increased off-target activities. However, such an increase in off-targeting was not observed, highlighting the need of more studies to detail the role of Cas9 domains in PAM, target recognitions and transition of the inactive to active state conversion of the cleavage (Guo *et al.* 2019).

Delivery method	Death mechanism	Construct	Strain targeted	Targeted gene	Gene function	Pros	Cons	Reference
Transfection	*S. pyogenes* Type II CRISPR-cas	nanocomplex of Cas9 conjugated with branched polyethylenimine polymer	Methicillin resistant *S. aureus* (MRSA)	*mecA*	methicillin resistance	Broad host range, delivery efficiency of 40%	high escape mutant frequency	(Kang et al. 2017)
RP4 conjugation machinery compared with phagemid (M13 phage)	*S. pyogenes* Type II CRISPR-cas	tracrRNA + CRISPR array + Cas9 into a mobilizable plasmid or in phagemid construction carrying f1 origin to be encapsidated by M13 phages	*E. coli*	bla_{SHV-18} and bla_{NDM-1}, *gyrAD87G*	β-lactam resistance, gyrase gene allowing resistance to quinolones	Conjugation : broad host range, Phage : high delivery efficiency	Conjugation : low delivery efficiency, Phage : Narrow host range	(Citorik, Mimee, and Lu 2014)
RP4 conjugation machinery	*S. pyogenes* Type II CRISPR-cas with dCas9	gRNA + dCas9 into a mobilizable plasmid	*E. coli*	*mRFP*	reporter gene	Broad host range	Low delivery efficiency, Cas9 under inducible promoter	(Ji et al. 2014)
RP4 conjugation machinery	*S. pyogenes* Type II CRISPR-cas	gRNA + Cas9 into a mobilizable plasmid then transformed in an autonomous plasmid	*E. coli*	*mcr-1*	collistine resistance	Broad host range	Low delivery efficiency, low modularity	(Dong et al. 2019)
RP4 conjugation machinery	*S. pyogenes* Type II CRISPR-cas modified with TevSpCas9	tracrRNA + CRISPR array + TevSpCas9 into a mobilizable plasmid then transformed in an autonomous plasmid	*S. enterica*	65 genes	38 essential, 23 non-essential genes and 4 with unresolved phenotypes	Broad host range, delivery efficiency high (with beads)	Low modularity	(Hamilton et al. 2019)
RP4 conjugation machinery	*S. pyogenes* Type II CRISPR-cas	tracrRNA + CRISPR array + Cas9 into a mobilizable plasmid	*E. coli*	*blaTEM-52b*, *blaCTX-M-14*	Extended-spectrum β-lactamase (ESBL), β-lactam resistance	Broad host range	Low delivery efficiency	(Ruotsalainen et al. 2019)
pPD1 plasmid of *E. faecalis* conjugative machinery	*E. faecalis* Type II CRISPR-cas	tracrRNA + CRISPR array + Cas9 into an autonomous plasmid	*E. faecalis*	*tetM erm*	tetracycline resistance, erythromycin resistance	High delivery efficiency, In vivo experimentation with eradication of the pathogenic strain	Narrow host range, Low modularity	(Rodrigues et al. 2019)

Table 3 : List of non-antibiotic microbial delivered by conjugation or phage (Part 1)

Utilization of CRISPR-Cas based tools to fight bacterial infection or antibiotic resistance is a promising option allowing a lot of possibilities. There is now a need to develop an adapted delivery system.

II.3. CRISPR-Cas systems used as antimicrobials

CRISPR-Cas systems have been used to fight bacterial infections or to prevent antibiotic resistance. Studies of different CRISPR-Cas antibacterial engineered systems are reported in Table 3. The majority of the CRISPR-Cas-based antimicrobial tools have been developed using the Type II-A CRISPR-Cas system of *S. pyogenes* (Bikard *et al.* 2014; Citorik, Mimee and Lu 2014; Ji *et al.* 2014; Kang *et al.* 2017; Park *et al.* 2017; Ram *et al.* 2018; Hamilton *et al.* 2019; Ruotsalainen *et al.* 2019). Two studies used type I CRISPR-Cas systems of *E. coli* and *Clostridium difficile* (Yosef *et al.* 2015) and one the type VI system of *Leptotrichia shahii* (Kiga *et al.* 2020).

Type I and type VI CRISPR-Cas systems differ from the Type II-A of *S. pyogenes*. For instance, it was shown that Type I Cas3 nuclease carries helicase activity allowing the degradation of the targeted DNA and preventing the repair by HR (Newsom *et al.* 2021). After recognition of the targeted sequence, Cas3 induces a cleavage and continues to degrade the targeted DNA thanks to its helicase activity. Contrary to Cas9 and Cas3 nucleases, Cas13 degrades RNA. Indeed, upon recognition by the Cas13-RNA complex, foreign single stranded RNA is cleaved by the Cas13 which in turn also degrades non-targeted RNA either produced by the invader or the host bacterial cell (Garcia-Doval and Jinek 2017). Degradation of the bacterial transcripts leads to dormancy of bacteria (Meeske, Nakandakari-Higa and Marraffini 2019). In nature, this is thought to prevent the release of the invader and spreading to proximal cells (Garcia-Doval and Jinek 2017). The Type VI CRISPR/Cas13 of *L. shahii* was used to target drug resistance determinants in *E. coli* and *S. aureus* (Kiga *et al.* 2020). Using the type VI system with the activity of Cas13 allows killing of bacteria carrying resistant determinants on plasmids (Kiga *et al.* 2020) while the Cas9 will only eliminates the plasmid without killing the bacteria. However it is not really known if targeted bacteria were effectively killed or put in dormancy state. No escape mutant was observed using this system, probably signifying the death of targeted bacteria (Kiga *et al.* 2020).

II.3.1. Delivery methods of antimicrobial CRISPR systems

Efficient delivery efficiency is also a major challenge of CRISPR-based antimicrobials. Different delivery methods were listed in the Table 3. One study proposed to bind a nanocomplex of Cas9-RNA to a branched polyethylenimine polymer and transfect it to kill *Staphylococcus aureus* (Kang *et al.* 2017). Host range of this delivery system is not discussed by the authors however it seems plausible that it could have a broad host range (at least towards gram-positive bacteria which have the same wall composition than *S. aureus*). Apart from this paper, the majority of studies focus on the use of conjugation or phages to ensure the delivery of CRISPR-Cas systems.

Phage delivery is very efficient (Bikard *et al.* 2014; Citorik, Mimee and Lu 2014; Yosef *et al.* 2015; Park *et al.* 2017; Ram *et al.* 2018; Kiga *et al.* 2020; Selle *et al.* 2020). Indeed, phage/bacterial cell ratio also called Multiplicity of Infection (MOI) can be adjusted to ensure satisfying CRISPR-Cas delivery. The MOI is monitored to use the most efficient targeting without being detrimental for the bacteria. MOI rarely falls under 20 and it is readjusted for *in vivo* delivery in several studies. The only study using MOI under 20 proposes a system with a replicating phage allowing multiplication of the antimicrobial as it kills targeted bacteria (Selle *et al.* 2020).

Delivery method	Death mechanism	Construct	Strain targeted	Targeted gene	Gene function	Pros	Cons	Reference
Phagemid (SaPI capsid)	*S. pyogenes* Type II CRISPR-cas with Cas9 and dCas9	tracrRNA + CRISPR array + Cas9/dCas9 into SaPI2 deleted of toxin and small capsid genes	*S. aureus* and *L. monocytogenes*	*agrA*, *agrP2P3 hly*	virulence regulator conserved in *S. aureus*, listeriolysin O in *L. monocytogenes*	High delivery efficiency, In vivo experimentation with eradication of the pathogenic strain	Narrow host range	(Ram et al. 2018)
Phagemid (Φ-NM1 capsid)	*S. pyogenes* Type II CRISPR-cas	tracrRNA + CRISPR array + Cas9 into phagemid encapsidated by Φ-NM1	*S. aureus*	*aph-3* *mecA* *sek* pUSA02 pUSA01	Kanamycin resistance, methicillin resistance, superantigen enterotoxin gene, tetracycline resistance (pUSA02) , no resistance (pUSA01)	High delivery efficiency, In vivo experimentation with eradication of the pathogenic strain	Narrow host range	(Bikard et al. 2014)
Phage (Φ-SaBov)	*S. pyogenes* Type II CRISPR-cas	tracrRNA + CRISPR array + Cas9 into the non-coding sequence of Φ-SaBov	*S. aureus*	nuc esxA	conserved in all *S. aureus*, thermostable nuclease, virulence factor implied in host immunity escaping	High delivery efficiency	Narrow host range	(Park et al. 2017)
λ prophage	*E. coli* Type I-E CRISPR-cas	CRISPR cascade genes + Cas3 + CRISPR array into a λ integrative prophage + utilisation of T7 engineered phage containing sequences targeted by spacers to eliminate escape mutants	*E. coli*	*ndm-1* *ctx-M-15*	carbapenem resistance	High delivery efficiency, eradication of escape mutants with T7 phage	Narrow host range	(Yosef et al. 2015)
Phage (Φ-CD24-2)	*C. difficile* Type I-B CRISPR-cas (endogenous)	CRISPR array compatible with Type I-B *C. difficile* CRISPR-cas endogenous system into the Φ-CD24-2 phage genome to enhance its antibacterial activity. CRISPR-cas interference machinery is provided in trans by the genome of *C. difficile*	*C. difficile*	*rnY*	Ribonuclease Y	High delivery efficiency, combination of phage and CRISPR-mediated antibacterial activity, in vivo experimentation with eradication of the pathogenic strain	Narrow host range, the targeted pathogen must have endogenous CRISPR-cas systems.	(Selle et al. 2020)
Phagemid PICI for *E. coli* and SaPI for *S. aureus*	*L. shahii* Type VI CRISPR-cas	Cas13 ad CRISPR array with f1 origin to be encapsidated by M13 phage for delivery in *E. coli* or with into SaPI2 deleted of toxin and small capsid genes for delivery in *S. aureus*	*E. coli* and *S. aureus*	bla_{IMP-1}, bla_{OXA-48}, bla_{VIM-2}, bla_{NDM-1}, bla_{KPC-2} ; *mcr-1*, *mcr-2* ; *mecA*	carbapenem resistance, colistine resistance, methicillin resistance	High delivery efficiency	Narrow host range	(Kiga et al. 2020)

Table 3 : List of non-antibiotic microbial delivered by conjugation or phage (Part 2)

Conjugation-based delivery has also been monitored in term of ratio of donor versus recipient strain and early studies have shown that recipient cannot bear a too high donor over recipient ratio. This is why most of the studies use a 1:1 donor over recipient ratio (Ji *et al.* 2014; Dong *et al.* 2019; Rodrigues *et al.* 2019; Ruotsalainen *et al.* 2019). Only one study uses a 10:1 donor over recipient ratio, allowing an increase in the conjugation efficiency (Hamilton *et al.* 2019). Conjugation-based tools are generally elaborated with two types of plasmids : a helper plasmid which encodes the conjugation machinery and a mobilizable "CRISPR" plasmid which produces the CRISPR-Cas system. Indeed, the conjugation machinery carried by the helper plasmid is composed of a large set of genes, resulting in a large DNA plasmid (>30kb) which complicates molecular biology engineering. The "CRISPR" plasmid, on the contrary, is conceived to be short and easily editable by molecular biology approaches to adapt the conjugation-CRISPR method to target a large variety of applications like pathogen killing or resistance gene targeting (Citorik, Mimee and Lu 2014; Ji *et al.* 2014; Dong *et al.* 2019; Hamilton *et al.* 2019). All Studies use broad-host range conjugation machineries of the RP4 plasmid in order to reach a large panel of bacterial species (Citorik, Mimee, and Lu 2014; Ji et al. 2014; Dong et al. 2019; Hamilton et al. 2019).

Targeting gram-positive bacteria with conjugation requires gram-positive conjugation machinery. The conjugative pheromone responsive pPD1 plasmid of *Enterococcus faecalis* was used as a vector to target *E. faecalis ermB* and *tetM* genes conferring resistance to erythromycin and tetracycline respectively. Although this system lacks modularity and broad host range, it achieves satisfying conjugation efficiencies *in vitro*. Moreover, *in vivo* experiments demonstrate possibility of this construct to re-sensitize *E. faecalis* in a mouse model (Rodrigues *et al.* 2019).

II.3.2. Limits of the antimicrobial CRISPR systems

Delivering CRISPR-Cas systems to fight bacterial infection have been proven to be a good option to specifically kill a bacterial specie among a population. However, some limitations still arose from those studies. First, phage delivery have narrow host range which limits their utilisation to only one bacterial population. Second, broad host-range conjugative plasmids have limited delivery efficiency which restricts the effect of the CRISPR-Cas antimicrobial. Third, escape mutants have been shown to emerge from CRISPR-Cas based antimicrobials. Finally, the identification of specific spacers among multispecies community to achieve antimicrobial activity is not an easy task. I will discuss all those limitations in the following parts.

II.3.2.1. Narrow host-range (phage)

Phage host-range is dictated by the interaction of the phage binding proteins and the bacterial receptor involved in the adsorption step which is very specific for each phage. As previously mentioned, adsorption of the phage is linked to a very specific interaction with a bacterial receptor. Phages are chosen depending on the targeted bacteria to ensure their adsorption. This makes the antimicrobial hardly adaptable to other bacterial pathogens.

It is possible to choose phage capsids that are able to infect diverse bacterial species. For instance, Pathogenic Islands of *S. aureus* (SaPI) are genetic element encompassing toxic super-antigen producing genes that can be excised from the chromosome and encapsidated with the help of bacteriophage 80α or ϕ-NM1 (Lindsay *et al.* 1998). These genetic elements interfere with the phage replication, are encapsidated in phage-produced virions and released in the media after cell lysis to confer virulence factors to adjacent cells (Ruzin, Lindsay and

Novick 2001; Tallent *et al.* 2007). It was shown that these SaPI were able to be efficiently transferred to *Listeria monocytogenes* (Chen and Novick 2009) probably because of similar wall teichoic acids that are the receptor for 80α phage (Winstel *et al.* 2013). This capacity was used to transfer CRISPR-Cas systems encapsidated as SaPI particles to target resistance determinant and virulence genes in *S. aureus* and *L. monocytogenes* (Ram *et al.* 2018).

A recent study took example on eukaryote antibodies to extend T3 phage host range (Yehl *et al.* 2019). Indeed, antibodies are composed of a constant structural domain and a variable domain which is able to recognize the antigen. The idea is to build a T3 phage with a constant capsid structure and variable tail to recognize divergent receptors on the surface of bacteria and generate the larger host range possible. Four host-range determining region (HRDR) were found in the T3 tail fibre gene. A library was created with plasmids encompassing random HRDR regions while keeping the structure of the T3 phage capsid intact to create mutated "phagebodies" (for bacteriophage and antibodies) (Yehl *et al.* 2019). Phagebodies infecting a broad host range of *E. coli* cells and even infecting *Yersinia tuberculosis* were recovered. This strategy is a first step in the engineering of broad host range phage and could be applied to other phages to extend their host range.

II.3.2.2. Low transfer efficiency (conjugation)

Conjugation with the RP4 machinery is associated with low delivery efficiencies making difficult to see an efficient effect of the delivered CRISPR system on the total targeted population (Citorik, Mimee and Lu 2014; Ji *et al.* 2014; Dong *et al.* 2019). Most studies use non-mobilizable helper plasmid that results to only one event transfer of the mobilizable CRISPR plasmid and not an exponential spreading of the antimicrobial tool. To solve this problem, Dong *et al.* fused the helper and the CRISPR plasmids increasing by 4 the conjugation efficiency, reaching 1,43% in filter condition (Dong *et al.* 2019). Hamilton *et al.* did the same construct and increased the conjugation efficiency by 10,000-fold from 1.10^{-6} % to 1.10^{-2} % in liquid condition. In both cases, it was still not enough to see a reasonable effect on the recipient population. Improved conjugation efficiencies in liquid were only observed by adding glass beads. In these conditions, 100 % efficiency of conjugation has been observed (Hamilton *et al.* 2019). It was suggested that glass beads provide the solid surface contact for cell to cell contact as filter condition does.

While conjugation rates can be increased by fusing the CRISPR plasmid and the helper plasmid these combined plasmids are not easy to engineer especially to insert small 20 nt spacer. Indeed, helper plasmids generally measure under 10 kb whereas conjugative plasmids encompassing all mobilization genes can measure between 13 kb to 1 Mb, depending on the conjugative apparatus (Smillie *et al.* 2010). It turns out that smaller plasmids are easier to engineer and modify with biomolecular techniques, thus keeping the killer and helper plasmids apart seems better. Moreover, the use of autonomous CRISPR conjugative plasmids poses problems in term of biocontainment. Indeed, conjugative plasmids can harbour several cargo genes encoding a panel of metabolic properties, notably antibiotic and/or metal resistance, and sometimes contains transposons or insertion sequences. The transfer of these properties to pathogens could be deleterious to fight an infection. In this context, it seems better to favour constructions allowing the transfer of the CRISPR plasmid only while inhibiting the transfer of the helper plasmid by deletion of the *oriT*.

Furthermore, transfer efficiency *in vitro* does not always reflect transfer efficiency *in situ* (Neil *et al.* 2020). For example, mating pair formation is a crucial step for the conjugation. It was shown that IncI conjugative plasmids which encode two pili stabilizing mating pair are

more efficient at delivering plasmids in the gut microbiota than other plasmids (Neil *et al.* 2020). More comprehensive studies on the bottlenecks of conjugation *in situ* could help to develop a better conjugative delivery tool adapted to the target's environment. Moreover, *in situ* testing of the conjugative transfer should be realized even if *in vitro* efficiency is not as high as expected.

II.3.2.3. Escape mutants

The use of CRISPR-Cas system leads to the emergence of escape mutants able to survive the CRISPR-mediated cleavage. Among the listed studies, two indicate an escape mutant emergence rate around 10^{-4} (Bikard *et al.* 2014; Ruotsalainen *et al.* 2019). When CRISPR-Cas systems are delivered by phage, escapers also depend on the MOI with an increase of the MOI resulting in the decrease of escape mutants (Ram *et al.* 2018). Escape mutants can emerge by several mechanisms. Insertion of transposable elements and deletion of the cas9 gene were reported (Bikard *et al.* 2014; Citorik, Mimee and Lu 2014) as well as inactivation of the CRISPR array by deletion (Citorik, Mimee and Lu 2014; Ram *et al.* 2018; Selle *et al.* 2020), inactivation of the sgRNA by insertion of transposons (Hamilton *et al.* 2019) and even a spontaneous mutation leading to an insertion of an A nt into the tracrRNA loci between the 140 and 141 nt (Citorik, Mimee and Lu 2014). Authors further reported nucleotide polymorphism flanking the PAM in the targeted sequence rendering it unrecognizable for the CRISPR-Cas system (Hamilton *et al.* 2019). Other study investigating the action of the CRISPR-Cas9 system in *E. coli* reported that large deletions from 12.9 kb and up to 35 kb can occur to suppress the targeted sequence (Cui and Bikard 2016).

The use of Type I CRISPR-Cas system also lead to escape mutations (Selle *et al.* 2020). In this study, a CRISPR array was delivered by the ϕCD24-2 phage into *Clostridium difficile* which allowed to integrate the array thanks to lysogenic activity of this phage. The CRISPR array exerted antibacterial activity thanks to the endogenous Type I CRISPR-Cas system of *C. difficile* which provides the interference module. Several escapers lacking the CRISPR array were recovered. To reduce the rate of escapers, authors deleted the lysogeny genes of the ϕCD24-2 phage which resulted in enhanced killing activity due to both CRISPR-Cas activity and phage replication. During successful *in vivo* assays, *C. difficile* escapers were recovered in the faeces of mice and it was found that these escapers retained the CRISPR array in their genome. No information is given on the presence of functional Type I CRISPR-Cas system or the presence of the targeted sequence in those escapers. The mechanism allowing for integration of the CRISPR array in *C. difficile*'s genome is also unclear.

As resistance was described to depend in the balance between Cas9-mediated DSB and the efficiency for the homologous recombination (HR) repair mechanism, it has been proposed to impair HR pathway. To achieve more efficient Cas9-mediated killing, it is possible to use an inhibited form of RecA protein (RecA56) which competes with wild-type RecA, reducing induction of the SOS response and blocking the HR-mediated repair. Thanks to this mutant RecA allele, killing can occur even with non-efficient spacers with Cas9-mediated DSB (Moreb *et al.* 2017).

Other strategies were used to avoid the emergence of escape mutants. First, it was proposed to add a selective advantage to the system. Yosef *et al*. proposed an elegant strategy to first re-sentitize bacteria by eliminating a plasmid conferring drug resistance and second to eliminate bacteria that have escaped the CRISPR system (Yosef *et al.* 2015). To do so the CRISPR-Cas system targeting resistance determinants was first integrated into the bacterial chromosome using a lysogenic phage construction. Following this step, the bacteria are

infected with a lytic engineered phage containing sequences recognized by spacers produced by the integrated CRISPR-Cas system. Bacteria producing an intact CRISPR system are immunized against the phage while escape mutant resulting of an inactivated CRISPR will die. If mutations in the CRISPR-Cas system cannot arise thanks to this counter-selection, it is still possible that the targeted carbapenem resistance genes can be mutated and not recognized anymore by the CRISPR-Cas system. To prevent these escape mutations authors designed the CRISPR-Cas system with several spacer sequences targeting different sequences of the resistance genes. Mutation of the targeted sequence is unlikely to produce a functional resistance to carbapenem (Yosef *et al.* 2015).

Furthermore, using different CRISPR-Cas system could be a solution to prevent escape mutants emergence. For instance, the use of the Type VI CRISPR-Cas system with the Cas13 allows a degradation of untargeted RNA, that induces a dormancy state in bacterial hosts and no emergence of escape mutants were reported (Kiga *et al.* 2020). However, as mentioned above, this system seems to kill bacteria even if the target is found on a plasmid. In the case of resistance determinant targeting in the microbiota, it could be better not to kill a resistant bacteria but only to eliminate the conjugative plasmid conferring resistance. Indeed, the microbiota is composed of various bacterial species that are involved in the host health and can contain plasmid-encoded resistance. Killing these bacteria does not seem the better way to fight against antibiotic resistance because it could result in dysbiosis.

II.3.2.4. Identifying spacer sequences

Many spacer-finding algorithms have been developed for biotechnological applications related to CRISPR-Cas systems (Torres-Perez *et al.* 2019). Comparative algorithms exist to efficiently compare and detect absent and present sequences in a define genome in order to choose spacers (Zhu *et al.* 2014; Stemmer *et al.* 2015; Park, Kim and Bae 2016; Spoto *et al.* 2020). Moreover, it is possible for the user to search spacers in a favourite genome by submitting a genome file (Stemmer *et al.* 2015; Spoto *et al.* 2020).

In the long-term, the use of CRISPR-Cas based antimicrobial tools could allow the targeting of specific bacterial specie in a bacterial community thanks to the ability of CRISPR-Cas to target a specific ~20 bp sequence in a whole genome. The choice of the spacer becomes challenging as it implies to identify a sequence unique to the targeted specie and absent in the others species present in the community. Finding such spacer requires to compare large number of genomes, which is not feasible manually. When I started my thesis no algorithm able to select a spacer targeting a specific specie in a complex microbial population existed.

III. Investigating the cellular mechanistic of conjugation

Bacterial DNA conjugation was first discovered when researchers observed that the mixing of two parental *E. coli* strains with different auxotrophic markers led to the formation of new type of strains with mixed genotypes (Lederberg and Tatum 1946). It was later realized that this sexual process in bacteria was due to a contact-dependent transfer of an extra-chromosomal replicon, called the F plasmid for fertility factor (Lederberg and Tatum 1953). The F plasmid is a ~100 kb genetic element carrying all the genes required for its maintenance (replication origin, partition system) and autonomous transfer (transfer origin, *tra* genes encoding the conjugation machinery). In the following section I will review the mechanistic detail of the conjugation process step-by-step, with specific focus on the F plasmid, which I use as a model study during my PhD. For a better understanding of the genetic nomenclature related to the F genes and functional homologs in other model conjugative plasmids, please refer to the Table 1 of Virolle, Goldlust, Djermoun *et al.* (2020).

III.1. Mating pair formation

The first step of bacterial conjugation is the mating pair formation by establishment of the contact between donor and recipient cells. These steps are realized by two components of the conjugation machinery *i.e.*, the conjugative pilus and the Type IV Secretion System (T4SS). I will describe in more detail implications of these two actors in the mating pair formation.

III.1.1. Role of the conjugative pilus

The conjugative pilus is an extracellular appendage with a tubular structure exposed at the surface of the donor cell. Its function is to establish contact between the donor and the recipient bacteria. Among the different conjugative plasmids, distinctive pili are encoded and processed. Pili can be classified into three main types, defined by Bradley according to their morphology (Bradley 1980): thin flexible (encoded by IncI1 R64 plasmid), thick flexible (encoded by IncF F plasmid and IncI1 R64 plasmid) and rigid (encoded by IncP1α RP4 plasmid). Flexibility of the pilus seems to be related to its thickness as thin flexible pili have a 6 nm diameter, thick flexible pili a 9 nm diameter, and rigid pili a 10-11 nm diameter. These distinct pili types are adapted for conjugation in diverse media (Bradley, Taylor and Cohen 1980). Indeed, thin flexible pili were able to ensure conjugation in liquid and solid media whereas rigid pili obtained particularly reduced conjugation efficiencies in liquid media. Thick flexible pili are able to perform conjugation in both solid and liquid media although liquid conjugation efficiency can be reduced for some plasmids encoding those pili. Moreover, in another study, Bradley determined that IncI plasmids encode two types of pilus : a thick flexible essential for the conjugation and a thin flexible proven to enable liquid mating (Bradley 1983; Komano, Kim and Nisioka 1990). Thick flexible pili and rigid pili of the IncP group have a strong tendency to aggregate. This aggregation phenotype is thought to promote conjugation by facilitating cell-to-cell contact (Samuels, Lanka and Davies 2000; Kalkum 2002). In addition to their direct role in conjugation, pili encoded by conjugative plasmids were shown to mediate adherence to eukaryotic cells and abiotic surfaces, witch suggest a role in biofilm formation (Ghigo 2001; Reisner *et al.* 2003; Dudley *et al.* 2006).

The F plasmid encodes a thick flexible pilus without adhesin at the tip. The F pilus is composed of the TraA pilin subunits in helicoidal organization assembled by the T4SS machinery and has the ability to extend and retract (Hospenthal, Costa and Waksman 2017). During the biosynthesis of the pilus, the pilin go through post-transcriptional modifications, notably they are cleaved by the LepB protease and subsequently acetylated (Finlay *et al.* 1985;

Frost *et al.* 1985). During processing, the F pilin associates with phosphatidylglycerol of the inner membrane, thus making the inner channel of the pilus hydrophobic (Costa *et al.* 2016). Other pili of broad-host range plasmids, like Ti and RP4, are produced with cyclized pilin (Eisenbrandt *et al.* 1999).

TraA pilin does not recognize a specific receptor on the recipient bacteria, so it was proposed that the pilus's role is to grab the recipient cell and bring it closer to the donor to form the mating pair (Curtiss 1969; Anthony *et al.* 1994). However, there is still a controversy on whether or not the pilus can serve as a channel for DNA transfer (Harrington and Rogerson 1990). The structure of the pilus and diameter of the inner channel (28.2 Å) could allow the passage of the ssDNA plasmid molecule with unfolded protein (Costa *et al.* 2016). In addition, TraA association with phosphatidylglycerol has been proposed to neutralize interaction with the charge carried by the DNA during transfer (Ilangovan, Connery and Waksman 2015). Yet, only two articles indirectly report the ability for the F plasmid to be transferred between cells in liquid culture separated by a membrane (Harrington and Rogerson 1990), and between distant cells under the microscope (Babic *et al.* 2008). Further studies are required to provide an unambiguous answer to this question.

III.1.2. The Type IV secretion system (T4SS)

Type IV secretion system (T4SS) is the membrane-associated machinery that forms a pore through the two membranes of the donor cell. The T4SS is strictly required for pilus biogenesis as well as DNA transfer. Solved structures of the T4SS of different model plasmids showed that the T4SS composed of various subunits forms two major complexes in the inner and the outer membrane connected by periplasmic proteins (Low *et al.* 2014; Ilangovan, Connery and Waksman 2015; Hu, Khara and Christie 2019).

To enable the T4SS machinery to go through the gram-negative cell-wall, a T4SS glycosylase protein degrades peptidoglycan in the periplasm (Zupan *et al.* 2007). The inner membrane channel is composed of TraE, TraL, TraF and TraC proteins involved in pilus assembly and DNA translocation, which are ATP-dependent and are also implied in the positioning of the T4SS (Low *et al.* 2014). The outer membrane channel is composed of TraK and TraV pore-forming proteins and the large TraB protein ensuring the stability of the channel by crossing the periplasm and the inner membrane.

Moreover, to ensure energy-dependent DNA transfer, conjugative plasmids generally encode three ATPases, including two allowing pilus assembly and retractation (Atmakuri, Cascales and Christie 2004; Llosa and Alkorta 2017; Álvarez-Rodríguez *et al.* 2020). However, only one ATPase is ubiquitous to all conjugative machineries, which is TraC and TrbE in the F and RP4 plasmids, respectively. TraC ATPase is required for the F pilus assembly (Lawley *et al.* 2003) and in IncX families of plasmids it is fused to proteins forming the inner membrane channel (Batchelor *et al.* 2004). In the structure of the R388 plasmid revealed by Low *et al.* this ubiquitous ATPase formed two hexamers bound to the base of the inner membrane channel (Low *et al.* 2014). For the F plasmid, Hu *et al.* report that TraC ATPase structure forms hexamer of dimers (Hu, Khara and Christie 2019). The second most conserved ATPase is the T4SS coupling protein (T4CP) essential for DNA transfer but not implicated in pilus biogenesis (TraD and TraG respectively in F and RP4 plasmids). Importance of this protein is discussed in more details in the next section. Last ATPase is the Traffic ATPase family inner membrane protein TrbB in the RP4 plasmid (not conserved in F plasmid T4SS). Traffic ATPases are generally associated with gram-negative Type II, III, IV and VI secretion systems. Although R388 plasmid encodes this ATPase, it was not part of the T4SS structure published by Low *et*

al. suggesting that interaction of this protein with the channel is weak (Low *et al.* 2014). In the Ti plasmid of *Agrobacterium tumefaciens*, this protein seems to be implicated in pilus biogenesis (Atmakuri, Cascales and Christie 2004). Genetic analysis of proteobacterial T4SS allowed their classification into four different MPF families (Table 1). The F plasmid is classified in MPF_F whereas the RP4 plasmid is classified into the MPF_T family with other broad-host range plasmids like the Ti plasmid (Smillie *et al.* 2010).

III.2. Plasmid pre-processing in the donor cell

Within the donor cell, the conjugation process requires the pre-processing of the plasmid by the relaxosome components, and the subsequent recognition of the processed plasmid and addressing to the T4SS via the Type IV coupling protein (T4CP).

III.2.1. Relaxosome

The relaxosome is a complex of proteins able to recognize a specific sequence of the conjugative plasmid termed origin of transfer (*oriT*). It is composed of a plasmid-encoded relaxase and several accessory proteins, which can be plasmid- or chromosome-encoded. Accessory proteins recognize the *oriT* and act as molecular wedges to melt the dsDNA to favour the recruitment of the relaxase recombinase. Accessory proteins contain a ribbon-helix-helix motif allowing their binding to the *oriT*. The processing of the F plasmid is realized by relaxosome accessory proteins TraM, TraY, the host-encoded Integration Host Factor (IHF) and the TraI relaxase which introduce a nick in the *oriT* (Ragonese *et al.* 2007; Dostál, Shao and Schildbach 2011).

The relaxase is a multifunctional protein composed of two distinct domains : a trans-esterase and a helicase (Ilangovan *et al.* 2017). The main role of the relaxase is to introduce a nick at the *nic* site on the *oriT*. To do so, the relaxase recognizes the *nic* site thanks to inverted repeats on the *oriT* locus (Lucas *et al.* 2010). The relaxase also contains Tyrosine (Tyr) residues allowing DNA cleavage through a transesterification reaction that covalently binds the Tyr residue to the 5' end of the plasmid DNA. The helicase domain of the relaxase then unwinds the plasmidic DNA and extrudes the single-stranded plasmid molecule, named the transferred strand (T-strand) because only this strand will be translocated into the recipient cell (Draper *et al.* 2005). It was then suggested that two relaxase are needed during the conjugation event. A first relaxase remains linked to the 5' end of the T-strand and is transferred into the recipient cell, while the second relaxase unwinds the T-strand within the donor cell during transfer (Becker and Meyer 2012; Ilangovan *et al.* 2017). Importantly, the nicked 3' end of the T-strand serves as primer for rolling-circle-replication (RCR), allowing the replication of the remaining plasmid strand into dsDNA in the donor cell. Replication of the plasmid in the donor is not necessary for the conjugation process (Kingsman and Willetts 1978) but ensures that the plasmid is conserved by the donor in the process of conjugation. The transfer is complete when the relaxase performs a second nick to separate the T-strand of the newly replicated strand.

Among MOB families, only MOB_F relaxase harbour several catalytic Tyr residues. Interestingly, it was shown that the two Tyr residues on the TrwC relaxase of the MOB_F family R388 plasmid were essential for a complete conjugation process (Garcillán-Barcia *et al.* 2007; Gonzalez-Perez *et al.* 2007). However, single mutations showed that among the four Tyr residues found on the TraI F relaxase, only one is required for complete conjugation (Dostál, Shao and Schildbach 2011).

III.2.2. The Type IV coupling protein (T4CP)

The T4CP ATPase is essential to the DNA transfer, and are present in all conjugative T4SS. T4CP recognizes the relaxosome-T-strand complex, connects it with the rest of the T4SS and energizes the transport of this complex through the T4SS. T4CP are proteins ensuring substrate recognition through interaction with the relaxosome proteins and associated T-DNA. In the F plasmid, the T4CP is the TraD protein.

T4CPs are particularly diverse proteins, however, they all contain a nucleotide binding domain (NBD) enabling ATPase activity to energize the transport of the DNA substrate into the T4SS thanks to the Walker A and Walker B domains involved in ATP binding and hydrolysis. Indeed, it was shown that mutations in the NBD of T4CP abolish conjugation (Moncalián *et al.* 1999; Schröder and Lanka 2003; Atmakuri, Cascales and Christie 2004; Parsons *et al.* 2007; Lang and Zechner 2012). Most T4CP proteins have transmembrane domains (TMD) to associate with the cell membrane and form the base of the T4SS, a cytoplasmic All-Alpha Domain (AAD) and a C-terminal domain both responsible for Relaxosome-DNA substrate recruitment.

TMD domain allows the inner membrane anchoring, regulation of ATPase activity and oligomerization. Indeed, the TMD of the R388 plasmid TrwB confers ATP/GTP specificity (Hormaeche *et al.* 2006) and both T4CPs of R388 and RP4 plasmids do not have ATPase activity when their N-terminal TMD is absent (Hormaeche *et al.* 2002; Schröder and Lanka 2003). Moreover, T4CPs deleted of their TMD are monomeric whereas full-length T4CPs have the ability to oligomerize (Hormaeche *et al.* 2002; Schröder and Lanka 2003). A previous study already demonstrated that T4CPs of the F and RP4 plasmids have a tendency to form oligomers (Schröder *et al.* 2002). The structure of the TrwB T4CP protein of the R388 plasmid with its T4SS showed interaction between dimeric T4CP and the core T4SS structure, notably structural proteins crossing both inner and outer membranes and a conserved ATPase (Redzej *et al.* 2017). It has further been proposed that T4CPs could be responsible for the positioning of the T4SS. For instance, R388 and Ti plasmids T4CPs are positioned in the membrane at the pole of the bacteria even without any plasmid or relaxosome protein (Kumar and Das 2002; Segura *et al.* 2014). These same T4CPs with mutated TMDs showed a random positioning in the cytoplasm. It was further demonstrated that the pole positioning of the Ti plasmid T4CP also needed its NBD domain intact, whereas this is not the case for R388 plasmid. Finally, R27 plasmid T4CP was reported to forms discrete foci distributed all along the cell membrane (Gunton *et al.* 2005). However, TMD does not always play a preponderant role in the subcellular localization of the T4CP, as in the case of the CloDF13 plasmid whose T4CP does not need the TMD to localize at the cell pole, only to be membrane anchored (Álvarez-Rodríguez *et al.* 2020). Nevertheless, fixed subcellular localization of the T4CP suggest a role for the positioning of the T4SS machinery, likely mediated through the TMD.

The AAD and C-terminal domain of T4CPs are thought to be responsible for the specificity of the transferred DNA by interaction with the relaxosome proteins. For the F plasmid, a direct interaction between the relaxosome component TraM and the C-terminal domain of the TraD T4CP allows the addressing of the T-strand to the T4SS (Beranek *et al.* 2004; Lu and Frost 2005; Lu *et al.* 2008). Chimeric TraD proteins showed that the substrate is recruited by the C-terminal domain and that the T4SS is recognized by the TMD domain (Whitaker *et al.* 2016). Moreover, AAD domain of the Ti and pCF10 plasmid T4CPs were shown to bind DNA (without specific sequence recognizing), the relaxase and the entry ATPase of the core T4SS, suggesting an implication in signal transmission for T-strand injection in the T4SS (Whitaker *et al.* 2015).

However, if the T4CP substrate is highly specific, this is not the case for its interaction with the T4SS. Indeed, it was observed that T4CP of R388, pKM101 and R6K plasmids are able to interact with varying strength to each heterologous T4SS (Llosa, Zunzunegui and de la Cruz 2003). Moreover, the CloDF13 plasmid, lacking for a T4SS, encodes for a T4CP that hijacks T4SS of R388, RP4 or F T4SS to be transferred (Cabezón, Sastre and de la Cruz 1997).

III.3. Establishment of the plasmid in the recipient

Within the recipient cell, the newly acquired plasmid must be processed to ensure its maintenance and vertical transmission to the progeny of the transconjugant cell. First, the plasmid internalized as single-stranded linear DNA will be recircularized and then converted into dsDNA by the complementary strand synthesis reaction. Moreover, plasmid DNA needs to be replicated and segregated in the recipient bacteria before the cell division.

III.3.1. Recircularization/ssDNA conversion to dsDNA

Entry of the T-strand in the recipient cell is led by the relaxase protein. It is thought that the relaxase is unfolded through the T4SS and refolds in the recipient cell. Studies showed that active relaxase form was transferred in the recipient cell (Draper *et al.* 2005; Dostál, Shao and Schildbach 2011). The *oriT* region is composed of inverted repeats which helps the relaxase to find the *nic* site in the donor. In the recipient cell, inverted regions of the T-strand forms a hairpin shape allowing again the relaxase recognition as proved by the crystal structure of the R388 plasmid TrwC relaxase with inverted repeats near to the *nic* site (Guasch *et al.* 2003). After recovery of the 3' end through the helicase activity, the relaxase catalyses the ligation between the 5' and the 3' end of the T-strand. If the relaxase only uses 1 Tyr residue, this imply to use at least two relaxases, one performing the first nick, transferred in the donor and catalysing the last ligation reaction, and another to ensure nick between the T-strand and the newly synthetized DNA in the donor strain (Dostál, Shao and Schildbach 2011).

The mechanism involved in the complementary strand synthesis in the recipient cell remains largely elusive. It was shown that F, R6K, R100 and ColE2 plasmids possess single stranded initiator sequences (*ssi*) forming a stem loop structure which allow RNA primase to synthetize primers. These *ssi* are notably able to complement the replication of the M13 phage lacking its own *ssi* (Nomura *et al.* 1991). Thus *ssi* are thought to be structures enabling the complementary strand priming for subsequent synthesis of the complementary strand by the host-encoded DNA polymerase III (Wilkins and Hollom 1974; Böldicke *et al.* 1981). For the RP4 plasmid however, it was found that the *oriT* region was enough to complement the growth of the M13 phage in presence of the RP4 primase, suggesting that *oriT* contains sequences enabling the initiation of the complementary strand synthesis (Yakobson *et al.* 1990). Moreover, studies on RP4-like RP1 plasmid and the ColIb-P9 plasmid showed that the plasmid primase was transferred into the recipient cell, suggesting that it is able to synthetize primers to induce replication (Chatfield and Wilkins 1984; Merryweather, Barth and Wilkins 1986; Merryweather *et al.* 1986).

Next, the synthesis of the complementary strand was shown to depend on the host-encoded DNA polymerase III for the F and ColEI plasmids (Wilkins and Hollom 1974). After the complementary strand synthesis reaction, the dsDNA plasmid is produced. Its maintenance will then depend on functional replication and partition mechanisms.

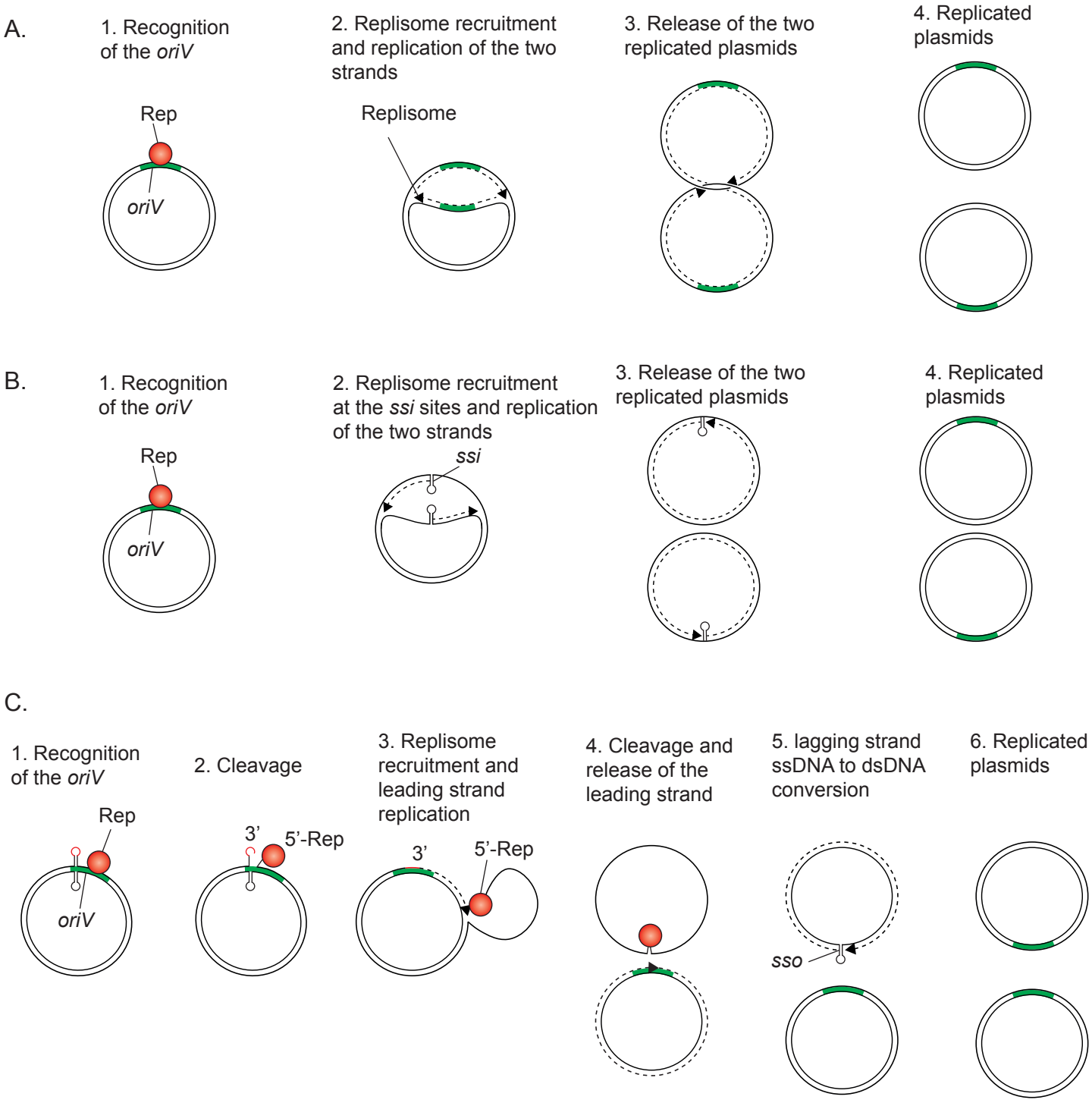

Figure 9 : Illustration of the three replication mechanisms described for conjugative plasmids.
A. Theta replication occurs by the recruitment of the Rep protein to the replication origin (*oriV*). Replisome recruitment allow the bidirectionnal replication of both strands. The replication is completed by the release of the two replicated plasmids. Adapted from Viret *et al.* 1991.
B. Strand displacement replication also begins with the recruitment of the rep protein to the *oriV*. Formation of two single stranded initiator (*ssi*) sites allow for the recruitment of the replisomes which perform the replication of one strand each. The two plasmids are next released. Adapted from Lilly and Camps 2015.
C. Rolling circle replication starts with the recruitment of the Rep protein with the subsequent cleavage at the *oriV*. the Rep protein stays bound to the 5' cleaved strand and rolling circle replication is initiated at the 3' of the cleaved DNA for the replication of the leading strand. At the end of the leading strand replication, another cleavage is realized by the Rep protein to release the first plasmid copy and the lagging strand. The lagging strand forms a hairpin single strand origin (*sso*) which allows for its conversion into dsDNA. Adapted from Ruiz-Mazo *et al.* 2015

III.3.2. Plasmid replication

All plasmids possess an origin of replication (*oriV*) and sometimes encode replication initiator proteins (Rep). Three types of replication were described for plasmids (Figure 9): theta replication used by most studied plasmids like F and RP4 plasmids (Lilly and Camps 2015), strand displacement replication, typically used by IncQ plasmids and rolling circle replication used by model plasmid pMV158 of *S. pneumoniae*.

Theta replication (Figure 9A) is the most documented replication mode since it is the same mechanism for the replication of bacterial chromosomes. It is initiated by the Rep protein encoded by the plasmid or by the host which will bind *oriV* of the plasmid. This will lead to the recruitment of a nucleoprotein complex to open the DNA duplex and allow the DnaB helicase to load on the replication fork, a mechanism which is dependant of DnaA or PriA. The replisome assembles after the loading of DnaB. The replisome is formed with the following actors. The DnaB helicase, the DnaC loading factor ATPase and the DnaG primase form a complex destined to synthetize RNA primers for the lagging strand synthesis (Fang, Davey and O'Donnell 1999). The SSB protein binds single stranded DNA which protects and stabilizes exposed DNA of the replication fork. Finally, the DNA polymerase III holoenzyme (Pol III) also takes part in the replisome. Pol III is composed of diverse subunits to perform DNA replication: α (catalytic subunit) and ε (3'→5' exonuclease) forming the core, β_2 processivity factor and DnaX (McHenry 2011). DnaX allows the loading of β_2 onto the DNA and recruits the core (α and ε subunits) to β_2. Pol III core (α and ε subunits) is stimulated the DnaB relaxase activity whereas DnaG modulates it. This allows the coordination of the synthesis between the leading and the lagging strand (Wu *et al.* 1992; Tanner *et al.* 2008). The replication is performed bidirectionally (Scott 1984) and is next resolved to obtain the two resulting plasmids.

Strand displacement replication (Figure 9B) initiation is independent of host factors. In the IncQ model RSF1010 plasmid, like for theta replication, the RepC replication initiator protein binds to *oriV* which initiate bending and melting of the DNA. Recruitment of the RepA helicase will unwind bidirectionally the single-stranded DNA, creating *ssi* sites on each strands forming DNA hairpins (Honda *et al.* 1993; Miao *et al.* 1993). DNA hairpins will be recognized by RepB primase which synthetizes primers and the Pol III holoenzyme recruited by RepA will extend the synthetized primer (Rawlings and Tietze 2001). During the continuous strand replication, RepA helicase will perform DNA unwinding to separate the two replicated plasmids.

Finally, rolling circle replication (Figure 9C) is identical as the one performed during conjugation and is marked by the decoupling of leading and lagging strand replication. Indeed, a Rep helicase initiates the replication by sequence-specific nick at the *oriV* with a trans-esterification leading to covalent binding between the Rep helicase and the 5' end of the parental strand. The 3'-OH end liberated will serve as primer for the host DNA polymerase to perform the leading strand replication. To complete the leading strand synthesis and generation of the first replicated plasmid, a nick needs to be performed at the initiation of the replication where the synthetized DNA remained attached to the parental DNA. This reaction is catalysed by the Rep helicase that remained attached to the 5' end of the parental DNA. The parental strand is released and serves as a matrix for the replication of the lagging strand which depends on host-encoded enzymes and is initiated by a *ssi* forming a stem-loop structure (Ruiz-Masó *et al.* 2015; Wawrzyniak, Płucienniczak and Bartosik 2017).

Conjugative plasmids encode numerous functions and are generally maintained at low copy number to limit the metabolic burden for the bacterial host cell. Therefore, plasmids

ensure that their copy number is high enough to be segregated into the daughter cells without detrimental effect for the bacteria which could lead to its loss. Two types of regulation have been reported, sometimes they are found into the same plasmid.

The first regulation can be due to iterons (Chattoraj 2002; Konieczny *et al.* 2014). Iterons are directly repeated sequences which are present in the *oriV* and sometimes outside. Iterons recruit Rep replication initiator proteins to perform replication. Sometimes the *oriV* overlaps the *rep* gene promoter, this is a way to prevent over replication because Rep binding to the *oriV* will impede the *rep* gene expression (Shingler and Thomas 1984; York and Filutowicz 1993; Ishiai *et al.* 1994). Iterons are able to sequestrate Rep dimer proteins by handcuffing: a Rep protein dimer is associated with iterons situated on two different plasmid copies. Iteron sites titrates the Rep proteins.

A second way for plasmid to regulate replication is the use of antisense RNA (Del Solar and Espinosa 2002; Brantl 2014). RNA are produced and hybridize to essential sequences needed for the replication of the plasmid. For example, in the ColE1 family of plasmids, the antisense RNA inhibits the primer formation. Moreover, the antisense RNA can hybridize to the *rep* gene transcript to block Rep production. In most of cases, antisense RNA are constitutively produced and their copy number are controlled with plasmid copy number, which allows regulation. This regulation can be assumed by auxiliary proteins too.

Lastly, some plasmids encode chaperones and proteases. Indeed, Rep proteins can be found in two state : active monomers and inactive dimers (Nakamura, Wada and Miki 2007). Chaperones are able to change the conformation of inactive dimers, liberating active monomers whereas protease can degrade monomers and dimers of Rep proteins (DasGupta *et al.* 1993; Sozhamannan and Chattoraj 1993; Zzaman, Reddy and Bastia 2004; Kubik *et al.* 2012).

Regulation of the replication can lead to incompatibility phenotypes exerted by co-resident plasmids. Indeed, when regulation of replication is realized with iterons on the promoter of the *rep* gene, Rep proteins encoded by the co-resident plasmid can bind to iterons (on the origin of replication), which blocks the *rep* gene expression. Moreover, antisense RNA interacts directly or not with the mRNA of the Rep initiator protein to impede its translation and therefore its production. If the antisense RNA is able to recognize the co-resident plasmid's Rep mRNA, then incompatibility occurs between those two plasmids (Rivera-Urbalejo *et al.* 2015).

III.3.3. Plasmid partition

Some plasmids are regulated to have high copy-numbers and their stability rely on random partitioning during cell division. However, large plasmids impose a high metabolic burden to their bacterial host and are consequently maintained at low copy-number. It this case, the plasmid copies must be segregated into the daughter cells by dedicated active mechanisms (Baxter and Funnell 2014; Brooks and Hwang 2017). Generally, segregation is mediated by 3 main actors, two segregation proteins and a *par* site. The *par* site can be assimilated to the centromere found in eukaryotic cells. Plasmids can harbour several or one *par* site, usually placed next to the segregation genes. One of the protein is named "centromere binding protein" (CBP) and recognizes and binds to the *par* site. The other protein is an NTPase that uses ATP or GTP hydrolyzation energy to drive DNA into the cell. Two types of partition systems were described for conjugative plasmids depending on the NTPase (Figure 10).

The F and RP4 plasmids use the type I partition system: the walker type (Figure 10A). It is based on the diffusion rachet model of the ParAB*S* system. ParA is the ATPase, ParB the

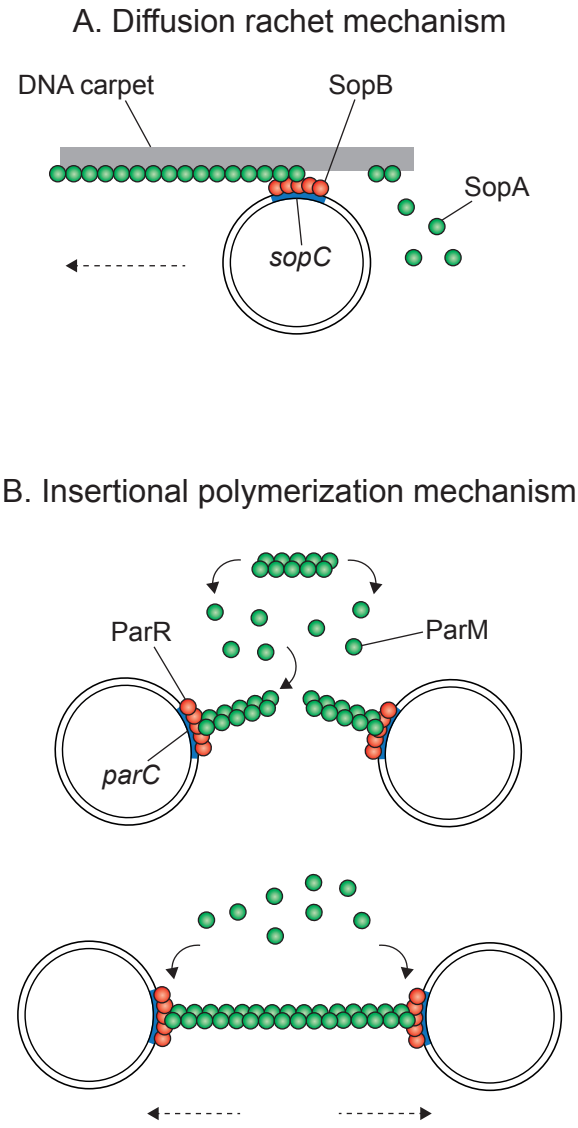

Figure 10 : Schematic view of the two partition mechanisms described for conjugative plasmids
A. Diffusion rachet mechanism for the F plasmid. SopA protein binds unspecifically to the chromosomic DNA carpet while SopB binds to *sopC* sequence. SopB then binds SopA which induces ATP hydrolysis and the subsequent release of SopA in the media. As SopB is prefers SopA bound to DNA, it will silde in the SopA carpet thus moving the plasmid thanks to its *sopC* binding.
B. Insertional polymerization mechanism for the R1 plasmid. ParM NTPase forms two-stranded filament bundles. ParR recognize the *parC* sequence of the R1 plasmid. After R1 replication, ParM polymerization occurs at the ParR-*parC* complex. The ParM polymerization allows the pysical separation of the two replicated plasmids.

Adapted from 2017 Brooks et Hwang Plasmid

CBP and *parS* the *par* site. ParB binds to *parS* and a large quantity of ParA is linked to the bacterial host DNA, acting like a ParA carpet. The ParB/*parS* cargo is attracted to the ParA carpet linked to the DNA. The approach of ParB/*parS* cargo triggers the ParA-mediated ATP hydrolysis releasing ParA of the DNA. ParA could rebind the DNA only after a delay. This is why after the plasmid replication, there is a formation of two ParB/*parS* cargos on the two replicated plasmids and these cargos tend to slide on the ParA carpet on the DNA which allows to separate them (Vecchiarelli, Neuman and Mizuuchi 2014).

F and RP4 plasmids have similar type I partition systems. In F and RP4, CBPs (respectively SopB and KorB) are Helix Turn Helix (HTH) proteins. C-terminal domain (adjacent to the HTH domain) mediate the dimerization of the CBPs. N-terminal domain interact with the ATPase (SopA and IncC respectively) to mediate oligomerization of the CBP at and around the *par* site (*sopC* and O_B respectively). To be recognized by HTH proteins, the *par* sites contain inverted repeat recognition elements. For example, KorB of the RP4 plasmid binds to 12 inverted repeats operators O_B, only one is thought to be the *par* site (O_B3). In the F plasmid *sopC* consists of 12 copies of 43 pb repeat, only one of them is considered essential for partition. Moreover, 16 bp in the 43 bp repeat serve as the binding site for the CBP SopB.

One other partition type was reported on other conjugative plasmids. The type II partition system is the actin-like type (Figure 10B), based on the ParMR*C* model of the IncFII R1 plasmid. ParM is a NTPase which can form two-stranded filament bundles. After replication, in the two replicated plasmids, ParR CBP binds to *parC* site. ParM polymerization occurs at the ParR/*parC* partition complex. ParM polymerization allows the physical separation of the two replicated plasmids which will be segregated in two daughter bacterial cells (Ebersbach and Gerdes 2005).

III.3.4. Toxin-Antitoxin

Conjugative plasmids provide several advantages for the bacteria to survive and adapt to its environment. However, plasmids are not only beneficial to bacteria and impose a fitness cost to their hosts. Indeed, they need to be maintained in the bacterial progeny and can also be transferred to adjacent bacteria. Both those needs imply costly mechanisms, encoded by the plasmid and expressed by the bacterial host only to ensure essential plasmidic functions. It can lead to extreme measures taken by the plasmid to avoid being cleared of the bacterial host. For instance, many conjugative plasmids encode Toxin-Antitoxin systems also called addiction systems. They are composed of two genes expressed in the bacterial host, a toxin and the cognate antitoxin. However, the antitoxin is a labile protein whereas the toxin is stable. Thus, if the plasmid is lost, the antitoxin and toxin are not produced anymore but as the toxin is more stable than the antitoxin, the bacterial host dies.

One example of TA systems found on the F plasmid is CcdAB (Ogura and Hiraga 1983). CcdB is a toxin targeting and inhibiting the DNA gyrase, which is essential for the bacterial host, notably to relax DNA supercoiling during the replication (Critchlow *et al.* 1997; Nöllmann, Crisona and Arimondo 2007). The DNA gyrase is a heterotetrameric protein composed of two GyrA subunits responsible for DNA binding and cleavage, and two GyrB subunits containing the ATPase domain (Reece and Maxwell 1991). GyrA was shown to dimerize in presence of GyrB to form the functional gyrase. CcdB toxin interacts with GyrA to prevent its dimerization (Dao-Thi *et al.* 2005). In a bacteria possessing the F plasmid, the CcdA antitoxin blocks the action of CcdB toxin by forming a CcdA-CcdB complex (Dao-Thi *et al.* 2005). If the bacterium loses the F plasmid, the labile CcdA degrades before CcdB, allowing the latter's toxic activity on the DNA gyrase. Thus the bacterial host is killed due to the loss of the plasmid.

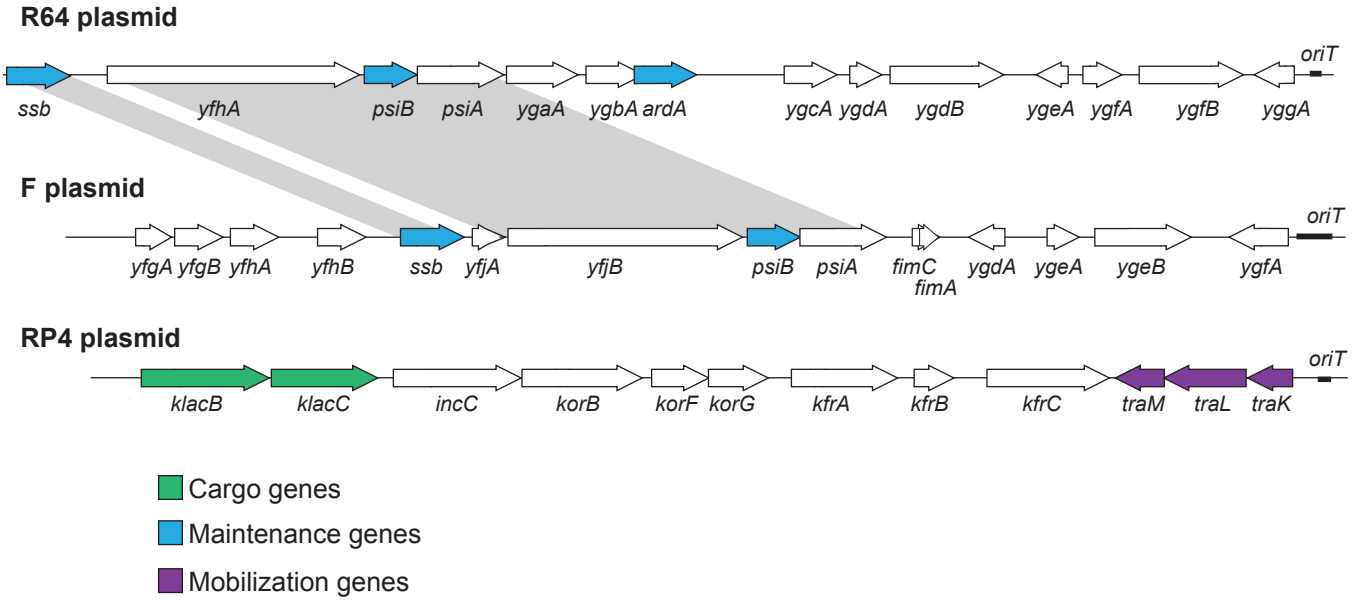

Figure 11 : Comparison of the genetic organization of the leading region of three representative plasmids.
Genetic organization of the leading region of F, R64 and RP4 plasmids are represented using (i) blue to indicate genes implicated in maintenance (genes implicated in the stabilization of the T-strand in the recipient, replication genes and partition genes) (ii) violet to indicate mobilization genes (T4SS, T4CP and relaxosome genes), (iii) green for cargo genes (antibiotic or metal resistance genes, transposons and isertion sequences), (iv) white to indicate unknown genes and (v) black dash to show the *oriT*. Homologous genes are related in grey.

Alignment between *yfhA* and *yfjB* was done with clustalw, using protein sequences and obtained a score of 92.4847, suggesting high homology.

III.4. Plasmid gene expression and phenotypic conversion of the recipient cell

Plasmid acquisition will be followed by plasmid-gene expression that will result in the conversion of the recipient cell into a transconjugant bacteria exhibiting new metabolic functions.

III.4.1. Leading region expression

The leading region of the plasmid is the first region of the T-strand to be transferred in the recipient. The structure of the leading region is not universally conserved among conjugative plasmids. As a mean of comparison, leading region of RP4 plasmid is not organized the same way than F plasmid leading region. However, R64 plasmid also have a leading region encompassing *psiB* and *ssb* highly similar to the F plasmid (figure 11).

Early gene expression of the leading region genes in transconjugant was reported. Cell measurement of the expression of *ssb* and *psiB* using transcriptional fusion of their promoter with the *lacZ* reporter gene showed a zygotic expression of these two genes. Indeed it seems that these genes are only expressed transiently in the transconjugant cell and not in the donor (Jones, Barth and Wilkins 1992). This has been also reported for genes of the leading region of the ColIB-P9 plasmid (Althorpe *et al.* 1999). Moreover a recent study showed that pED208 IncFII plasmid leading genes produce proteins that are translocated into the recipient cell by the T4SS during conjugation, including SSB and PsiB (Al Mamun, Kishida and Christie 2021).

SSB (single-strand binding) protein produced by the F plasmid (SSB_F) is homologous to the essential and universally conserved chromosomic SSB (SSB_C) able to bind DNA during the replication to stabilize and protect single stranded intermediary (Chase and Williams 1986). The role of SSB_F protein is not well known, however a study showed its ability to partially complement the inactivation of the essential SSB_C (Golub and Low 1986). PsiB (plasmid SOS interference/inhibition) is a protein allowing the repression of the SOS response in *E. coli* by binding to RecA thus preventing the auto-proteolysis of LexA (Petrova *et al.* 2009). PsiB would then prevent the induction of the SOS response due to the T-strand entry in the recipient, to prevent its degradation.

The leading region organization could be linked to the early expression of these genes, the first region to enter the recipient bacteria would also be the first to be expressed in order to help establish the plasmid. As previously mentioned, to perform the complementary strand synthesis *ssi* sequences are present in the plasmid and are thought to form stem loop structures to allow the primers synthesis by the primase. In the F plasmid, the *Frpo ssi* is present in the leading region. *In vitro*, *Frpo* has been shown to form stem-loop structures recruiting the RNA polymerase, thus serving as single-stranded promoters controlling the transcription of downstream genes (Masai et Arai 2000). This led to the hypothesis that early expression of the leading genes could be due to the transcription initiation activity of *ssi* sequences. In this view, the *ssi* sequence enables the early and transient expression the leading genes, immediately after the entry of the plasmid in single-stranded form (Nomura *et al.* 1991). The later conversion of the ssDNA T-strand into dsDNA plasmid would avoid the single-stranded promoter formation. Consequently, the expression of the leading genes would be switched off while the expression of all other plasmid genes under the control of double-stranded promoters are switched on. This will then allow the expression of genes involved in plasmid maintenance (replication and partition), and conjugation *tra* genes, converting the transconjugant into a new plasmid donor.

III.4.2. Entry exclusion

After the acquisition of the dsDNA plasmid, the transconjugant cell will produce the exclusion factors encoded by the newly acquired plasmid. Entry exclusion is a physical barrier to the DNA transfer between bacterial cells carrying related conjugative elements. It has two main functions, first it prevents competition between identical plasmids and ensure the stable replication of the plasmid residing in donor strain. Indeed, F donors deficient for entry exclusion genes are not stable (Helmuth and Achtman 1975). Their second function is to prevent recipient death due to excessive rounds of conjugation, termed lethal zygosis. Mating assay containing an excess of Hfr donors indeed showed that recipient cells tend to die of lethal zygosis (Skurray and Reeves 1974).

Most of the plasmids encode an entry exclusion protein (Eex) which is required in the recipient cell to mediate entry exclusion. This protein is typically localized in the inner membrane and interacts with a T4SS protein involved in the mating pair stabilization. These proteins are highly divergent as showed by the analysis of entry exclusion systems of Garcillan-Barcia and de la Cruz (Garcillán-Barcia and de la Cruz 2008). However, it seems that the N-terminal part of the protein with a conserved cysteine residue allows the localization at the periplasmic side of the inner membrane (Haase, Kalkum and Lanka 1996). The highly divergent C-terminal part of Eex proteins seem to be the one implicated in the exclusion of specific T4SS (Jakubowski *et al.* 2004). In the F plasmid, TraS is the entry exclusion protein which was shown to interact with TraG of other donor cells (Audette *et al.* 2007).

Some plasmids, notably IncF and IncH plasmids, also encode a surface exclusion (Sfx) protein located in the outer membrane which prevents the formation of the mating pair by interaction with outer membrane proteins. This could allow the destabilization of the mating pair mediated by their thick flexible pilus strongly attached to the recipient (Garcillán-Barcia and de la Cruz 2008). Notably, F plasmid TraT protein has been suggested to interfere with the interaction between TraN and OmpA to destabilize mating pair (Riede and Eschbach 1986).

III.5. Plasmid conjugation and the acquisition of drug-resistance in real-time

As presented, the key steps of conjugation are well documented, specially concerning the F model plasmid. However, there is still a gap in our understanding of the organisation of conjugation at the cellular scale. Also, the timing of conjugation remains largely elusive in terms of chronology, dynamics, rate, speed and cell interaction. First, how conjugation events are coordinated to ensure the maintenance of the plasmid in the recipient? How much time does the ssDNA stays in the recipient cell before being converted into dsDNA? Are there plasmid factors expressed during this ssDNA phase and how are they involved in the establishment of the plasmid in the recipient? What are the recipient factors implicated in the recircularization, complementary strand synthesis and subsequent expression of the plasmid genes?

Recently, *in vivo* microscopy approaches have been developed in the laboratory to study conjugation in real-time and at the single-cell level. Being transferred at high conjugation frequency in liquid conditions, the F plasmid turned out to be a relevant plasmid model for live cell imaging with fluorescence microscopy. The use of fluorescence microscopy combined with microfluidics allowed to see the actual timing of conjugation transfer. Using these tools, it was shown that upon T-strand injection in the recipient cells, T-strand of the F

plasmid only dwells ~5 min in a single-stranded form (Nolivos *et al.* 2019). This is shortly followed by complementary strand synthesis that converts the plasmid into dsDNA.

This study also addressed the acquisition timing of tetracycline resistance carried by the conjugative plasmid. Tetracycline resistance gene expression starts immediately after dsDNA conversion of the plasmid, resulting in the rapid conversion of the initially drug-sensitive bacterium into a drug-resistant one. More surprisingly, acquisition of tetracycline resistance by conjugation is possible, even in the presence of tetracycline, which is an inhibitor of protein synthesis (Nolivos *et al.* 2019). The question then became, how can plasmid encoded proteins be produced despite the inhibition of protein synthesis by the tetracycline? Using single-cell microscopy, it was demonstrated that recipient factors are required for the production of the tetracycline resistance protein TetA in the presence of tetracycline. More specifically, the basal activity of the conserved multidrug efflux pump AcrAB-TolC encoded by the host genome allows the bacteria to extrude enough tetracycline to ensure the maintenance of a residual activity of protein synthesis and the production of the TetA specialized efflux pump. This work demonstrates an unanticipated interaction between hosts factors and the acquisition of new properties via conjugation.

Besides, it showed how relevant is the use of real-time microscopy for the deeper understanding of the conjugation process. The use of appropriate reporter systems allows to differentiate donor, recipient and transconjugant populations and also to synchronize cells during the conjugation event. From that perspective, real-time microscopy allow to see the chronology of the sequence of events in the conjugation phenomenon.

IV. Thesis objectives

All along this introduction, I emphasized on the two faces of conjugation. First, it is a ubiquitous and conserved phenomenon in bacterial populations and permits environment adaptation. Second, it is a powerful tool that can be used in biotechnological applications and notably to deliver antimicrobial agents. My thesis has focused on those two aspects of the conjugation phenomenon.

My first objective was to elaborate an antibacterial strategy using CRISPR-Cas systems delivered by conjugative machinery to fight antibiotic resistance and kill desired pathogens in a bacterial community. My main goal was to develop a versatile tool, which would be suitable for diverse applications using both CRISPR-Cas9-mediated DSB to kill or CRISPRi to repress gene expression. Moreover, my objective was to adapt this tool to any bacterial community, by using a bioinformatic algorithm to predict spacer sequences able to target any desired bacterial genome while sparing environmental bacteria. I focused on generating a proof of concept of this tool and on adapting it to the microbiota, one of the environments for which this tool is intended.

Furthermore, I was interested in the conjugation mechanism itself and investigated the dynamic of expression of the leading region genes and the timing of acquisition of tetracycline resistance by conjugation with the F plasmid. Indeed, as already discussed, the leading genes seem to be expressed only transiently in the transconjugant and not in the donor. This could be explained by a single stranded promoter locus in the leading region. It also seems that the proteins produced by those genes have functions related to the plasmid establishment in the recipient. Establishment is a crucial step for the plasmid dissemination in the bacterial community. Thus, during my thesis I observed the production of fluorescent recombinant proteins of the leading region as a proxy for the gene expression. Thanks to fluorescent microscopy, I was able to determine the production timing and dynamic of these proteins which informed us on the plasmid strategy to ensure its establishment in the recipient cell.

I also worked on tetracycline resistance acquisition via the conjugative F plasmid. Fluorescence microscopy allowed to evaluate the dynamics of tetracycline entry and efflux thanks to the F plasmid resistance genes.

All my thesis work is based on fluorescence microscopy in real-time assay that allowed to visualize, at the single cell level and using relevant fluorescent markers, the dynamics of the observed phenomenon, in particular conjugation and double-stranded breaks induced by Cas9.

Results

V. Development of Targeted-Antibacterial-Plasmids (TAPs) to fight antibiotic resistance and bacterial pathogens

V.1. Reuter *et al*. Nucleic Acids Research paper

V.1.1. Introduction

Antibiotic resistance is a global issue threatening human health. Indeed, the overuse of antibiotics leads to the emergence and dissemination of antibiotic resistant strains. In this context, there is an urgent need to develop non-antibiotics alternatives to tackle the problem of bacterial infection and drug-resistance. In the introduction, I presented several studies combining conjugation with CRISPR-Cas systems to fight either bacterial infections or antibiotic resistance. Most of these studies use the broad host-range RP4 conjugative machinery (Table 3 part 1) for which the conjugation efficiency is relatively low. During my thesis, I developed a tool that combines the conjugative machinery of the narrow host-range but highly transferrable F plasmid, and customizable strain- or gene-specific CRISPR-Cas systems. Our system consists in a donor strain containing a helper F-Tn*10* plasmid (the F plasmid containing the Tn*10* transposon) and a mobilizable Targeted-Antibacterial-Plasmid (TAP), which contains the F-Tn*10* origin of transfer *oriT* and the CRISPR-Cas system. The donor strain produces the conjugative machinery encoded on the F-Tn*10* plasmid to mobilize the TAP from donor to recipient cells. In this system, the F-Tn*10* helper plasmid is autonomous, meaning that it can be transferred into the recipient strain as well as the TAP. In the new host cell, the CRISPR-Cas system is constitutively produced and exerts an antimicrobial activity in strains that contain the sequence targeted by the spacer sequence only.

A major specificity of the TAP system is the development of the CRISPR Search Tool for Bacteria (CSTB) bioinformatic algorithm that allows the identification of strain- or gene-specific spacer sequences on the basis of their presence or absence within the targeted bacterial specie(s). CSTB was developed by Christian Lesterlin, Erwan Gueguen in collaboration with Guillaume Launay and Cécile Hilpert before I started my PhD. TAPs were also already constructed by Sarah Bigot at the beginning of my thesis. My contribution was to insert a range of spacers into TAPs, to validate their transfer efficiency and the specificity of their antibacterial activity *in vitro*, in bi- or multi-species bacterial populations.

V.1.2. Results and conclusion

Our results show that the TAPs can be used as a tool to kill specifically bacterial species into a defined community thanks to the CSTB algorithm. We determined that this killing is mediated by the introduction of DSB into the chromosome. We demonstrated that the spacers designed by the CSTB software are highly reliable and specific allowing a precise targeting of a unique species among a multispecies bacterial population. We also showed that TAPs can be used to target antibiotic resistance determinants and resensitize bacteria to antibiotics using the pOXA-48a conjugative plasmid responsible of carbapenem dissemination as an example. The main bottlenecks of our strategy are the efficiency of transfer and the emergence of TAP escapers mutants.

3584–3598 *Nucleic Acids Research, 2021, Vol. 49, No. 6* *Published online 28 February 2021*
doi: 10.1093/nar/gkab126

Targeted-antibacterial-plasmids (TAPs) combining conjugation and CRISPR/Cas systems achieve strain-specific antibacterial activity

Audrey Reuter[1], Cécile Hilpert[1], Annick Dedieu-Berne[1], Sophie Lematre[1], Erwan Gueguen[2], Guillaume Launay[1,*], Sarah Bigot[1,*] and Christian Lesterlin[1,*]

[1]Microbiologie Moléculaire et Biochimie Structurale (MMSB), Université Lyon 1, CNRS, Inserm, UMR5086, 69007 Lyon, France and [2]University of Lyon, Université Lyon 1, INSA de Lyon, CNRS UMR 5240 Microbiologie Adaptation et Pathogénie, 69622 Villeurbanne, France

Received November 26, 2020; Revised February 10, 2021; Editorial Decision February 11, 2021; Accepted February 16, 2021

ABSTRACT

The global emergence of drug-resistant bacteria leads to the loss of efficacy of our antibiotics arsenal and severely limits the success of currently available treatments. Here, we developed an innovative strategy based on targeted-antibacterial-plasmids (TAPs) that use bacterial conjugation to deliver CRISPR/Cas systems exerting a strain-specific antibacterial activity. TAPs are highly versatile as they can be directed against any specific genomic or plasmid DNA using the custom algorithm (CSTB) that identifies appropriate targeting spacer sequences. We demonstrate the ability of TAPs to induce strain-selective killing by introducing lethal double strand breaks (DSBs) into the targeted genomes. TAPs directed against a plasmid-born carbapenem resistance gene efficiently resensitise the strain to the drug. This work represents an essential step toward the development of an alternative to antibiotic treatments, which could be used for *in situ* microbiota modification to eradicate targeted resistant and/or pathogenic bacteria without affecting other non-targeted bacterial species.

INTRODUCTION

The worldwide proliferation of drug-resistant bacteria is predicted to cause a dramatic increase in human deaths due to therapeutic failures in the next decades (1). The constant emergence of bacterial resistances and the current low rate of antibiotic discovery emphasize the need to develop innovative antibacterial strategies that represent a real alternative to the use of antibiotics. Moreover, antibiotics generally lack specificity as they target processes that are essential to bacterial proliferation. Antibiotics consequently affect the whole treated bacterial community without discriminating between harmful and commensal strains, and lead to the population enrichment in drug-resistant strains.

Recent reports have demonstrated the possibility to achieve specific antimicrobial activity through the use of clustered regularly interspaced short palindromic repeats (CRISPR) and the associated Cas proteins. CRISPR/Cas systems can achieve bacterial killing through the induction of double-strand breaks (DSBs) to the chromosome by the Cas9 nuclease (2,3). The expression of specific genes can also be inhibited through CRISPR interference (CRISPRi), when using the dead catalytic Cas9 enzyme (dCas9) (4,5). CRISPR targeting relies on the ∼16–20 nucleotide (nt) target-specific guide RNA (gRNA) sequence, which allows the recruitment of the Cas nuclease to the complementary DNA sequence (2,6). Yet, to be used as practical antibacterial tools, CRISPR/Cas genes need to be delivered to the targeted bacterium. Bacterial DNA conjugation precisely offers the possibility to transfer long DNA segments to a range of bacterial species, with the transfer specificity depending on the considered conjugation system. Methodologies using conjugation to deliver CRISPR/Cas systems have been recently developed to target *Escherichia coli* (7–10) or *Salmonella* Typhimurium (11). These methods rely on the RK2 plasmid conjugation machinery that perform broad-host range transfer, but with the drawback of low efficiency. Besides, these studies report the targeting of a single bacterial strain within mono-species populations only. One major challenge is to develop an antibacterial strategy that selectively alter one or several targeted bacterial strains, without affecting the other species present in a multispecies population. This objective requires the development of bioinformatics tools to identify gRNA sequence able to achieve such strain-specific targeting.

In this work, we present an innovative antibacterial methodology based on mobilizable plasmids that carry

*To whom correspondence should be addressed. Tel: +33 472 72 26 89; Fax: +33 472 72 26 01; Email: sarah.bigot@ibcp.fr
Correspondence may also be addressed to Guillaume Launay. Email: guillaume.launay@ibcp.fr
Correspondence may also be addressed to Christian Lesterlin. Email: christian.lesterlin@ibcp.fr

CRISPR/Cas systems designed to induce antibacterial activity into specifically targeted recipient strains. These so-called targeted-antibacterial-plasmids (TAPs) use the conjugation machinery (*tra* genes) encoded by a F plasmid to be efficiently transferred to *E. coli* strains and to closely related Gram-negative Enterobacteriaceae. TAPs were designed to produce the CRISPR Cas system in a constitutive manner and can easily be redirected against any bacterial species of interest by changing gRNA sequence in one-step cloning. The gRNA sequence carried by the TAP determines the targeting of the antibacterial activity towards specific recipient strains only. To identify strain-specific gRNA, we have developed a bio-informatic program CSTB (CRISPR Search Tool for Bacteria) that allows the rapid and robust identification of ∼16–20 nt sequences on the basis of their presence or absence in the genome of bacterial strains selected on a phylogenetic tree. Consequently, the CRISPR/Cas system will only be active in recipients that contain the DNA sequence complementary to the chosen gRNA sequence, while being inactive in other strains of a multispecies population mix. Here we demonstrate TAPs ability to induce efficient and strain-specific antibacterial activity against a range of Gram-negative Enterobacteriaceae within multispecies population *in vitro*.

MATERIALS AND METHODS

Bacterial strains, plasmids, primer and growth culture conditions

Bacterial strains construction and growth procedures. Bacterial strains, plasmids and primers are listed in Supplementary Tables S1, S2 and S3, respectively. Plasmid cloning were done by Gibson Assembly (12) and verified by Sanger sequencing (Eurofins Genomics). Chromosome mutation were transferred by phage P1 transduction to generate the final strains. Strains were grown at 37°C in Luria-Bertani (LB) broth, M9 medium supplemented with glucose (0.2%) and casamino acid (0.4%) (M9-CASA) or M63 medium supplemented with glucose (0.2%) and casamino acid (0.4%) (M63). When appropriate, the media were supplemented with the following antibiotics: 50 μg/ml kanamycin (Kn), 20 μg/ml chloramphenicol (Cm), 10 μg/ml tetracycline (Tc), 20 μg/ml nalidixic acid (Nal), 20 μg/ml streptomycin (St), 100 μg/ml ampicillin (Ap), 10 μg/ml gentamycin (Gm), 50 μg/ml rifampicin (Rif). When appropriate 40 μg/ml 5-bromo-4-chloro-3-indolyl-β-D-galactopyranoside (X-Gal) and 40 μM isopropyl β-D-1-thiogalactopyranoside (IPTG) were added for screening of LAC phenotype.

TAPs construction and one-step-cloning change of the spacer sequence on the TAPs

Plasmid construction was performed by IVA cloning (13), expect for changing the spacer sequence in the TAPs, which was performed by the replacement of the spacer in pEGL129 by a SapI-spacer-SapI DNA sequence. The nsp (non-specific) spacer sequence is flanked by two SapI restriction sites that allow for liberation of non-cohesive DNA ends upon SapI digestion. To replace the nsp spacer, a new spacer is constructed by annealing two oligonucleotides (listed in Supplementary Table S3) with oriented complementary sequences to the non-cohesive ends generated by SapI restriction of TAP-Cas9-nsp or TAP-dCas9-nsp plasmids. Ligation production between the new spacer fragment and the TAP backbone was transformed into DH5α or TB28 strains. Constructions were verified by PCR reaction and sequencing.

Congo red assay

Curli production colony assay. *Escherichia coli* strain OmpR234 with or without plasmids were plated on Congo Red medium (10 g bacto tryptone, 5 g yeast extract, 18 g bacto agar, 40 μg/ml Congo Red and 20 μg/ml Coomassie Brilliant blue G) and incubated 4 days at 30°C. Colonies were visualized at ×10 magnification with a M80 stereomicroscope (Leica). Digital images were captured with an IC80-HD integrated camera coupled to the stereomicroscope, operated via LASv4.8 software (Leica).

Liquid aggregation test. Overnight culture of *E. coli* strain OmpR234 with or without plasmids were diluted to an A_{600} of 0.05 in 1 ml M9-CASA medium supplemented with 25 μg/ml of Congo Red. Culture were grown without agitation at 30°C for 24 h and image captured.

Conjugation assay

Overnight cultures grown in LB of donor and recipient strains were diluted to an A_{600} of 0.05 and grown until an A_{600} comprised between 0.7 and 0.9 was reached. 50 μl of donor and 150 μl of recipient cultures were mixed into an Eppendorf tube to obtain a 1:3 donor to recipient ratio. At time 0 min, 100 μl of the mix were diluted into 1 ml LB, serial diluted and plated on LB agar supplemented with antibiotics selecting for donor, recipient and transconjugant cells. The remaining 100 μl were incubated for 1h30 at 37°C. 1 ml of LB was added gently and the tubes were incubated at 37°C for another 1h30, 4h30 or 22h30. Conjugation mix were then vortexed, serial diluted and plated as for time 0 min.

Long-term conjugation experiment. Conjugation mixes were prepared and incubated at 37°C without agitation. Every 24 h, 100 μl of the mix were diluted into 1 ml of LB and re-incubated at 37°C. The remaining of the mixes were vortexed, serial diluted and plated on LB agar supplemented with antibiotics selecting for donor, recipient and transconjugant cells. At day 1 and day 7, 100 clones of the resulting ampicillin resistant recipients mixed with the TAP-dCas9-OXA48 carrying donor were streaked on LB agar supplemented with Tc or Kn to evaluate the presence of the F-Tn*10* or TAP-dCas9-OXA48 plasmids respectively.

Multispecies conjugation. Overnight cultures grown in LB of donor and recipient strains were diluted to an A_{600} of 0.05 and grown until an A_{600} comprised between 0.7 and 0.9 was reached. A recipient mix is prepared by mixing *C. rodentium*, *E. cloacae*, *E. coli* EPEC and *E. coli* HS recipients strains in indicated proportions (Figure 5C). This mix is serial diluted and plated on LB agar supplemented with

antibiotics to select for each recipient. 100 μl of donor and 100 μl of the recipient mix were added to an Eppendorf tube to perform mating. At time 0 min, 100 μl of the mix were diluted into 1 ml LB, serial diluted and plated on LB agar supplemented with antibiotics to select for donor, recipients and transconjugants. The remaining 100 μl were incubated for 1h30 at 37°C. 1 ml of LB was gently added and the tubes were incubated for an additional 1h30 at 37°C. Conjugation mix were then vortexed, serial diluted and plated on LB agar supplemented with antibiotics to select for donor, recipients and transconjugants. In the figures, the efficiencies of conjugation are represented either as the final concentration of transconjugant cell (CFU/ml) or as the percentage of transconjugant cells calculated from the ratio (T/R + T).

Transformation assay

Overnight cultures grown in LB were 1/100 diluted and grown until an A_{600} comprised between 0.4 and 0.6. Cells were treated with Rubidium Chloride and 90 μl of the resulting competent cells transformed with 100 ng of plasmid and heat shock. Following the 1h incubation at 37°C for phenotypic expression, cells were centrifugated 5 min at 5000 rpm, resuspended in 100 μl of LB, and plated on LB-agar plates supplemented with the appropriate antibiotics.

Live-cell microscopy imaging and analysis

Time-lapse experiments. Overnight cultures in M9-CASA (between *E. coli*) or M63 (between *E. coli* and *C. rodentium*) of donor and recipient cells were diluted to an A_{600} of 0.05 and grown until an A_{600} comprised between 0.7 and 0.9. 25 μl of donor and 75 μl of recipient were mixed into an Eppendorf tube and 50 μl of the mix was loaded into a B04A microfluidic chamber (ONIX, CellASIC®). Nutrient supply was maintained at 1 psi and the temperature maintained at 37°C throughout the imaging process. Cells were imaged every 10 min for 3 h.

Image acquisition. Conventional wide-field fluorescence microscopy imaging was carried out on an Eclipse Ti-E microscope (Nikon), equipped with ×100/1.45 oil Plan Apo Lambda phase objective, FLash4 V2 CMOS camera (Hamamatsu), and using NIS software for image acquisition. Acquisition were performed using 50% power of a Fluo LED Spectra X light source at 488 and 560 nm excitation wavelengths. Exposure settings were 50 ms for sfGFP and 50 ms for mCherry produced from the TAPs; 100 ms for RecA-GFP, HU-mCherry and DnaN-mCherry.

Image analysis. Quantitative image analysis was done using Fiji software with MicrobeJ plugin (14). The Manual-editing interface of MicrobeJ was used to optimize cell detection and the Mean intensity fluorescence, skewness and cell length parameters were automatically extracted and plotted. We defined the timing of TAP acquisition (time $t = 0$) by analyzing the increase of the fluorescence signal conferred by the TAPs (sfGFP or mCh). Plasmid acquisition was validated when a 15% sfGFP or a 30% mCherry fluorescence increase was observed in the transconjugant cells. Fluorescence profiles of each cells were then aligned according the defined $t = 0$ to generate the graphs presented in Figures 2B, C, E, F, 3C and Supplementary Figure S5d.

Flow cytometry

Conjugation was done as described in the conjugation assay section in 0.1 μm filtered LB. At time 90 min and 180 min, conjugation mix were diluted to an A_{600} of 0.03 in 0.1 μm filtered LB and analysed into an Attune N×T acoustic focusing cytometer at a 25 μl/min flow rate. Forward scattered (FSC), Side scattered (SSC) as well as fluorescence signal BL1 (sfGFP) and YL2 (mCherry) were acquired with the appropriate PMT setting and represented with the Attune™ N×T analysis software. To verify the absence of toxicity of the Cas9 or dCas9 constitutive expression from the TAPs, we compared the growth of *E. coli* MS388/TAP with the *cas9* or *dcas9* or without any *cas9* gene. Those strains were grown overnight in 0.1 μm filtered LB and diluted to an A_{600} of 0.05 in 0.1 μm filtered LB. They were grown during 8 h and the A_{600} and CFU/ml were estimated by plating assays at 0, 2, 4, 6 and 8 h. In parallel, at 1 h, 2 h and 5h30 the strains were analysed into the Attune NxT acoustic Focusing cytometer at a 25 μl/min flow rate. Forward scattered (FSC) was acquired and represented with the Attune™ NxT software.

Analysis of TAP-escape mutants

In *E. coli.* The 31 TAP-escape mutants were streaked on medium supplemented with X-Gal and IPTG to determine their LAC phenotype. TAP-escape mutants exhibiting lac+ phenotype were classified as 'Blue' and the others as 'White' in Supplementary Figure S3. To determine the acquisition of point mutation or deletion that modify the targeted *lacZ2* locus, a PCR was realized with OL240 and OL654 that amplify a fragment of 748 pb encompassing the *lacZ2* locus in wt strain. For escape mutants that exhibited no deletion of the *lacZ2* locus but still had an active TAP CRISPR system, the PCR product was sequenced and the mutations identified. A PCR was also done with OL655 and OL656 to amplify a larger fragment around *lacZ2* and observe large deletion as previously described (15). To determine the activity of the TAPs extracted from escape mutants, conjugation was performed between the TAP-escape mutants and an *E. coli* MS388 lac+ strain as described in the conjugation assays section. In parallel, the activity of the TAPs extracted with the Machery Nagel NucleoSpin® Plasmid kit from escape mutants were verified by transformation into lac^+ and lac^- strains as described in the transformation assay section. Seven inactive TAPs were sequenced to identify mutations inactivating CRISPR system.

C. rodentium. For the 20 TAP-Cas9-Cr1-escape mutants, a PCR with OL686 and OL687 was performed to determine deletions in the chromosome locus. To verify the CRISPR activity of the TAPs from *C. rodentium* TAP-escape mutants, conjugation was performed during 5 h between the *C. rodentium* mutants and the *E. coli* MS388 strain to generate new *E. coli* TAPs donors. Then conjugation was performed during 24 h between those new donors and fresh *C. rodentium* recipients and plated to select for recipient

and transconjugants. To confirm the activity of the TAPs isolated form *C. rodentium* escape mutants, TAPs were extracted with Machery Nagel NucleoSpin® Plasmid kit and transformed by electroporation (2.5 kV) into wt *C. rodentium* cells treated with 10% sucrose. Following 1 h of incubation at 37°C, cells were plated on LB-agar supplemented or not with Kn to evaluate the transformation efficiency. Two inactive TAP-Cas9-Cr1 and two inactive TAP-Cas9-Cr22 isolated from escaper clones were sequenced.

CSTB algorithm

The CSTB web site can be freely accessed at https://cstb.ibcp.fr. The CSTB web service enables the comparative analysis of CRISPR motifs across a wide range of bacterial genomes and plasmids. Currently considered motifs are NGG-anchored sequences of 18–23 bp long. The CSTB back-end database indexes all occurrences of these CRISPR motifs present in 2914 complete genomes labeled as representative or reference in the release 99 of RefSeq (03/12/20). In addition, seve bacterial genomes and five plasmids of interest were added. The mean number of distinct motifs among bacterial genomes is 55 923 (5719 and 2 729 570 as respective minimum and maximum). Genomes are classified according to the NCBI taxonomy (07/22/20). Each genome is inserted in the database of motifs by processing the corresponding complete fasta using the following procedure. Firstly, all words satisfying the CRISPR motif regular expression are detected and their chromosomal coordinates stored in a database of motifs. Secondly, all unique words are converted into an integer representation using a 2 bits per base encoding software we developed (https://github.com/glaunay/crispr-set). These integers are then sorted in a unique flat file per genome. The indexing of CRISPR motifs as integers enables computationally efficient comparison of the sets of motifs across several organisms. Finally, the original fasta file is added to a blast database. All related software can be freely accessed at https://github.com/MMSB-MOBI/CSTB_database_manager. The CSTB input interface displays the 2914 genomes available for searching as two taxonomic trees. The left-hand tree allows for the selection of species whose genomes have to feature identical/similar CRISPR motifs. This set of genomes defines the targeted CRISPR motifs. Meanwhile, the right-hand tree allows for the selection of 'excluded' organisms, which must have no motif in common with the targeted ones. The set of motifs that satisfies the user selections will effectively be equal to the union of the motifs found in the selected organisms subtracted from the intersection of the motifs found in the 'excluded' organisms. Computation time ranges from seconds to a few minutes according to the size of the selections and an email is sent upon completion.

All the solutions CRISPR motifs are presented in an interactive table of gRNA sequences and their occurrences in each selected organism. The table has sorting and filtering capabilities on motif counts and sequence composition. This allows for the easy selection of motifs of interest. Detailed information can be downloaded for the entire set of solutions or for the selected motifs only. This detailed information is provided in tabulated file with lines featuring the coordinates of each sgRNA motif in the targeted organisms. Alternatively, the user may explore the results using a genome-based approach. Hence, each targeted genome has its graphical view. The graphic is a circular histogram of the entire distribution of solution sgRNA motifs in a selected genome. The graphic is interactive to display the local breakdown of sgRNA distribution.

RESULTS

Targeted-antibacterial-plasmids (TAPs) modular design

TAPs derivate from the synthetic pSEVA plasmid collection (16), and carry the pBBR1 origin of replication, a choice of resistant gene cassettes, and the $oriT_F$ origin of transfer of the F plasmid (Figure 1A). TAPs are consequently mobilizable by the conjugation machinery produced in *trans* from the conjugative F-Tn*10* helper plasmid contained in the donor cells (Figure 1B and Supplementary Figure S1a) (17,18). We inserted the *Streptococcus pyogenes* wild-type *cas9* (for CRISPR activity) or catalytically dead *dcas9* gene (for CRISPRi activity) and the guide gRNA sequence composed of the constant tracrRNA scaffold and the target-specific crRNA spacer sequence (Figure 1A). Changing the crRNA spacer sequence in one-step-cloning allows reprogramming the targeting of the TAPs against any specific chromosome or plasmid DNA. Optionally, TAPs also carry either the *superfolder green fluorescent protein* (*sfgfp*) or the *mcherry* gene highly expressed from the broad-host range synthetic BioFab promoter (19) to serve as plasmid transfer fluorescent reporter in microscopy and flow cytometry assays (Figure 1A).

Validation of TAPs CRISPR and CRISPRi activities

We addressed the ability of TAPs to induce efficient and specific Cas9-mediated killing (CRISPR) or dCas9-mediated gene expression inhibition (CRISPRi). First, TAPs ability to induce Cas9-mediated killing was confirmed using the previously described lacZ2 spacer that targets the *lacZ* gene of *E. coli* (15). Transformation of the TAP-Cas9-lacZ2 plasmid into the lac+ MG1655 wt strain was ∼1000-fold less efficient than in the isogenic lac– strain carrying a deletion of the targeted *lacZ* locus (Supplementary Figure S1b). By contrast, the TAP-Cas9-nsp plasmid, which contains a non-specific (nsp) crRNA spacer that does not target *E. coli* genome, was transformed with equal efficiency in both lac+ and lac– strains (Supplementary Figure S1b). Second, TAPs ability to induce dCas9-mediated CRISPRi activity was validated by using the csgB spacer that targets the *csgB* promoter driving the production of cell-surface curli fimbriae (20) in the MG1655 *E. coli* mutant strain OmpR234 (21). Congo Red (CR) staining on agar-plates and aggregation clumps formation in liquid medium were used as direct readouts for curli production (21,22). The TAP-dCas9-csgB efficiently inhibits curli production by the OmpR234 strain, as reflected by the formation of white colony in the presence of CR and the inability to form aggregation clumps (Supplementary Figure S1c). By contrast, the non-specific TAP-dCas9-nsp had no effect on curli formation or aggregation in the OmpR234 strain. Besides, we confirmed that the constitutive production of the Cas9 or dCas9 from the TAPs do not cause growth defects (Supplementary Figure S1d)

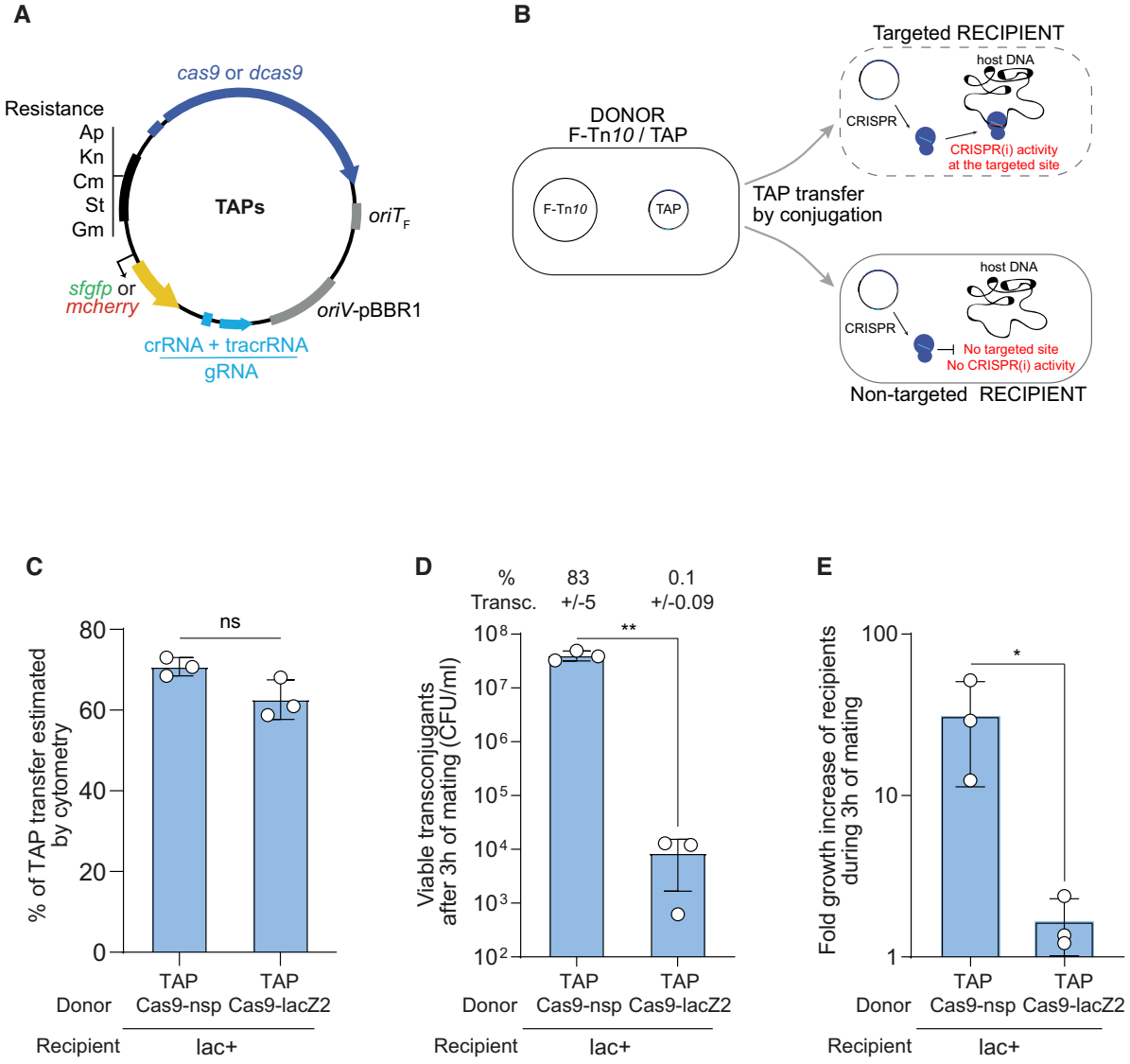

Figure 1. Transfer of TAP by F plasmid machinery mediates killing of a targeted *E. coli* strain. (**A**) TAPs modules consist of CRISPR system composed of wild type (*cas9*) or catalytically dead *cas9* (*dcas9*) genes expressed from the weak constitutive *BBa_J23107* promoter and a gRNA module expressed from the strong constitutive *BBa_J23119* promoter; the F plasmid origin of transfer (*oriT*$_F$); the pBBR1 origin of replication (*oriV*), and a set of resistance cassettes (Ap, ampicillin; Kn, kanamycin; Cm, chloramphenicol; St, streptomycin; Gm, gentamycin), an optional cassette carrying the *sfgfp* or *mcherry* genes highly expressed from the broad-host range synthetic BioFab promoter. (**B**) Diagram of the TAP antibacterial strategy. A donor strain produces the F plasmid conjugation machinery to transfer the TAP into the recipient strain. Targeted recipient carries a sequence recognized by CRISPR(i) system that induces killing or gene expression inhibition. Non-targeted recipient lacking the spacer recognition sequence are insensitive to CRISPR(i) activity. (**C**) Histogram of TAPs transfer estimated by flow cytometry show that TAP$_{kn}$-Cas9-nsp-GFP and TAP$_{kn}$-Cas9-lacZ2-GFP are transferred with similar efficiency in recipient cells after 3 h of mating. Donors TAP-Cas9-nsp (LY1371) or TAP-Cas9-lacZ2 (LY1380), recipient HU-mCherry lac+ (LY248). Two-tailed unpaired *t*-test was performed. ns: non-significant *P*-value >0.05. (**D**) Histograms of the concentration of viable transconjugants estimated by plating assays show viability loss associated with the acquisition of TAP-Cas9-lacZ2. The corresponding percentage of viable transconjugants (ratio T/R+T) is shown above each bar. Two-tailed unpaired t-test was performed. ***P*-value <0.0021 (**E**) Fold-increase of the recipient population counts over the 3 h of mating. Donors TAP-Cas9-nsp (LY1369) or TAP-Cas9-lacZ2 (LY1370), recipient lac+ (LY827). Two-tailed unpaired t-test was performed. **P*-value <0.05 (C–E) Mean and SD are calculated from three independent experiments.

or elongated cell morphology (Supplementary Figure S1e), contrasting with the toxic effects reported in some systems (23–26). These results demonstrate that TAPs ability to induce Cas9-mediated killing or dCas9-mediated gene expression inhibition is efficient and depends on the accurate targeting by the spacer sequence.

TAPs-mediated killing of targeted recipient cells

Next, we addressed the ability of the TAPs to be transferred by conjugation and induce antibacterial activity in *E. coli* recipient cells. Conjugation was performed using the *E. coli* MG1655 donor strain that contains the F-Tn*10* helper plasmid and either the TAP-Cas9-nsp or TAP-Cas9-

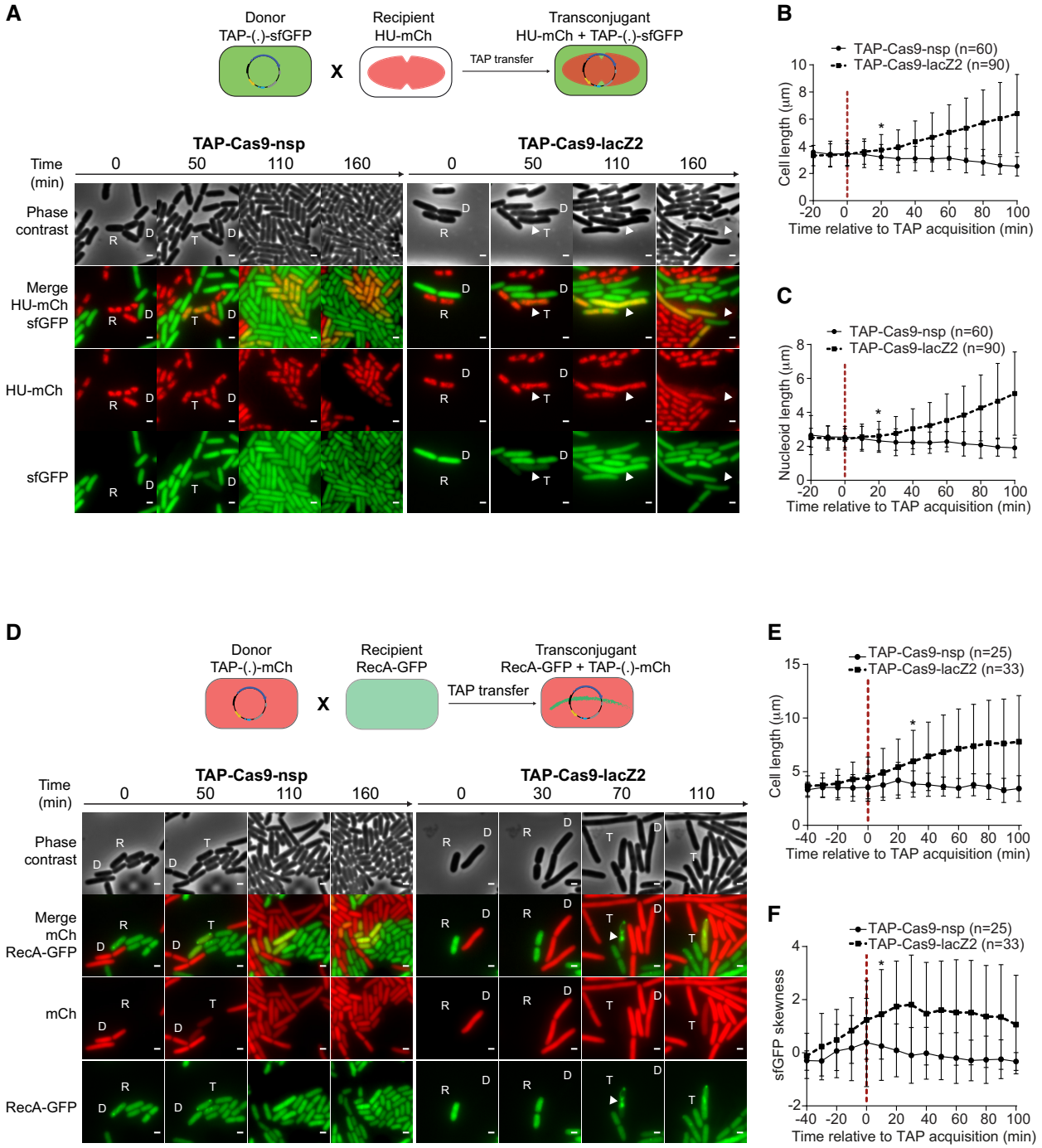

Figure 2. Real-time visualization of *E. coli* killing after acquisition of TAP. (**A**) Upper panel: diagram of the fluorescent reporter system allowing microcopy visualization of TAP transfer and subsequent nucleoid disorganization in transconjugants. Donor cells exhibit diffuse green fluorescence due to sfGFP production from TAP; HU-mCherry recipients exhibit red nucleoid associated fluorescence; transconjugants are identified by the production of both green and red fluorescence. Lower panel: time-lapse microscopy images performed in a microfluidic chamber. D (donor), recipient (R), and transconjugant (T) cells are indicated. Scale bar 1 μm. Donors TAP-Cas9-nsp (LY1371) or TAP-Cas9-lacZ2 (LY1380); recipient HU-mCherry lac+ (LY248). (**B**, **C**) Single-cells time-lapse quantification of transconjugants (**B**) bacterial and (**C**) nucleoid lengths. Average and SD are indicated (n cells analysed). The time of TAP acquisition (red dashed line at 0 min) corresponds to a 15% increase in the green fluorescence in the transconjugant cells. (**D**) Upper panel: diagram of the fluorescent reporter system. Donor cells exhibit diffuse red fluorescence from the mCherry produced by TAP; recipients exhibit diffuse RecA-GFP fluorescence; transconjugants are identified by the production of red fluorescence followed by RecA-GFP polymerization. Lower panel: time-lapse microscopy images performed in a microfluidic chamber. Donor (D), recipient (R), and transconjugant (T) cells are indicated. Scale bar 1 μm. Donors TAP-Cas9-nsp (LY1537) or TAP-Cas9-lacZ2 (LY1538), recipient RecA-GFP (LY844). (E, F) Single-cells time lapse quantification of transconjugants (**E**) cell length and (**F**) skewness of RecA-GFP fluorescence signal. Average and SD are indicated (*n* cells analysed). The time of TAP acquisition (red dashed line at 0 min) corresponds to a 30% increase in the green fluorescence in the transconjugant cells. (B–C and E–F) Multiple *t*-test were performed corrected with Holm–Sidak method. Stars indicate the time with significant difference (*P*-value < 0.05). Significant difference was observed from this point until the end of the analysis.

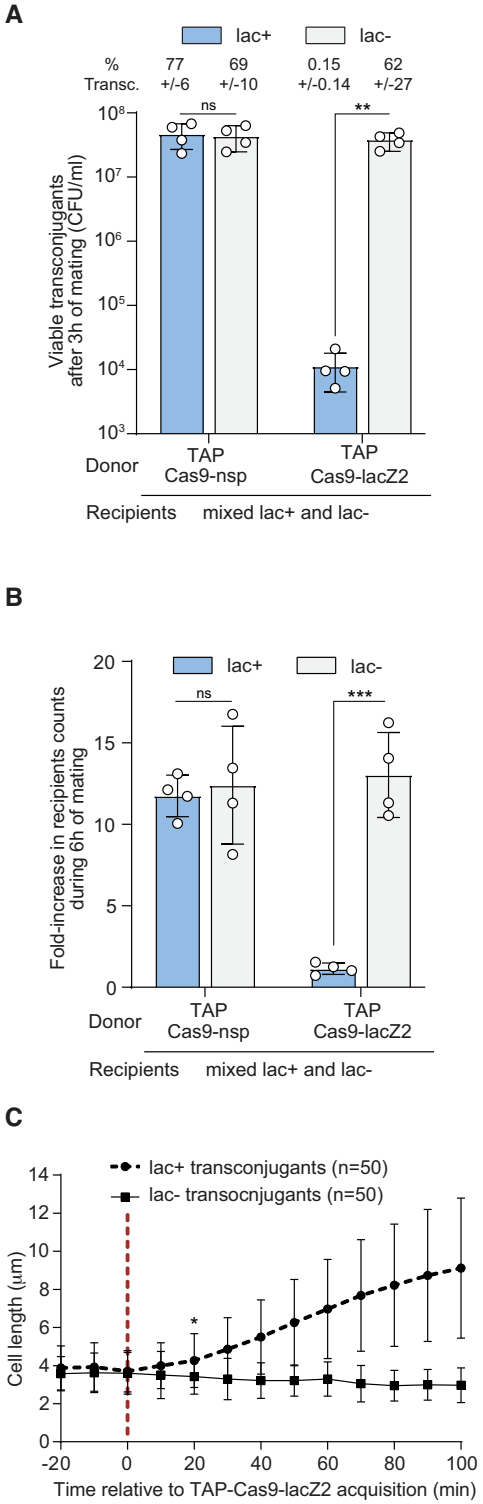

Figure 3. TAP system specifically kills targeted recipients in a mix of targeted and non-targeted *E. coli* recipient cells. (**A**) Viable transconjugant cells and percentage of transconjugants (ratio T/R + T) through TAP_{kn}-Cas9-nsp or TAP_{kn}-Cas9-lacZ2 transfer from donor to a mixed lac+ and lac– recipient population. Two-tails unpaired *t*-test was performed on log_{10}-transformed values. ns = non-significant *P*-value >0.05; ****P*-value <0.0002. (**B**) Quantification of fold-increase in lac+ and lac– recipient populations counts over the 6h of mating. Mean and SD are calculated from 4 independent experiments. Donors: TAP-Cas9-nsp (LY1369) or TAP-Cas9-lacZ2 (LY1370); recipients lac+ (LY827) and lac– (LY848). Two-tails unpaired *t*-test was performed. ns = non-significant *P*-value >0.05; ***P*-value <0.0021. (**C**) Single-cell quantification showing cell length increase in the targeted lac+ transconjugant cells but not non-targeted lac- transconjugants. The time of TAP acquisition (red dashed line at 0 min) corresponds to a 15% increase in the green fluorescence in the transconjugant cells. Cell length average is indicated with SD (n cells analysed). Donor TAP-Cas9-lacZ2 (LY1380); recipients HU-mCherry lac+ (LY248) and DnaN-mCherry lac– (LY1423). Multiple *t*-test were performed corrected with Holm–Sidak method. Stars indicate the time with significant difference (*P*-value < 0.05). Significant difference was observed from this point until the end of the analysis.

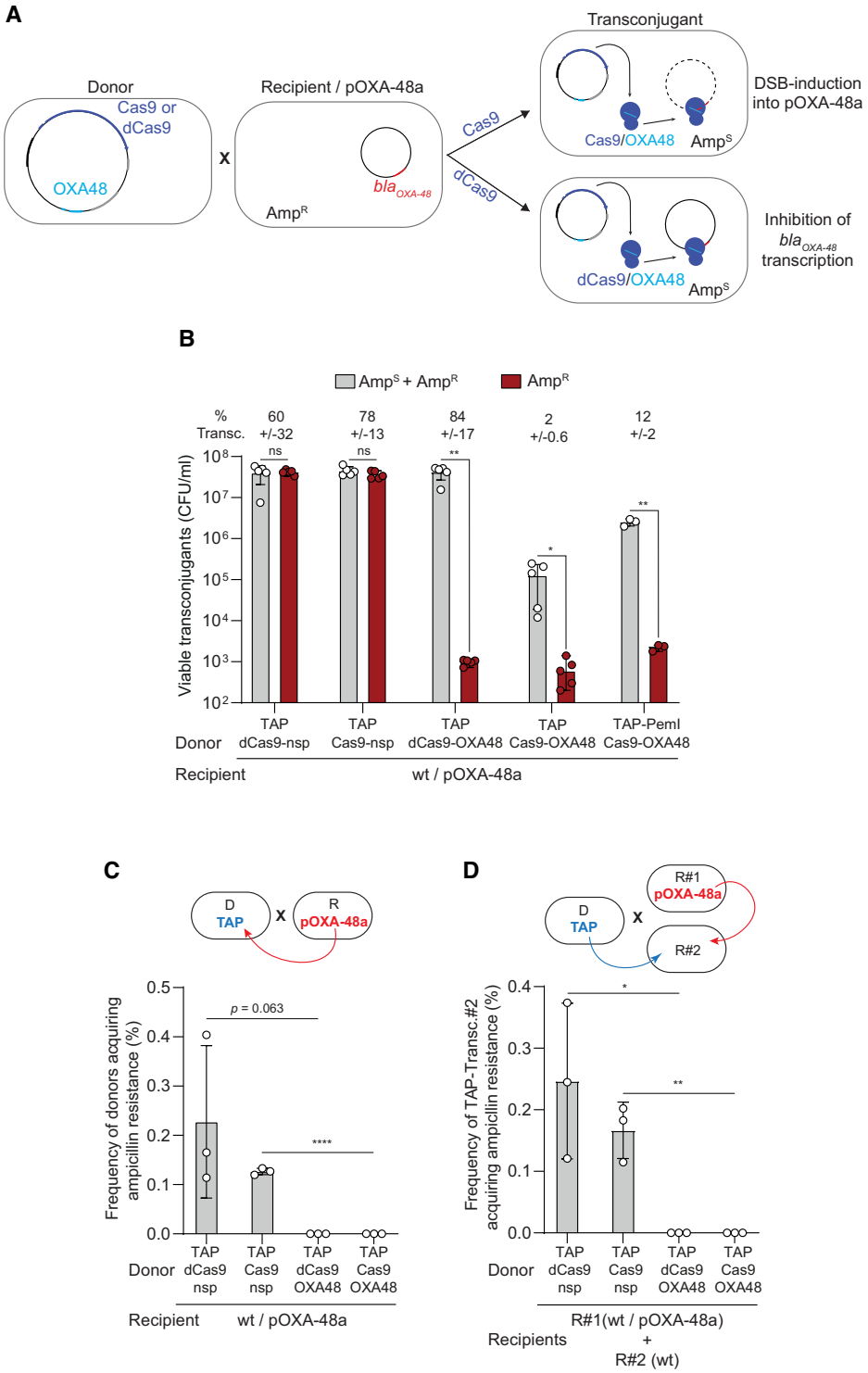

Figure 4. TAP re-sensitises pOXA48-carrying recipient cells and impedes resistance dissemination. (**A**) Diagram of the TAP-mediated anti-resistance strategy. TAP-Cas9-OXA48 targeting the bla_{OXA48} promoter is transferred from a donor to an ampicillin resistant recipient cells carrying the pOXA-48a plasmid. Acquisition of the TAP-Cas9-OXA48 induces double-strand-breaks (DSBs) into the plasmid, while the TAP-dCas9-OXA48 inhibits bla_{OXA48} gene expression. Both TAPs sensitize the transconjugant cells to ampicillin. (**B**) Histograms showing reduction of ampicillin resistance in transconjugants cells after acquisition of the TAP_{kn}-Cas9-OXA48, TAP_{kn}-dCas9-OXA48 and TAP_{kn}-Cas9-OXA48-PemI. Percentages of transconjugants (ratio T/R + T) are indicated. (**C**) Histograms showing the frequency of donor cells acquiring ampicillin resistance through transfer of pOXA-48a from the recipients (as depicted in the above diagram). (**D**) Histograms show the frequency of ampicillin-resistance acquisition through pOXA-48a transfer into R#2 plasmid-free wt recipient that have received the TAPs (TAP-transc.#2) (as depicted in the above diagram). Mean and SD are calculated from at least three independent experiments. Donors TAP-dCas9-nsp (LY1524), TAP-Cas9-nsp (LY1369), TAP-dCas9-OXA48 (LY1523), TAP-Cas9-OXA48 (LY1522) or TAP-PemI-Cas9-OXA48 (LY1549); Recipients R#1 wt/pOXA-48a (LY1507) and R#2 wt (LY945). (B–D) Two-tailed unpaired *t*-tests were performed. ns = non-significant *P*-value >0.05; **P*-value <0.05, ***P*-value <0.0021; *****P*-value <0.0001.

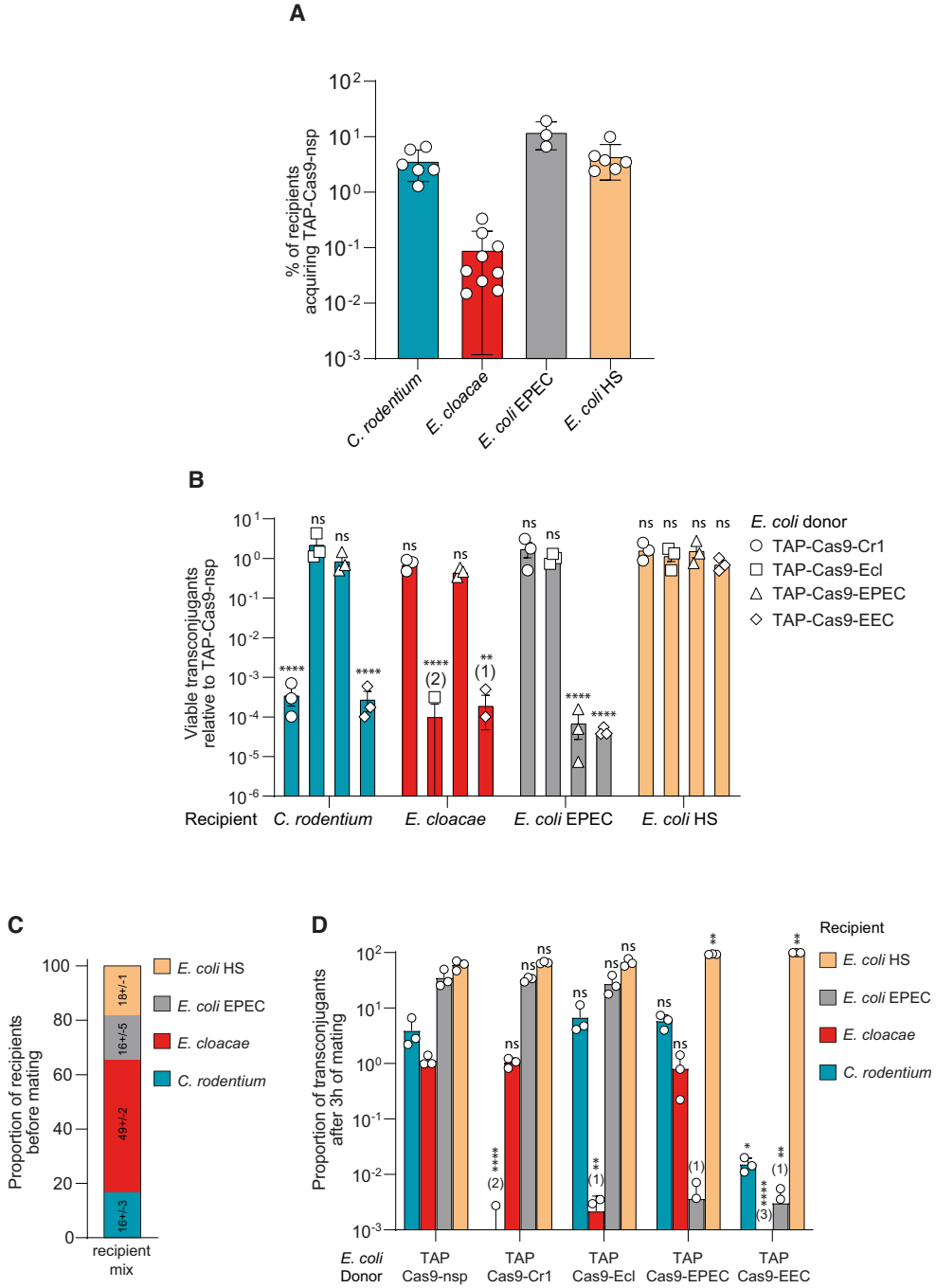

Figure 5. Efficient and strain-specific killing of TAPs within a multispecies recipient population. (**A**) Efficiency of TAP-Cas9-nsp transfer from *E. coli* (LY1369) donor to *C. rodentium*, *E. cloacae, E. coli* EPEC or HS recipients. Histograms show the percentages of tranconjugants (T/R + T) after 24 h of conjugation for *C. rodentium*, *E. cloacae, E. coli* EPEC recipients and 3 h for *E. coli* HS recipient; mean and SD are calculated from at least three independent experiments. (**B**) TAPs carrying specific spacers identified with the CSTB algorithm were tested against each recipient cells. To account for the variability of TAP transfer in the different recipient strains, the histograms show the relative abundance of viable transconjugants normalized by viable transconjugants obtained for the TAP_{Kn}-Cas9-nsp. Numbers in brackets indicate replicates with detection limit of transconjugants below 10^{-8}. Mean and SD are calculated from 3 independent experiments. One-way ANOVA with Sidak's multiple comparisons test were performed on $\log_{10}$-transformed values and *p*-value show comparison with the TAP-Cas9-nsp data. ns = non-significant *P*-value >0.05; ** *P*-value <0.0021; **** *P*-value <0.0001. (**C**) Proportion of recipients estimated by plating assay before mating with donors. Mean and SD calculated from three independent experiments are indicated for each recipient strains. (**D**) Each TAP carrying specific spacers were tested through conjugation between *E. coli* donors and a recipient population containing all recipient species. Histograms show the proportion of viable transconjugants in the mixed population after 3 h of mating. Numbers in brackets indicate replicates with detection limit of transconjugants below 10^{-8}. Mean and SD are calculated from three independent experiments. One-way ANOVA with uncorrected Fisher's LSD test were performed on the $\log_{10}$-transformed values and *P*-value show comparison with the TAP-Cas9-nsp data. ns = non-significant *P*-value >0.05; * *P*-value<0.05; ** *P*-value<0.0021; **** *P*-value<0.0001. Donors TAP-Cas9-nsp (LY1369), TAP-Cas9-Cr1 (LY1597), TAP-Cas9-Ecl (LY1566), TAP-Cas9-EPEC (LY1618), TAP-Cas9-EEC (LY1665); recipients *C. rodentium* (LY720), *E. cloacae* (LY1410), *E. coli* EPEC (LY1615) or HS (LY1601).

lacZ2 mobilizable plasmids. Using flow cytometry analysis, we quantified the transfer efficiency of these TAPs (carrying the sfGFP green fluorescent reporter) into a lac+ recipient strain that produces the red fluorescent histone-like protein HU-mCherry, encoded on the chromosome (Supplementary Figure S2a). Quantification of the transconjugants exhibiting combined red and green fluorescence show that TAP-Cas9-nsp and TAP-Cas9-lacZ2 are both transferred to ∼65% of the recipient cell population after 3h of mating (Figure 1C and Supplementary Figure S2b). As expected, TAPs transfer requires the presence of the F-Tn*10* plasmid in the donor strain (Supplementary Figure S2c–e). Most importantly, the parallel plating of the conjugation mixes revealed a ∼3.5-log decrease in the viability of TAP-Cas9-lacZ2 transconjugants compared to TAP-Cas9-nsp transconjugants (Figure 1D). This killing activity is also reflected by the lack of increase in the total recipient cells count during the three hours of mating with the TAP-Cas9-lacZ2 donor strain, compared to a ∼20-fold increase with TAP-Cas9-nsp donors (Figure 1E). Importantly, no killing effect is observed for either TAPs when using the isogenic lac- recipient strain lacking the targeted *lacZ* locus (Supplementary Figure S2f). These results show that TAP-Cas9-nsp and TAP-Cas9-lacZ2 are transferred with equal efficiency through the F-Tn*10* conjugation machinery. Yet, the acquisition of TAP-Cas9-lacZ2, but not TAP-Cas9-nsp, is associated with a loss of viability of the transconjugant cells.

Using live-cell microscopy, we characterized the cellular response of the recipient cells to the acquisition of TAPs (Figure 2). In these experiments, the TAPs carry the sfGFP reporter system that confers green fluorescence to the donor and transconjugant cells. The lac+ recipient cells produce the nucleoid-association protein HU-mCherry, which localization reveals the global organization of the chromosome. As expected, the acquisition of the TAP-Cas9-nsp reported by the production of sfGFP green fluorescence in red recipient cells has no impact on growth, cell morphology or nucleoid organization (Figure 2A–C and movie 1). By contrast, the acquisition of the TAP-Cas9-lacZ2 triggers the rapid disorganization of the nucleoid that grows into an unstructured DNA bulk, followed by cells filamentation and occasional cell lysis (Figure 2A–C and movie 2). Furthermore, we analyzed in recipient cells the localization pattern of a RecA-GFP fusion, which has been reported to polymerize into large intracellular structures in response to DNA-damage induction (27). In this experiment, TAPs carry the mCherry reporter system that confers red fluorescence to donors and transconjugant cells. Image analysis reveals that the acquisition of the TAP-Cas9-lacZ2 (Figure 2D and movie 4), but not the TAP-Cas9-nsp (Figure 2D and movie 3), is followed by cells filamentation (Figure 2E) as well as the RecA-GFP polymerization, which was quantified using fluorescence skewness analysis (Figure 2F, see Materials and Methods). Nucleoid disorganization, cell filamentation and RecA-GFP bundle formation confirm that TAP-Cas9-lacZ2 acquisition is followed by CRISPR-mediated induction of DSBs that result in the death of the transconjugants.

TAPs-mediated selective killing within a mixed *E. coli* recipient population

We verified the specificity of TAPs-mediated killing within a mixed recipient population composed of the targeted lac+ and the non-targeted lac- *E. coli* strains. We observed a ∼4 log-fold decrease in viable lac+ transconjugants compared to lac- transconjugants when using the TAP-Cas9-lacZ2, while no difference is observed with the TAP-Cas9-nsp (Figure 3A). TAP-Cas9-lacZ2 specific killing activity is also reflected by the stagnation of the targeted lac+ recipient total population, while the non-targeted lac- population is able to grow during the 6 h of mating (Figure 3B). We performed live-cell microscopy imaging where the lac+ and lac– recipients are distinguished by the typical localization pattern of nucleoid associated HU-mCherry and the replisome associated DNA clamp DnaN-mCherry, respectively. Time-lapse analysis shows that both strains receive the plasmids reported by the increase of green fluorescence, yet only the targeted lac+ transconjugants exhibits cell filamentation, symptomatic of Cas9-mediated DNA-damage induction (Figure 3C). These results recapitulate the effects obtained when using individual recipient strains, and demonstrate that the TAPs achieve selective killing of the targeted strain within a mixed population.

Analysis of TAP-escape mutants

Transfer of the TAP-Cas9-lacZ2 is associated with a ∼3.5-log viability loss of the lac+ transconjugant cells, yet we noticed a proportion of transconjugants that are able to survive despite the acquisition of the TAP (Figure 1D). Genotyping and sequence analysis of 31 clones escaping the TAP-Cas9-lacZ2 activity revealed two types of escape mutants (Supplementary Figure S3a and b). One third (12 out of 31) have acquired a transposase or IS insertion in the plasmid-born *cas9* gene, thus inactivating the CRISPR system. Two-thirds have acquired mutations that modify the targeted *lacZ* chromosome locus, either by small or large deletions (12 out of 31) as already described (15), or by single point mutation in the seed region of the PAM (7 out of 31), which was shown to be key for recognition by the Cas9–gRNA complex (28) (Supplementary Figure S3c).

TAPs directed against carbapenem-resistant population

Conjugative plasmids are major contributors to the spread of multi-drug resistance in bacteria (29), those conferring carbapenem resistance being of severe clinical concern (30). The IncL/M pOXA-48a plasmid carries the bla_{OXA-48} gene that encodes the OXA-48 carbapenemase, which confer resistance to carbapenem and other beta lactams, such as imipenem and penicillin (31). We designed TAPs targeting the pOXA-48a and assessed their ability to sensitize the plasmid-carrying population to ampicillin. Using an OXA48 spacer that targets the 5′-end of the bla_{OXA-48} gene, we constructed the TAP-Cas9-OXA48 to induce Cas9-mediated DSBs on pOXA-48a, and the TAP-dCas9-OXA48 to inhibit bla_{OXA-48} gene transcription by CRISPRi (Figure 4A). Transfer of TAP-Cas9-OXA48 and

TAP-dCas9-OXA48 plasmids into pOXA-48a-carrying *E. coli* recipients lead to a ∼4.5-log decrease in ampicillin resistance level, while the TAP-Cas9-nsp or the TAP-dCas9-nsp have no effect (Figure 4B). Unexpectedly, we observe that significantly less viable transconjugant are obtained without ampicillin selection when using the TAP-Cas9-OXA48 compared to TAP-dCas9-OXA48 (Figure 4B). We ruled out the possibility of a decrease in TAP-Cas9-OXA48 transfer ability as all four tested plasmids are acquired with similar frequency by pOXA-48a plasmid-free *E. coli* recipients (Supplementary Figure S4a). However, analysis of the pOXA-48a plasmid sequence revealed the presence of the *pemIK* toxin-antitoxin (TA) system, which is involved in plasmid stability by inhibiting the growth of daughter cells that do not inherit the plasmid (7,32,33). Indeed, the arrest of *pemIK* expression due to plasmid loss results in the rapid depletion of the labile PemI antitoxin, which can no longer repress the toxic activity of the more stable PemK toxin. This regulation was reported using CRISPR-associated phage therapy to cure antibiotic resistance carried by the pSHV-18 plasmid (7). We then hypothesized that the observed reduction of viable TAP-Cas9-OXA48 transconjugants could be due to PemK toxic activity in cells that have lost of the pOXA-48a targeted by the Cas9 cleavage. This possibility was confirmed by inserting a constitutively expressed antitoxin *pemI* gene into the TAP-Cas9-OXA48, which results in a ∼1.5 log increase in transconjugants viability, while retaining the inhibition of ampicillin resistance (Figure 4B).

We further investigated the long-term evolution of resistance of the strain carrying the pOXA-48a during conjugation with a TAP donor. We observed that while the TAP-dCas9-nsp had no effect, the transfer of the TAP-dCas9-OXA48 and the resulting re-sensitization of the recipient population to ampicillin reached equilibrium after 24 h (Supplementary Figure S4b). From this point on, a stable 90% of the recipients have received the TAP-dCas9-OXA48 and became sensitive to ampicillin. We hypothesized that the remaining 10% of ampicillin-resistant recipient cells could result from the acquisition of the F-Tn*10* plasmid only, thus resulting in the establishment of the F-encoded exclusion systems in the recipient cells and the permanent inability to acquire the TAP through a subsequent conjugation event. This hypothesis was confirmed by showing that all ampicillin-resistant recipients present in the population after 1 and 7 days of co-culture do contain the F-Tn*10* plasmid but not the TAP-dCas9-OXA48 (Supplementary Figure S4c). One way to modulate the transfer efficiency of the mobilizable TAPs would be to prevent the transfer of the F plasmid by deletion of its origin of transfer. First, this would prevent the acquisition of the F plasmid only and the consequent establishment of the exclusion mechanism in the recipient cells. Second, the recipient cells that receive the TAP only would be unable to transmit it to other recipient bacteria due to the absence of the F-encoded conjugation machinery. In this situation, TAPs are expected to disseminate more slowly, but potentially to all recipient cells in the population.

The pOXA-48a is an autonomous conjugative plasmid that disseminates among *Enterobacteriaceae*, raising the possibility that the recipient containing the pOXA-48a could transfer ampicillin resistance to the TAPs-donors during mating. We observed that ampicillin resistance is indeed transmitted to ∼0.2% and 0.12% of donors carrying the TAP-dCas9-nsp or the TAP-Cas9-nsp (Figure 4C). However, donors carrying the TAP-dCas9-OXA48 or the TAP-Cas9-OXA48 do not acquire ampicillin resistance (Figure 4C). Assuming that the efficiency of pOXA48 transfer is insensitive to the presence of the TAPs in the cells, this result suggests that TAPs directed against OXA48 impedes the development of resistance, even if the pOXA48 plasmid is acquired. We tested this possibility by performing the same conjugation experiments with an additional plasmid-free recipient wt strain (R#2) in the conjugation mix (see diagram in Figure 4D). Among R#2 cells that have received the TAP-Cas9-nsp or the TAP-dCas9-nsp, ∼0.24% and 0.15% become ampicillin resistant, respectively. However, no ampicillin resistance is observed in R#2 cells that have received the TAP-Cas9-OXA48 or the TAP-dCas9-OXA48 (Figure 4D). Altogether, these results demonstrate that directing TAPs against the $bla_{OXA\text{-}48}$ gene is an efficient strategy to sensitize the pOXA-48a-carrying strain to ampicillin. In addition, TAPs also appear to impede drug-resistance dissemination by protecting the donor and other plasmid-free recipients from developing the resistance.

CSTB software: targeting specific strains within multispecies bacterial population

Numerous bioinformatic tools have been developed to identify and design gRNA spacers specific of one species (34). However, designing TAPs that perform antibacterial activity against specific bacterial species, without affecting other bacterial strains, requires the robust identification of spacer sequences that are present in the genome of the targeted organism(s), but not in the genomes of other non-targeted strains. Since no such tools existed to achieve this task, we developed a 'Crispr Search Tool for Bacteria' CSTB algorithm (https://cstb.ibcp.fr.) that enables the comparative analysis of ∼18–23 nt long spacer sequences across a wide range of bacterial genomes and plasmids. The CSTB backend database indexes all occurrences of these motifs present in 2919 complete genomes classified according to the NCBI taxonomy. CSTB allows identifying appropriate spacer sequences to reprogram TAPs against unique or multiple sites in the targeted chromosome or plasmid DNA.

We asked the CSTB algorithm to generate spacer sequences that target the attachment/effacement (A/E) pathogen *Citrobacter rodentium* strain ICC168 (Cr spacers), or the enteropathogenic *E. coli* EPEC strain E2348/69 (EPEC spacer), or the nosocomial pathogen *Enterobacter cloacae* (Ecl spacer), or the three of them (EEC spacer), without targeting other bacterial genome present in the database. TAPs directed against *C. rodentium* carry a Cr1 spacer that target a unique locus, or a Cr22 that targets 22 loci distributed throughout the genome (Supplementary Figure S5a). Transfer of TAP-Cas9-Cr1 from an *E. coli* donor reduces by 4-log the viability of *C. rodentium* transconjugant cells (Supplementary Figure S5b). Live-cell microscopy revealed that TAP-Cas9-Cr1 acquisition induces *C. rodentium* filamentation and lysis, while no growth defect was induced by the TAP-Cas9-nsp (Supplementary Figure S5c and d; movies 5 and 6). This indicates that, as

observed in *E. coli,* the induction of a single DSB by the Cas9 is lethal to *C. rodentium*. Consistently, targeting 22 chromosome loci by the TAP-Cas9-Cr22 results in comparable transconjugant killing efficiency (Supplementary Figure S5b). However, multiple targeting unbalances the contribution of the mechanisms by which transconjugants escape to the TAPs activity. Analysis of twenty clones escaping Cr1 single targeting revealed either deletions of the targeted chromosomal locus or inactivation of the CRISPR system on the TAP, in equal proportion. By contrast, all 19 clones escaping the Cr22 multiple targeting carry mutations that inactivate the TAP CRISPR system (Supplementary Figure S6). This is consistent with the prediction that mutations of the 22 targeted chromosome sites within the same call is highly infrequent, if even possible.

TAP transfer through F conjugation machinery is highly efficient towards MG1655 *E. coli* laboratory strain reaching up to 90% efficiency in 3h of mating (Figures 1, 2 and Supplementary Figure S2). We quantified the efficiency of TAP-Cas9-nsp transfer in non-laboratory strain and observed a disparity between recipients with an overall ∼7- to 900-fold decrease in TAP acquisition frequency in comparison to MG1655 *E. coli* (Figure 5A). To account for this variability, we normalized the frequency of viable transconjugants obtained for TAP-Cas9-Cr1, -Ecl, -EPEC and -EEC to the frequency of TAP-Cas9-nsp transconjugants in the corresponding bacterial strain (Figure 5B). We quantified that the TAP-Cas9-Cr1 induces a transconjugant viability loss only in *C. rodentium*, TAP-Cas9-Ecl in *E. cloacae*, TAP-Cas9-EPEC in *E. coli* EPEC, while the TAP-Cas9-EEC targets the three pathogenic strains. As a control, we show that the commensal *E. coli* HS recipient, which genome is not targeted by any spacer, is affected by none of these antibacterial TAPs (Figure 5B). These results demonstrate that the spacer sequences generated by the CSTB algorithm allow the robust reprograming of the TAPs for efficient and strain-specific antibacterial activity on mono-species recipient populations. It also demonstrates that one given TAP can target several species at the time.

Next, we addressed TAPs ability to induce strain-specific antibacterial activity within a multi-species recipient population composed of the three pathogenic strains and the commensal *E. coli* HS (Figure 5C). The proportion of transconjugants obtained after 3 h of mating with TAP-Cas9-nsp varies (Figure 5D) and reflects the efficiency of TAP transfer among the different recipient strains (Figure 5A). We observed that within the multispecies recipient mix, *C. rodentium* transconjugant viability is dramatically reduced by TAP-Cas9-Cr1, that of *E. cloacae* by TAP-Cas9-Ecl and that of *E. coli* EPEC by TAP-Cas9-EPEC, while all three species are affected by the triple-targeting TAP-Cas9-EEC. The viability of transconjugants of the control commensal *E. coli* HS is not affected by any of the antibacterial TAPs (Figure 5D). These results validate that TAPs achieve selective killing within a multispecies mixed recipient population without affecting the non-targeted species. Although the antibacterial TAPs impact selectively the viability of the transconjugant populations, their activity is not significantly reflected by the total recipient counts of each species (Supplementary Figure S7), due to the limited efficiency of TAP transfer to the pathogenic recipient strains and the differential fitness of these strains in competition within the conjugation mix.

DISCUSSION

Tools for *in situ* microbiota manipulation are currently in their infancy. Here, we demonstrate the ability of the TAP antibacterial strategy to exert an efficient and strain-specific antibacterial activity within multi-species populations *in vitro*. TAPs selective-killing activity induces a ∼4-log viability loss of the tested species. TAPs targeting the pOXA-48a carbapenem resistance-plasmids results in a 4- to 5-logs increase of the strain susceptibility to the drug. Most CRISPR delivery methodology currently in development focus on the use of bacteriophages, which have intrinsically narrow host-range (35,36,7). Besides, several recent studies successfully use the broad host range RK2 conjugation systems to deliver CRISPR system that target *E. coli* (7–9,37) or *S. enterica* (11) *in vitro*. One key advantage of our strategy over these approaches is the versatility conferred by the CSTB algorithm that enables the robust identification of gRNA that should be used to specifically re-target the TAPs against one or several bacterial strains of interest, without targeting other species. Despite the availability of numerous programs dedicated to the identification of CRISPR motifs, the CSTB has no equivalent so far (34). Another advantage is the modular design and the relatively small size of the mobilizable TAPs (compared to autonomous conjugation plasmids) that are easily modifiable. The spacer sequence that directs the TAP against the targeted strain(s), as well as the other constituent biobricks (origin of replication, origin of transfer, Cas9, resistance gene) can be changed in one-step-cloning (see methods), thus enabling the rapid construction of a library of TAPs adapted to the considered applications. Finally, the constitutive expression of the CRISPR system (and the fluorescent reporters) from promoter that are active in a wide range of Enterobacteriaceae avoids the requirement for an external inductor, rendering the TAP approach more suitable for the modification of natural bacterial communities *in vivo*.

TAPs designed to induce Cas9-mediated double-stranded-breaks (DSBs) to the chromosome of the targeted bacteria trigger significant viability loss. However, we observe the emergence of targeted bacteria that have evolved mutations allowing them to survive despite the acquisition of the TAP. The frequency of these TAP-escape mutants varies from $\sim 3 \times 10^{-4}$ to 6×10^{-5} depending on the spacer and the recipient strains used (Figures 1D, 3A, 4B and 5B). The phenotypic and sequence analysis of *E. coli* and *C. rodentium* escape-mutants reveal two main mechanisms to escape TAP activity: (i) The first mechanism is the acquisition of insertions (transposase or Insertion Sequences, IS) or single nucleotide deletions that inactivate the *cas9* gene carried by the TAP. These types of mutations allowing bacteria to escape CRISPR activity have been previously reported to occur with comparable frequency (7,38,39,11). It has also been reported that mutations or deletions within either tracrRNA or crRNA sequences is another way to inactivate CRISPR systems (7,40,39,38). Yet, no such mutations were found in the *C. rodentium* nor *E. coli* TAP-escape mutants analysed,

potentially due to their lesser frequency of occurrence. (ii) The second mechanism we have identified is the acquisition of point mutations or deletion that modify the targeted locus, thus impeding the recognition by the gRNA. These were also previously described (15,28,11,38,7). When using TAPs that target one chromosome locus in *E. coli* and *C. rodentium*, escape-mutations occur by *cas9*-inactivation (first mechanism) in 38.7 and 42.8%, and by modification of the targeted locus (second mechanism) in 61.3% and 57.2%, correspondingly.

We show that the contribution of escape mutations by modification of the chromosome sequence can be dramatically, if not completely reduced by directing the TAPs against multiple chromosome loci. Indeed, the probability of mutating multiple chromosome sites within the same bacterial cell is expected to decrease as the number of targeted sites increases. When using the Cr22 spacer that targets 22 loci of *C. rodentium* chromosome, all the nineteen escape-mutants tested carry mutations that inactivate the TAP-born *cas9* gene. Consequently, we observe a 2.9-fold decrease in the frequency of TAP-Cas9-Cr22 escapers (8.56×10^{-5}) compare to TAP-Cas9-Cr1 (2.47×10^{-4}) that targets one single chromosome locus. This decrease is consistent with our estimates of the relative contributions of each escape mechanisms.

The observed frequency of escape mutations by *cas9* inactivation is likely related to the intrinsic rate of transposition estimated to oscillate between 10^{-5} to 10^{-6} in *E. coli* (41) and the rate of spontaneous mutations (10^{-8} and 10^{-10} per base pair and generation). In the case of TAPs, it is also possible that the induction of DSBs results in the increase of the mutation rates through the triggering of SOS-induced hypermutator phenotype. Cui and Bikard demonstrated that one way to improve CRISPR efficiency in *E. coli* host cell is to inhibit RecA activity, which is essential to DSB repair and to the induction of the SOS-response (15). Moreb *et al.* further proposed to inhibit RecA activity by co-expressing the CRISPR system with a dominant negative allele of the *recA* gene (42). These strategies are however less relevant in the case of the TAPs approach, as they would likely alter the recombination proficiency and thus the viability of the untargeted population.

We also addressed the possibility that part of the mutations in TAPs already emerge in the donor cells, thus resulting in the transfer of already inactive TAPs into the recipient target. This possibility is supported by the sequencing analysis of one *C. rodentium* escape mutant that has received TAP-Cas9-Cr1 from an *E. coli* donor. The sequencing revealed the insertion in *cas9* of *insAB* genes coding for transposase elements present in *E. coli* but absent from *C. rodentium* genomes. This result indicates that mutation leading to TAPs inactivation can occur in the donor cells prior to transfer, without excluding that they might also emerge in the targeted recipient after plasmid acquisition.

Our work reveals that TAPs efficiency is primarily determined by two main limiting factors. The first limiting factor is the $\sim 10^{-4}$–10^{-5} frequency of escaper clones that acquire mutations inactivating the plasmid-born *cas9* gene, or mutations that modify the targeted sequence. The occurrence of escaper clones due to the acquisition of TAPs that have been inactivated before transfer could be reduced by using a transposon-free *E. coli* donor strain (43). As shown in *C. rodentium*, the emergence of escaper clones by mutation of the targeted sequence can be avoided by targeting multiple sites on the genome. Alternatively, it has been shown that another way to avoid the emergence of escape mutants through the modification of the chromosome is to target essential genes, which mutation is often lethal for the cell (40). The second limiting parameter is the efficiency of TAPs transfer towards the targeted strain(s). This efficiency primarily depends on the conjugative system chosen to mobilize the TAPs. Here, we use the F plasmid as a helper plasmid that mediates relatively efficient TAPs transfer (10^{-1}–10^{-2}) to closely related Enterobacteriaceae. Therefore, TAPs appear appropriate to target a range of clinically relevant pathogenic or resistant Gram-negative bacteria (*E. coli*, *Citrobacter*, *Enterobacter*, *Klebsiella*, *Salmonella*, *Yersinia*, *Shigella*, *Serratia*,etc.). Recently, the narrow host range pPD1 plasmid has also been used to transfer CRISPR/Cas systems to the Gram-positive *Enterococcus faecalis* (44). Other reported antibacterial (7,11) or anti-drug (8–10) methodology using conjugation are mostly based on the incP RK2 conjugative system, which offer broad-host range, but low efficiency of transfer (10^{-4}–10^{-5}). Hamilton *et al.* have shown that transfer efficiency can be artificial increased using glass beads *in vitro* (11). It is also possible to isolate broad-host range conjugation systems with increased transferability. Such superspreader plasmid mutants have been successfully isolated through Tn-seq approach (45,46) and could represent an valuable option to widen the range of bacteria toward which TAPs could be efficiently transferred.

Translating the present *in vitro* proof of concept to *in situ* settings would represent an important step towards the development of a non-antibiotic strategy for the *in situ* manipulation of microbiota composition, in a directed manner. The efficiency of the TAPs methodology within host-associated bacterial communities would primarily depend on conjugation rates *in situ*, which often differs from rates achieved *in vitro* (47). For instance, it was recently reported that the IncI2 plasmid TP114 and IncX type plasmids are very actively transferred in the mouse intestinal tract (47) and in human fecal microbiomes (48), respectively, making them good candidate to mobilize TAPs in these given ecosystems. TAPs could be used for the inhibition of harmful pathogenic and resistance strains from an infected host or environments, or as anti-virulence strategy through inhibition of virulence effector genes or genes involved in biofilm formation. The future implementation of the TAPs approach in clinical or environmental settings would require the consideration of the rapidly evolving regulations on GMO, CRISPR and biocontainment (49–51).

DATA AVAILABILITY

Software and source codes: The CSTB web service can be freely accessed at https://cstb.ibcp.fr. The software we developed to convert all unique words (spacers) into an integer representation using a 2-bits per base encoding is also available at https://github.com/glaunay/crispr-set. All additional related software can be freely accessed at https://github.com/MMSB-MOBI/CSTB_database_manager.

Flow Cytometry: Data from flow cytometry experiments have been submitted to the FlowRepository (https://flowrepository.org/id/FR-FCM-Z35C and FR-FCM-Z35E).

SUPPLEMENTARY DATA

Supplementary Data are available at NAR Online.

ACKNOWLEDGEMENTS

The authors thank Gregory Jubelin, François Cornet, Claire Prigent-Combaret, Pierre Bogaerts for the gift of strains and plasmids. Lisa Rubio, Brice Simon-Letcher, ShangNong Hu and Timothée Sluys, for earlier involvement in the project.
Author contributions: C.L. provided funding. C.L. and S.B. conceived the project, designed the study and wrote the paper. A.R., A.D. and S.B. performed the experiments and analyzed the data. The CSTB algorithm was conceived by G.L., C.H. and S.L. in discussion with E.G., S.B. and C.L. All the authors gave intellectual input throughout the project.

FUNDING

French National Research Agency [ANR-19-ARMB-0006-01]; Schlumberger Foundation for Education and Research [FSER2019]; Foundation for Innovation in Infectiology [FINOVI-2014]; Foundation pour la Recherche Médicale [FRM-ECO201806006855 to A.R.]. Funding for open access charge: French National Research Agency [ANR-19-ARMB-0006-01].
Conflict of interest statement. None declared.

REFERENCES

1. WHO (2015) In: *Global Priority List of Antibiotic-Resistant Bacteria to Guide Research, Discovery, and Development of New Antibiotics*. ISBN: 9789241509763.
2. Jinek,M., Chylinski,K., Fonfara,I., Hauer,M., Doudna,J.A. and Charpentier,E. (2012) A programmable dual-RNA-guided DNA endonuclease in adaptive bacterial immunity. *Science*, **337**, 816–821.
3. Gasiunas,G., Barrangou,R., Horvath,P. and Siksnys,V. (2012) Cas9-crRNA ribonucleoprotein complex mediates specific DNA cleavage for adaptive immunity in bacteria. *Proc. Natl. Acad. Sci. U.S.A.*, **109**, E2579–E2586.
4. Qi,L.S., Larson,M.H., Gilbert,L.A., Doudna,J.A., Weissman,J.S., Arkin,A.P. and Lim,W.A. (2013) Repurposing CRISPR as an RNA-guided platform for sequence-specific control of gene expression. *Cell*, **152**, 1173–1183.
5. Bikard,D., Jiang,W., Samai,P., Hochschild,A., Zhang,F. and Marraffini,L.A. (2013) Programmable repression and activation of bacterial gene expression using an engineered CRISPR-Cas system. *Nucleic Acids Res.*, **41**, 7429–7437.
6. Anders,C., Niewoehner,O., Duerst,A. and Jinek,M. (2014) Structural basis of PAM-dependent target DNA recognition by the Cas9 endonuclease. *Nature*, **513**, 569–573.
7. Citorik,R.J., Mimee,M. and Lu,T.K. (2014) Sequence-specific antimicrobials using efficiently delivered RNA-guided nucleases. *Nat. Biotechnol.*, **32**, 1141–1145.
8. Dong,H., Xiang,H., Mu,D., Wang,D. and Wang,T. (2019) Exploiting a conjugative CRISPR/Cas9 system to eliminate plasmid harbouring the mcr-1 gene from Escherichia coli. *Int. J. Antimicrob. Agents*, **53**, 1–8.
9. Ruotsalainen,P., Penttinen,R., Mattila,S. and Jalasvuori,M. (2019) Midbiotics: conjugative plasmids for genetic engineering of natural gut flora. *Gut Microbes.*, **10**, 643–653.
10. Wang,P., He,D., Li,B., Guo,Y., Wang,W., Luo,X., Zhao,X. and Wang,X. (2019) Eliminating mcr-1-harbouring plasmids in clinical isolates using the CRISPR/Cas9 system. *J. Antimicrob. Chemother.*, **74**, 2559–2565.
11. Hamilton,T.A., Pellegrino,G.M., Therrien,J.A., Ham,D.T., Bartlett,P.C., Karas,B.J., Gloor,G.B. and Edgell,D.R. (2019) Efficient inter-species conjugative transfer of a CRISPR nuclease for targeted bacterial killing. *Nat. Commun.*, **10**, 4544.
12. Gibson,D.G., Young,L., Chuang,R.-Y., Venter,J.C., Hutchison,C.A. and Smith,H.O. (2009) Enzymatic assembly of DNA molecules up to several hundred kilobases. *Nat. Methods*, **6**, 343–345.
13. García-Nafría,J., Watson,J.F. and Greger,I.H. (2016) IVA cloning: a single-tube universal cloning system exploiting bacterial in vivo assembly. *Sci. Rep.*, **6**, 27459.
14. Ducret,A., Quardokus,E.M. and Brun,Y.V. (2016) MicrobeJ, a tool for high throughput bacterial cell detection and quantitative analysis. *Nat. Microbiol.*, **1**, 16077.
15. Cui,L. and Bikard,D. (2016) Consequences of Cas9 cleavage in the chromosome of *Escherichia coli*. *Nucleic Acids Res.*, **44**, 4243–4251.
16. Martínez-García,E., Aparicio,T., Goñi-Moreno,A., Fraile,S. and de Lorenzo,V. (2015) SEVA 2.0: an update of the Standard European Vector Architecture for de-/re-construction of bacterial functionalities. *Nucleic Acids Res.*, **43**, D1183–D1189.
17. Nolivos,S., Cayron,J., Dedieu,A., Page,A., Delolme,F. and Lesterlin,C. (2019) Role of AcrAB-TolC multidrug efflux pump in drug-resistance acquisition by plasmid transfer. *Science*, **364**, 778–782.
18. Crisona,N.J. and Clark,A.J. (1977) Increase in conjugational transmission frequency of nonconjugative plasmids. *Science*, **196**, 186–187.
19. Mavridou,D.A.I., Gonzalez,D., Clements,A. and Foster,K.R. (2016) The pUltra plasmid series: a robust and flexible tool for fluorescent labeling of Enterobacteria. *Plasmid*, **87–88**, 65–71.
20. Bhoite,S., van Gerven,N., Chapman,M.R. and Remaut,H. (2019) Curli biogenesis: bacterial amyloid assembly by the Type VIII secretion pathway. *EcoSal Plus*, **8**, doi:10.1128/ecosalplus.ESP-0037-2018.
21. Vidal,O., Longin,R., Prigent-Combaret,C., Dorel,C., Hooreman,M. and Lejeune,P. (1998) Isolation of an *Escherichia coli* K-12 mutant strain able to form biofilms on inert surfaces: involvement of a new ompR allele that increases curli expression. *J. Bacteriol.*, **180**, 2442–2449.
22. Serra,D.O. and Hengge,R. (2017) Experimental Detection and Visualization of the Extracellular Matrix in Macrocolony Biofilms. In: Sauer,K. (ed). *c-di-GMP Signaling, Methods in Molecular Biology*. Springer, NY, Vol. **1657**, pp. 133–145.
23. Rock,J.M., Hopkins,F.F., Chavez,A., Diallo,M., Chase,M.R., Gerrick,E.R., Pritchard,J.R., Church,G.M., Rubin,E.J., Sassetti,C.M. *et al.* (2017) Programmable transcriptional repression in mycobacteria using an orthogonal CRISPR interference platform. *Nat. Microbiol.*, **2**, 16274.
24. Cho,S., Choe,D., Lee,E., Kim,S.C., Palsson,B. and Cho,B.-K. (2018) High-level dCas9 expression induces abnormal cell morphology in *Escherichia coli*. *ACS Synthetic Biology*, **7**, 1085–1094.
25. Zhang,S. and Voigt,C.A. (2018) Engineered dCas9 with reduced toxicity in bacteria: implications for genetic circuit design. *Nucleic Acids Res.*, **46**, 11115–11125.
26. Misra,C.S., Bindal,G., Sodani,M., Wadhawan,S., Kulkarni,S., Gautam,S., Mukhopadhyaya,R. and Rath,D. (2019) Determination of Cas9/dCas9 associated toxicity in microbes. *Microbios.*, doi:10.1101/848135.
27. Lesterlin,C., Ball,G., Schermelleh,L. and Sherratt,D.J. (2014) RecA bundles mediate homology pairing between distant sisters during DNA break repair. *Nature*, **506**, 249–253.
28. Semenova,E., Jore,M.M., Datsenko,K.A., Semenova,A., Westra,E.R., Wanner,B., van der Oost,J., Brouns,S.J.J. and Severinov,K. (2011) Interference by clustered regularly interspaced short palindromic repeat (CRISPR) RNA is governed by a seed sequence. *Proc. Natl. Acad. Sci. U.S.A.*, **108**, 10098–10103.
29. Barlow,M. (2009) What antimicrobial resistance has taught us about horizontal gene transfer. *Methods Mol. Biol.*, **532**, 397–411.

30. Codjoe,F. and Donkor,E. (2017) Carbapenem resistance: a review. *Medical Sciences*, **6**, 1.
31. Poirel,L., Bonnin,R.A. and Nordmann,P. (2012) Genetic features of the widespread plasmid coding for the carbapenemase OXA-48. *Antimicrob. Agents Chemother.*, **56**, 559–562.
32. Hayes,F. (2003) Toxins-antitoxins: plasmid maintenance, programmed cell death, and cell cycle arrest. *Science*, **301**, 1496–1499.
33. Mnif,B., Vimont,S., Boyd,A., Bourit,E., Picard,B., Branger,C., Denamur,E. and Arlet,G. (2010) Molecular characterization of addiction systems of plasmids encoding extended-spectrum beta-lactamases in Escherichia coli. *J. Antimicrob. Chemother.*, **65**, 1599–1603.
34. Alkhnbashi,O.S., Meier,T., Mitrofanov,A., Backofen,R. and Voß,B. (2020) CRISPR-Cas bioinformatics. *Methods*, **172**, 3–11.
35. Bikard,D. and Barrangou,R. (2017) Using CRISPR-Cas systems as antimicrobials. *Curr. Opin. Microbiol.*, **37**, 155–160.
36. Bikard,D., Euler,C.W., Jiang,W., Nussenzweig,P.M., Goldberg,G.W., Duportet,X., Fischetti,V.A. and Marraffini,L.A. (2014) Exploiting CRISPR-Cas nucleases to produce sequence-specific antimicrobials. *Nat. Biotechnol.*, **32**, 1146–1150.
37. Ji,W., Lee,D., Wong,E., Dadlani,P., Dinh,D., Huang,V., Kearns,K., Teng,S., Chen,S., Haliburton,J. *et al.* (2014) Specific gene repression by CRISPRi system transferred through bacterial conjugation. *ACS Synth. Biol*, **3**, 929–931.
38. Fischer,S., Maier,L.-K., Stoll,B., Brendel,J., Fischer,E., Pfeiffer,F., Dyall-Smith,M. and Marchfelder,A. (2012) An archaeal immune system can detect multiple protospacer adjacent motifs (PAMs) to target invader DNA. *J. Biol. Chem.*, **287**, 33351–33363.
39. Jiang,W., Bikard,D., Cox,D., Zhang,F. and Marraffini,L.A. (2013) RNA-guided editing of bacterial genomes using CRISPR-Cas systems. *Nat. Biotechnol.*, **31**, 233–239.
40. Gomaa,A.A., Klumpe,H.E., Luo,M.L., Selle,K., Barrangou,R. and Beisel,C.L. (2014) Programmable removal of bacterial strains by use of genome-targeting CRISPR-Cas systems. *mBio*, **5**, doi:10.1128/mBio.00928-13.
41. Sousa,A., Bourgard,C., Wahl,L.M. and Gordo,I. (2013) Rates of transposition in *Escherichia coli*. *Biol. Lett.*, **9**, 20130838.
42. Moreb,E.A., Hoover,B., Yaseen,A., Valyasevi,N., Roecker,Z., Menacho-Melgar,R. and Lynch,M.D. (2017) Managing the SOS response for enhanced CRISPR-Cas-based recombineering in *E. coli* through transient inhibition of host RecA activity. *ACS Synth. Biol.*, **6**, 2209–2218.
43. Pósfai,G., Plunkett,G., Fehér,T., Frisch,D., Keil,G.M., Umenhoffer,K., Kolisnychenko,V., Stahl,B., Sharma,S.S., de Arruda,M. *et al.* (2006) Emergent properties of reduced-genome Escherichia coli. *Science*, **312**, 1044–1046.
44. Rodrigues,M., McBride,S.W., Hullahalli,K., Palmer,K.L. and Duerkop,B.A. (2019) Conjugative delivery of CRISPR-Cas9 for the selective depletion of antibiotic-resistant Enterococci. *Antimicrob. Agents Chemother.*, **63**, e01454-19.
45. Yamaichi,Y., Chao,M.C., Sasabe,J., Clark,L., Davis,B.M., Yamamoto,N., Mori,H., Kurokawa,K. and Waldor,M.K. (2015) High-resolution genetic analysis of the requirements for horizontal transmission of the ESBL plasmid from *Escherichia coli* O104:H4. *Nucleic Acids Res.*, **43**, 348–360.
46. Poidevin,M., Sato,M., Altinoglu,I., Delaplace,M., Sato,C. and Yamaichi,Y. (2018) Mutation in ESBL plasmid from *Escherichia coli* O104:H4 leads autoagglutination and enhanced plasmid dissemination. *Front Microbiol*, **9**, 130.
47. Neil,K., Allard,N., Grenier,F., Burrus,V. and Rodrigue,S. (2020) Highly efficient gene transfer in the mouse gut microbiota is enabled by the Incl2 conjugative plasmid TP114. *Commun. Biol.*, **3**, 523.
48. Munck,C., Sheth,R.U., Freedberg,D.E. and Wang,H.H. (2020) Recording mobile DNA in the gut microbiota using an *Escherichia coli* CRISPR-Cas spacer acquisition platform. *Nat. Commun.*, **11**, 95.
49. Fellmann,C., Gowen,B.G., Lin,P.-C., Doudna,J.A. and Corn,J.E. (2017) Cornerstones of CRISPR-Cas in drug discovery and therapy. *Nat. Rev. Drug Discov.*, **16**, 89–100.
50. Davison,J. and Ammann,K. (2017) New GMO regulations for old: determining a new future for EU crop biotechnology. *GM Crops Food*, **8**, 13–34.
51. Brokowski,C. and Adli,M. (2019) CRISPR ethics: moral considerations for applications of a powerful tool. *J. Mol. Biol.*, **431**, 88–101.

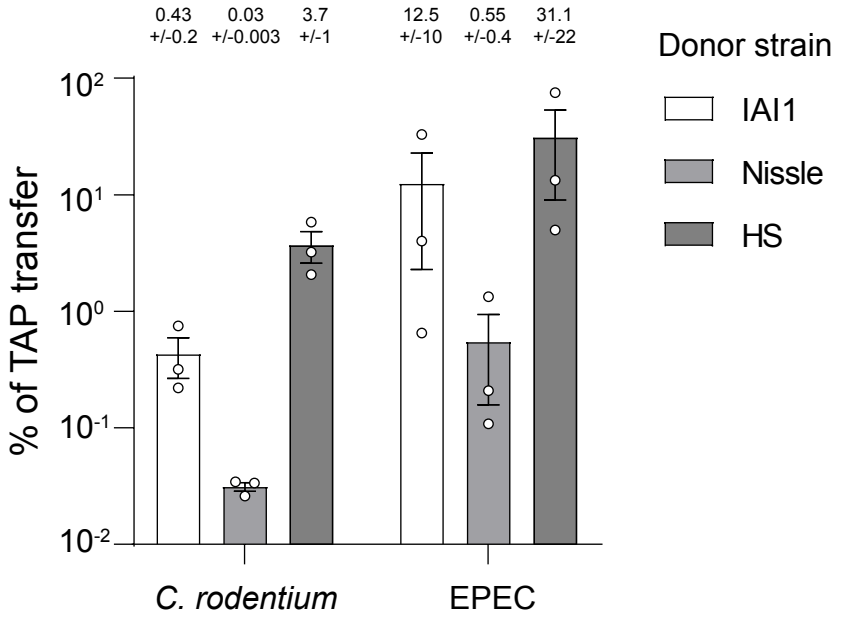

Figure R1 : Comparison of the ability of the commensal *E. coli* strain IAI1, HS and Nissle to transfer the TAP. Histogram showing the TAP-Cas9-nsp transfer efficiency after 3h of mating assay estimated by plating assay. Donor strains: *E. coli* strain HS / F-Tn*10* / TAP-Cas9-nsp (LY1675); IAI1 / F-Tn*10* / TAP-Cas9-nsp (LY1908); Nissle / F-Tn*10* / TAP-Cas9-nsp (LY1676). Recipients: *C. rodentium* (LY720); EPEC (LY1615). Means of percentage of transconjugant (ratio T/R+T) and SEM are calculated from three independant experiments and indicated above the histograms.

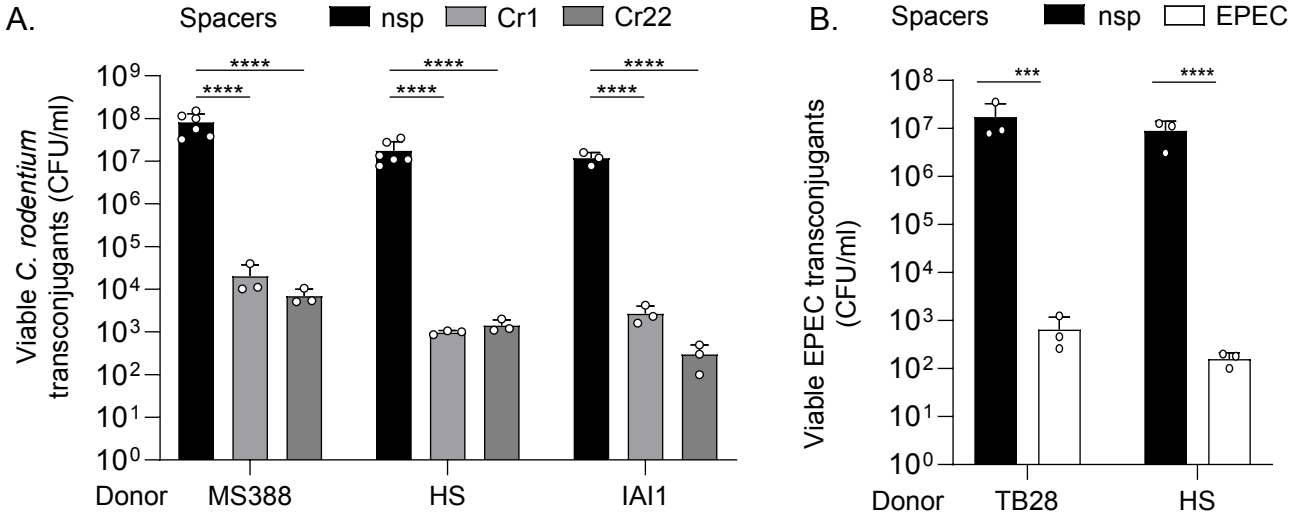

Figure R2 : Comparison of Killing efficiency of *C. rodentium* and EPEC by TAP using different donors A. Histogram showing the viability of *C. rodentium* transconjugants after acquisition of TAP carrying nsp, Cr1 or Cr22 spacer transferred from the *E. coli* donor strain MS388, HS or IAI1. B. Histogram showing the viability of EPEC transconjugants after acquisition of TAP carrying nsp or EPEC spacer transferred from *E. coli* donor strain TB28 or HS. Viability was estimated after 24h of mating. Mean and SEM were calculated from trhee independant experiments. Multiple T-test corrected with Holm-Sidak method were performed on $\log_{10}$ transformed values. **** *P*-value<0.0001 and *** *P*-value<0.001. Donors: MS388 F-Tn*10* TAP-Cas9-nsp (LY1244), MS388 F-Tn*10* TAP-Cas9-Cr1 (LY1239), MS388 F-Tn*10* TAP-Cas9-Cr22 (LY1276), HS F-Tn*10* TAP-Cas9-nsp (LY1675), HS F-Tn*10* TAP-Cas9-Cr1 (LY1723), HS F-Tn*10* TAP-Cas9-Cr22 (LY1846), IAI1 F-Tn*10* TAP-Cas9-nsp (LY1907), IAI1 F-Tn*10* TAP-Cas9-Cr1 (LY1908), IAI1 F-Tn*10* TAP-Cas9-Cr22 (LY1909), TB28 F-Tn*10* TAP-Cas9-nsp (LY1369), TB28 F-Tn*10* TAP-Cas9-EPEC (LY1618), HS F-Tn*10* TAP-Cas9-EPEC (LY1724). Recipients: *C. rodentium* (LY720), EPEC (LY1615).

V.2. Unpublished results

In the publication we showed that the TAP strategy allows the specific targeting and killing of bacterial pathogens *in vitro*. Nonetheless, several modifications could be imagined to improve the efficiency of the TAPs and test its efficiency *in situ*. I first had to adapt the TAP strategy to be used in a murine model. Then I have made several optimization of the system by first testing the effect of a biocontainment of the helper plasmid and secondly by widening the TAPs' host range. Finally, I begun to explore the impact of plasmids' acquisition on fitness of recipient cells.

V.2.1. Use of TAPS *in situ*: selection of murine host adapted donors

In the long term, we expect to use the TAPs in the gut microbiota to fight infections with intestinal pathogens or to decolonize drug resistant strains. The first step is to evaluate and validate the efficiency of TAPs *in situ* using an infection model and try to impede bacterial infection using TAPs. To do so, we have initiated a collaboration with Grégory Jubelin (INRAE Clermont-Ferrand) which has developed mouse models of infection to study the virulence of intestinal pathogens such as *Citrobacter rodentium* and Enteropathogenic *E. coli* (EPEC). The validation of the TAPs presented in the Reuter *et al*. manuscript has been performed using *E. coli* laboratory strains K12 that are not efficient gut colonizers. Indeed, we observed that the MS388 strain is not able to persist in the mouse gut long enough to efficiently disseminate the TAPs, as it is cleared from the gastrointestinal tract of mice in ~24h after gavage. We then chose three *E. coli* commensal strains, IAI1, HS and Nissle, shown to persist in the mouse gut (Leatham *et al.* 2009; Touchon *et al.* 2009). The F-Tn*10* plasmid and TAPs were transferred into these strains and I evaluated their capacity as donors. Figure R1 shows that the *E. coli* strain HS is an efficient donor strain able to transfer TAP-Cas9-nsp into *C. rodentium* and EPEC at an efficiency of 3.7% and 31.1% respectively. TAP-Cas9-nsp carried by the *E. coli* strain IAI1 are also transferred efficiently (0.43% in *C. rodentium* and 12.5% in *EPEC*) while the *E. coli* strain Nissle is not an efficient donor *in vitro*. Based on these results, I have further used the *E. coli* donor strains HS and IAI1 to test the effect of TAPs with spacers targeting *C. rodentium* or EPEC.

Plating of the conjugation mixes between laboratory or commensal *E. coli* donors and *C. rodentium* recipients revealed a ~3 to 4 log decrease in the viability of the TAP-Cas9-Cr1 and TAP-Cas9-Cr22 *C. rodentium* transconjugants compared to TAP-Cas9-nsp transconjugants (Figure R2A). Furthermore, the TAP-Cas9-EPEC transferred by the laboratory *E. coli* strain TB28 or the commensal *E. coli* strain HS is able to kill efficiently EPEC recipient strain as we observed a ~4 log decrease in the viability of transconjugants (Figure R2B). These results showed that the commensal strains are efficient donors in killing experiments *in vitro*. These donors have been sent to the lab of Gregory Jubelin which performed preliminary tests to treat mice infected with *C. rodentium*. As the better conjugation efficiency was observed for the HS strain, this strain was used for *in vivo* assays.

First tests were conducted with HS strain containing F-Tn*10* and TAP-Cas9-nsp or TAP-Cas9-Cr22 (Figure R3). Mice were infected (I) or not (NI) with *C. rodentium* at day 0. Then the mice were fed at days 1, 3, 5, 7 and 9 or only at day 1 (brown curve) with *E. coli* donor strain HS carrying the F-Tn*10* and the TAP-Cas9-nsp or TAP-Cas9-Cr22 (Figure R3). Feeding non-infected mice with the donor strains does not impact their viability. Infection of mice with *C. rodentium* leads to the death of all the mice after 11 days. Treatment of mice with donor strains containing either the TAP-Cas9-nsp or the TAP-Cas9-Cr22 improve their survival rate. Indeed, in the two cases we observe a final survival rate of 60%. No significant effect of the

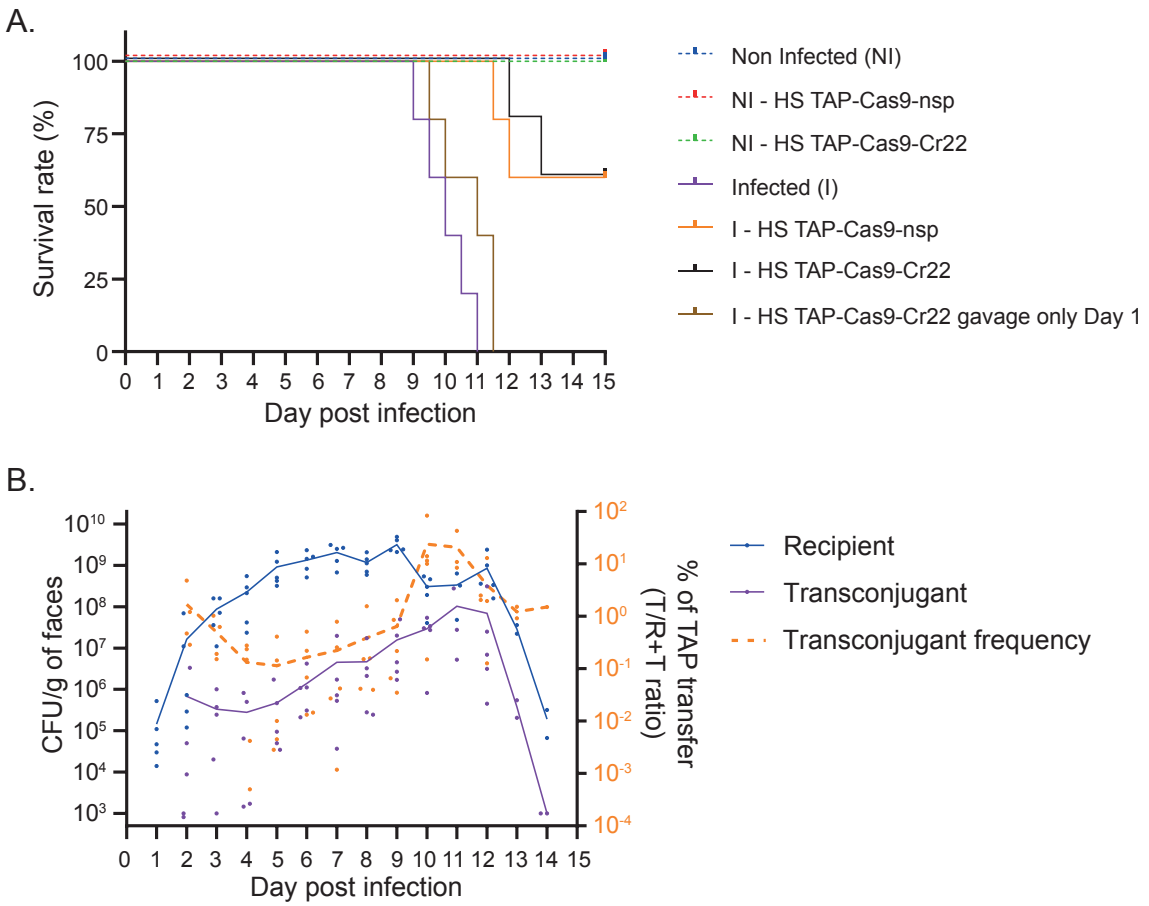

Figure R3 : Efficiency of TAP in a mouse model *in vivo*.
A. Survival rate of mice infected (I) or not (NI) with *C. rodentium* after addition of *E. coli* donor strain HS carrying the TAP-Cas9-nsp or the TAP-Cas9-Cr22 at days 1,3, 5, 7 and 9. B. Analysis of the proportion of CFU/g of feces of *C. rodentium* recipient and transconjugant during the addition of the *E. coli* strain HS carrying the TAP-Cas9-nsp . Transconjugant frequency estimated by the ratio T/R+T was calculated and reported on the graph (right axis, orange curve). Donors : HS F-Tn*10* TAP-Cas9-nsp (LY1675), HS F-Tn*10* TAP-Cas9-Cr22 (LY1846). Recipient : *C. rodentium* (LY720)

TAP-Cas9-Cr22 over the TAP-Cas9-nsp was detected. This suggests that the improvement of the survival rate observed in presence of both TAPs is most certainly due to a competition between HS and *C. rodentium* in the mouse gut. Further analysis on *C. rodentium* content in the feces of mice revealed that transconjugant frequency (T/R+T) ratio of TAP-Cas9-nsp vary between 10 and 0.1 % with an average of 4 %. This shows that conjugation occurs in the gut of the mouse, however it is not efficient enough to lower the relative abundance of *C. rodentium*. These preliminary results show the importance to improve the system and increase the frequency of conjugation in the gut which is the bottleneck of the strategy used here.

Thus, the principal amelioration of TAPs will be the utilization of conjugative systems that are reported to be efficient in the gut microbiota. In particular, is was shown that the $IncI_2$ plasmid TP114 is a good candidate for this environment (Neil *et al.* 2020, 2021). Thus using this plasmid as a helper plasmid could improve the TAP strategy.

V.2.2. TAP optimization

V.2.2.1. Biocontainment to prevent the transfer of the helper plasmid

As previously mentioned, in the TAP strategy the helper F-Tn*10* plasmid (providing the conjugative machinery to mobilize the TAP plasmid) is autonomous and can be transferred into the targeted recipient. Among reviewed papers that use CRISPR-Cas systems combined with conjugative machineries, two employ an helper RP4 plasmid integrated on the chromosome of the donor strain (Citorik, Mimee and Lu 2014; Ji *et al.* 2014). All the other studies use an autonomous helper plasmid (Ruotsalainen *et al.* 2019) or combined their helper plasmid with their CRISPR plasmid (Dong *et al.* 2019; Hamilton *et al.* 2019; Rodrigues *et al.* 2019). In the case of autonomous helper plasmid, it could be the only one transferred and not the CRISPR plasmid (or TAP in our case). The acquisition of the helper plasmid alone can have counter-productive effects. Notably, cells that have received the helper plasmid only would become unable to receive the TAP plasmid due to the expression of the exclusion systems from the already acquired helper plasmid. On the other hand, in the case of the acquisition of both F-Tn*10* plasmid and TAP, the transconjugant cell will become a new donor which is not our goal. The transfer of the helper plasmid carrying antibiotic resistance could contribute to the dissemination of resistance into bacterial populations. This is indeed the case of the F-Tn*10* helper plasmid that carries tetracycline resistance genes.

In the Reuter *et al.* paper, we evaluated the efficiency of the TAP to resensitize a pOXA-48a carrying recipient population to ampicillin over a week mating experiment. We were able to show that 90 % of the recipient cells were resensitized to ampicillin after 24h of mating but this proportion did not decrease after this time. We found that the remaining 10 % recipient population only received the F-Tn*10* plasmid resulting in the establishment of the F-encoded exclusion systems and the permanent inability to acquire the TAP by a subsequent conjugation event. Constituently with these results, a study using an autonomous helper plasmid indeed showed that it tends to be transferred alone in recipient strains (Ruotsalainen *et al.* 2019). We suggested that using a non-transferrable F-Tn*10* plasmid deleted of its origin, the TAP could potentially transfer to all the recipient population and resensitize it more efficiently.

In the article, we already showed that mobilization of the TAP could be mediated by a non-mobilizable F-Tn*10*-Δ*oriT* plasmid. Thus, I conducted a long-term experiment using a donor strain containing the F-Tn*10* Δ*oriT* plasmid to see if this would limit the appearance of the population that does not receive the TAP. I performed mating assays between donor strains carrying F-Tn*10*-Δ*oriT* and TAP-dCas9-nsp or TAP-dCas9-OXA48 against a recipient

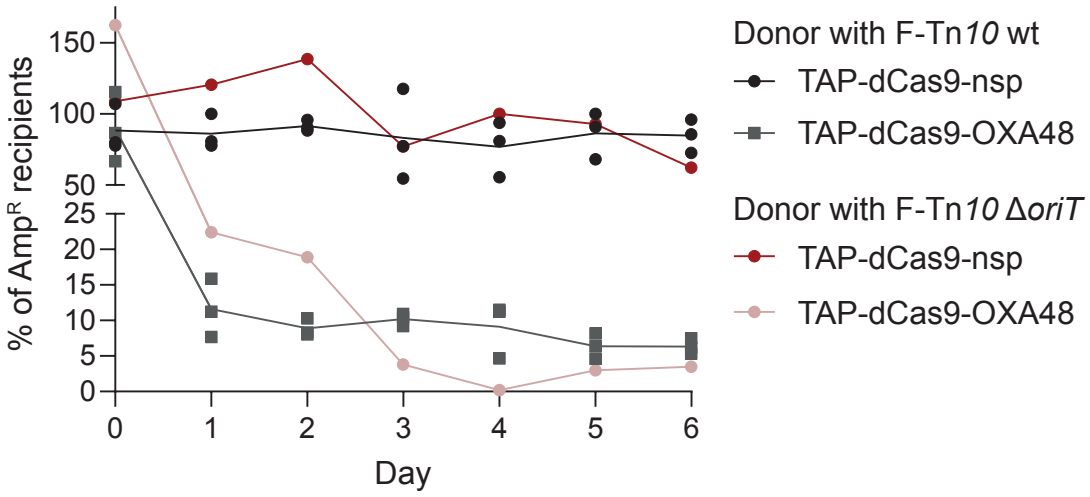

Figure R4 : preventing the transfer of the F-Tn*10* helper plasmid increases the resensitization of the pOXA48a-carrying recipient cells.
Graph showing the proportion of ampicillin resistant recipient strains carrying pOXA-48a plasmid over a 6 days co-culture with either TAP-dCas9-nsp or TAP-Cas9-OXA48 donors carrying the F-Tn*10* or F-Tn*10* Δ*oriT* plasmids. Line represent the mean of replicates. Donors with F-Tn*10* : TAP-dCas9-nsp (LY1524), TAP-dCas9-OXA48 (LY1523). Donors with F-Tn*10* Δ*oriT* : TAP-dCas9-nsp (LY1973), TAP-dCas9-OXA48 (LY1975).Recipient containing the pOXA-48a (LY1507).

strain carrying the pOXA-48a which holds the *bla*$_{OXA-48}$ gene targeted by TAP-dCas9-OXA48. Only one replicate was realized for this experiment and this should be reproduced to ensure its trustworthiness. Figure R4 shows that using the F-Tn*10* Δ*oriT* helper plasmid, at day 1 and 2, 20 % of the recipient strain remain resistant to ampicillin in comparison of 10 % observed at day 1 with F-plasmid carrying donors. In absence of F transfer, cells receiving the TAP are unable to transmit this plasmid to other bacteria. The delay observed between the wild-type and F-Tn*10*-Δ*oriT* mutant suggest a slower dissemination of the TAP. The ampicillin resistant recipient proportion then drops to 4 % on day 3, to reach 0.2 % on day 4. This shows that even if the transfer of the TAP is delayed by the lack of transfer of the helper plasmid, in the long-term, the TAP-dCas9-OXA48 is transferred to a larger proportion of recipient strains and resensitize to ampicillin a larger proportion of cells. These results indicate that the use of non-transferable helper plasmid is a more efficient strategy in the long term than autonomous helper plasmid.

V.2.2.2. Broadening the host-range of TAPs

The F-Tn*10* plasmid encodes a narrow host-range conjugative system able to transfer only to *Enterobacteriaceae* and we noticed that the transfer is relatively inefficient in other species than *E. coli*. The idea of TAPs is to have a very simple system using a small plasmid in a wide range of applications. In this perspective, we wanted to widen the host-range of the TAPs to be able to target a large set of pathogens. We chose to use the broad-host range RP4 conjugative plasmid as a helper plasmid to transfer TAPs. To do so, TAPs in which *oriT*$_F$ was replaced by the *oriT* of RP4 (*oriT*$_{RK2}$) was constructed in the lab, renamed TAP$_{RK2}$-Cas9-nsp and I used it to test its efficiency on three selected pathogens : *Salmonella enterica* serovar Typhimurium LT2, *Vibrio cholerae* N16961 and *Klebsiella pneumoniae* LM21.

Both *S. enterica* and *V. cholerae* are food-borne pathogens causing typhoid fever and cholera respectively (Pui *et al.* 2011; Clemens *et al.* 2017). The CDC estimates that *Salmonella* cause about 1.35 million infections, 26,500 hospitalizations and 420 death in the US per year (Salmonella Homepage | CDC 2021). Recently, outbreaks of *Salmonella* were reported in diverse food products in the US (CDC 2021a, 2021b). *V. cholerae* was reported to cause 95,000 deaths between 2008 and 2012 (Ali *et al.* 2015) and is still considered as a major public health issue in South-East Asia and Sub-Saharan Africa. *K. pneumoniae* is an opportunistic pathogen which can cause diverse diseases : urinary tract infection, bacteremia, pneumonia and liver abscesses (Wang *et al.* 2020). Nowadays, *K. pneumoniae* is a major threat to human health due to its drug resistance and was included in the ESKAPE list of pathogens (Rice 2008). All three of these pathogens were reported to acquire resistance determinants, notably towards β-lactams (Mąka and Popowska 2016; Verma *et al.* 2019; Wang *et al.* 2020) leading to therapeutic failures (Jajere 2019; Tang *et al.* 2020; Dutta *et al.* 2021; Portes *et al.* 2021).

First, the Figure R5A shows that the TAP$_{RK2}$-Cas9-nsp can be transferred into the three pathogenic recipient strains. However, transfer efficiencies vary between recipient strains as we observed 7.4%, 2.10^{-3} % and 0.386 % efficiency of transfer in *S. enterica*, *V. cholerae* and *K. pneumoniae* respectively.

Using the CSTB server, three spacers were designed to specifically target the chromosome of *S. enterica* sv Typhimurium, *V. cholerae* and *K. pneumoniae,* and renamed respectively St, Vc and Kp. I then constructed the corresponding TAP$_{RK2}$-Cas9-St, TAP$_{RK2}$-Cas9-Vc, TAP$_{RK2}$-Cas9-Kp. Figures 5B, C and D show that all pathogen recipients are efficiently killed after receiving the targeting-TAP. In *Salmonella enterica*, transfer of TAP$_{RK2}$-Cas9-St results in a 4-log loss of transconjugant viability (Figure R5B). Viable *V. cholerae* transconjugants

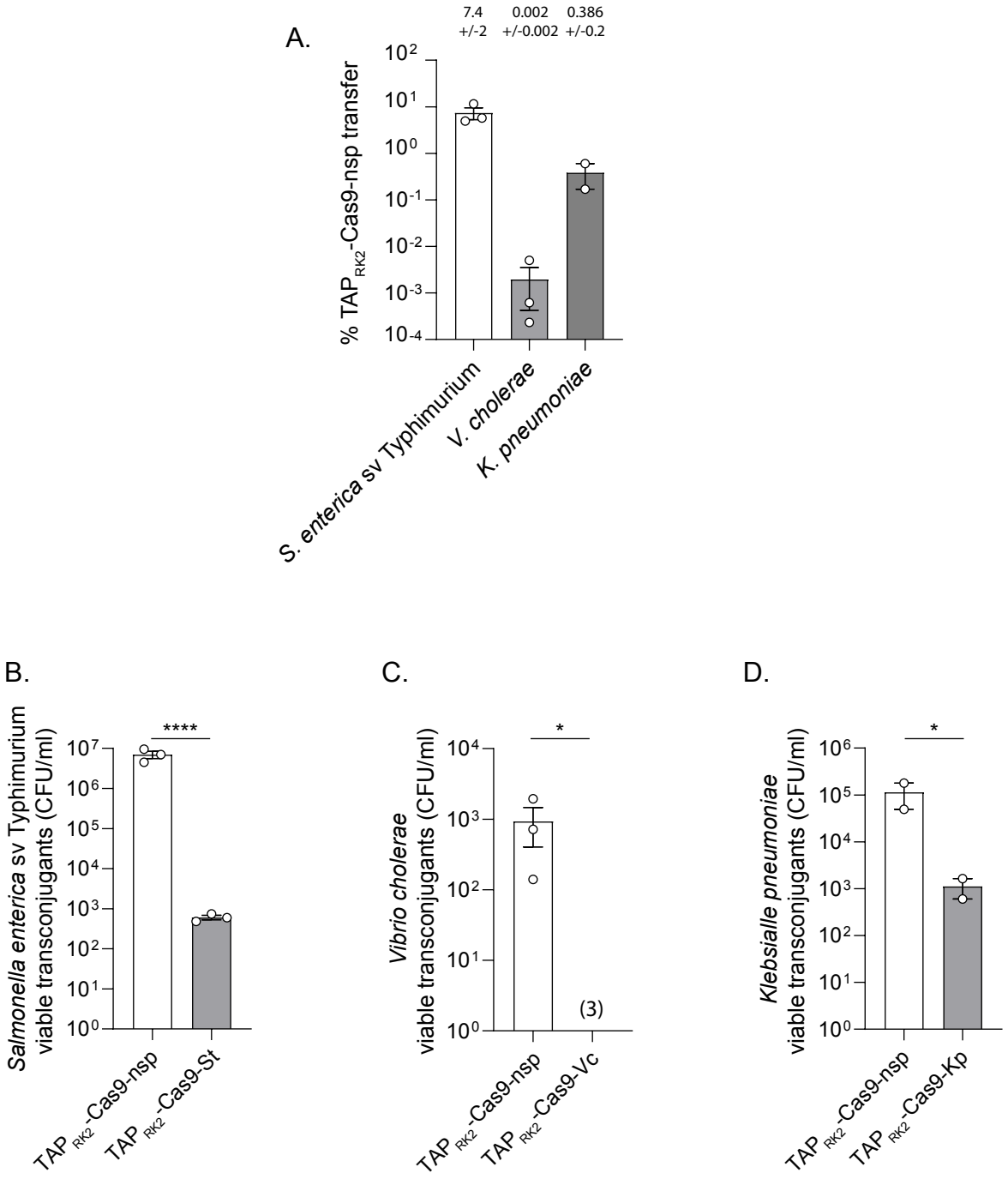

Figure R5 : transfering TAPs by the RP4 conjugative machinery allows the targetting and killing of *S. enterica* sv Typhimurium, *V. cholerae* and *K. pneumoniae.*

A. Histogram showing the efficiency of TAP_{RK2}-Cas9-nsp transfer (T/R+T ratio) estimated by plating assay after 2h of mating on filter. Mean of the percentage and SEM are indicated above each bar. B, C and D. Histogram showing the viability of *S. enterica* vs Typhimurium (B), *V. cholerae* (C) and *K. pneumoniae* (D) transconjugants after acquisition of the TAP_{RK2}-TAP-Cas9-nsp or respective targeting TAPs. Number in brackets indicates replicates with detection limit of transconjugants under 10^{-3}. Unpaired t-test were realized on the $\log_{10}$ transformed values. * P-value<0.05 ; **** P-value<0.0001. Donor strains : Donor strain *E. coli* TAP_{RK2}-Cas9-nsp (LY1981), *E. coli* TAP_{RK2}-Cas9-St (LY2013), TAP_{RK2}-Cas9-Vc (LY2012) and TAP_{RK2}-Cas9-Kp (LY2052). recipient strains : *S. enterica* sv Typhimurium (LY1977), *V. cholerae* (LY1708) and *K. pneumoniae* (LY1182).

carrying the TAP_{RK2}-Cas9-Vc were under the limit of detection, most probably due to the poor transfer efficiency towards this strain (Figure R5C). Transfer of the TAP_{RK2}-Cas9-Kp results in a 2-log reduction of the transconjugant viability only (Figure R5D), suggesting that *K. pneumoniae* might be more resistant than *S. enterica* to the TAP activity.

Less efficient cutting of *K. pneumoniae's* genome can be the result of different phenomenon. This could either be due to less efficient cutting by the Cas9 or more efficient repair by the homologous recombination repair machinery. Indeed, the killing efficiency of TAPs is the result of the balance between DSB induction by the Cas9 and the repair by the homologous replication machinery. CRISPR effect depends on the targeted site. Indeed, it was shown that targeting *E. coli*'s genome does not result in homogenous killing efficiencies (Cui and Bikard 2016). Notably, two spacer lacZ1 and lacZ2 targeting two sites located in the *lacZ* gene show differential efficiency of killing with lacZ2 being more efficient than lacZ1 spacer. The survival of *E. coli* was attributed to the homologous recombination because no escape mutants were obtained in a *recA* mutant background. This allowed to show that even if lacZ1 targeting was not as efficient as lacZ2's one, it stills perform DSB in *E. coli*'s genome (Cui and Bikard 2016). Moreover, divergent killing efficiencies depending on the targeted sequence was observed in *S. enterica* (Hamilton *et al.* 2019). It might be due to the inefficiency for the Cas9 to perform simultaneously DSB on each targeted sequence. For now, there does not appear to be a common thread between targeted sites which do not lead to a high killing efficiency (Cui and Bikard 2016; Hamilton *et al.* 2019). In the case of *K. pneumoniae*, it is then possible that some targeted sites are more efficiently repaired by the homologous recombination machinery than others. This could be the case for the spacer used to target *K. pneumoniae*. Another way for *K. pneumoniae* to escape from Cas9-mediated DSB would be to perform NHEJ repair. However, to my knowledge, *K. pneumoniae* does not possess any NHEJ repair system so this hypothesis seems unlikely.

Another hypothesis that could explain the lower activity of TAP in *K. pneumoniae* is that the constitutive promoters controlling the expression of the CRISPR system are less active in *K. pneumoniae*. Indeed, the constitutive promoters used in TAP plasmids to express the Cas9 and the gRNA are respectively Bba_J23107 and J23119 synthetic promoters that were developed and tested in the *E. coli* model (http://parts.igem.org/Part:BBa_J23119). Thus maybe these constitutive promoters are not as efficient in *K. pneumoniae* which could reduce the Cas9 and gRNA concentration resulting in less efficient killing activity.

An alternative hypothesis would be that *S. pyogenes*'s Cas9 activity is reduced in *K. pneumoniae* strain. For instance, it was shown that the dCas9 of *S. pyogenes* is less active in *Mycobacterium smegmatis*, whereas the dCas9 of *Streptococcus thermophilus* or *Streptococcus pasteurianus* respectively are more suitable for CRISPRi (Rock *et al.* 2017). The dCas9 of *S. pasteurianus* was also used to develop CRISPRi in Pseudomonas species (Tan, Reisch and Prather 2018).

Finally, we can consider that the frequency of escaper mutants is higher in *K. pneumoniae*. In Reuter *et al.*, we analyzed *E. coli* and *C. rodentium* escape mutants and revealed that escapers result from two strategies: rendering the genomic target non-recognizable for the CRISPR-Cas system by deletions of the targeted site or point mutations near the PAM sequence, or disrupting the TAP activity by transposase insertions in the *cas9* gene. Targeting 22 genome loci in *C. rodentium*, showed that all escapers result from Cas9 inactivation as it is very unlikely for the recipient strain to mutate 22 chromosome sites at the same time. The Kp spacer hits twice the genome of *K. pneumoniae* in two different genes : *KPLM21v1*_340090 and *KPLM21v1*_820007 which encode conserved proteins of unknown

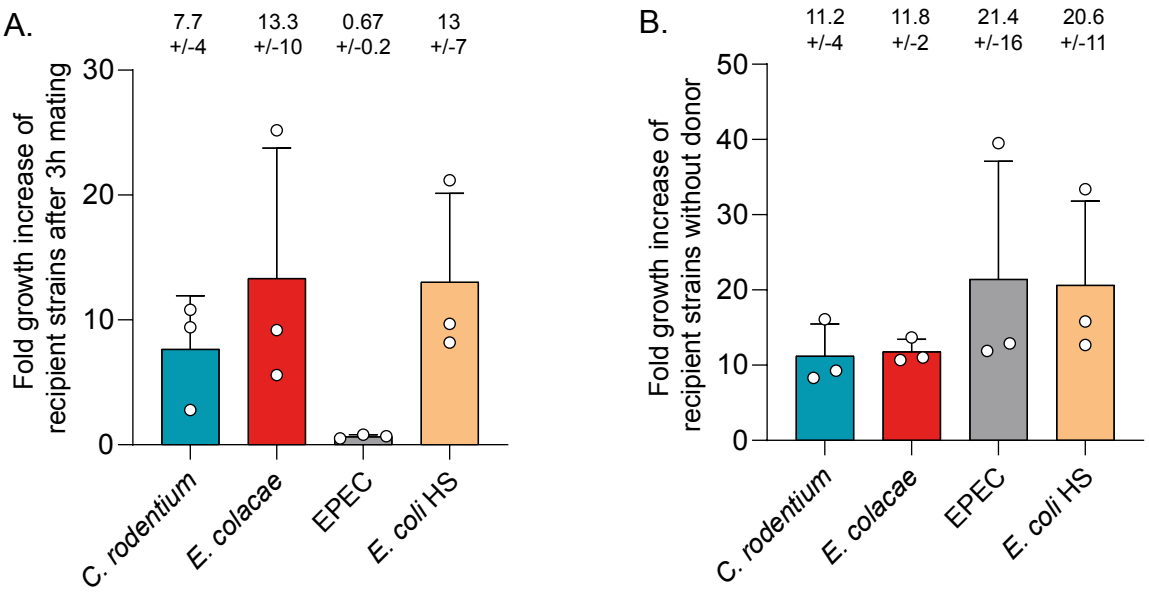

Figure R6: The fitness of EPEC strain is impacted in presence of donor strain carrying the F-Tn*10* palsmid and TAP-Cas9-nsp. Histograms showing the fold growth increase of recipients strains in presence (A) or in absence (B) of the donor. Mean and SD are indicated above the histograms and were calculated from 3 independent replicates. Donor : TAP-Cas9-nsp (LY1369). Recipients : *C. rodentium* (LY720), *E. cloacae* (LY1410), EPEC (LY1615) and *E. coli* HS (LY1601).

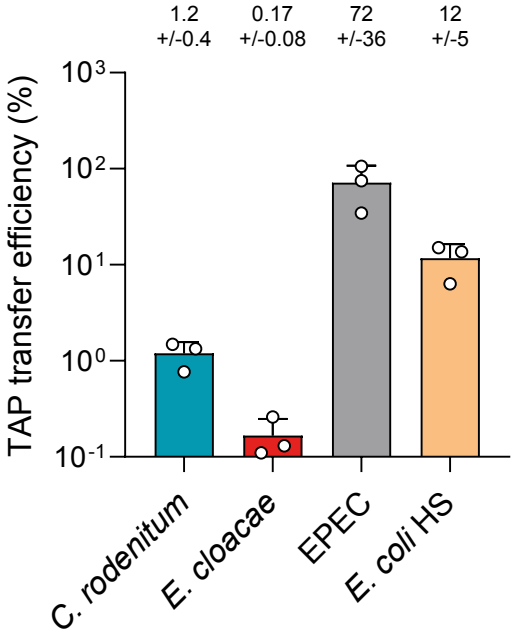

Figure R7 : TAP transfer efficiency in muiltispecies mix
Histograms showing the transfer efficiency of TAPs in the different recipient strains into multispecies mix after 3h mating. Mean and SD are indicated above the histograms and were calculated from 3 independent replicates. Donor : TAP-Cas9-nsp (LY1369). Recipients : *C. rodentium* (LY720), *E. cloacae* (LY1410), EPEC (LY1615) and *E. coli* HS (LY1601).

function. To delete or mutate two loci in a genome is more likely to occur that the mutation/deletion of 22 loci. These two genes seem conserved in various *Enterobacteriaceae*, suggesting an importance. They are not necessarily essential, thus the targeted loci could be mutated/deleted. However, we can suggest that *K. pneumoniae* escapers arise more likely from the disruption the TAP activity than from mutations of the two genes simultaneously. Our analysis in *E. coli* and *C. rodentium* escapers revealed that disruption of the TAP activity was related to insertion of transposable elements into the Cas9 open reading frame. It is possible that *K. pneumoniae* contains more transposable element and it thus more efficient to disrupt the CRISPR-Cas activity of the TAP.

V.2.3. Impact of the F-Tn*10* plasmid acquisition on the fitness of EPEC strain

In Reuter *et al.*, we performed conjugative assays with multispecies mix containing *E. coli* HS, *C. rodentium*, *E. cloacae* and EPEC. After 3h mating with a TAP-Cas9-nsp carrying donor, we observed that EPEC recipient strain proportion was reduced compared to other strains and the fold growth was below 1 meaning that EPEC either stopped growing or suffered a significant viability loss (Figure R6A). Our first thought was that this phenotype might be due to conjugation exerted by the presence of the donor in the mix. To verify this hypothesis, culture of the recipient strain mix without the donor strain was realized in the same conditions than the conjugative mix. The proportion of each recipient strain was counted at time 0h and 3h. Figure R6B shows that without donor the fold growth of *C. rodentium* and *E. cloacae* do not change. The *E. coli* HS strain presents a better fold growth that increases from 13 to 20.6. Finally, the EPEC strain fold growth rises drastically from 0.67 to 21.4. This result suggests that the presence of the TAP-Cas9-nsp donor strain in the mix has a fitness impact on the two *E. coli* strains HS and EPEC.

We also quantified the proportion of each recipient strains acquiring the TAP-Cas9-nsp in multispecies mix after 3h of mating (Figure R7). Delivery efficiency of the TAP-Cas9-nsp is 1.2 %, 0.17 %, 72 % and 12 % for *C. rodentium*, *E. cloacae*, EPEC and *E. coli* HS recipient strains, respectively. It seems that EPEC and *E. coli* HS recipients that acquire the TAP more efficiently are also the most impacted in their fold growth during mating in multispecies (Figure R7). The conjugation process *per se* might affect the fitness cost applied by the donor strain on the EPEC.

In the TAP strategy, both F-Tn*10* and TAP are generally transferred into the recipient strains. It was shown that plasmid acquisition can lead to a fitness cost in transconjugant cells compared to plasmid-free cells but also compared to strains with already established plasmids (Diaz Ricci and Hernández 2000; Prensky *et al.* 2021). Thus, our data are consistent with the proposal that the acquisition of the mobilizable TAP and/or the F-Tn*10* plasmid would be responsible of the observed fitness cost on the EPEC strain. On the other hand, CRISPR-Cas systems can induce off-target activity toxic for the cell (Cui *et al.* 2018). Then, the CRISPR-Cas9 system itself may induce a fitness cost to the EPEC strain. To test these hypothesis, I performed multispecies mating assays containing different donors strains and measured the fold growth of the EPEC strains after 3h of mating. As a control, a multispecies recipients mix without donor strain was realized to evaluate the fold growth of EPEC in multispecies mix without any donor strain. Figure R8 shows the results of one replicate.

To test the impact of F-Tn*10* acquisition on the fitness of EPEC, I have calculated the fold growth increase of EPEC in a multispecies mix containing a donor strain carrying either no plasmid, the non-transferable F-Tn*10*-Δ*oriT* or the F-Tn*10* plasmid (Figure R8). First of all, the presence of the donor strain alone without plasmid in the mating mix reduces the fitness of

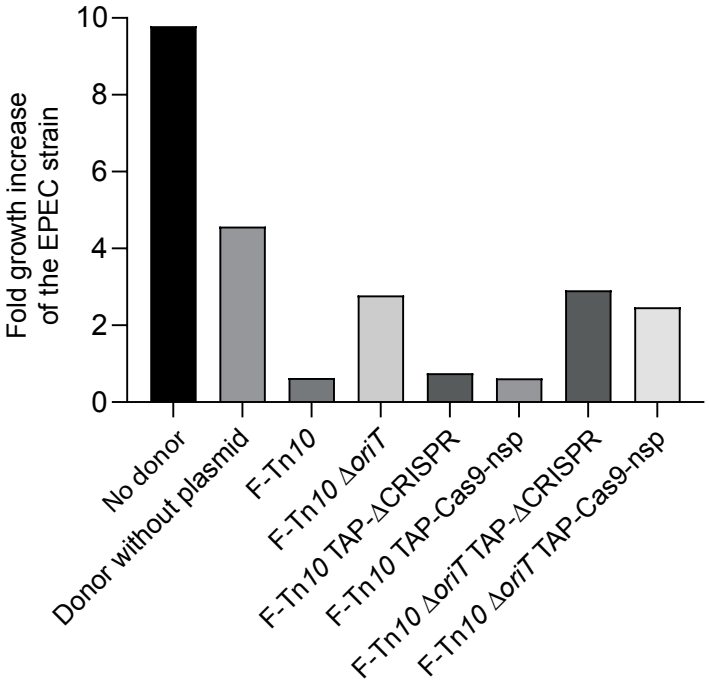

Figure R8: Acquisition of the F plasmid has a fitness cost on the EPEC strain.
Histogram showing the fold growth increase of the EPEC strain after 3h of mating in multispcies mix with different donor strains. Donor strains : *E. coli* without plasmid (LY636), with F-Tn*10* (LY1361), F-Tn*10* Δ*oriT* (LY1932), F-Tn*10* TAP-ΔCRISPR (LY1379), F-Tn*10* TAP-Cas9-nsp (LY1369), F-Tn*10* Δ*oriT* TAP-Δ CRISPR (LY1971) and F-Tn*10* Δ*oriT* TAP-Cas9-nsp (LY1972). Recipient strains : *C. rodentium* (LY720), *E. cloacae* (LY1410), EPEC (LY1615) and *E. coli* HS (LY1601).

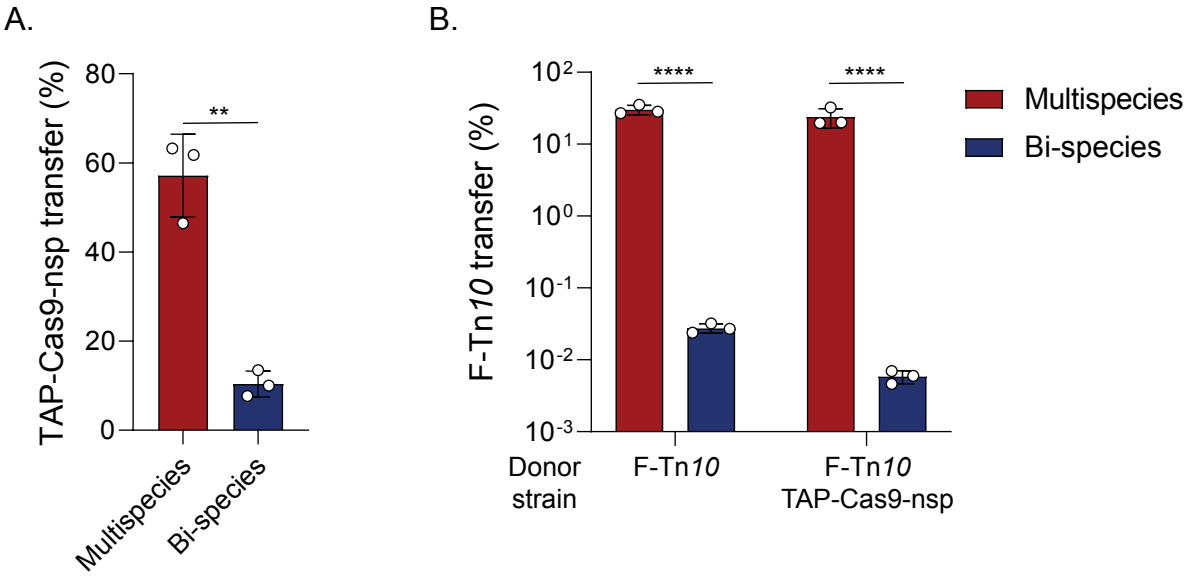

Figure R9: Transfer of the TAP-Cas9-nsp and F-Tn*10* plasmid into EPEC are increased in multispecies mix.
A. Histogram showing the TAP-Cas9-nsp transfer efficiency (T/T+R ratio) after 3h of mating in multispecies or bi-species mixes. Unpaired T-test was performed. ** P-value < 0.01. B. Histogram showing the F-Tn*10* transfer efficiency (T/T+R ratio) after 3h of mating in multispecies or bi-species mixes. Multiple T-tests corrected with Holm-Sidak method were performed on the $\log_{10}$ transformed values. **** P-value < 0.0001. Donors: F-Tn*10* (LY1361) and F-Tn*10* TAP-Cas9-nsp (LY1369). Recipients: *C. rodentium* (LY720), *E. cloacae* (LY1410), EPEC (LY1615) and *E. coli* HS (LY1601).

EPEC for which the fold growth drops from 9.79 to 4.57. This is due to the competition induced by the introduction of the donor strain without plasmid. Indeed, it was shown that bacteria in the same media tend to compete for the available nutrients (Stubbendieck and Straight 2016). Interestingly, the fold growth of the EPEC collapse to 0.63 with a donor transferring the F-Tn*10* plasmid alone, while the growth is restored to 2.78 using a donor carrying the non-transferable F-Tn*10* Δ*oriT* plasmid. This suggests that the acquisition of the F-Tn*10* plasmid impacts the fitness of EPEC. However, the EPEC fitness cost associated to the F-Tn*10* Δ*oriT* plasmid is higher than the one observed with a donor strain without plasmid. The formation of the mating pair is still performed by the F-Tn*10* Δ*oriT* plasmid and it might have an impact on the fitness cost of the recipient strain.

To test the hypothesis of a reduced fitness cost due to the acquisition of the CRISPR-Cas system, I tested the effect of a donor strain carrying the non-transferable F-Tn*10*-Δ*oriT* plasmid able to transfer only the TAP-Cas9-nsp. In addition, I included in the experiment a donor transferring a TAP deleted of the CRISPR system (TAP-ΔCRISPR) to determine whether the acquisition of the mobilizable plasmid itself could induce a fitness cost. Figure R7 shows that the acquisition of TAP carrying or not CRISPR system is not responsible of the observed fitness cost. Transfer of these plasmids by a donor carrying the non-transferable F-Tn*10* plasmid led to a fold growth increase of 2.47 and 2.91 respectively while transfer of both F-Tn*10* and TAP still lead to drastic drop of the EPEC growth. These results clearly show that only the acquisition of the F-Tn*10* by EPEC affect the growth of this strain.

Conjugative transfer of the TAP-Cas9-nsp plasmid in EPEC strains in multispecies mix after 3h mating was estimated to 72%. However, the transfer of the F-Tn*10* plasmid was not estimated in multispecies mix, neither in bi-species mix. Thus, the transfer efficiency of the TAP-Cas9-nsp and the F-Tn*10* plasmid in bi-species or multi-species mix after 3h mating was evaluated and represented in the Figure R8. In this condition, the transfer of the TAP-Cas9-nsp is significantly more efficient in multispecies (57%) than in bi-species experiment (10.4%) (Figure R9A). In addition, transfer efficiency of the F-Tn*10* plasmid from two donors containing or not the TAP-Cas9-nsp plasmid is also significantly higher in multispecies mix (Figure 9B). This means that multispecies conditions increase the transfer efficiency of both F-Tn*10* plasmid and TAP in the EPEC recipient strain. This can be due to the formation of new donor strains in the multispecies recipient population which could be more efficient at transferring F-Tn*10* and TAP.

All together those results indicate that the fitness cost observed in the EPEC population of recipient is due to the acquisition of the F-Tn*10* plasmid and maybe the mating pair formation mediated by the F plasmid machinery. We also showed that TAP acquisition and the constitutive expression of the CRISPR-Cas9 system does not affect the EPEC fold growth. These *in vitro* results realized in controlled population settings implicate that the efficiency of TAP transfer and killing will be hard to predict *in situ* within complex bacterial communities. Many parameters come into play, notably in the microbiota where the relative abundance and growth of the different species can be related to the host health, age, diet and immune system activity (Hooper, Littman and Macpherson 2012; David *et al.* 2014; Saraswati and Sitaraman 2014; Carmody *et al.* 2015; Rodríguez *et al.* 2015). Transfer of the TAP can also be influenced by the composition of the gut microbiota and the physico-chemical properties of this environment.

V.3. Discussion

During my thesis, I was interested in developing an alternative to antibiotics which would be specific of the targeted pathogen. To do so, I combined CRISPR-Cas system with conjugation into TAPs to deliver specific antimicrobials to kill diverse pathogens and disrupt antibiotic resistance genes carried by plasmids. My work led to the proof of principle of this tool which validates the capacity and the applications of this strategy. Notably, I showed:

- The killing of the diverse transconjugant pathogens,
- The ability of the tool to selectively kill the targeted strain and to perform multiple targeting thanks to the CSTB web-service,
- The versatility of this tool as the target is easily switchable and the conjugative machinery too.

If this tool was validated *in vitro*, TAPs can be ameliorated to overcome their limitations. Indeed, our results *in vitro* and *in vivo* show a clear eradication of the transconjugant population, yet the recipient population is not impacted by the TAP strategy. This clearly indicates that the conjugation efficiency of TAPs is too low to have an impact on the recipients. Moreover, we showed with long-term experiments that the transfer of the helper plasmid can make recipient strain immune to the conjugation and impedes the transfer of TAPs in this population. As for antibiotics, escape mutants to the TAP strategy were observed at a frequency of 1/1,000 to 1/10,000, which has to be reduced. Once optimized the TAP strategy, it will be necessary to adapt them for a use in human health. Finally, our results brought an interesting view of the conjugation phenomenon in complex environments thanks to multispecies mix. Notably, the impact of conjugation in the EPEC strain was unexpected and emphasizes the need to study conjugation with stetting closer to the environment, in this particular case the microbiota.

These results bring more questions that need to be answered to enhance the TAP strategy :

- How does the conjugative efficiency can be enhanced ?
- How to limit the transfer of the helper plasmid ?
- How to reduce the resistance to TAPs ?
- How to adapt TAP strategy for an utilization in human health ?
- How does conjugation influence bacterial populations ?

These questions are the ones I will now address.

V.3.1. Enhancing conjugation efficiency

As was highlighted in the introduction with the review of CRISPR-Cas antimicrobials delivered by conjugation (Table 3) and as our results show, the conjugation efficiency is the main bottleneck impairing the TAP strategy. Our results show that conjugation efficiency is related to several factors including the conjugative machinery and the donor strain.

V.3.1.1. Conjugation machinery engineering or replacing

I used two conjugative machineries, that of the narrow host range F-Tn*10* plasmid and that of the broad host range RP4 plasmid. If those machineries achieve high conjugation efficiency when the donor and the recipient belong to the same species, this is decreased when the donor and recipient strains are not related. Interestingly, the only counter-example to this rule is the transfer of the TAP with the F-Tn*10* machinery into the EPEC strain which is relatively low considering that it is performed between two *E. coli* strains. This could be due to the TraN interaction with outer membrane proteins (OmpA in *E. coli*) and LPS stabilizing the

mating pair. Outer membrane proteins from other bacterial species are not necessarily mediating a stable mating pair. However, it cannot explain the reduced transfer efficiency between our MG1655 *E. coli* and EPEC strains because their OmpA proteins share sequence 98,55 % identity.

The conjugation efficiency can also be influenced by the donor strain used to transfer the TAP. TAP transfer with the RP4 machinery seems better between two related donor-recipient species than between distant species. Indeed, in our results, transfer efficiency of the TAP from *E. coli* to *V. cholerae* is 2.10^{-3} % whereas the transfer efficiency of the RP4 plasmid between two *E. coli* was tested in the laboratory and shown to be 100 %. It could be due to the formation of the mating pair by RP4 machineries which was shown to melt the two bacterial membranes (Samuels, Lanka and Davies 2000) and is probably easier to realize when membrane composition is similar. Indeed, in closely related species membranes lipid compositions are more likely to be homologous than between distantly related species (Sohlenkamp and Geiger 2016).

To enhance the conjugation efficiency, it is possible to test other conjugative machineries. For example, the IncI TP114 conjugative plasmid was shown to perform high conjugation efficiency in the gut microbiota (Neil *et al.* 2020). In this study, the authors emphasize the role of the mating pair establishment for the conjugative efficiency, notably the type 4 pilus (T4P) encoded by TP114 enabling the formation of a strong mating pair. T4P are generated with an adhesin on the tip, which can be switched thanks to its shufflon genetic construction. These tips are thought to ensure adherence between the donor and the recipient and the modularity of the tip would serve to contact several bacterial species. We could then modify the helper plasmid to produce a T4P to try enhancing the conjugation efficiency, notably towards distant bacterial species. However, plasmids encoding T4P belonging to the IncI incompatibility family are known to be narrow host range plasmids (Datta and Hedges 1972; Suzuki *et al.* 2010). Thus, changing the helper plasmid in order to produce the T4P could enhance only the transfer into *Entrebacteriaceae* which are the hosts of IncI plasmids.

It would be better to keep the wide host range that is offered by the RP4 conjugative machinery. Indeed, it was shown that RP4 is able to be disseminated into indigenous bacteria of the rhizosphere and the spermosphere of plants, notably pseudomonads, *Erwinia herbicola* and *Enterobacter agglomerans* (Sørensen and Jensen 1998). One of the early goals of my project was to develop TAPs to target *Pseudomonas syringae*, a pathogen of *Arabidobsis thaliana* model plant. To accomplish this goal, it is possible to use the RP4 conjugative machinery which allow conjugative transfer in bacteria of the rhizosphere. Moreover, this conjugative machinery could promote the transfer of TAPs directed against antibiotic resistance genes in different bacteria of the environment. This is why, the RP4 conjugative machinery is a suitable candidate to easily adapt TAPs to any desired application. The RP4 pilus does not seem to rely on any receptor to mediate cell-to cell contact (Pérez-Mendoza and de la Cruz 2009), which is a strength allowing a broad host range but also can impede the formation of solid mating pair and thus decrease the transfer efficiency. For instance, it is known that conjugation efficiency in liquid medium is drastically reduced with the RP4 plasmid (Bradley 1980). To enhance the conjugative efficiency and the mating pair formation by the RP4 machinery, it is possible to draw inspiration from the F-Tn*10* conjugative plasmid. Indeed, in the case of the F-Tn*10* plasmid, conjugation efficiency is high due to derepression of the *tra* genes due to the insertion in *finO* (Frost, Ippen-Ihler and Skurray 1994). The conjugative apparatus is thus constitutively induced. It is possible to imagine genetic modifications that

could enhance the production of the RP4 conjugative machinery and notably the pilus and T4SS production. In the RP4 plasmid, the conjugative machinery is distributed in two locations of the plasmid, named Tra1 and Tra2. Tra2 operon contains the genes responsible for the mating pair formation (Mpf) and pilus assembly (Haase *et al.* 1995). The only Mpf protein lacking from the Tra2 operon is the TraF protein which is the peptidase performing peptidoglycan degradation to facilitate the position of the T4SS (Haase *et al.* 1995). The Tra2 operon is under the control of the *trbB* promoter (*trbBp*) which is regulated by KorB and TrbA proteins acting in synergy to repress it (Zatyka, Jagura-Burdzy and Thomas 1997; Zatyka *et al.* 2001). TrbA was reported to act also on the replication of the RP4 plasmid and KorB is an actor in its partition (Bingle and Thomas 2001). This is why suppressing these proteins could lead to a deleterious effect on the stability of the RP4 plasmid. The interaction of these two proteins to repress the *trbBp* is mediated by the C-terminal domain of TrbA (Zatyka *et al.* 2001). Therefore, to enhance the expression of the RP4 Mpf machinery, it could be tried to mutate the C-terminal domain of TrbA in the RP4 plasmid.

Other techniques could help to recognize genes enabling increased conjugation efficiencies towards non-related strains. For example, TnSeq method could help identifying plasmidic genes that are required to enhance conjugation (van Opijnen, Bodi and Camilli 2009). This technique consists in creating a mutant library by insertion of transposons. Next, selection of mutants that mediate conjugation with enhanced or decreased frequencies can be realized. Mutants with increased conjugation efficiencies can be kept and tested for their efficacy to kill other bacteria using the TAP strategy. This is a non-directed way to obtain helper plasmid able to efficiently transfer the TAPs.

Another way, as mentioned in the introduction to widen the host range of phages, is to use enhanced evolution. For instance, techniques were developed to induce more mutations during the replication, as the MP6 plasmid which was proven to increase the mutation rate of *E. coli* by 322,000 fold, notably thanks to inducible expression of polymerase III variant mutated for its proofreading domain (Badran and Liu 2015). This polymerase introduces many mismatches during replication and other genes of the MP6 plasmid impair the correction by mismatch repair or induce other mutations. Thanks to arabinose induction, MP6 is able to introduce many mutations in replicated DNA. Usage of this plasmid in strains containing our favourite helper plasmid could allow to select plasmids with enhanced efficiency and/or host range (Neil *et al.* 2021).

V.3.1.2. Adaptation of the donor strain

Using the F-Tn*10* conjugation machinery, I showed that different *E. coli* donor strains such as HS, IAI1 and Nissle perform conjugation with highly varying efficiency. One hypothesis will be that host-encoded factors are implicated in these variations. For instance, it was found that three mutants Δ*frmR*, Δ*sufA* and Δ*iscA* could increase the transfer efficiency of the RP4 plasmid in both *E. coli* and *Saccharomyces cerevisiae* recipients. FrmR is a transcriptional regulator which repress the formaldehyde operon in *E. coli* (Herring and Blattner 2004). SufA and IscA have redundant activity in iron binding and delivery in the iron-sulfur cluster assembly (Lu *et al.* 2008). Deletion of *iscA* or *sufA* genes do not result in a growth defect in *E. coli*, whereas deletion of both genes impact the fitness of the bacteria. However, the impact of the product of these three genes on the conjugation steps of RP4 plasmid is not yet known (Zoolkefli *et al.* 2021). It could be interesting to use Δ*frmR*, Δ*sufA* and Δ*iscA* mutants to see if the TAP_{RK2} transfer is enhanced in recipient strains, notably in *V. cholerae*, in which the TAP_{RK2} is weakly transferred.

The donor strain should be adapted to the tested environment. In our case, enterobacteria targeted by the TAPs are mostly found in the gut microbiota. This is why my first improvement to the TAP strategy was to adapt the donor strain to the mouse gut. Indeed, if donor strains are able to stably colonize the environment, it is more likely to deliver its antibacterial CRISPR system. In our conditions, the colonization by the donor strain was shown to impact the colonization of the mouse pathogen *C. rodentium*. Unfortunately, the presence of the TAP did not show any differences to fight the pathogen. This reflects the main bottleneck of the TAP tool which is the transfer efficiency.

Interestingly, our results also show that complex interactions in the multispecies mix enhance the transfer of the TAP and the F-Tn*10* in the EPEC strain. This would suggest that an intermediary donor is formed in the multispecies mix which would be able to better spread F-Tn*10* plasmid and TAP in the EPEC recipient. It was demonstrated that donors can play a role on the host range of the transferred plasmid. In particular, the pB10 plasmid was shown to be transferred to different recipient strains depending on the donor strain used to perform conjugation (De Gelder *et al.* 2005).

Consequently, the choice of the donor strain is determinant and it should be adapted to the desired application.

V.3.2. Preventing helper plasmid dissemination

In our system, the F-Tn*10* or RP4 plasmids are both helper and autonomous plasmids able to transfer into the targeted recipient strains. As previously addressed, this has great impact in the recipient population and promotes the acquisition of resistance determinants by conjugation. We were able to show that F-Tn*10* plasmid can be transferred alone and then block the acquisition of the TAP probably through expression of exclusion systems (Reuter *et al.* 2021). To avoid this, I constructed a F-Tn*10* plasmid without the *oriT* sequence. It is impossible for this helper plasmid to be transferred. Experiments of the long-term impact of TAPs using this donor strain showed that the autonomous property of the helper plasmid can impede the TAP strategy. Without autonomous transfer of the helper plasmid, recipients do not become active mobilisers of the TAP which delays the transfer efficiency. However, in the long term this allows to transfer the TAP to a larger proportion of recipients. This experiment further showed that TAPs are able to be maintained in recipient strains without selection pressure even if their copy number is low. Finally, conjugative transfer of the helper plasmid impedes the growth of some recipients. This was shown for the EPEC strain. Thus using a non-mobilizable helper plasmid would be beneficial in complex bacterial communities, like the gut microbiota. The gut microbiota plays a major role in the individual health and TAPs should not impact its composition. Thus, utilisation of a non-transferrable helper plasmid is better to prevent dysbiosis.

V.3.3. Avoiding escape mutants apparition

As observed with CRISPR-Cas delivered antimicrobials, bacteria are able to evolve escape mutations to avoid death by the TAP system. We observed two types of resistance:

- Mutation of the targeted site which renders it unrecognizable by the CRISPR-Cas system
- Disruption of the CRISPR-Cas9 system held by the TAP.

Mutations on the targeted locus can occur either by point mutations near the PAM sequence which make the recognition by the spacer impossible or by small and large deletions around the targeted locus. How to prevent these events from happening in bacteria ? It is

possible to target essential genes which would be impossible to delete as it will be detrimental. Using the Cr22 spacer, we showed that it is very difficult, if not impossible, for bacteria to mutate 22 loci on their chromosome. Spacers able to target multiple loci in a given chromosome can be easily found thanks to the CSTB web-service.

In other studies, multiple-targeting of the chromosome was performed using several spacer sequences (Bikard *et al.* 2014; Citorik, Mimee and Lu 2014; Yosef *et al.* 2015; Park *et al.* 2017; Ram *et al.* 2018; Rodrigues *et al.* 2019; Ruotsalainen *et al.* 2019; Kiga *et al.* 2020; Selle *et al.* 2020). To do so, the CRISPR-Cas system used does not contain a gRNA but a CRISPR array with a tracrRNA. This allows to target several genes on the chromosome, which could prevent escape mutations in the same way than the targeting of multiple identical loci does. It is an interesting feature in the fighting of antibiotic resistance genes. Indeed, to use different spacer targeting the same resistance determinant is a way to force the selection of bacteria with mutated or deleted resistance gene. Thus, even if bacteria manage to escape the CRISPR-Cas activity, it will no longer be able to resist to the antibiotic. Multiple targeting could also be relevant to improve targeting in the genome. Indeed, some genomic targets do not seem to be as efficient as others to kill a bacterial cell (Cui and Bikard 2016; Hamilton *et al.* 2019). This could be linked to a competition between the action of the homologous repair machinery on one hand and the Cas9-mediated DSB on the other hand. Indeed, it was shown in *recA* mutant *E. coli* cells that Cas9-mediated DSB are lethal (Cui and Bikard 2016). Thus, targeting *recA* gene with the TAP simultaneously with another genomic sequence could lead to enhanced cell death. It is possible to modify the TAPs to include a CRISPR array and the tracrRNA constitutively expressed. However, this could suppress the modularity of the TAPs. Indeed, TAPs have a switchable spacer locus which can be changed easily with one step cloning. Adding a CRISPR array would require more effort but could be worth to try.

In our observations, disruption of the CRISPR-Cas system of the TAP consists in the insertion of transposable elements into the *cas9* gene. Such insertions and deletions into the CRISPR array were also reported in other systems and also insertion of nucleotide into the *tracrRNA* locus and deletion of the *cas9* gene (Bikard *et al.* 2014; Citorik, Mimee and Lu 2014; Ram *et al.* 2018; Hamilton *et al.* 2019; Ruotsalainen *et al.* 2019). Interestingly, we were able to show that insertion of transposable elements in the *cas9* gene could be already done in the donor strain as well as in the recipient cell. It was reported that spontaneous mutations in *E. coli* reference strain MG1655 occur at a rate of ~1 $.10^{-3}$ per genome per generation (Lee *et al.* 2012). Mutagenesis could be enhanced due to the presence of the TAP and possible off-target which would apply stress on the donor strain and trigger stress-induced mutagenesis. Our published results showed that TAPs do not impact the donor cell viability (Reuter *et al.* 2021). Particularly, we monitored cell with or without the TAP-Cas9-nsp or the TAP-ΔCRISPR, verified their growth and performed cytometry experiment to see their morphology. No difference was observed, indicating that the CRISPR-Cas system might not perform off-target in these strains. Thus, the apparition of defective TAPs in the donor cell should be due to the intrinsic mutagenesis rate, in *E. coli*. To limit the apparition of mutated TAPs, notably by transposition, it is possible to use donor strain which does not possess transposable elements as was proposed in the discussion of our publication (Pósfai *et al.* 2006).

The inactivation of the TAP in the recipient strain seems difficult to avoid, yet systems were imagined to provide selective markers with the CRISPR-Cas system. For instance, Yosef *et al.* provided with their CRISPR-Cas system a defence mechanism against an engineered lytic phage (Yosef *et al.* 2015). Thus, strains that disrupted their CRISPR-Cas system were not able

to fight the infection mediated by the lytic phage and were killed. This would be difficult to implement on TAPs.

Other CRISPR-Cas system could be a solution to avoid resistance. For example, Kiga *et al.* using the Type VI CRISPR-Cas system did not observe any escape mutants (Kiga *et al.* 2020). This system, after the recognition and the subsequent cleavage of the targeted RNA, degrade non-targeted RNAs of the bacteria which leads to its death. Their system allows to kill bacteria even if the targeted sequence is on a plasmid. This is not our goal with the TAP system. Indeed, we targeted the bla_{OXA-48} resistance gene on the pOXA-48a and showed that it only eliminates the plasmid. This is lethal for bacteria only if the plasmid harbours toxin-antitoxin systems, like in the pOXA-48a. As our system is made to be transferred in the widest host range possible, it seems safer to not kill any targeted bacteria. In this regard, it even seems better to use the CRISPRi property of type II CRISPR-Cas systems. Indeed, to fight antibiotic resistance and/or virulence it is possible to target genes involved in these properties. Bacteria should not be impaired in their capacity to grow and thus less incline to develop resistance to such a tool.

As discussed in the introduction, some properties in the recipient cells could also impair the TAP tool:

- The NHEJ repair system which could repair the Cas9-mediated DSBs.
- A CRISPR system that could target the TAP
- Anti-CRISPR proteins (Acr) generally encoded by phages which impede the function of the CRISPR-Cas system.

If any of these properties are detected in a targeted bacteria, it could lead to an increase rate of escape mutants. These properties should be targeted by the TAP system to prevent resistance.

V.3.4. Adapting the TAP system for human health

The goal of the TAP strategy is to be used to fight bacterial infection, to reduce the bacterial load, to impede virulence mechanisms or to re-sensitize bacteria to antibiotics. In order to realize these tasks, TAPs should be modified, notably to ensure that TAPs are not able to disseminated antibiotic resistance determinants.

First, TAPs carry a resistance cassette which was used to select transconjugants. Of course, the TAPs use in the future should not contain any resistance genes. This could impact the stability of TAPs. As already evoked, the helper plasmid should not be able to be transferred due to the presence of resistance determinants. It would be even better if the helper plasmid did not contain any resistance determinant. Indeed, when the donor strain dies, it could liberate the TAP and the helper plasmid in the medium. It would be possible that the liberated DNA was acquired by other bacteria *in situ* due to active transformation mechanisms (Griffith 1928).

TAPs cannot be used without the bacterial donor strain which deliver them. However, it seems plausible that the bacterial donor will trigger an immune response. This could reduce the efficiency of TAPs to reduce the bacterial infection and also worsen the patient's condition. To avoid this, donor strains have to be species from the commensal population. Indeed, these bacteria co-evolved with the immune system and can colonize the gut microbiota (Hooper, Littman and Macpherson 2012). This offers more chances that the bacteria reach and deliver the TAP to the targeted pathogen.

TAPs are designed to target a specific bacteria or function. However, it could be possible to engineer TAPs designed to target multiple pathogens as was presented in the Reuter *et al.* paper with the EEC spacer targeting EPEC, *Enterobacter cloacae* and *Citrobacter*

rodentium. Moreover, we could use homology between genes and promoters to silence the expression of antibiotic resistance genes. This is an option that was imagined during the creation of TAPs and it is implemented in the CTSB. Indeed, the web service contains a gene specific branch that is designed for this purpose. Notably, TAPs could be used with traditional antibiotic treatment. If a resistance to antibiotic is identified in a pathogen, TAPs could be used first as a way to sensitize the pathogen and next antibiotics should allow elimination of the pathogen. It could also be imagined TAPs targeting specifically virulence genes, notably for the most virulent pathogens. For example, it is possible to target the *stx* gene of Shiga toxin-producing *E. coli* allowing the shiga toxin production (Yokoyama *et al.* 2000). These TAPs could allow to slow down the bacterial infection while the immune system of the patient would fight the pathogen and eradicate it. Finally, the microbiota and its composition was shown to be a factor in diseases like obesity and diabetes, for example (Fan and Pedersen 2020). The TAPs could be directed against gut microorganisms that were found to be linked to these diseases. For instance, it is possible to target *Eubacterium ventriosum* and *Roseburia intestinalis* that were associated with a higher body mass index (Tims *et al.* 2013). Moreover, it is possible to target genes in metabolism pathways that are associated with Type 2 diabetes like membrane transport of sugars, branched-chain amino acid transport, methane metabolism, xenobiotic degradation and sulphate reduction (Qin *et al.* 2012).

All these requirements should be completed and the efficacy of TAPs should be then approved in pre-clinical and clinical trials to prove their capacity to fight bacterial infection and to decolonize resistant bacteria. A difficulty for the TAP to be used in human health is the drug category they could be classified in. Indeed, TAPs are only plasmids but cannot have any antimicrobial activity without the donor strain which delivers them. Thus, the TAP strategy can be considered as probiotics. Probiotics are “live microorganisms that, when administered in adequate amounts confer a health benefit on the host” (Wolrd Health Organization and Food and Agriculture Organization of the United Nations 2002). According to the FDA, probiotics can have three uses : dietary supplement, foods or drugs which defines their regulation and the guidelines for their evaluation (Research 2020). Moreover, regulations on Genetically Modified Microorganisms (GMOs) should be applied to the TAP strategy (European Medicines Agency 2018). This is why it is crucial to apply biocontainment guidelines to the TAP strategy. This would ensure that TAPs benefit/risk balance is clearly in favour of the benefits.

V.3.5. Influence of bacterial conjugation on bacterial populations

Our results revealed that the conjugation phenomenon have an impact on the recipient strains. Notably, we showed that EPEC growth can be affected by the acquisition of the F-Tn*10* plasmid. Interestingly, our results suggest that the mating pair formation alone could reduce the fold growth of recipient strains. Decreasing the growth of targeted strains could be beneficial, however it is not our goal to impair the fitness of microbiota microorganisms. Indeed, the TAPs are designed to only target a bacterial specie or function, while the microbiota should remain unaffected by TAPs, contrary to antibiotics that have a broad host range targeting. Of course, it is impossible that the transfer of the TAP does not affect the recipient strain. Indeed, the acquisition of the single stranded form of the plasmid triggers the SOS response (Baharoglu, Bikard and Mazel 2010), and thus has an impact on the recipient. We still have to minimize the impact of the TAP in non-targeted recipients. Our results also indicate that the TAP itself does not influence the bacterial growth, which is encouraging. We were able to show that if the helper plasmid is not transferred, the EPEC strain is still able to

grow. These are promising results that emphasize the need to prevent the transfer of the helper plasmid in the TAP strategy.

Therefore, the conjugation efficiency and effectiveness of the TAP *in vivo* is difficult to estimate *in vitro*. First, the conjugation efficiencies estimated *in vitro* are not a good indicator of the conjugation rates *in vivo* (Neil *et al.* 2020). Moreover, our results with the multispecies experiments demonstrated the importance of the composition of the bacterial community. This mix was only a defined and controlled environment encompassing 4 different recipients and already revealed a surprising influence of the conjugation in bacterial growth into complex environments. This emphasizes the need to study conjugation dynamics and the implication of plasmid and host factors which can play a role in the crucial steps of conjugation. This would help develop a more efficient delivery machinery based on conjugation for the TAP strategy.

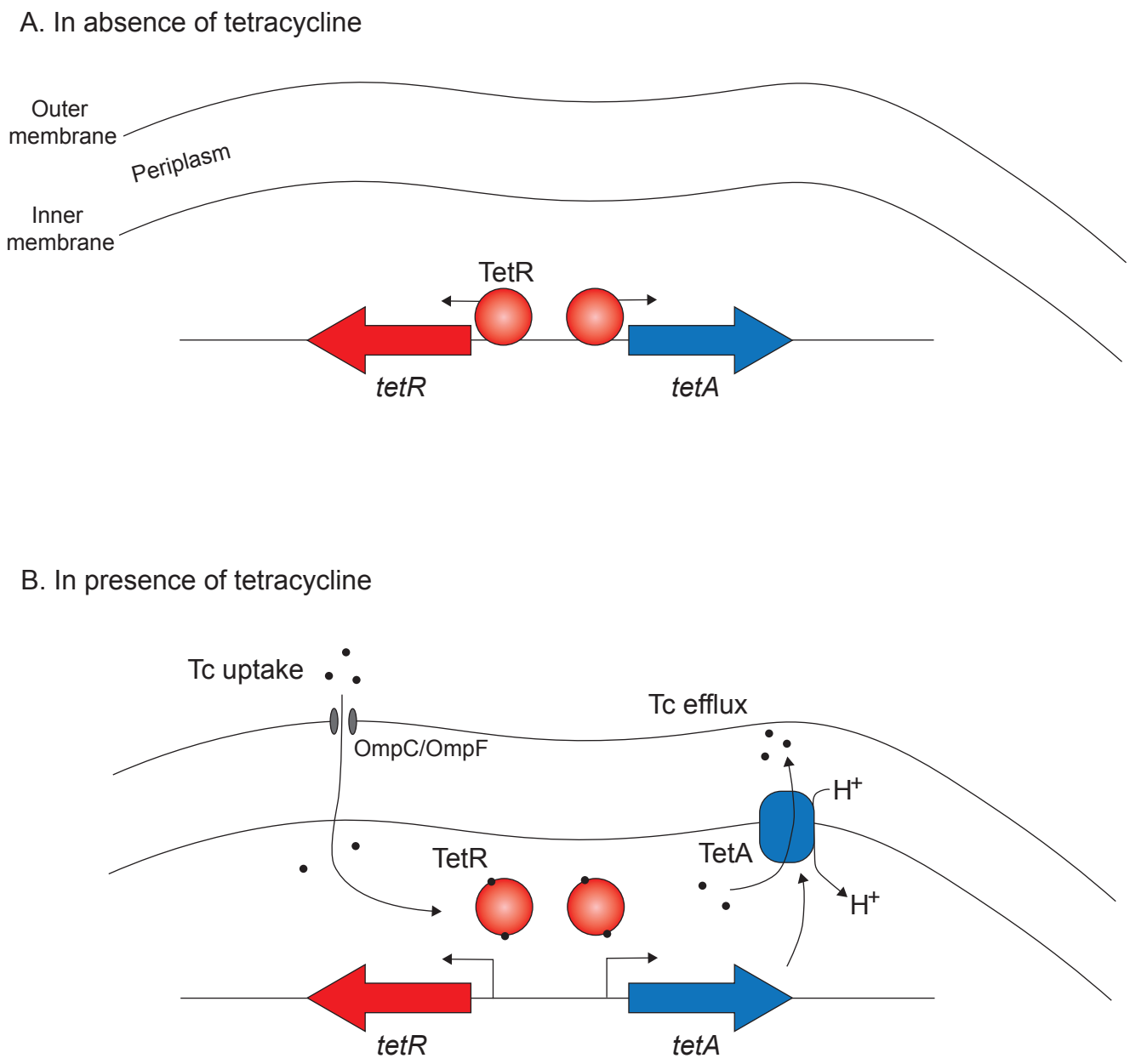

Figure R10 : Regulation of TetA efflux pump
A. In absence of tetracycline (Tc), TetR binds to *tetA* and *tetR* promoters, inhibiting their expression. B. In presence of Tc, that is uptake through the outer membrane thanks to OmpC/OmpF porins and diffuses to the inner membrane, Tc binds to TetR inducing a conformational change and release binding from *tetR* and *tetA* promoters. TetA is then produced and exchange protons (H+) to efflux Tc into the periplasm. Adapted from Cuthbertson and Nodwell, 2013.

VI. Dynamic and mechanistic of conjugation

During my thesis I worked on the model F-Tn*10* plasmid in *E. coli*. Notably, I took interest in the dynamics of antibiotic resistance acquisition mediated by this plasmid. Furthermore, I studied the early expression of the leading region genes.

VI.1. Article Reuter, Virolle, Goldlust *et al*. FEMS Microbiology Reviews

VI.1.1. Introduction

It is now well established that conjugative plasmids largely contribute to the spread of antibiotic resistance among bacterial strains, including clinically relevant bacteria. However, the conjugation phenomenon is not yet fully understood, and we still lack understanding regarding the timing of establishment of the newly acquired metabolic properties within the transconjugant cells. The F-Tn*10* plasmid harbours the Tn*10* transposon, which carry tetracycline resistance genes. Tetracycline (Tc) is a bacteriostatic antibiotic inhibiting the protein synthesis by interacting with the 30S ribosomal subunit. Tc resistance conferred by the Tn*10* transposon is mediated by two genes: *tetA* and *tetR*. The *tetA* gene encodes a specialized efflux pump that transports Tc from the intracellular compartment to the periplasm, thus limiting the binding of the drug to their ribosomal target. The *tetR* gene encodes a transcriptional regulator, which binds to the *tetA* promoter and its own promoter in the absence of Tc. Tc entry into the cell's periplasm is mediated by outer membrane proteins, and entry into the cell's cytoplasm occurs by passive diffusion. The Tc molecule then binds to the TetR repressor, triggering a conformational change that unbinds TetR from the promoters, resulting in the derepression of *tetR* and *tetA* gene expression (Figure R10). Efflux of Tc by TetA has been well described by biochemical and genetics studies (Cuthbertson and Nodwell 2013; Nguyen *et al.* 2014). However, the dynamics and timing of TetA production and Tc efflux activity remained unexplored. In our laboratory, we revealed that Tc resistance can be established after acquisition of the F-Tn*10* plasmid, even in the presence of Tc that inhibits protein synthesis (Nolivos *et al.* 2019). How can cells produce the TetA efflux pump after plasmid entry despite the inhibitory effect of Tc on protein synthesis? Nolivos *et al.* demonstrated that synthesis of TetA in the presence of tetracycline is only possible through the activity of chromosomally encoded AcrAB-TolC multidrug efflux pump. AcrAB-TolC was previously described to allow cell growth in the presence of sub-inhibitory doses of a wide range of toxic compounds, among which several antibiotics including tetracycline (Nikaido 1996). Our work showed that the basal efflux activity of AcrAB-TolC is required to maintain a low level of protein synthesis in the presence of Tc. This residual translation activity is not sufficient for the cell to grow in the presence of inhibitory doses of Tc. However, if the recipient cell receives the F-Tn*10* plasmid from a donor, the residual translation activity is sufficient to allow the production of proteins encoded by the newly acquired plasmid, including TetA. This work was the first evidence for the importance of AcrAB-TolC system in the acquisition of resistance by plasmid conjugation.

The Nolivos *et al.* article set the basis for the follow-up project I worked on, which was to describe the real-time dynamics of TetA production and Tc efflux within recipient cells that carry the F-Tn*10* plasmid. To do so, we took advantage of the intrinsic autofluorescent property of the unmodified Tc molecule (Dubuy *et al.* 1964) and we quantified the production of TetA (TetA-mCherry fusion) in response to Tc addition. To carry out this project, I worked with Chloé Virolle and Kelly Goldlust who were just starting their PhD in the laboratory. I could then share my acquired expertise in microscopy analysis, growth and viability assays to successfully complete this project.

VI.1.2. Conclusion

This work showed the real-time dynamics of TetA production and the efflux of Tc during Tc-induced stress. Analysis of single-cell populations revealed the dynamics of Tc entry during the first 30 minutes after addition of the drug. We quantified how Tc entry triggers the production of the TetA pump, and the balance between TetA intracellular levels and Tc efflux activity. Analysis showed that the basal level of TetA (before Tc treatment) is finely tuned to allow the initial activity of Tc efflux required for the production of additional TetA pump, while avoiding the deleterious effect of TetA overproduction that is known to be toxic for the cells. Unexpectedly, we also showed that the basal intracellular TetA levels dictated by TetR repression is significantly heterogeneous in the cell population, with cells that contained low TetA levels accumulating more Tc than cells with high TetA contents. Interestingly, even when TetA efflux activity is fully established, we still detected low intracellular levels of Tc that are sufficient to avoid repression by TetR, thus allowing the maintenance of TetA production.

Importantly, the pre-induction of cells with anhydrotetracycline (aTc) (an analogue to Tc that retains TetR binding but not translation inhibition effect) showed that cells already containing high levels of TetA did not accumulate Tc and were insensitive to the drug, even at high concentration. Tc efflux mediated by TetA rapidly surpasses the Tc entry, which confers the resistance phenotype to bacterial cells. Induction with aTc also allowed to correlate the TetA cellular content with the level of resistance to Tc. Notably, we were able to show that 24h pre-induction with either Tc or aTc permit the cells to accumulate enough TetA pumps to resist to 20 and even 40 times the minimum inhibitory concentration (MIC) of Tc.

Our study clearly showed that Tc resistance depends on a balance between the production of the efflux pump and the ability of the Tc to block this production. The establishment of the Tc resistance phenotype is helped by the leakiness of *tetA* promoter allowing the production of basal quantity of TetA to efflux Tc thus permitting the production of additional TetA.

FEMS Microbiology Reviews, fuaa031, 44, 2020, 782–792

doi: 10.1093/femsre/fuaa031
Advance Access Publication Date: 6 August 2020
Research Article

RESEARCH ARTICLE

Direct visualisation of drug-efflux in live *Escherichia coli* cells

Audrey Reuter†, Chloé Virolle†, Kelly Goldlust†, Annick Berne-Dedieu, Sophie Nolivos‡ and Christian Lesterlin*,§

Microbiologie Moléculaire et Biochimie Structurale (MMSB), Université Lyon 1, CNRS, Inserm, UMR5086, 69007, Lyon, France

*Corresponding author: Microbiologie Moléculaire et Biochimie Structurale CNRS-UMR5086, 7 passage du Vercors 69007, Lyon, France. E-mail: christian.lesterlin@ibcp.fr

One sentence summary: Real-time visualization of tetracycline (Tc) and the Tc-specific TetA efflux pump protein reveals the dynamics of drug accumulation and extrusion in live *Escherichia coli* cells.

Editor: Tam Mignot

†These authors contributed equally
‡Current address: Université de Pau et des Pays de l'Adour, CNRS, UMR5254, IPREM, 64000, Pau, France
§Christian Lesterlin, http://orcid.org/0000-0002-9108-0848

ABSTRACT

Drug-efflux by pump proteins is one of the major mechanisms of antibiotic resistance in bacteria. Here, we use quantitative fluorescence microscopy to investigate the real-time dynamics of drug accumulation and efflux in live *E. coli* cells. We visualize simultaneously the intrinsically fluorescent protein-synthesis inhibitor tetracycline (Tc) and the fluorescently labelled Tc-specific efflux pump, TetA. We show that Tc penetrates the cells within minutes and accumulates to stable intracellular concentration after ~20 min. The final level of drug accumulation reflects the balance between Tc-uptake by the cells and Tc-efflux by pump proteins. In wild-type Tc-sensitive cells, drug accumulation is significantly limited by the activity of the multidrug efflux pump, AcrAB-TolC. Tc-resistance wild-type cells carrying a plasmid-borne Tn*10* transposon contain variable amounts of TetA protein, produced under steady-state repression by the TetR repressor. TetA content heterogeneity determines the cells' initial ability to efflux Tc. Yet, efflux remains partial until the synthesis of additional TetA pumps allows for Tc-efflux activity to surpass Tc-uptake. Cells overproducing TetA no longer accumulate Tc and become resistant to high concentrations of the drug. This work uncovers the dynamic balance between drug entry, protein-synthesis inhibition, efflux-pump production, drug-efflux activity and drug-resistance levels.

Keywords: microscopy in live bacterial cells; drug-efflux; drug-resistance; TetA efflux pump protein

INTRODUCTION

Drug-resistant microorganisms have been isolated soon after the introduction of antibiotherapy in the early 20th century. Microbiology analysis and systematic sequencing of drug-resistant bacteria from natural and clinical environments have since uncovered a vast collection of genes that confer resistance to most classes of antibiotics currently used in clinical treatments. Bacterial drug-resistance is consequently a significant obstacle to the successful treatment of infections and is recognized as an increasingly severe threat to public health worldwide. Due to its biological importance, bacterial drug-resistance has attracted lots of attention and has been the focus of extensive research. Various mechanisms of antimicrobial resistance have been characterised, including inactivation or modification of the drug, modification of a drug target, limiting drug uptake by changing the cell membrane permeability and active efflux of the drug. Drug efflux mechanism, first described in

Received: 29 January 2020; **Accepted:** 22 July 2020

1980 (McMurry, Petrucci and Levy 1980), play a prominent role in antimicrobial resistance (Nikaido 1998, 2009; Li and Nikaido 2004, 2009). Efflux of drugs from the cellular compartment to the extracellular medium can be performed by multidrug or drug-specific efflux pumps proteins.

Multidrug pumps are generally chromosome-encoded and able to extrude a wide range of toxic compounds, thus conferring a certain intrinsic level of multidrug resistance (MDR). In *E .coli*, the AcrAB-TolC tripartite complex transports a variety of antibiotics and other antimicrobials (Sulavik *et al.* 2001; Tal and Schuldiner 2009; Du *et al.* 2014; Li, Plésiat and Nikaido 2015; Bergmiller *et al.* 2017). AcrAB-TolC production is controlled by a complex network of transcriptional regulators (Li, Plésiat and Nikaido 2015), thus allowing for tight regulation of the efflux activity in response to environmental conditions or the presence of antimicrobials. Mutations in transcriptional repressor genes (such as *soxR*, *marR*, *acrR* or *envR*), which result in overproduction of the multidrug efflux pump, are often found in drug-resistant bacteria from natural and clinical origins.

Drug-specific pumps extrude and confer resistance to a single drug. Genes coding for drug-specific pumps are often found on mobile genetic elements such as conjugative plasmids or transposons, which acquisition is sufficient to confer resistance to minimal inhibitory concentration (MIC) of the drug. In this work we focus on the study of the paradigmatic Tetracycline-specific efflux pump TetA. Tetracycline (Tc) is a bacteriostatic protein-synthesis inhibitor that binds reversibly to the ribosome, thus preventing the association of aminoacyl-tRNA (Chopra and Roberts 2001). This fundamental mode of action renders Tc active in a broad-spectrum of both gram-positive and gram-negative bacteria. Since the introduction of Tc in 1948, resistant strains have emerged dramatically in both animal and humans (Roberts 1996; Chopra and Roberts 2001; Coenen *et al.* 2011). Tc-resistance dissemination together with the development of other effective antibacterial drugs led to the reduction of Tc usage in human treatments, yet Tc remains one of the most used antibiotics in livestock worldwide and is even used in plant agriculture (Eliopoulos, Eliopoulos and Roberts 2003). Notably, Tc is a substrate for the AcrAB-TolC multidrug pump. Indeed, AcrAB-TolC performs low levels of Tc-efflux activity, thus allowing *E. coli* to grow in the presence of sub-inhibitory concentration of the drug (Sulavik *et al.* 2001; Li, Plésiat and Nikaido 2015). However, AcrAB-TolC activity alone is not sufficient to support cell growth in the presence of minimal inhibitory concentration (MIC) of Tc (10 μg/ml). At this concentration, growth is only possible for strains carrying Tc-specific resistance genes (*tet* genes). To date, 36 *tet* genes have been identified across most bacterial genera. Ten of these genes encode ribosomal protection proteins (such as Tet(M) and Tet(O)), which prevent binding of the Tc molecule to the ribosomes (Burdett 1993; Warburton, Amodeo and Roberts 2016). However, Tc-resistance is largely mediated by efflux mechanisms as 23 of the 36 *tet* genes encode efflux pumps proteins belonging to the major facilitator superfamily (MFS). Efflux pumps of the TetA family were the first identified (Levy and McMurry 1978; McMurry, Petrucci and Levy 1980) and are among the most frequently found in resistant Gram-negative bacteria (Bryan, Shapir and Sadowsky 2004). In fact, *tetA* genes are often carried by transposons inserted in conjugative plasmids, which propagate by horizontal gene transfer between a broad-range of unrelated bacterial species. The paradigmatic Tn*10* transposon carries the *tetA* gene coding for the TetA efflux pump and the *tetR* gene encoding the TetR repressor. TetA is a proton motive force-dependent metal-tetracycline/H1 antiporter that selectively transports Tc through the inner membrane in exchange of a proton (Schnappinger and Hillen 1996; Thaker, Spanogiannopoulos and Wright 2010). By exporting Tc from the cytoplasm to the periplasm, TetA decreases the intracellular concentration of the drug, thus reducing protein translation inhibition. TetR is a Tc-responsive repressor protein that regulates *tetA* expression as follows. In the absence of Tc, TetR binds to the promoter region of the *tetA* gene and limits TetA production to basal steady-state levels. When present in the medium, Tc is transported into the periplasm, presumably via OmpF and OmpC porins, and then diffuses passively through the inner membrane (Mortimer and Piddock 1993; Roberts 1996; Fernández and Hancock 2012; Møller *et al.* 2016). Once in the cytoplasm, Tc binds to the ribosome and inhibits protein synthesis. In parallel, Tc also binds to TetR inducing a conformational change that releases the repressor from P_{tetA} promoter. This results in the induction of TetA production and Tc-efflux activity, thus helping to restore normal protein synthesis level. The level of Tc accumulation within the cells is then resulting from the balance between Tc-uptake (Tc entry) and Tc-efflux by pump proteins. Noteworthy, the non-antibiotic Tc analogue anhydrotetracycline (Atc) retains TetR binding and *tetA* induction activity, but does not inhibit protein synthesis and has no antibiotic effect.

Our current understanding of the mechanism of Tc resistance by the TetA efflux pump results from several decades of study (Roberts 1996; Chopra and Roberts 2001; Eliopoulos, Eliopoulos and Roberts 2003). Regulation of TetA production by TetR in response to the drug has been extensively investigated using genetics approaches, transcriptional analysis (Muthukrishnan *et al.* 2012; Møller *et al.* 2016) or using computational modelling (Biliouris, Daoutidis and Kaznessis 2011; Schultz, Palmer and Kishony 2017). Besides, biochemical works have provided a well-documented description of the structure and function of TetA and TetR proteins (Yamaguchi *et al.* 1990; Yamaguchi, Udagawa and Sawai 1990; Aldema *et al.* 1996; Ramos *et al.* 2005; Chow *et al.* 2012; Kumar and Varela 2012; Cuthbertson and Nodwell 2013). However, mainly due to previous technological limitations, the *in vivo* dynamics of Tc-efflux by the TetA pump in real-time at the single-cell level remains poorly understood. Here, we have developed an experimental system that enables to address this question. We use live-cell fluorescence microscopy associated with microfluidics chamber to perform the simultaneous visualization and quantification of both Tc and TetA intracellular concentrations. Tetracycline was visualized directly by taking advantage of its autofluorescence property (Dubuy *et al.* 1964)). In parallel, we use the fully functional carboxy-terminal fusion of TetA to the mCherry fluorescent protein (TetA-mCh) expressed from the FTn*10* plasmid endogenous locus (Nolivos *et al.* 2019). We characterise the dynamics of entry and accumulation of Tc within the intracellular compartment and the influence of AcrAB-TolC overproduction by deletion of the *acrR* gene. We also characterise Tc accumulation in Tc-resistant strain carrying the FTn*10tetA-mCh* plasmid and we correlate the induction of TetA production with Tc-efflux activity.

RESULTS

Tc accumulation in the intracellular compartment

We performed time-lapse fluorescence microscopy imaging of live *E. coli* cells placed in microfluidic chamber during the injection of growth medium containing minimal inhibitory concentration (1MIC) of Tc (10 μg/ml) or 10MIC of Tc (100 μg/ml). Image

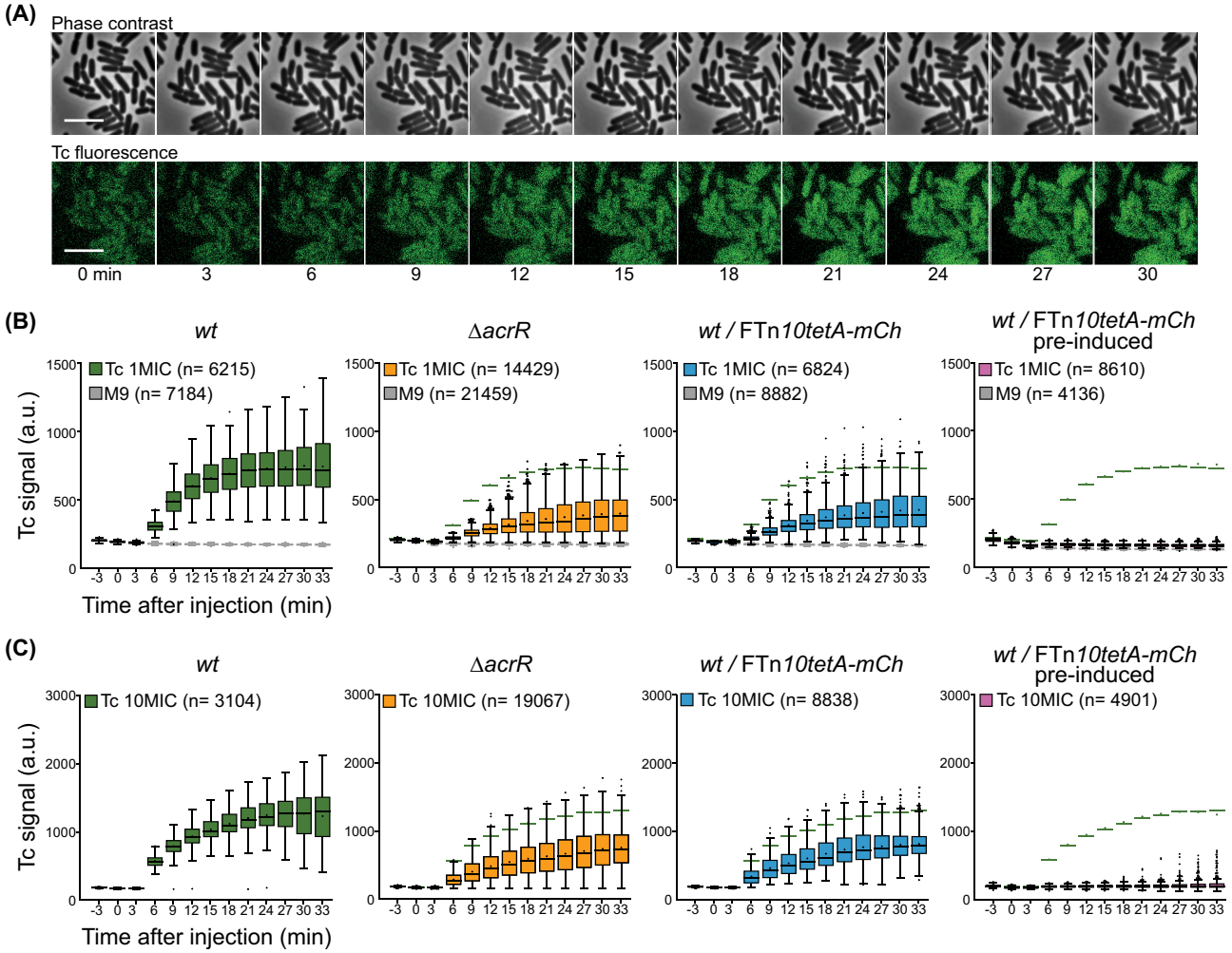

Figure 1. Dynamics of tetracycline accumulation in live *E. coli* cells. **(A)**, Time-lapse microscopy phase contrast (top) and green fluorescence channel (bottom) images of *wt E. coli* cells in microfluidics chamber during injection of Tc 1MIC (10 μg/ml). Imaging intervals 3 min. Scale bar 5 μm. **(B)**, Box plots presenting the quantification of green fluorescence intracellular signal (a.u., arbitrary unit) during time-lapse experiments after injection of M9 glucose medium with (coloured boxes) or without (grey boxes) Tc 1MIC (10 μg/ml). From left to right, results are presented for *wt*, Δ*acrR*, *wt*/FTn*10tetA-mCh* strains and for *wt*/FTn*10tetA-mCh* after overnight pre-induction with Atc (0.2 μg/ml). The median, quartile 1 and quartile 3 are indicated by horizontal lines and the mean by a black dot. Black dots above and below the max and min values correspond to outlier cells. The median and the mean obtained for the *wt* strain are reported on each plot by a green line and a green dot, respectively. The total number of cells analysed and plotted (n =) is indicated. **(C)**, Same as 1B for injection of Tc 10MIC (100 μg/ml).

analysis was achieved by running automated cell detection and quantification of Tc and TetA-mCh intracellular fluorescent signal in the course of the experiments. The early steps of Tc entry and accumulation in the cellular compartment were analysed using time-lapses with 3 min imaging intervals (Fig. 1A and Movie S1). When growth medium containing Tc at 1MIC is injected, the intracellular green fluorescence signal increases significantly, reflecting the entry of the intrinsically fluorescent Tc molecules within the cell compartment (Fig. 1A-B and Movie S1). Intracellular Tc is first detected between 3 and 6 minutes after injection, and accumulates to eventually reach a steady-state level after 21 min ± 3. When Tc concentration is increased to 10MIC (Fig. 1C and Movie S1), we also detect the entry of the Tc between 3 and 6 minutes after injection. However, it takes a longer 27 min ± 3 period for Tc intracellular concentration to eventually stabilize. Most importantly, the final concentration of Tc accumulated is increased by 2-fold compared to cells exposed to 1MIC. This shows that a 10-fold increase in Tc concentration in the medium only results in a 2-fold increase accumulation within the cells. These observed levels of Tc accumulation reflect the balance between Tc-uptake by the cells (Tc entry) and the extrusion of Tc mediated by efflux pump proteins. Our observations suggest that the efficiency of Tc-uptake and Tc-efflux do not respond similarly to the increase of Tc concentration in the medium, resulting in Tc accumulation levels that are not proportionally dose-dependent (see discussion).

To better understand the contribution of Tc-efflux activity on the dynamics of accumulation within *wt* cells, we investigated the importance of the main multidrug pump in *E. coli*, the AcrAB-TolC complex. AcrAB-TolC is known to extrude Tc, thus allowing resistance and cell growth in the presence of sub-inhibitory concentrations of the drug (Sulavik *et al.* 2001; Li, Plésiat and Nikaido 2015). Consistently, we have previously reported that Δ*acrA*, Δ*acrB* and Δ*tolC* single mutants strains accumulate significantly more Tc than the isogenic *wt* strain (Nolivos *et al.* 2019). We then tested the effect of AcrAB-TolC overproduction induced by deletion of the *acrR* repressor gene (Nolivos *et al.* 2019). The entry of Tc in Δ*acrR* cells is detected between 3 and 6 min after injection of the drug at 1MIC, as observed for the *wt* strain (Fig. 1B). However, the final level of Tc accumulation is significantly reduced in

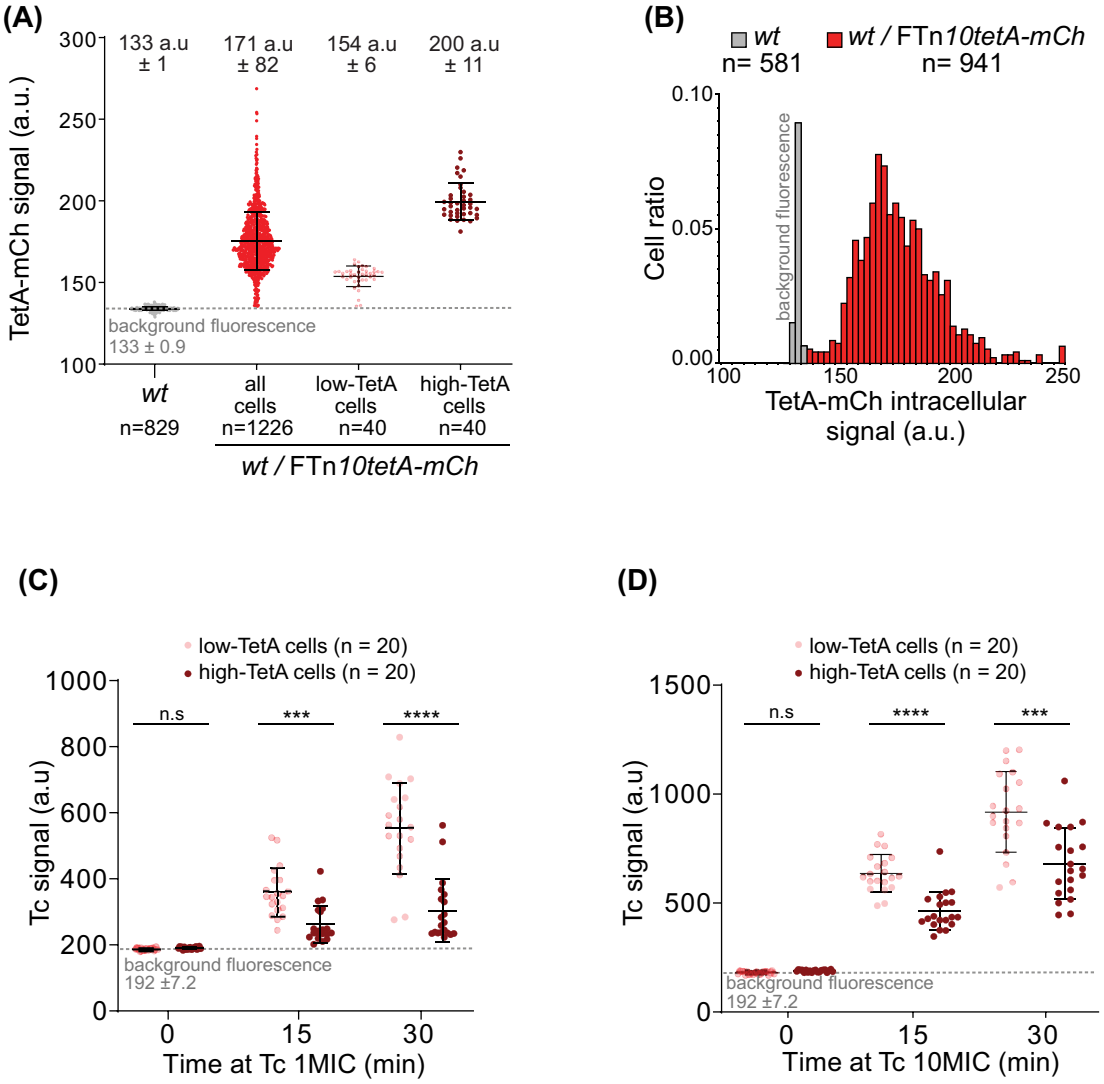

Figure 2. Influence of the initial cellular TetA-mCh content on the dynamics of Tc accumulation. **(A)**, Jitter plots present the quantification of red fluorescence intracellular signal of single-cells (a.u., arbitrary unit). The autofluorescence background of the *wt* strain is shown by grey dots and the grey-dashed line (133 a.u. ±0.9). Results for the *wt*/FTn*10tetA-mCh* cells are shown by red dots reflecting TetA-mCh signal plus the autofluorescence background. Light red and dark red dots correspond to *wt*/FTn*10tetA-mCh* cells selected for the low- or high-TetA initial content, respectively. Each dot corresponds to a single-cell, mean and standard deviations are shown in black lines and reported in numbers above the plots. **(B)**, Histogram of the red fluorescence distribution in *wt* (grey) and *wt*/FTn*10tetA-mCh* (red) cell populations. **(C and D)**, Jitter plots of green fluorescence intracellular signal for *wt*/FTn*10tetA-mCh* single-cells with initially low-TetA content (light red) or high-TetA content (dark red). Value at t = 0 min and the grey dashed line correspond to the green autofluorescence background of the cells before the injection of Tc (192 a.u. ±7.2). Data presented for cells 15 and 30 min after injection of Tc 1MIC **(C)**, and 10MIC **(D)**, show a reduction of Tc accumulation in high-TetA content cells compared to low-TetA content cells. The total number of cells analysed (n =) is indicated in each plot. *P-Value* significance from unpaired statistical *t-test* is indicated by n.s. (>0.05, non-significant), *** (<0.001 significant) and **** (<0.0001 significant).

Δ*acrR* cells compare to *wt* and is attained later (27 min ± 3 compared to 21 min ± 3 for *wt*). At Tc 10MIC, Tc final accumulation was also decreased by ∼2-fold in the Δ*acrR* strain compared to *wt* strain (Fig. 1C). These observations show that the overproduction of AcrAB-TolC pump induced by *acrR* deletion enhances the cells ability to efflux Tc, consequently limiting its accumulation in the cytoplasm. Reduction of Tc intracellular accumulation is expected to attenuate the inhibition of protein synthesis. Consistently, mutations inactivating AcrR or other repressors of AcrAB-TolC (MarR, SoxR) are often found in clinical or environmental strains exhibiting partial resistance to a range of antibiotics, including Tc (Vinué, Hooper and Jacoby 2018; Hoeksema *et al.* 2019).

Next, we analysed Tc accumulation in *wt* cells carrying the Tc-resistant FTn*10tetA-mCh* plasmid (Nolivos *et al.* 2019). Again, Tc entry is detected between 3 and 6 min after drug injection (Fig. 1B). The final level of accumulation is attained after 21 min ± 3 and is decreased by 2-fold compared to *wt* cells. Similar results are observed in the presence of Tc at 10 MIC (Fig. 1C). These results indicate that even before exposure to Tc, *wt*/FTn*10tetA-mCh* cells already contain TetA pump proteins readily available to perform efflux of Tc. Consistently, we quantified a significant increase of red intracellular fluorescence in *wt*/FTn*10tetA-mCh* cells compared to *wt* cells, reflecting the basal amounts of TetA-mCh molecules in plasmid-containing cells (Fig. 2A). These data show that even before exposure to Tc,

the steady-state repression of the *tetA* gene mediated by the TetR repressor allows for the production of a basal level of TetA molecules. This initial TetA-mCh cellular pool is immediately available to perform efflux of Tc and limit the accumulation of the drug in the cellular compartment.

Population heterogeneity in TetA initial content influences Tc accumulation levels

We noticed a certain level of heterogeneity in the initial amounts of TetA-mCh proteins contained in the *wt*/FTn*10tetA-mCh* cell population (Fig. 2B). We wanted to know whether this initial heterogeneity in TetA content influences the dynamics of Tc accumulation at the single-cell level. To test this possibility, we selected cells with low-TetA initial contents and cells with high-TetA initial contents (Fig. 2B). After subtraction of the red background fluorescence (133 a.u ± 1), we estimated that high-TetA content cells initially possess ∼3.2 times more TetA molecules than low-TetA content cells (see methods). We then quantified Tc accumulation in these two cells categories, 15 and 30 minutes after Tc injection at 1MIC and 10MIC (Fig. 2C and D). Results show that high-TetA cells accumulate significantly less Tc than low-TetA cells. More specifically, the 3.2-fold increase in TetA-mCh initial content results in a 2.5-fold and 1.5-fold decrease in Tc accumulation at 1MIC and 10MIC, respectively. These findings reveal that TetR steady-state repression induces a slight heterogeneity in TetA cellular amounts, which is sufficient to translate into population phenotypic heterogeneity where cells containing more TetA pumps are predisposed to efflux Tc more efficiently. This raised the possibility that cells with very high initial amounts of TetA proteins would perform maximum Tc-efflux activity, thus reducing drug accumulation to minimal levels. To test this hypothesis, we pre-induced *wt*/FTn*10tetA-mCh* cells with anhydrotetracycline (Atc 0.2 μg/ml), a Tc analogue that has no antibiotic activity, while retaining the ability to bind to TetR and induce the production of TetA proteins. Pre-induced cells exhibit a ∼60-fold increase in TetA-mCh cellular content compared to non-induced cells (Fig. S1A and B, Supporting Information). Time-lapse analysis shows that these cells accumulate virtually no Tc either at 1MIC or 10MIC concentrations (Fig. 1B and C). In these cells, Tc-efflux activity is maximized and outcompetes the constant entry of Tc within the cells.

Correlation between TetA induction and efflux of tetracycline

No increase of TetA-mCh fluorescence was detected during the first 30 minutes after injection of Tc (Fig. S1C, Supporting Information). We then performed time-lapses over 300 minutes periods (30 min imaging intervals) to analyse the induction of TetA-mCh production and correlate with Tc-efflux activity in *wt*/FTn*10tetA-mCh* cells (Fig. 3A and Movie S2). At Tc 1MIC, the accumulation of drug during the first 30 min is followed by a subtle but detectable increase of intracellular TetA-mCh signal at 60 min (Fig. 3B and C). This indicates that the internalized level of Tc is not sufficient to fully inhibit protein synthesis. The modest increase in TetA-mCh content is concomitant with the extrusion of Tc, which concentration rapidly reduces between 30 and 60 min to stabilize at low levels (Fig. 3B). Noteworthy, the low amount of Tc remaining in the cells is sufficient to maintain the induction of TetA-mCh synthesis, which ends up being produced at high levels (Fig. 3C). Importantly, the growth of *wt*/FTn*10tetA-mCh* cells in the microfluidic chamber in the presence of Tc 1MIC is comparable to growth without antibiotic (Fig. S2A and Movie S2, Supporting Information). This is confirmed by OD monitoring of the *wt*/FTn*10tetA-mCh* strain grown in liquid culture (Fig. S2B, Supporting Information). These results indicate that the initial pool of cellular TetA reduces Tc accumulation to levels that allow protein synthesis to continue, allowing for the production of additional TetA and the continuation of cell growth and normal rate. By contrast, in the presence of Tc 10MIC, *wt*/FTn*10tetA-mCh* cells stop growing over the duration of time-lapse experiments (Figure S2A and Movie S2). Meanwhile, microscopy analysis reveals that high amount of Tc remain in the cells for a long period of time (Fig. 3D). At ∼120 min ± 30 min, we observed that TetA-mCh is produced at low rate compared to Tc 1MIC (compare Fig. 3C to E). This modest increase in TetA-mCh cellular content in nonetheless concomitant with the initiation of the efflux of Tc, which intracellular concentration reduces slowly to reach low levels at 270 min ± 30 (Fig. 3D). OD monitoring consistently reveals that in the presence of Tc 10MIC, cell growth is arrested for a period of about 5 hours before restarting progressively (Fig. S2B, Supporting Information). Height hours after exposure to Tc10MIC, TetA-mCh cellular content is significantly increased (Fig. S2C, Supporting Information). These results indicate that at 10MIC concentration, the amount of Tc accumulated in the cells strongly alters the cells' ability to synthesis new TetA proteins. The cells remain in relative latency for several hours, but eventually manage to produce additional TetA-mCh proteins, which initiate the extrusion of Tc and slowly allows cells growth to restart and more TetA to be produced after 5 hours. We finally observed that pre-induced *wt*/FTn*10tetA-mCh* cells, which initially contain very high amount of TetA-mCh, accumulate virtually no Tc at 1MIC (Fig. S3A, Supporting Information) and very low levels of Tc at 10MIC (Fig. S3C, Supporting Information), and exhibit no growth latency at either concentration (Fig. S2B, Supporting Information). Similar results were observed for *wt*/FTn*10tetA-mCh*Δ*tetR* strain, in which TetA overproduction is triggered by deletion of the *tetR* gene from the *wt*/FTn*10tetA-mCh* plasmid (Fig. S2B, Supporting Information).

Correlation between TetA cellular content and the level of resistance to tetracycline

We next addressed the level of Tc-resistance of cells containing low or high cellular levels of TetA. To do so, we pre-induced *wt*/FTn*10tetA-mCh* cells with Tc 1MIC or Atc (0.2 μg/ml) for 2, 4, 8 or 24 hours. These pre-induced cell cultures were observed by snapshot microscopy to quantify TetA-mCh intracellular contents and plated on medium containing 1MIC, 10MIC, 20MIC or 40MIC of Tc in parallel (Fig. 4A-C). Snapshot analysis shows that Tc 1MIC and Atc (0.2 μg/ml) induce similar rate of TetA-mCh synthesis. In both case, the increase in TetA cellular content is clearly associated with the enhanced resistance to Tc 10MIC, 20MIC and even 40MIC to some extent. This finding reveals that cells exposed to non-lethal concentration of drug develop very high levels of acquired resistance due to the overproduction of TetA pump protein. However, we also observe that cells with high TetA contents (pre-induced *wt*/FTn*10tetA-mCh* cells and *wt*/FTn*10tetA-mCh*Δ*tetR* cells) exhibited slower growth in M9 compared to the *wt* or non-induced *wt*/FTn*10tetA-mCh* cells (Fig. S2B, Supporting Information). These results show that the overproduction of TetA is associated with a selective advantage in

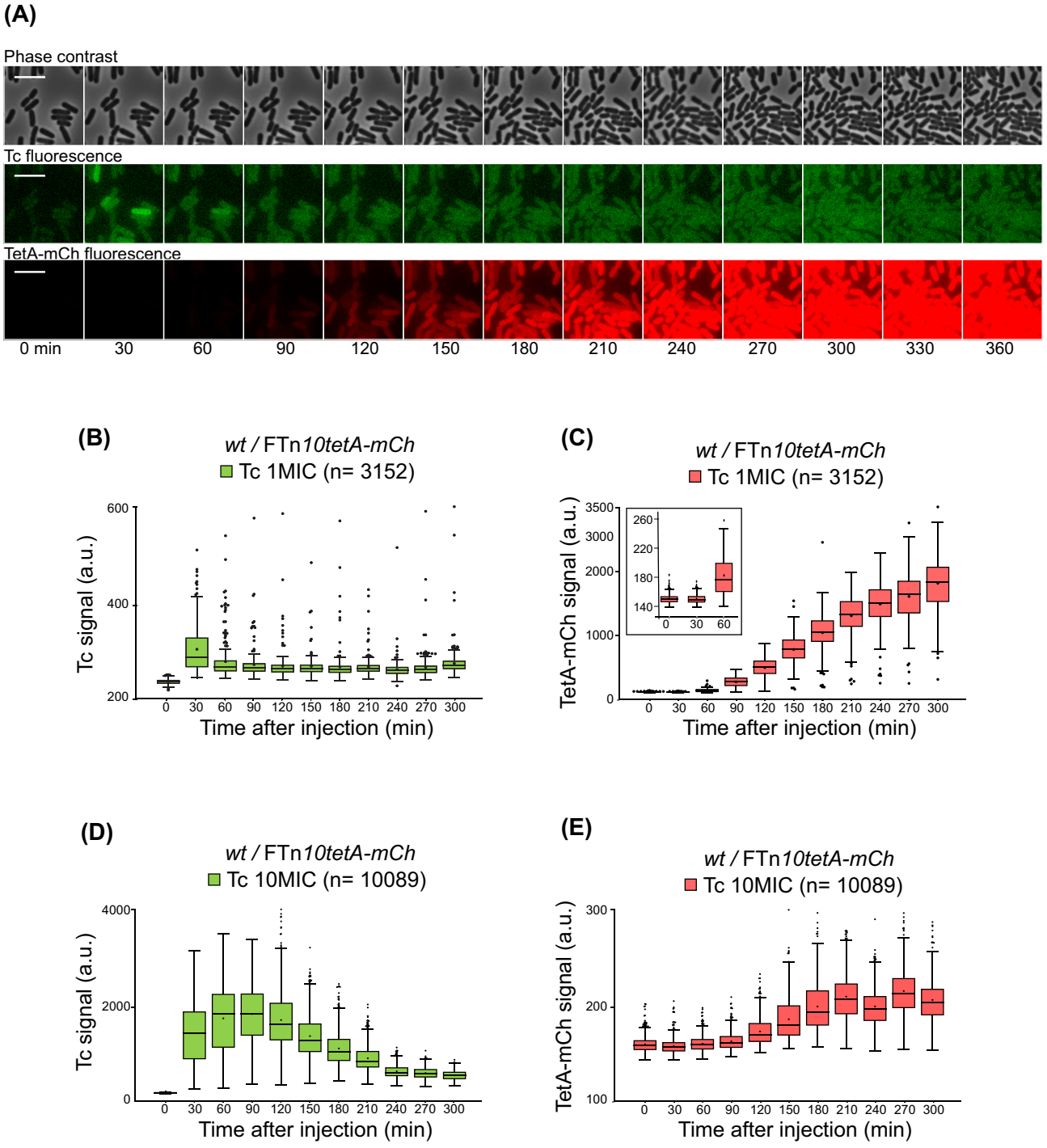

Figure 3. Dynamics of tetracycline accumulation and efflux in correlation with TetA-mCh production in live *E. coli* cells. **(A)**, Time-lapse microscopy phase contrast (top), green fluorescence (middle) and red fluorescence (bottom) images of *wt*/FTn*10tetA-mCh* cells in microfluidics chamber during injection of Tc 1MIC (10 μg/ml). Imaging intervals 30 min. Scale bar 5 μm. **(B and C)**, Box plots presenting the quantification of Tc (B) and TetA-mCh (C) during time-lapse experiments after injection of M9 glucose medium containing Tc 1MIC (10 μg/ml). **(D and E)**, Box plots presenting the quantification of Tc (D) and TetA-mCh (E) after injection of M9 glucose medium containing Tc 10MIC (100 μg/ml). For B, C, D and E the median, quartile 1 and quartile 3 are indicated by horizontal lines, and the mean by a black dot. Black dots above and below the max and min values correspond to outlier cells. The total number of cells analysed and plotted (n =) is indicated. In these time-lapses, medium supplemented with Tc 1 or 10MIC was injected for 30 min, the injection was then stopped for the rest of the experiment.

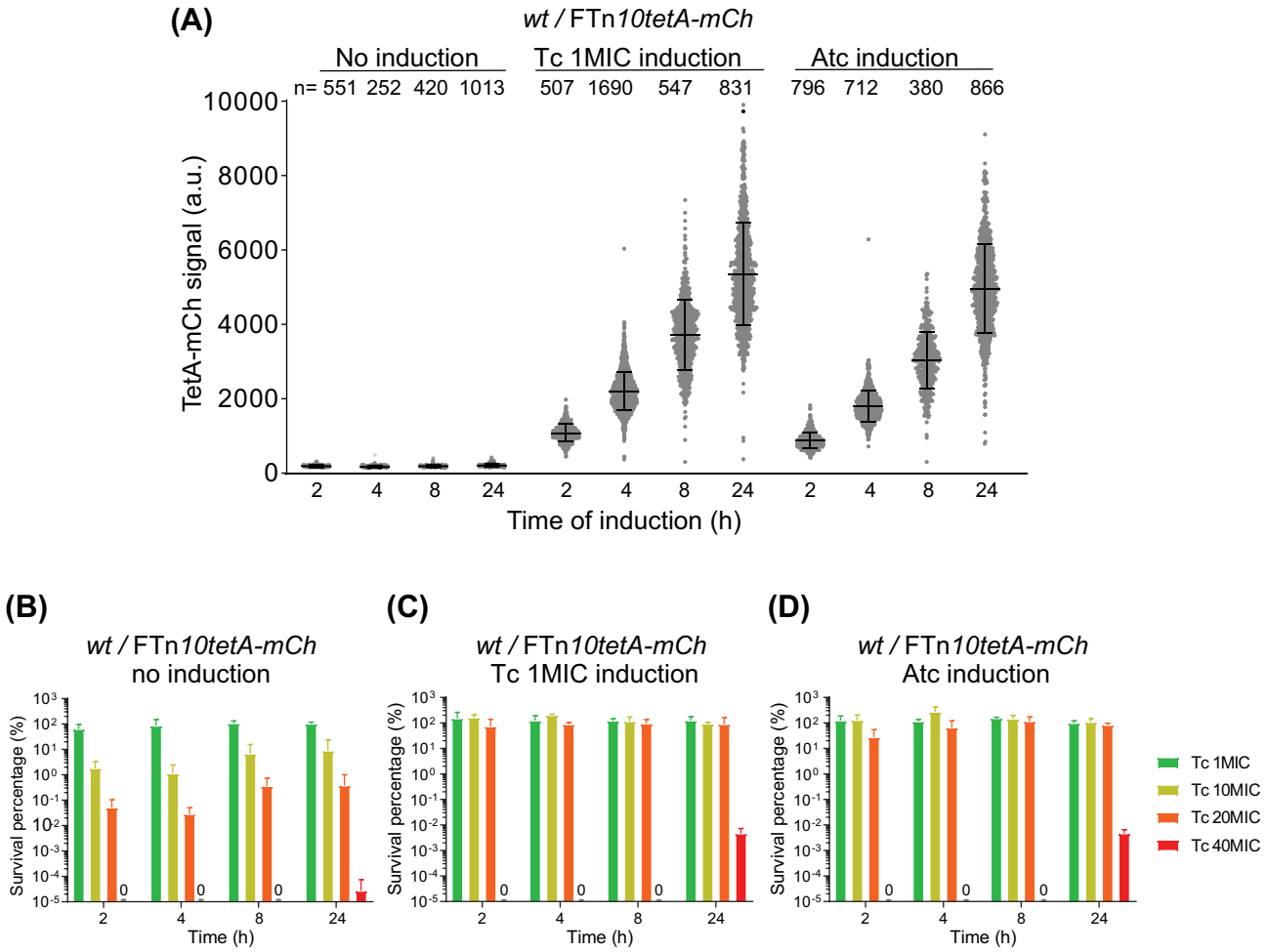

Figure 4. TetA-mCh intracellular content determines the level of Tc-resistance. **(A)**, Jitter plots presenting the quantification of TetA-mCh intracellular signal (a.u., arbitrary unit) from snapshot microscopy imaging of the *wt*/FTn*10tetA-mCh* strain in the absence of induction or 2, 4, 8 and 24 hours after induction with Tc 1MIC and Atc (0.2 μg/ml). Each dot corresponds to a single-cell, mean and standard deviations are shown in black lines. The number of cells analyzed and plotted (n =) is indicated. **(B, C and D)**, Histogram presenting the survival of *wt*/FTn*10tetA-mCh* cells in the presence of increasing doses of Tc. Results are shown for *wt*/FTn*10tetA-mCh* cells corresponding to the panel **(A)**, i.e. without induction **(B)**, or 2, 4, 8 and 24 hours after induction with Tc 1MIC **(C)** or Atc (0.2 μg/ml) **(D)**. Survival was estimated by CFU/ml counting after plating on 1MIC, 10MIC, 20MIC or 40MIC of Tc.

the presence of Tc, but also with a loss of fitness in the absence of antibiotic (see discussion).

DISCUSSION

Live-cell fluorescent microscopy imaging represents a valuable tool to investigate bacterial responses to antibiotics in real-time. Most microscopy studies of antibiotics mode of action and interaction with bacterial cells generally requires the use of antibiotics conjugated with fluorescent moieties, such as Fluorescein or BODIPY (Stone *et al.* 2018). These studies are informative, yet often limited by the fact that the modification of the antibiotic might alter its biochemical properties, including the ability to penetrate the bacterial cell or to perform the inhibitory effect on the cellular machineries (Stone *et al.* 2018). In this work, we use the unmodified tetracycline, which is part of the few antibiotics that are intrinsically fluorescent. The simultaneous visualization of Tc and the fully functional fluorescently labelled TetA-mCh Tc-specific pump protein allowed us to characterize the real-time dynamics of drug accumulation and efflux in live bacteria.

Tc entry within the cells is observed 3 to 6 min after injection in the microfluidic chamber. Similar timing is observed for all tested strains, indicating that the rate of Tc-uptake is mostly unchanged in all tested genetic backgrounds. The observed levels of Tc accumulation reflect the balance between the two opposite effect of Tc-uptake (Tc entry) and Tc extrusion mediated by efflux pump proteins. Tc crosses the outer membrane via porins and the inner membrane by free diffusion. The internalized Tc is subsequently extruded to the extracellular medium by multidrug or drug-specific efflux pumps present in the cells. Interestingly, we observe that a 10-fold increase of Tc concentration in the medium only results in a ~2-fold increase of Tc accumulation levels in the cells. This absence of proportionality between Tc accumulation levels and the dose of antibiotic suggests that Tc-uptake and Tc-efflux activities do not respond similarly to the increase of Tc concentration. Tc-uptake is expected to be limited by the amount of outer membrane porins available, and Tc-efflux by the amount of efflux-pump present in the cells. Our results are compatible with a scenario where Tc 10MIC saturates Tc-uptake systems earlier than Tc-efflux systems, resulting in the relative reduction of Tc accumulation compared to Tc 1MIC condition. This proposal is consistent with the recent

reports that rate of drug-uptake is rate limited by the antibiotic's ability to diffuse through the inner membrane, which permeability properties also varies in response to conditions (pH, temperature and drug treatments) (Cama *et al.* 2015, 2016; Cama, Henney and Winterhalter 2019).

The ability of the cells to extrude the internalized Tc is significantly enhanced by the overproduction of the AcrAB-TolC multidrug pump in the Δ*acrR* strain, as well as by the presence of a basal pool of TetA produced from the FTn*10tetA-mCh* resistance plasmid. In both the Δ*acrR* and in *wt*/FTn*10tetA-mCh* cells, Tc accumulation is reduced by 2-fold compare to the *wt*. This reduction of Tc accumulation is not sufficient to improve the growth of the Δ*acrR* cells compared to the *wt*. However, similar reduction of Tc accumulation appears sufficient for protein synthesis to continue in *wt*/FTn*10tetA-mCh* cells, thus allowing the production of additional TetA pumps required for optimal Tc-efflux activity and subsequent cell growth. Increasing Tc concentration to 10 MIC increases Tc accumulation to levels that further inhibit protein synthesis, thus reducing significantly the rate of TetA production and delaying cell growth.

Quantitative image analysis reveals a certain level of heterogeneity of TetA-mCh initial content in the cell population. This shows that even in the absence of Tc or Atc inducers, TetR-mediated repression slightly varies at the single-cell level. Interestingly, this gene expression heterogeneity is sufficient to translate into significant phenotypic heterogeneity, where TetA initial content correlates directly with the cells initial ability to efflux Tc. Yet, Tc still accumulates in all cells, indicating that Tc-efflux activity mediated by the initial pool of TetA pumps is sub-optimal. It is only after TetA content adjustment that the equilibrium between Tc-uptake and efflux is reached, and that Tc intracellular levels become low and stable, presumably reflecting the constant entry of the drug within the cells. The low amount of Tc still detected in the cells is sufficient to induce the rapid production of TetA proteins. Using quantitative real-time PCR, it has been shown that the ratio *tetA*/*tetR* mRNA is increased by 4-fold in the presence of Tc 1MIC (Møller *et al.* 2016). This transcriptional response optimizes the synthesis rate of TetA, which accumulates to a final concentration increase by ∼60-fold compare to the initial levels. We show that such cells overproducing TetA accumulate virtually no Tc and are resistant to very high doses of the drug (up to 20 MIC and 40 MIC). If the overproduction of TetA is advantageous in the presence of the drug, then why does TetR-mediated repression maintain TetA initial concentration to low levels that are sub-optimal for Tc-efflux? This is most probably explained by our observation that TetA overproduction has a deleterious effect on the cells fitness in the absence of the drug. The phenotype of fitness loss associated with TetA overproduction was previously reported and attributed to unrestricted translocation of protons and ions across the membrane, which triggers partial loss of the membrane potential (Eckert and Beck 1989). TetR-mediated repression of the *tetA* gene is then finely tuned to allow the production of sufficient TetA proteins to limit Tc-accumulation and ensure the maintenance of translation activity required for the synthetized of additional TetA pumps. On the other hand, TetR repression also avoids TetA overproduction that would be deleterious for the cells, while allowing a sensitive detection of the presence of Tc as well as a fast regulatory response.

This work emphasises that the bacterial response to tetracycline depends on the equilibrium between two opposite parameters, the ability of efflux pumps to limit drug accumulation and the ability of the accumulated drug to avoid the production of additional pumps required for the establishment of effective resistance. The outcome of this dynamic balance primarily depends on the initial concentration of efflux pumps in the cells and the concentration of the drug in the medium.

METHODS

Bacterial strains, plasmids and growth

Bacterial strains and plasmids are listed in Table S1 (Supporting Information). Fusion of genes with fluorescent tags and gene deletion used λRed recombination (Datsenko and Wanner 2000; Yu *et al.* 2000). Chromosomal gene *loci* were transferred by phage P1 transduction to generate the final strains. F plasmids were transferred by conjugation. Unless otherwise stated, cells were grown at 37°C in M9 medium supplemented with glucose (0.2%). When appropriate, supplements were used at the following concentrations; Streptomycin (St) 20 μg/ml, Ampicillin (Amp) 100 μg/ml, and Tetracycline (Tc) 10 μg/ml. For pre-induction of TetA-mCh, *wt*/FTn*10tetA-mCh* strain was grown at 37°C in minimal medium supplemented with anhydrotetracycline (Atc) 0.2 μg/ml.

Spot assay and growth curves

Spot assays

Cells were grown overnight in M9 minimal medium supplemented with glucose 0.2% at 37°C and serial diluted. About 10 μl drop of each dilution was deposited on LB agar plates supplemented with Tetracycline (Tc) 10, 100, 200 or 400 μg/ml, corresponding to 1MIC, 10MIC, 20MIC and 40MIC, respectively. Plates were incubated overnight at 37°C, and the next day the concentration of Colony Forming Unit (CFU/ml) was estimated. The survival efficiency of each strain was calculated by normalizing the CFU/ml in the presence of Tc by the CFU/ml on plates without Tc (Fig. 4B-D). Plates were scanned using a Typhoon fluo-phosphoimager GE Healthcare with standard acquisition parameters.

Growth curves

Growth curves (Fig. S2B, Supporting Information) were performed automatically using TECAN Spark multimode plate reader. Flat transparent bottom 96-wells plates were loaded with 20 μl of exponentially growing cultures and incubated at 37°C, with 1 min agitation and A_{600} measurement every 5 min over 9 hours. Mean growth curves with standard deviation for experimental triplicates were generated using Excel and GraphPad Prism software.

Live-cell microscopy imaging and analysis

Cell imaging on agarose-pad

Overnight culture of cells in M9 minimal medium were diluted to an OD_{600nm} of 0.01 and grown with shaking at 37°C to an OD_{600nm} of 0.2. Treated or untreated cells cultures were collected at time points indicated and 5 μl samples were deposited on 1% agarose-M9 medium pad (Lesterlin and Duabrry 2016) and imaged by microscopy snapshots.

Time-lapse in microfluidic chamber

Time-lapse in microfluidic chambers were performed as described previously (Nolivos *et al.* 2019). Here, overnight cultures of cells in M9 minimal medium were diluted to an OD_{600nm} of 0.05 and grown at 37°C to an OD_{600nm} of 0.1–0.2. Cells were immediately loaded into a B04A microfluidic chamber (ONIX,

CellASIC®) preheated at 37°C. For Tc entry time-lapses (3 min imaging intervals; Fig. 1), minimal medium supplemented or not with Tc 10 μg/ml (1MIC), Tc 100 μg/ml (10MIC), or Atc 0.2 μg/ml was injected at 3 psi into the microfluidic chamber immediately after acquisition of frame 2 and for the duration of the experiment (45 min). For Tc efflux and TetA induction experiment time-lapses (30 min imaging intervals; Fig. 3), minimal medium supplemented or not with Tc 10 μg/ml (1MIC), Tc 100 μg/ml (10MIC) or Atc 0.2 μg/ml was injected at 3 psi into the microfluidic chamber immediately after acquisition of frame 1 and stopped after 30 min. Nothing else was injected for the rest of the experiment (330 to 400 min).

Image acquisition

Conventional wide-field fluorescence microscopy imaging was carried out on an Eclipse Ti-E microscope (Nikon), equipped with x100/1.45 oil Plan Apo Lambda phase objective, FLash4 V2 CMOS camera (Hamamatsu), and using NIS software for image acquisition. Phase contrast images were also acquired at each timepoint. Fluorescence signal acquisition settings were 100 ms for Tc and 100 ms for mCh for both snapshots on agarose-pad and time-lapses in microfluidic chamber, using 50% power of a Fluo LED Spectra X light source at 488 nm and 560 nm excitation wavelengths, respectively. FM 4–64 was acquired using 20 ms exposure at 50% power of a Fluo LED Spectra X light source 560 nm excitation. Structured-illumination microscopy in 3D (3D-SIM) presented in Figure 6 and in Movies was carried out on a standard Elyra PS1 Zeiss microscope. The raw 3D-SIM stacks were composed of 10 to 14 z-sections (110 nm interval for Tc signal and 126 nm interval for TetA-mCh), with 15 images per z-section with the striped illumination pattern rotated to three angles and shifted in five phase steps. Acquisition settings were 60 ms exposure with 593 nm laser (20% transmission) for TetA-mch and 40 ms exposure with 488 nm laser (10% transmission) for Tc. 3D-SIM was performed on exponentially growing cells observed cultivated in M9 minimal medium supplemented with glucose 0.2% with or without Tc.

Image analysis

Microscopy images processing was performed using the open source ImageJ/Fiji (download at [6]) and quantitative image analysis was performed using the free MicrobeJ plugin (download at http://microbej.com) (Ducret, Quardokus and Brun 2016). Cells outlines were detected automatically based on the segmentation of phase contrast image. When required, cell outlines were corrected using the Manual-editing interface of MicrobeJ plugin. Mean intracellular fluorescence values were extracted automatically using MicrobeJ plugin. Boxplots, fluorescence histograms, and split histograms were plotted using MicrobeJ interface. Jitter plots, growth curves with mean and standard deviation were generated using Excel and GraphPad Prism software. Imaris analysis software (Bitplane) was used to generate 3D-renderings of 3D-SIM stacks fluorescence signal presented in the Movies.

Consideration of the cells background autofluorescence

Wilt-type *E. coli* cells (without fluorescent marker) exhibit low fluorescence signal in both red and green fluorescence channels (shown in Figs 1B, 2 and Fig. S1, Supporting Information). Background red fluorescence (*Brf*) was 133 a.u. ±0.9 (calculated on n = 829 *wt* cells) and background green fluorescence (*Bgf*) was 192 a.u. ±7.2 (calculated on n = 474 *wt* cells). During time-lapse imaging where fresh medium (without Tc or Atc) was injected, these signals gradually decrease (Fig. 1B-C; Fig. S1C, Supporting Information), reflecting the bleaching of the cells autofluorescence. Figures showing the variation of Tc, Atc and TetA-mCh intracellular present the raw fluorescence values (*Rf*), which then reflect the combination of Tc, Atc or TetA-mCh specific fluorescence (*Sf*), plus the Background fluorescence (*Bf*) of the cells. However, these background fluorescence (*Bf*) values were subtracted from the Raw fluorescence (*Rf*) value to estimate the specific fluorescence (*Sf*) attributable to Tc or Atc *Sf*(Tc) or TetA-mCh *Sf*(TetA); (*Sf*(Tc) = *Rf*(Tc)—*Bgf*) and (*Sf*(TetA) = *Rf*(TetA)—*Brf*). The ratio of two specific fluorescence valued allowed calculating the fold-change in TetA-mCh, Tc or Atc intracellular content (Fold-change = *Sf2*/*Sf1*). For instance the fold-change in Tc accumulation between high-tetA content cells and low-tetA content cells was:

$$\text{Fold} - \text{change in Tc intracellular content} = Sf_{\text{high}-\text{tetA content cells}} / Sf_{\text{low}-\text{tetA content cells}}$$

where

$$Sf(Tc)_{\text{high}-\text{tetA content cells}} = Rf(Tc)_{\text{high}-\text{tetA content cells}} - Bgf_{wt\ \text{cells}}$$

and

$$Sf(Tc)_{\text{low}-\text{tetA content cells}} = Rf(Tc)_{\text{low}-\text{tetA content cells}} - Bgf_{wt\ \text{cells}}$$

SUPPLEMENTARY DATA

Supplementary data are available at FEMSRE online.

AUTHOR CONTRIBUTIONS

AR, CV, KG, AD, SN and CL made the bacterial strains and plasmids and performed the experiments. AR, CV, KG and CL analysed the data and prepared the figures. CL conceived the project and wrote the paper.

ACKNOWLEDGEMENTS

The authors thank the National BioResource Project, the Coli Genetic Stock Center and Vickers Burdett for providing strains; Nichola Teh, M Halte and M Bancale for early involvement in the project. A Ducret for valuable help with MicrobeJ.

FUNDING

CL acknowledges the ATIP-Avenir program, the Schlumberger Foundation for Education and Research (FSER 2019), FINOVI (AO-2014), the ANR PRC program (PlasMed) for funding to KG, the FRM (Foundation pour la Recherché Médicale) for funding to AR (ECO201806006855) and SN (ARF20150934201) and the University of Lyon for funding to CV.

Conflict of interest. None declared.

REFERENCES

Aldema ML, McMurry LM, Walmsley AR *et al.* Purification of the Tn 10-specified tetracycline efflux antiporter TetA in a

native state as a polyhistidine fusion protein. *Mol Microbiol* 1996;**19**:187–95.
Bergmiller T, Andersson AMC, Tomasek K *et al*. Biased partitioning of the multidrug efflux pump AcrAB-TolC underlies long-lived phenotypic heterogeneity. *Science* 2017;**356**:311–5.
Biliouris K, Daoutidis P, Kaznessis YN. Stochastic simulations of the tetracycline operon. *BMC Syst Biol* 2011;**5**:9.
Bryan A, Shapir N, Sadowsky MJ. Frequency and distribution of tetracycline resistance genes in genetically diverse, nonselected, and nonclinical Escherichia coli strains isolated from diverse human and animal sources. *Appl Environ Microbiol* 2004;**70**:2503–7.
Burdett V. tRNA modification activity is necessary for Tet(M)-mediated tetracycline resistance. *J Bacteriol* 1993;**175**:7209–15.
Cama J, Bajaj H, Pagliara S *et al*. Quantification of Fluoroquinolone Uptake through the Outer Membrane Channel OmpF of Escherichia coli. *J Am Chem Soc* 2015;**137**:13836–43.
Cama J, Henney AM, Winterhalter M. Breaching the Barrier: Quantifying Antibiotic Permeability across Gram-negative Bacterial Membranes. *J Mol Biol* 2019;**431**:3531–46.
Cama J, Schaich M, Al Nahas K *et al*. Direct Optofluidic Measurement of the Lipid Permeability of Fluoroquinolones. *Sci Rep* 2016;**6**:32824.
Chopra I, Roberts M. Tetracycline antibiotics: mode of action, applications, molecular biology, and epidemiology of bacterial resistance. *Microbiol Mol Biol Rev* 2001;**65**:232–60; second page, table of contents.
Chow D, Guo L, Gai F *et al*. Fluorescence Correlation Spectroscopy Measurements of the Membrane Protein TetA in Escherichia coli Suggest Rapid Diffusion at Short Length Scales. *PLoS One* 2012;**7**, DOI: 10.1371/journal.pone.0048600.
Coenen S, Adriaenssens N, Versporten A *et al*. European Surveillance of Antimicrobial Consumption (ESAC): outpatient use of tetracyclines, sulphonamides and trimethoprim, and other antibacterials in Europe (1997-2009). *J Antimicrob Chemother* 2011;**66 Suppl 6**:vi57–70.
Cuthbertson L, Nodwell JR. The TetR Family of Regulators. *Microbiol Mol Biol Rev* 2013;**77**:440–75.
Datsenko KA, Wanner BL. One-step inactivation of chromosomal genes in Escherichia coli K-12 using PCR products. *Proc Natl Acad Sci USA* 2000;**97**:6640–5.
Dubuy HG, Dubuy HG, Riley F *et al*. Tetracycline fluorescence in permeability studies of membranes around intracellular parasites. *Science* 1964;**145**:163–5.
Ducret A, Quardokus EM, Brun YV. MicrobeJ, a tool for high throughput bacterial cell detection and quantitative analysis. *Nat Microbiol* 2016;**1**:16077.
Du D, Wang Z, James NR *et al*. Structure of the AcrAB-TolC multidrug efflux pump. *Nature* 2014;**509**:512–5.
Eckert B, Beck CF. Overproduction of transposon Tn10-encoded tetracycline resistance protein results in cell death and loss of membrane potential. *J Bacteriol* 1989;**171**:3557–9.
Eliopoulos GM, Eliopoulos GM, Roberts MC. Tetracycline Therapy: Update. *Clin Infect Dis* 2003;**36**:462–7.
Fernández L, Hancock REW. Adaptive and Mutational Resistance: Role of Porins and Efflux Pumps in Drug Resistance. *Clin Microbiol Rev* 2012;**25**:661–81.
Hoeksema M, Jonker MJ, Brul S *et al*. Effects of a previously selected antibiotic resistance on mutations acquired during development of a second resistance in Escherichia coli. *BMC Genomics* 2019;**20**:284.
Kumar S, Varela MF. Biochemistry of Bacterial Multidrug Efflux Pumps. *Int J Mol Sci* 2012;**13**:4484–95.
Lesterlin C, Duabrry N. Investigating bacterial chromosome architecture. In: Leake MC (ed). *Chromosome Architecture*. **Vol 1431**. New York, NY: Springer New York, 2016, 61–72.
Levy SB, McMurry L. Plasmid-determined tetracycline resistance involves new transport systems for tetracycline. *Nature* 1978;**276**:90–2.
Li X-Z, Nikaido H. Efflux-Mediated Drug Resistance in Bacteria. *Drugs* 2004;**64**:159–204.
Li X-Z, Nikaido H. Efflux-Mediated Drug Resistance in Bacteria: an Update. *Drugs* 2009;**69**:1555–623.
Li X-Z, Plésiat P, Nikaido H. The Challenge of Efflux-Mediated Antibiotic Resistance in Gram-Negative Bacteria. *Clin Microbiol Rev* 2015;**28**:337–418.
McMurry L, Petrucci RE, Levy SB. Active efflux of tetracycline encoded by four genetically different tetracycline resistance determinants in Escherichia coli. *Proc Natl Acad Sci USA* 1980;**77**:3974–7.
Mortimer PG, Piddock LJ. The accumulation of five antibacterial agents in porin-deficient mutants of Escherichia coli. *J Antimicrob Chemother* 1993;**32**:195–213.
Muthukrishnan A-B, Kandhavelu M, Lloyd-Price J *et al*. Dynamics of transcription driven by the tetA promoter, one event at a time, in live Escherichia coli cells. *Nucleic Acids Res* 2012;**40**:8472–83.
Møller TSB, Overgaard M, Nielsen SS *et al*. Relation between tetR and tetA expression in tetracycline resistant Escherichia coli. *BMC Microbiol* 2016;**16**:39.
Nikaido H. Multidrug Resistance in Bacteria. *Annu Rev Biochem* 2009;**78**:119–46.
Nikaido H. Multiple antibiotic resistance and efflux. *Curr Opin Microbiol* 1998;**1**:516–23.
Nolivos S, Cayron J, Dedieu A *et al*. Role of AcrAB-TolC multidrug efflux pump in drug-resistance acquisition by plasmid transfer. *Science* 2019;**364**:778–82.
Ramos JL, Martínez-Bueno M, Molina-Henares AJ *et al*. The TetR Family of Transcriptional Repressors. *Microbiol Mol Biol Rev* 2005;**69**:326–56.
Roberts MC. Tetracycline resistance determinants: mechanisms of action, regulation of expression, genetic mobility, and distribution. *FEMS Microbiol Rev* 1996;**19**:1–24.
Schnappinger D, Hillen W. Tetracyclines: antibiotic action, uptake, and resistance mechanisms. *Arch Microbiol* 1996;**165**:359–69.
Schultz D, Palmer AC, Kishony R. Regulatory Dynamics Determine Cell Fate following Abrupt Antibiotic Exposure. *Cell Syst* 2017;**5**:509–17.e3.
Stone MRL, Butler MS, Phetsang W *et al*. Fluorescent Antibiotics: New Research Tools to Fight Antibiotic Resistance. *Trends Biotechnol* 2018;**36**:523–36.
Sulavik MC, Houseweart C, Cramer C *et al*. Antibiotic susceptibility profiles of Escherichia coli strains lacking multidrug efflux pump genes. *Antimicrob Agents Chemother* 2001;**45**:1126–36.
Tal N, Schuldiner S. A coordinated network of transporters with overlapping specificities provides a robust survival strategy. *Proc Natl Acad Sci USA* 2009;**106**:9051–6.
Thaker M, Spanogiannopoulos P, Wright GD. The tetracycline resistome. *Cell Mol Life Sci* 2010;**67**:419–31.
Vinué L, Hooper DC, Jacoby GA. Chromosomal mutations that accompany qnr in clinical isolates of Escherichia coli. *Int J Antimicrob Agents* 2018;**51**:479–83.

Warburton PJ, Amodeo N, Roberts AP. Mosaic tetracycline resistance genes encoding ribosomal protection proteins. *J Antimicrob Chemother* 2016;**71**:3333–9.

Yamaguchi A, Ono N, Akasaka T *et al*. Metal-tetracycline/H+ antiporter of Escherichia coli encoded by a transposon, Tn10. The role of the conserved dipeptide, Ser65-Asp66, in tetracycline transport. *J Biol Chem* 1990;**265**:15525–30.

Yamaguchi A, Udagawa T, Sawai T. Transport of divalent cations with tetracycline as mediated by the transposon Tn10-encoded tetracycline resistance protein. *J Biol Chem* 1990;**265**:4809–13.

Yu D, Ellis HM, Lee E-C *et al*. An efficient recombination system for chromosome engineering in Escherichia coli. *Proc Natl Acad Sci* 2000;**97**:5978–83.

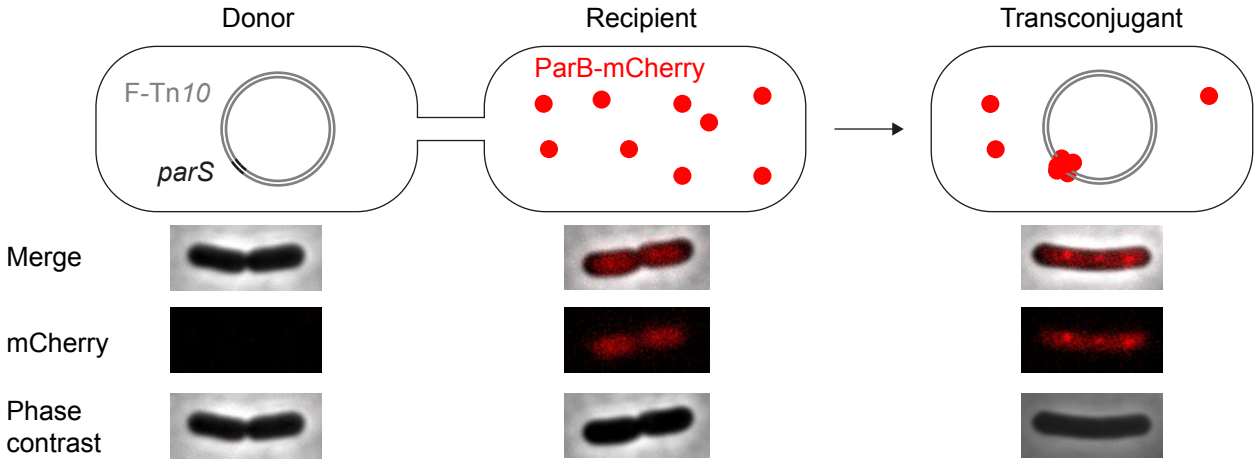

Figure R11 : Transfer visualization system
DNA transfer visualization. The donor strain contains the F-Tn*10 parS* plasmid and the recipient strain produce the ParB-mCherry protein which is diffuse in the cytoplasm. After the acquisition of the double stranded form of the F-Tn*10 parS* plasmid, the ParB-mCherry protein binds to the *parS* site forming a fluorescent focus allowing for the visualizaiton of transconjugant cells.

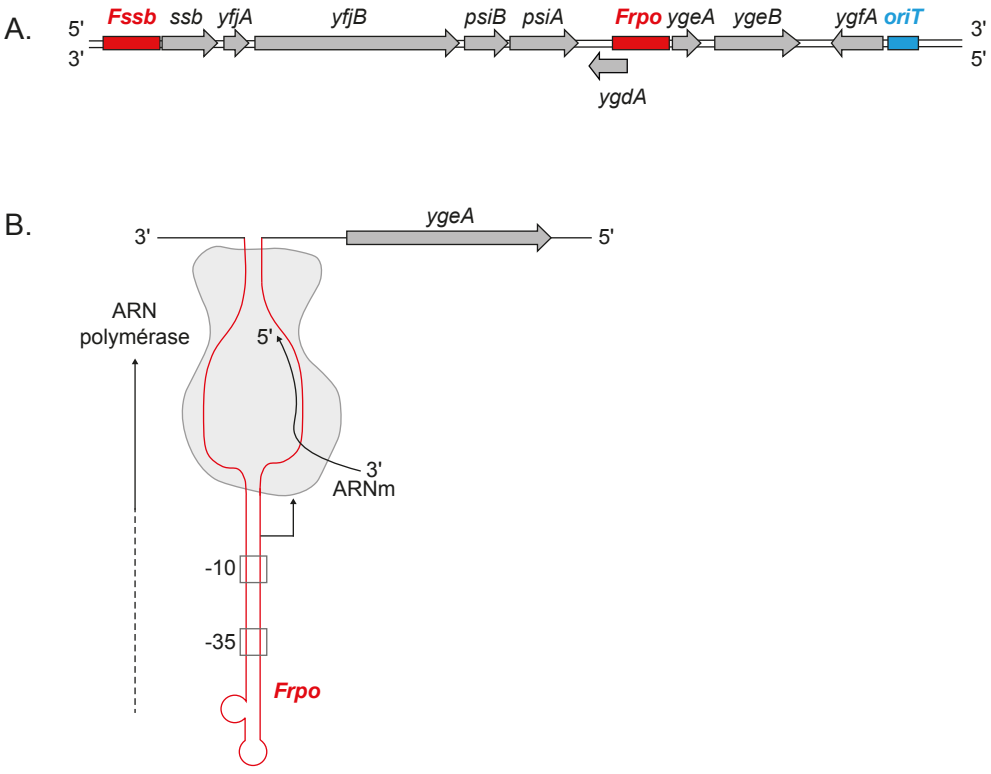

Figure R12 : Schematic view of the leading region and the *Frpo* stem loop.
A. Genetic map of the leading region with *Frpo* and potentially *Fssb* single stranded promoters. B. Stem loop folding model of the *Frpo* region. Before the complementary strand synthesis, the formation of the single stranded promoter initiates transcription by recruiting the RNA polymerase in grey to the -35 and -10 boxes.

VI.2. Expression of the leading region genes

VI.2.1. Introduction

The expression timing of the plasmidic genes in the fresh transconjugants remain poorly characterized. This is especially true for the genes of the leading region located on the first T-strand region that enters into the recipient cell during the conjugation process (see section III.4.1 in the introduction).

In the laboratory, we analyzed the dynamic and the timing of expression of the F-Tn*10* plasmid encoded genes in the transconjugant cell using real-time microscopy at the cellular level. Dynamics and localization of the proteins of interest were visualized thanks to C-termini fusion with the sfGFP (superfolder Green Fluorescent Protein). To synchronize the dynamic of gene expression to the acquisition of the plasmid, we use the reporter system developed in Nolivos *et al*. based on the fluorescent *parS/*ParB DNA labeling system (Nolivos *et al.* 2019) (Figure R11). Briefly, *parS* binding site is inserted near the *oriT* of the F-Tn*10* plasmid contained in the donor strain, while the fluorescently labeled ParB-mcherry protein is produced from a plasmid in recipient cells only, where it appears diffuse in the cytoplasm. The F-Tn*10* plasmid is transferred into the recipient cell in single-stranded DNA form (ssDNA) and is converted into double-stranded (dsDNA) by synthesis of the complementary strand. This DNA synthesis event triggers the recruitment of ParB-mCherry to the dsDNA *parS* site, revealed by the formation of a fluorescent ParB focus (Figure R11).

Using those tools, studies were realized before my arrival into the laboratory to determine the expression dynamic of the transfer (*tra*) genes. It was shown that these genes were expressed constitutively in the donor and 10 to 25 min after the acquisition of the double stranded form of the plasmid in the transconjugant revealed by the apparition of the ParB-mCherry focus. The timing of expression was also investigated for *ssb* gene, located in the leading region (Figure R12A). This region contains 9 genes with 2 in opposite direction. Preliminary results showed that the timing of expression of the *ssb* gene is quite different than *tra* genes. SSB is not produced in donor strains, but is early expressed in transconjugant cells before the acquisition of the double-stranded form of the F plasmid. This was consistent with the report that in ColIb-P9 plasmid, the *ssb* leading region gene is not expressed in the donor cells, but are expressed early in the transconjugants (Jones, Barth and Wilkins 1992). This expression phenotype is termed zygotic induction. Similarly, in the case of the F plasmid, the *psiB* gene located in the leading region was also reported to have a zygotic expression (Bagdasarian *et al.* 1992). One explanation could be linked to the role played by the *Frpo* region upstream *ygeA* and *ygeB* genes. *In vitro*, the single-stranded form of the *Frpo* region is able to form a stem-loop structure, where the double-stranded DNA region constituted at the stem creates a canonical -10 and -35 boxes that recruits the RNA polymerase of *E. coli* allowing the initiation of RNA synthesis (Figure R12B). This led to the proposal that *Frpo* could serve as a potential single-stranded promoter that controls the expression of the downstream genes in fresh transconjugant cells (Masai and Arai 1997). In the lab, we identified a region upstream the *ssb-yfjA-yfjB-psiB-psiA* genes that shares 92% identity with *Frpo* that we named *Fssb.* Our hypothesis was that upon entry of the ssDNA plasmid into the transconjugant cells, *Frpo* and *Fssb* could serve as single-stranded promoters to initiate the early transcription of downstream genes immediately after plasmid entry into the recipient cell.

As only *ssb* expression had been explored before my arrival as a master 2 internship, I determined during this training the expression profile of the genes downstream *Fssb* and *Frpo* regions during conjugation process.

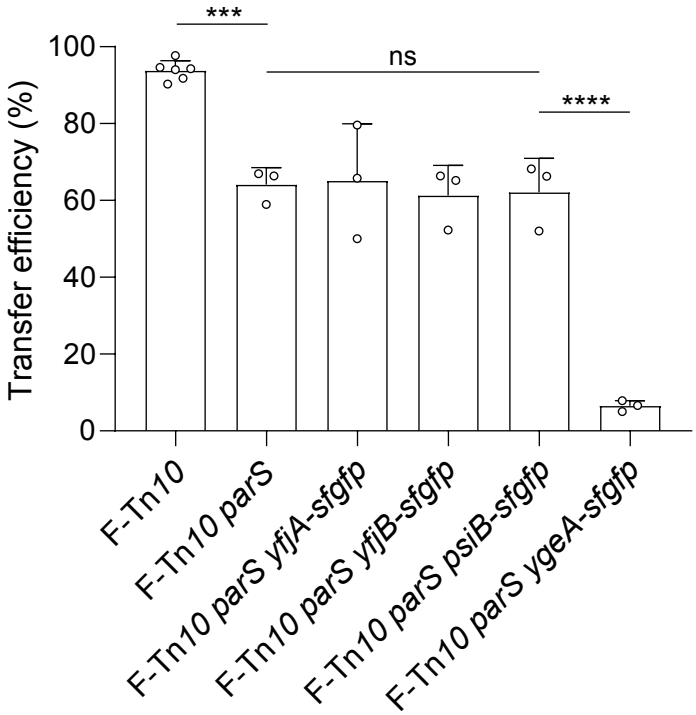

Figure R13 : Effect of protein fusions on the plasmid F conjugation efficiency. Effect of the Histogam showing the transfer efficiency (T/R+T ratio) of various F-Tn*10* construct estimated on plating assays after 3h mating. Bars represent the mean of three replicates and dots show each replicate value. Ordinary one-way anova with multiple comparison was performed. ns *P-value* > 0,05, *** *P-value* < 0,0002 and **** *P-value* < 0,0001. Donors : F-Tn*10* (LY5), F-Tn*10 parS* (LY875), F-Tn*10 parS yfjA-sfgfp* (LY791), F-Tn*10 parS yfjB-sfgfp* (LY792), F-Tn*10 parS psiB-sfgfp* (LY754), F-Tn*10 parS ygeA-sfgfp* (LY756). Recipient : MS428.

VI.2.2. Results

I first constructed protein fusion by fusing gene of interest to the *sfgfp* gene on the F-Tn*10*-*parS* plasmid that allows the reporting of the double stranded state of the plasmid in the transconjugant. I then verified the effect of the protein fusion on the transfer efficiency of the plasmid. Then, the analysis of the GFP fluorescence profile of all the fused proteins was conducted. We used two different approaches: a population level analysis which allow for robust analysis and a real time single-cell level analysis to follow conjugation chronology.

VI.2.2.1. Impact of the fused proteins on the conjugation process

Functionality of proteins can be impaired by the C-terminal fusion to sfGFP. For instance, it was observed that the fusion of TraM and TraD proteins with sfGFP impair conjugation efficiency. TraD is the T4CP and TraM a relaxosome accessory protein that are, both essential for the conjugation process. These results showed that the fusion to the sfGFP protein affect the activity of these proteins. Conjugation efficiency tests were realized to test the functionality of *parS* insertion and *yfjA*, *yfjB*, *psiB* and *ygeA* fusions. Figure R13 reveal that F-Tn*10* conjugation efficiency of the wild type (wt) F-Tn*10* plasmid is high (~90 % after 3h mating). The insertion of *parS* site between *ygeB* and *ygfA* reduced the conjugation efficiency to ~65 %, which is still suitable to visualize frequent F transfer events. This insertion is used in the laboratory to follow the F-Tn*10* plasmid in live cells because conjugation efficiency stays high compared to other insertion sites tested.

Figure R12 shows that *yfjB-sfgfp*, *yfjA-sfgfp* and *psiB-sfgfp* constructs do not affect conjugation efficiency. By contrast, *ygeA-sfgfp* fusion impact the function of *ygeA* gene. Indeed, conjugation efficiency of the F plasmid carrying this fusion drops to 6.52 %, suggesting that *ygeA* is important for conjugation. This result will need to be verified by complementing the deletion mutant with a *ygeA* copy in trans. YgeA does not have any described function but bioinformatic analysis revealed an homology of 92 % with a putative fimbrial-like adhesin coded by the AC28_5105 gene of *E. coli*. It is possible that *ygeA* also encodes for an adhesin essential during conjugation to maintain the mating pair between the donor and the recipient cell. Also, *ygeA* modification might affect *ygeB* gene expression by polar effect, as they seem to be in operon. Moreover, we were unable to obtain the *ygeB-sfgfp* fusion on the F-Tn*10* *parS* plasmid. Modification of the F-Tn*10* plasmid by λred introduced a FRT scar which could lead to recombination in case of multiple insertions. Thus the insertion of the *parS* site downstream the *ygeB* gene could impede the genetic modifications needed to build *ygeB-sgfp* fusion. This is why it was also tried to construct the *ygeB-sfgfp* fusion on a wild-type F-Tn*10* plasmid. It was unsuccessful, which suggest that *ygeB* is important for the maintenance of the F plasmid.

All fusions were then used to observe the production dynamic of the fused proteins under the microscope, in relation to the conjugation process.

VI.2.2.2. Dynamics of the genes downstream Fssb region

Our various donor strains with the different genetic constructs were mixed with the ParB-mCherry producing strain. Samples were taken and analyzed under the microscope at time 0 1, 2, 4, 6 and 9h after mating. Cells were classified into donors, recipient or transconjugant according to the principle described in the last part. Figure R14 shows the GFP fluorescence intensity in the three types of cells analyzed. At T=0h, no transconjugant can be seen because conjugation has not happened yet. Recipient cells that do not possess the F-Tn*10* plasmid with the genetic sfGFP construction only express a basal level of GFP intensity corresponding to

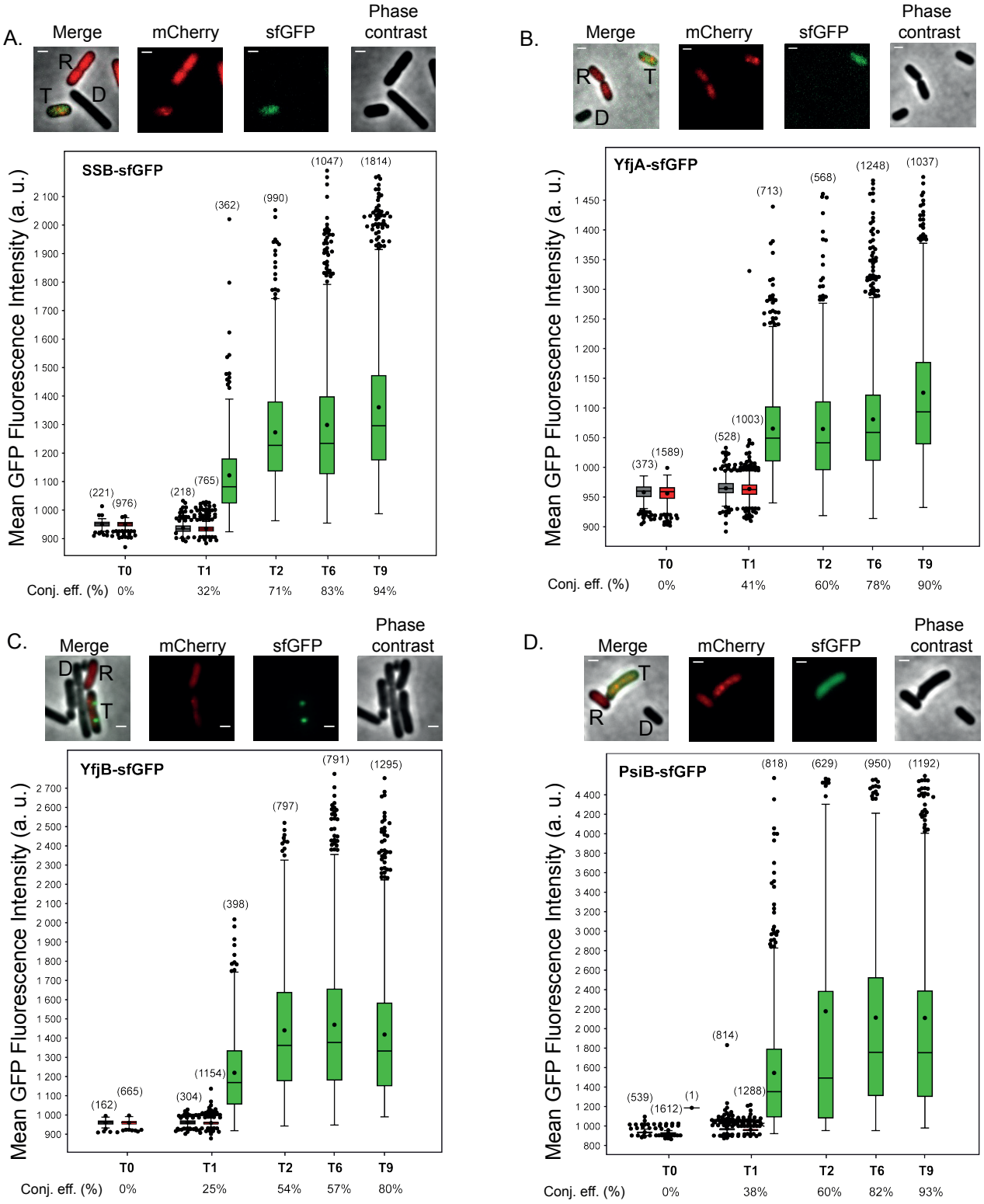

Figure R14 : SSB, YfjA, YfjB and PsiB proteins production profile.Top : Microscopy pictures of donor (D), recipient (R) and transconjugant (T) cells after 2h mating (scale bar = 1 µm). Bottom : Box plot representing thē mean GFP fluorescence intensity in arbitrary unit (a. u.) for each cell category during conjugation over time (donors in grey, recipients in red and transconjugants in green). Median, quartile 1 and quartile 3 are indicated by horizontal lines and mean is represented by the black dot. Black dots above and below the box plot represent the outlier cells. The number of cells analyzed is indicated beween brackets above each box. Conjugation efficiencies are indicated below each time. Mean GFP fluorescence intensity for donor and recipient cells at 0, 2, 6 and 9 h are identical, thus only the t=0h and t=1h is shown. Donors : F-Tn*10 parS yfjA-sfgfp* (LY791), F-Tn*10 parS yfjB-sfgfp* (LY792), F-Tn*10 parS psiB-sfgfp* (LY754), F-Tn*10 parS ssb-sfgfp*. Recipient : ParB-mCherry (LY318).

autofluorescence. Donor strains do not express more fluorescence than the recipient cells, showing that marked leading genes are not expressed in the donor. After 1h mating, fluorescence is present in the transconjugant cells only. The maximum production of the proteins in the population reaches its maximum at 2h after mating, except for *yfjA* for which the maximum production arrives at 1h after mating. Image analysis shows that YfjA, SSB and PsiB have a diffuse pattern in transconjugants. On the contrary, YfjB forms fluorescence focus in the transconjugants cells (Figure R14C). This pattern is addressed in the following results.

The same conjugation mix was realized and charged into microfluidics chambers to allow for media supply during visualization in real time. Images were taken each 5 minutes (min) during 90 min. Intensity fluorescence dynamics of each cell was normalized based on the apparition of the ParB-mCherry spot to synchronize conjugation events over time. Figure R15 shows the fluorescence intensity of five cells becoming transconjugants over time with F-Tn*10 parS* plasmids containing the different modified genes. It shows that SSB-sfGFP, YfjA-sfGFP, YfjB-sfGFP and PsiB-sfGFP proteins have been produced when the ParB-mCherry focus appears. The production of this protein is quick and reach a plateau at 15 min after ParB-mCherry focus apparition. PsiB protein production does not stabilize even 50 min after the acquisition of the double stranded form of the F plasmid. The localization of YfjA and PsiB still remain diffuse with no particular pattern. However, SSB was seen to form transiently one or two focus in transconjugants, this pattern will be addressed in the next results part. The ParB focus is the reflect of the double stranded form of the plasmid. As the maturation time of sfGFP is 13 min (Pédelacq *et al.* 2006), observation of the fluorescence of the fused proteins imply that the proteins were transcribed 13 min earlier. Thus, visualization of the fused proteins at the same time than the ParB-mCherry focus indicate that they are produced from the single stranded form of the plasmid.

VI.2.2.3. Specific localization of YfjB and SSB proteins

Besides the expression profile, microscopy analysis revealed a diffuse localization of YgeA, YfjA and PsiB proteins. On the other hand, YfjB forms well defined focus in the transconjugant cells (Figure R14C). Quantification and positioning inside transconjugant cells depending on their size was realized for the images taken 1h after mating (Figure R16A). This analysis indicate that short cells tend to have 1 YfjB focus at midcell whereas longer cells rather harbor two foci at the ¼ and ¾ of the cell. Based on observations, position of the YfjB focus does not seem to correlate with the position and number of F plasmid indicated by the ParB-mCherry focus.

Global analysis of the SSB-sfGFP protein did not reveal any precise localization of this protein. However, real time microscopy showed the formation of one or two SSB focus within 5 min before and 20min after the apparition of ParB-mCherry focus (Figure R15A). In analyzed cells, this focus is only visible during 1 frame, corresponding to 5 min maximum and then the protein is diffuse again (Figure R16B).

VI.2.2.4. YgeA dynamic

Although conjugation rates for *ygeA-sfGFP* construction was very low, we tried to visualize the conjugation process over time with this construction. Dynamic of the *ygeA* gene was observed first at different time points during the conjugation. The whole population of donor, recipient and transconjugant cells were analyzed. Figure R17A shows that as for the other observed proteins, YgeA is not produced in the donor cells and is present in the transconjugants only after 1h mating. The maximum protein production is also attained after 2h mating. The population analysis allowed us to determine the conjugation efficiency at each time thanks to

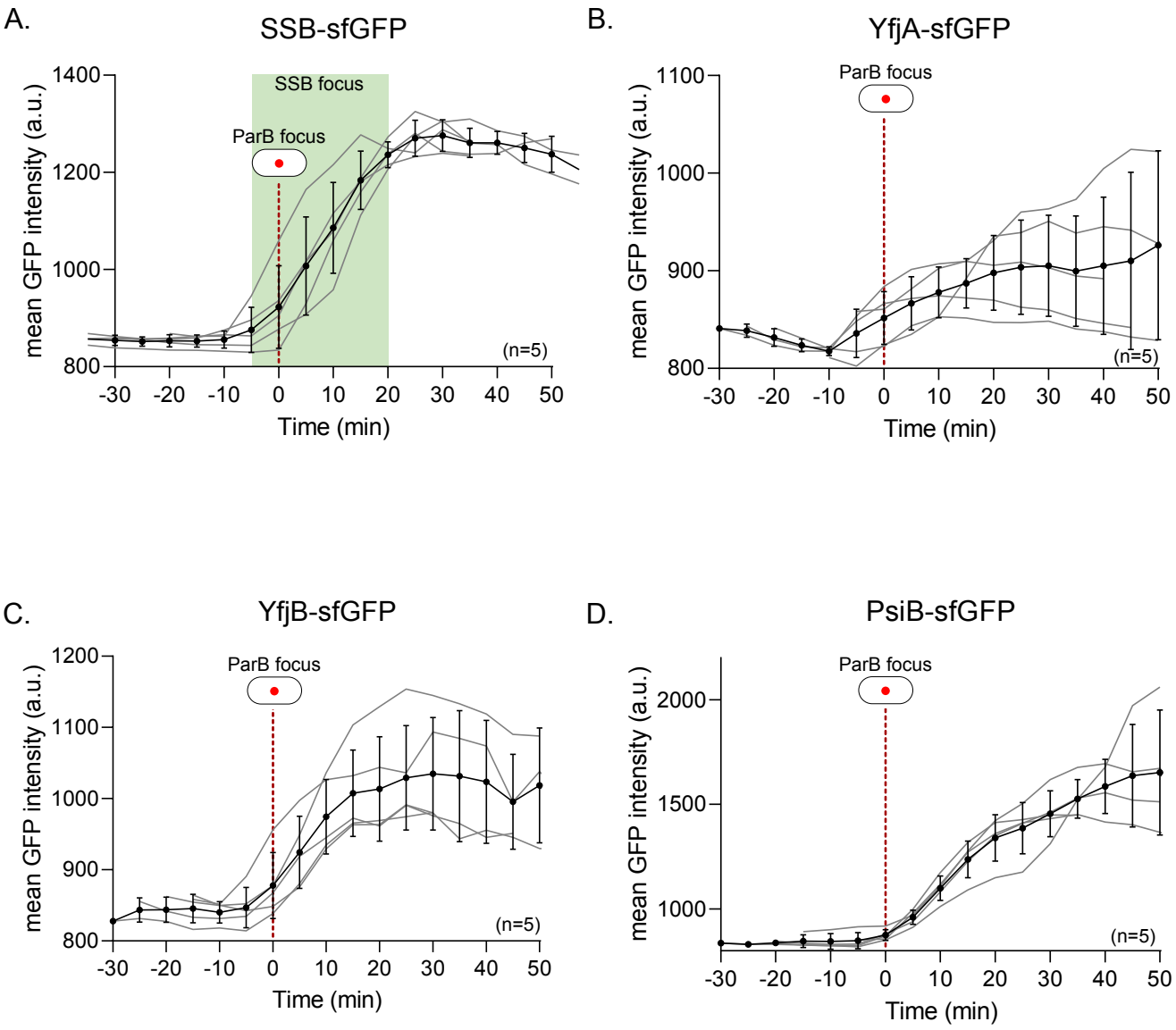

Figure R15 : SSB, YfjA, YfjB and PsiB proteins production dynamics.
Real time quantification of the fluorescence of the SSB-sfGFP (A), YfjA-sfGFP (B), YfjB-sfGFP (C) and PsiB-sfGFP (D) in transconjugant cells. Curves show the mean GFP fluorescence intensity over time. Each grey line represent one analysed cell and all cells are synchronized with the apparition of the ParB-mCherry focus (Time = 0 min). Average and standard deviation of the grey curves is represented in black. The number of analysed cells is indicated between brackets in the right corner. For SSB-sfGFP the apparition of the SSB focus is represented by the green box. Donors : F-Tn*10 parS yfjA-sfgfp* (LY791), F-Tn*10 parS yfjB-sfgfp* (LY792), F-Tn*10 parS psiB-sfgfp* (LY754), F-Tn*10 parS ssb-sfgfp*. Recipient : ParB-mCherry (LY318).

the transconjugant over transconjugant + recipient ratio. After 1h conjugation, it is estimated at 8% and increases over time to attain 63% after 9h mating. This suggest that YgeA-sfGFP fusion affects YgeA function and delay the conjugation process but does not abolish it.

To better understand the chronology of the production of this protein, we examined its dynamic in real time. Figure R17B reveals that the production of YgeA proteins arrive slightly before the ParB focus apparition in transconjugants cells. Similarly to other observed proteins, YgeA reach a maximum production level 20 min after the acquisition of double stranded form of the F plasmid.

Neither population nor single cell scale microscopic observations revealed a pattern in the intracellular localization of YgeA.

VI.2.3. Conclusion

All those results suggest that *Frpo* and *Fssb* region act as single stranded promoter in transconjugant cells. This could explain the early production of the leading genes in transconjugant cells. Genes downstream *Frpo*, namely *ygeA* and *ygeB* are thought to be important for conjugation as suggested by the reduced conjugation efficiency due to the fusion of YgeA with sfGFP and the unability to construct *ygeB* deletion or fusion. As mentioned in the introduction, SSB and PsiB could be implicated in the plasmid establishment, first step after single stranded acquisition by the recipient cells. Functions of YfjB and YfjA are not described for conjugation but these genes could also be maintenance genes. Moreover, *yfjB* gene seems to be conserved in the leading region of IncI R64 plasmid, suggesting an importance of this gene for the conjugation phenomenon.

This study is part of a larger project in the laboratory aiming to investigate the production of the plasmidic proteins produced from genes of the leading region, maintenance genes and transfer genes. For now, the results represented in the figure R18 show that genes of the leading region are early produced in the transconjugant, appearing at the same time than the double stranded form of the F plasmid. 3 min after the acquisition of the double stranded form F plasmid, the production of the maintenance proteins is observed. 10 to 20 min after, proteins involved in the transfer are produced. This production reveals a strategic production of the proteins which are produced in order to respond to the plasmid needs in the recipient strains. First, the plasmid has to be established, next to be stably maintained and finally it can be transferred in another recipient strain.

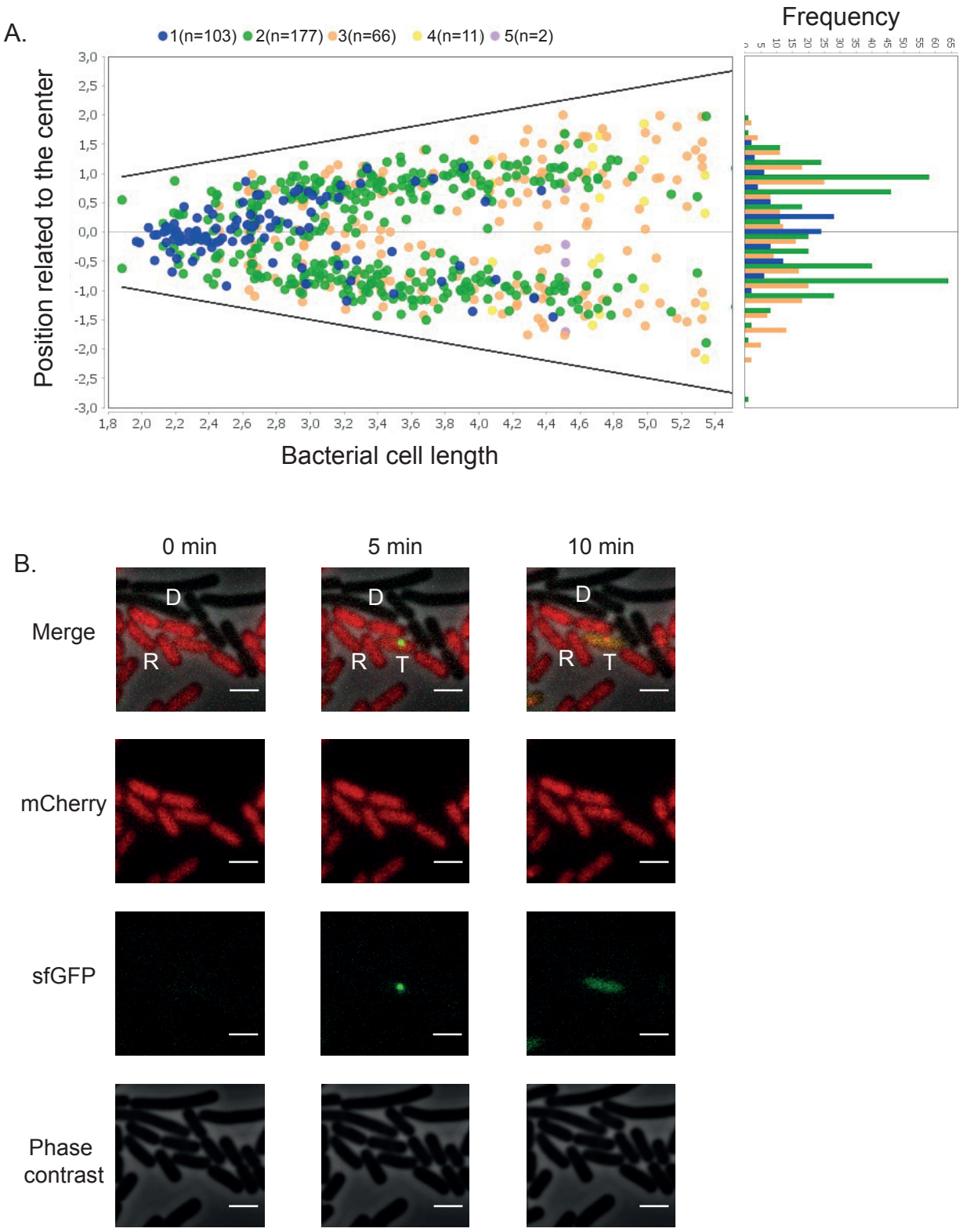

Figure R16 : YfjB localization and SSB dynamic analysis during the conjugation process
A. YfjB foci localization in the total population of transconjugant depending on the size of the cell after 1 h conjugation. Detected foci number within each bacteria is indicated in different colors and the number of analyzed bacteria are indicated in brackets. At the right is indicated the foci distribution depending on their relative disposition. B. Apparition of the SSB-sfGFP focus observed in real time during conjugation process every 5 min. Donor, recipient and transconjugant cells are indicated with D, R and T respectively. (scale bar = 2 µm).

VI.3. Discussion

During my thesis I studied the conjugation from a fundamental aspect. If the steps of conjugation within the donor strain are well-documented, we know much less about the event occurring within the recipient cells after plasmid entry and establishment, which will result into the phenotypic conversion of the recipient into transconjugant. Thus, I used microscopy to study the expression of the leading region genes of the F plasmid. The main goal in studying the leading region genes was to observe the expression dynamics of the genes downstream *Frpo* and *Fssb* by recording with fluorescence microscopy the production of protein fused with sfGFP during the conjugation phenomenon.

Microscopic observations reveal that these proteins are transiently produced in transconjugant cells immediately after internalization of the ssDNA plasmid, but are not produced in donor cells. Real-time analysis showed that proteins encoded by the leading region are produced even before the conversion of the ssDNA plasmid into dsDNA. These results are consistent with the hypothesis that *Fssb* and *Frpo* regions serve as single-stranded promoters allowing the expression of the downstream genes, immediately after the arrival of the F plasmid in recipient cells. In this view, these promoters would form a stem-loop structure recognized by the endogenous RNA polymerase when the plasmid is in single-stranded form. This allows the initiation of transcription of the leading genes in a limited time window, until the complementary strand synthesis converts the plasmid into dsDNA. This conversion results in the inactivation of *Fssb* and *Frpo* single-stranded promoters, thus explaining the absence of protein production in the donor cell that contains the dsDNA plasmid. In accordance with these conclusions, studies conducted on *psiB* and *ssb* genes of the ColIb-P9 plasmid revealed that no repressor was produced by the plasmid to silence those genes in vegetative conditions (Althorpe *et al.* 1999). Primary studies realized in the laboratory on *tra* genes showed that this zygotic induction is not common for F-encoded proteins. It seems that only proteins of the leading region are produced before the complementary strand synthesis in transconjugant cells. On the contrary, Tra proteins are produced 10 to 25 min after the acquisition of the double stranded form of the F plasmid and stay constitutively produced in these transconjugants, which become new donors. F plasmid seems to use a strategy based on differential expression of the genes to secure first its establishment and maintenance in transconjugant cells. Next, expression of transfer proteins produce the transfer machinery which ensure its transfer in a new recipient cell.

The production of these proteins early in the recipient cell and the fact that they are conserved in the leading region of several IncF and IncI plasmid suggest that they have an importance, especially in the first steps of plasmid establishment. A very recent study showed that several proteins encoded by genes of the leading region of the IncFV pED208 plasmid were translocated into the recipient cell (Al Mamun, Kishida and Christie 2021). It was demonstrated that SSB, PsiB, PsiA and ParB2 are transferred from the donor to the recipient cell. Moreover, other proteins that are not encoded on the leading region, like ParA and ParB, are also shown to be translocated by the conjugative machinery of this plasmid. Translocation of these proteins is dependant of the formation of the relaxosome and its recognition by the T4CP. Detectable amount of SSB and PsiB in the donor strains were reported. Authors propose a model in which SSB and PsiB are produced in the donor and upon the transfer of the T-strand are translocated into the recipient cell. These results also suggest that these proteins are actors in the establishment of the plasmid. PsiB and SSB can protect the T-strand during its entry and help to form *Frpo* stem-loop structure to enable the production of more SSB and PsiB proteins to protect the ssDNA entering. In our study, the leading region proteins were

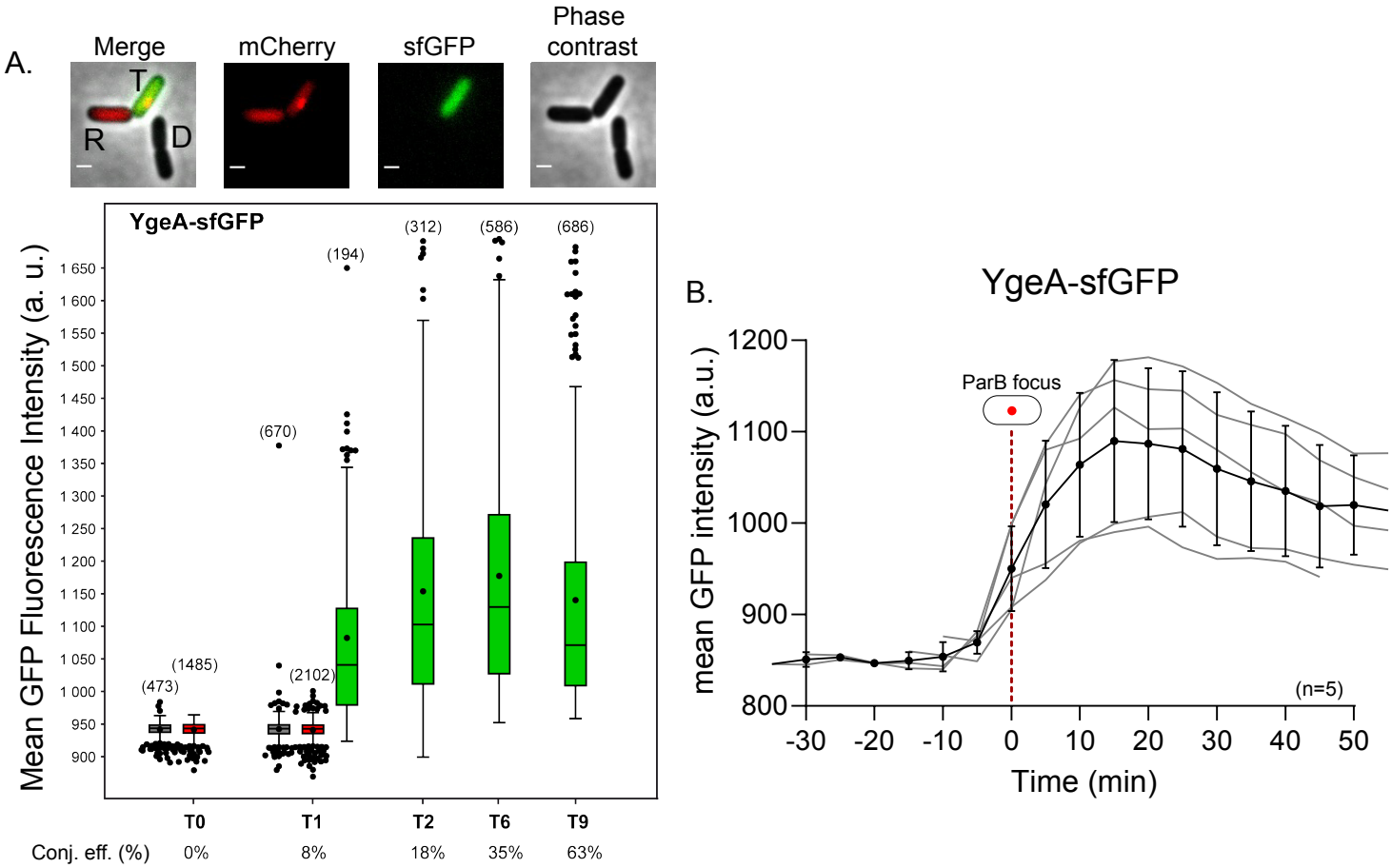

Figure R17 : *ygeA* expression profile at the poupulation and single cell level.
A. Top : pictures imaging the observed fluorescence phenotypes for donor (D), recipient (R) and transconjugant (T) cells (scale bar = 1 µm). Bottom : box plot representing the mean GFP fluorescence intensity in arbitrary unit (a. u.) for each cell category during conjugation over time (donors in grey, recipients in red and transconjugants in green). Median, quartile 1 and quartile 3 are indicated by horizontal lines and mean is represented by the black dot. Black dots above and below the box plot represent the outlier cells. The number of cells analyzed is indicated beween brackets above each box. Conjugation efficiencies are indicated below each time. Mean GFP fluorescence intensity for donor and recipient cells at 0, 2, 6 and 9 h are identical so only the t0 is shown. B. Real time quantification of the YgeA-sfGFP fluorescence in transconjugant cells. Curves showing the mean GFP fluorescence intensity over time. Each grey line represent one analysed cell and all cells are synchronized with the apparition of the ParB-mCherry focus (Time = 0 min). Average and standard deviation of the grey curves is represented in black. The number of analysed cells is indicated between brackets in the right corner. Donor strain : F-Tn*10 ygeA-sfgfp* (LY756). Recipient strain : ParB-mCherry (LY318).

not detected in the donor strain. However, it is not excluded that expression of the leading genes occurs in donor strains, notably during the processing of the T-strand by the relaxase which unwinds it. During a restrained time window, the T-strand is in ssDNA form which could allow the formation of the stem-loop structure and the expression of the leading region genes. It could be imagined that after this transient expression, proteins of the leading region are translocated into the recipient cell. Systems are developed to block the transfer of the T-strand. It is known that the TraI protein is transferred with the T-strand and has to unfold through the T4SS channel and then refolds out in the recipient. Thus inhibiting the unfolding of TraI could prevent the DNA transfer without inhibiting the recognition of the relaxosome with the T4CP. Then we could be able to see a production of the leading genes in the donor cell using our reporter constructs. To do so, it is possible to use ubiquitin fused TraI protein which was demonstrated to be resistant to unfolding and to prevent the translocation of the TraI homologous TrwC protein of the R388 plasmid (Trokter and Waksman 2018).

Among these proteins, the role of SSB encoded by the F plasmid (SSB_F) is not elucidated yet even though its zygotic expression was previously reported (Jones, Barth and Wilkins 1992). SSB_F homology with chromosomic SSB (SSB_C) indicates that it could bind to ssDNA and protect it upon its entry during conjugation (Golub and Low 1986). However, previously conducted experiments in the laboratory showed that SSB_C of *E. coli* ensures this function before the acquisition of the double stranded form of the F plasmid as a focus of SSB_C-YFP located at the cellular membrane can be observed during the entry of the F plasmid. The microscopic observation of SSB_F-sfGFP showed the formation of foci which are delayed compared to the entry of the plasmid. Then SSB_F is diffuse in transconjugants, which indicates that this protein does not perform the same task as SSB_C. ssb_F is a conserved gene in the majority of plasmid found in enterobacteria, suggesting an importance for the conjugation phenomenon (Golub and Low 1985). SSB_F could be implicated in the establishment or the early stabilization of the F plasmid. Other observations realized in the laboratory showed that the F plasmid is rapidly replicated after its transfer to retrieve 4 copies in the transconjugant. It seems plausible that observed SSB_F foci are due to the protection of the ssDNA during this rapid replication phase. This is why localization of the SSB_F protein regarding the SSB_C position should be characterized. Moreover, we want to observe if the rapid replication of the F plasmid following its transfer could be disturbed in absence of SSB_F. It was shown that a mutation of the *ssb* gene in the ColIb-P9 plasmid induce more quickly the SOS response (Howland *et al.* 1989) suggesting that plasmidic SSB could protect the single stranded form of the plasmid.

Observation of the inactivation of the SOS response was also reported for the PsiB protein. PsiB protein allow to repress the SOS response in *E. coli*. This response is triggered by an abnormal quantity of ssDNA in the bacterial cell. RecA protein binds to the ssDNA and polymerizes thus forming a nucleofilament. This structure catalyses the auto-proteolysis of LexA which is a repressor of the genes implicated in the SOS response. PsiB interacts with RecA and inhibit its polymerization which prevent the SOS response and allow the entry of the single stranded form of the plasmid into the recipient (Petrova *et al.* 2009). Our study proves that this protein is indeed produced only in transconjugant cells. It is a cytoplasmic protein with a diffuse pattern. Probably, the PsiB protein ensures a better stabilization of the plasmid and could favour its rapid replication in cooperation with SSB_F. It could be interesting to measure the induction of the SOS response in transconjugants in absence or in presence of PsiB and to visualize RecA protein in these conditions. The study of the SOS response induction was realized with the IncFV plasmid pED208 and showed that homologous PsiB and SSB genes

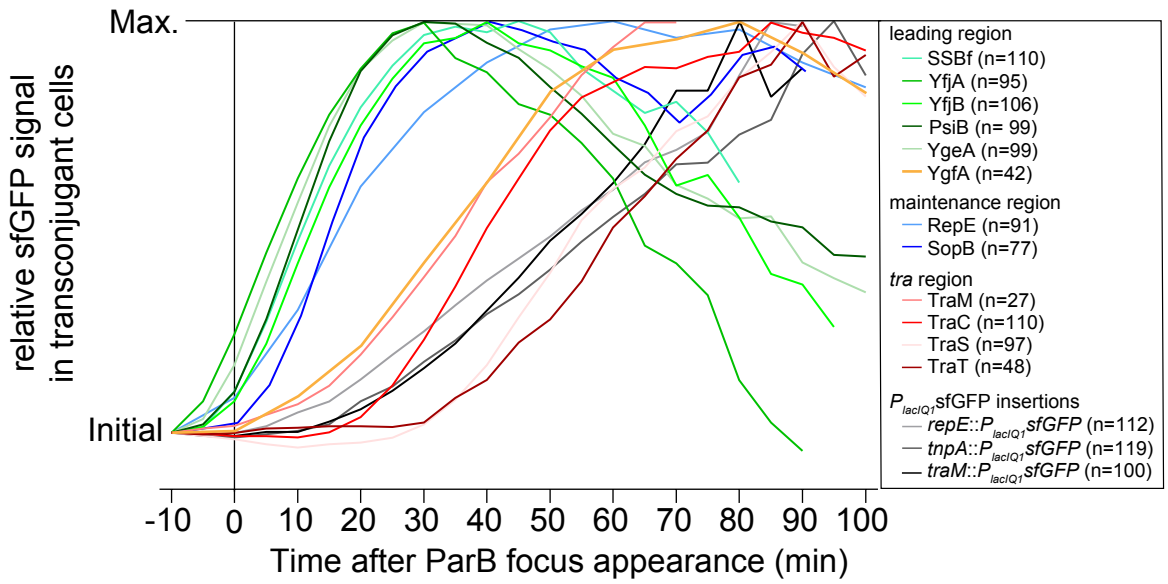

Figure R18 : Production of different F plasmid proteins in the transconjugant cell. Curves showing the relative sfGFP signal of different fused proteins relative to the acqui-sition of the double stranded form of the F plasmid in the transconjugant cells. Production of leading region proteins (SSB, YfjA, YfjB, PsiB, YgeA and YgfA), maintenance proteins (RepE and SopB) and proteins involved in the transfer (TraM, TraC, TraS and TraT) are analysed. The black, and grey curves correspond to the GFP signal generated by the transcritio-nal fusion of *sfgfp* with the *PlacIQ1* promoter in different regions of the F plasmid. Cells are synchronized by the apparition of the ParB-mCherry focus.

allowed the reduction of the SOS response whereas PsiA seems to slightly enhance the SOS response (Al Mamun, Kishida and Christie 2021). It could be interesting to see if the SOS response induced by the transfer of F plasmid is also induced in presence of $PsiA_F$ and reduced in presence of SSB_F and $PsiB_F$.

Concerning YfjB protein, no study was realized on its function until now. Bioinformatic analysis revealed the presence of a N-terminal ParB superfamily-associated domain in YfjB. ParB is a protein associated to the ParAB*S* partition system. As presented in the introduction, ParB is the "centromere-binding protein" (CBP) which binds to *parS* site and acts like a centromere recognized by the ParA protein. ParA distributes the plasmid copies thanks to its ATPase activity (Mierzejewska and Jagura-Burdzy 2012). The N-terminal domain of ParB encompass its liaison domain with ParA. Based on localization results of YfjB protein at the ¼ and ¾ of the bacterial cell, we could consider an implication in the segregation process of the plasmid as for partition proteins (Adachi, Hori and Hiraga 2006; Diaz, Rech and Bouet 2015). However the partition system of the F plasmid has already been described, and is the SopAB*C* system. Briefly, the SopA ATPase recognize the SopB CBP protein linked to *sopC* site and mediates the segregation of the F plasmid through the waler type partition system (Hiraga 2000; Brooks and Hwang 2017). A study realized in the laboratory in real time showed that SopB protein is produced 3 minutes after the acquisition of the double stranded form of the F plasmid. This protein is thus produced after YfjB and certainly not from a single stranded promoter transcription. Moreover, it is produced in the donor cell, contrary to YfjB. Foci formed by SopB protein correlate to observed F plasmid copy number, on the contrary to YfjB foci. Despite their similarities, those two proteins do not have equivalent analogous role. YfjB could allow future placement of the F plasmid by recognizing a chromosomic site. This could be accomplished with the help of a partner and/or a specific site as for partition systems. However, YfjA, product of the gene located upstream *yfjB*, which seems the more credible partner, does not forms foci as can be observed for SopA, for instance (Vecchiarelli, Hwang and Mizuuchi 2013).

Proteins analysed in this study have diverse importance relative to the conjugation phenomenon. Indeed, homologues of genes downstream *Fssb* are found in the leading region of conjugative plasmids like plasmids of incompatibility group IncFI, IncFII and in some IncI plasmids like R64 (Golub, Bailone and Devoret 1988; Howland *et al.* 1989). The conjugation experiments have only been realized between isogenic strains of *E. coli*. It is possible that leading region genes are necessary for the stabilization of the F plasmid during the transfer between unrelated strains. Indeed, if a specie is distant from the donor it is possible that its homologous SSB protein does not recognize the ssDNA of the plasmid or that activation of the SOS response could lead to the degradation of the transferred plasmid without PsiB and PsiA. Moreover, it was shown that SOS response was more induced during interspecies than during intraspecies mating (Matic, Rayssiguier and Radman 1995). Thus genes downstream *Fssb* could have more importance during interspecies conjugation. Genes downstream *Frpo* seem to have a great importance related to the bacterial conjugation. Among them, only *ygeB* is conserved, some plasmids do not possess the *ygeA* gene (Loh, Cram and Skurray 1989). In the case of the plasmid F, YgeA and surely YgeB seem to play a preponderant role in the conjugation phenomenon. However, our results do not indicate their function for now. Blast of YgeA sequence revealed an homology with another protein considered as a putative adhesin. It is possible that YgeA is produced in the recipient before the total transfer of the plasmid to consolidate the mating pair and ensure that the transfer is fully completed.

However, identification of a signal peptide to address the protein to the membrane was not succesfull. Thus, more work on this protein is needed to discover its function.

In conclusion, conjugation is a finely tuned process and surely adapted to efficiently realize the DNA transfer in all situations. This project was continued at the laboratory, notably for the study of YfjB function, and integrates into a larger study of the F plasmid genes expression dynamic. Our results show that F plasmid seem to express first genes related to establishment, next to maintenance and finally to the transfer, which is considered as a strategy to be first stably maintained in its host to then be disseminated into other hosts.

During my thesis, I was also interested in the expression of cargo genes which are carried by the plasmid and confer new metabolic properties to the transconjugant. These genes are not related to the conjugation phenomenon but are found on many conjugative plasmids. After establishment of the F plasmid, cargo genes are expressed and notably the tetracycline resistance genes *tetA* and *tetR* carried by the Tn*10* transposon of the F-Tn*10* plasmid. Tetracycline efflux system by TetA has been well characterized as well as its regulation by TetR (Cuthbertson and Nodwell 2013; Nguyen *et al.* 2014). Our study used fluorescence microscopy to show the dynamics of the balance between Tc efflux and entry into the bacterial cell. First, we show that *tetA* have a basal expression, leading to the formation of a pool of TetA pumps in the cell before tetracycline even enters. We demonstrate that efflux capacity of the cell is directly linked to TetA intracellular quantity. Indeed, single cell analysis revealed that cells carrying the highest TetA pool were more efficient to extrude Tc out, compared to cells which have less basal TetA pump. Basal TetA expulsion of tetracycline allow the continuation of the protein synthesis and Tc entry favours the production of more TetA pumps. When TetA pumps quantity attains a shift, tetracycline can be efficiently extruded. Moreover, pre-induction of TetA production with Tc or anhydrotetracycline allowed to show that cells producing large quantities of TetA are able to resist to 20 to 40 times the Minimum Inhibitory Concentration (MIC) of Tc. Thus, our study emphasizes the well-known property of antibiotics to trigger enhanced antibiotic resistance.

Moreover, in this study we show the influence of the overproduction of the multi-drug efflux pump AcrAB-TolC. Indeed, in a Δ*acrR* mutant which overexpress AcrAB-TolC, Tc efflux is as efficient as in cells which have basal intracellular TetA pool. A previous study already showed that Tc resistance can be acquired in presence of inhibitory concentration of Tc thanks to AcrAB-TolC (Nolivos *et al.* 2019). This shows that acquisition of conjugative plasmids and their properties can be mediated in stressful environments thanks to recipient factors. Another study shows that plasmid acquisition can depend on recipient factors. Indeed, stress induced by meropenem, an antibiotic of the carbapenem family, selects transconjugants which have reduced porins expression and are thus less incline to internalize carbapenems. It was shown that the acquisition of pNDM-HK plasmid that carry bla_{NDM-1} gene responsible for carbapenem resistance was facilitated into OmpR G63S mutant recipient strains selected by meropenem (Kong *et al.* 2018). OmpR is a transcriptional regulator responsible for the expression of *ompF* and *ompC* genes depending on its phosphorylation level (Head, Tardy and Kenney 1998). However, mutant OmpR G63S cannot be phosphorylated and is thus unable to induce the production of OmpF and OmpC porins. These porins regulate the entry of metabolites into the bacteria and carbapenems can notably pass through them (Delcour 2009). Thus the downregulation of these porins confers an enhanced resistance to carbapenems and cephalosporin (Doumith *et al.* 2009; Lou *et al.* 2011). These studies highlight the fact that stress in the environment does not necessarily suppress conjugation and that it

could result in enhanced antibiotic resistance due to the selection of genomic determinants in transconjugant allowing resistance to multiple antibiotics (Gullberg *et al.* 2011).

General discussion

During my thesis, I worked on the bacterial conjugation from a practical and fundamental perspectives. First, I proved that bacterial cells could die following the acquisition of the TAP and I also could establish the expression profile of genes regarding the conjugation phenomenon. These analysis have be realized thanks to fluorescence microscopy in real time at the population and single cell level. Indeed, in the laboratory several fluorescent reporters were developed to monitor the different steps of the conjugation. This allowed the synchronization of conjugation events and to perform quantitative analysis regarding this phenomenon. Fluorescence microscopy on live cells at real time is a powerful tool to observe timing, chronology and the sequence of events during the observed process. I will focus on fluorescence microscopy advances that allowed to have a better view of the bacterial conjugation and the developments that can be made using this technique to increase our knowledge.

The usage of fluorescent reporters with different techniques allowed to prove the ubiquity and host range of the conjugation process. For example, it was shown using microscopy and fluorescent reporters on conjugative plasmid that conjugation can take place in the phylloplane of leaves, in biofilms or that conjugative plasmids can be transmitted to different marine bacteria (Dahlberg, Bergström and Hermansson 1998; Normander *et al.* 1998). Moreover, the transfer of pJP14 and pMAS2027 plasmids was recorded by microscopy in soil biofilms developed in flow chambers using similar fluorescent reporter system (Aspray, Hansen and Burns 2005; Ong *et al.* 2009). During my thesis I also used a constitutively expressed fluorescent reporter to see in real time the acquisition of the TAPs in *E. coli* and *C. rodentium*. Synchronization of the conjugative events thanks to the reporter system allowed to produce quantitative analysis, notably regarding the shape of the bacteria after the transfer. Furthermore, the use of fluorescent proteins, allowed to see the nucleoid as well as RecA protein in the recipient cells. Notably, we were able to observe in the targeted cells the elongation of the bacteria, nucleoid disorganisation and RecA bundles. Observation of these reporters proved that TAP acquisition triggers, in the targeted strains, symptoms of bacterial stress linked to the induction of double stranded breaks on the chromosome.

Moreover, the association of fluorescence reporters on conjugative plasmid with flux cytometry, cell sorting and sequencing also allowed to show that the conjugation process occurs in the gut microbiota and to identify the genus of the bacteria that become transconjugants in this medium (Ronda *et al.* 2019). During my thesis I clearly focused on the development of TAPs. However, it was proposed in my project to observe the dissemination of the TAPs in the gut microbiota of mice. To do so, I would have used the capacity of a fluorescence reporters in a TAP construction to be able to see the extent of the conjugation in this environment. Notably, we proposed to use the infrared fluorescence protein (iRFP) reporter to be able to see macroscopically the diffusion of the plasmid in the gut of mouse. Indeed, iRFP allows to perform non-invasive visualization of the plasmid dissemination in live mouse (Filonov *et al.* 2011). Next, analysis of faecal samples would have helped identifying the transconjugants. Indeed, with another reporter like GFP on the same plasmid, we could use flux cytometry, cell sorting and sequencing to show what target can be reached by the TAP. The combination of these techniques would have allowed to have a broader view of the comportment of TAPs from a macroscopic to the microscopic level.

During my thesis, I also used fluorescent reporters to study the expression timing of the F-Tn*10* plasmid genes regarding the conjugation event. In the laboratory, the developed

different fluorescent reporter allow to monitor conjugation in real time at the single cell level. In particular, we are able to see the acquisition of the double stranded form of the plasmid thanks to the *parS* sequence on the F-Tn*10* plasmid and the reporter ParB-mCherry (Nolivos *et al.* 2019). Moreover, these constructions also allow to see the replication and the segregation of the plasmid in the transconjugant. It is also helpful to determine the average copy number of plasmids in bacterial cells in different conditions and allowed to see the rapid replication of the plasmid in new transconjugants (Nolivos *et al.* 2019).

The single stranded form of the plasmid can be seen thanks to the chromosomic protein SSB_C fused with the yellow fluorescent protein (YFP) (Nolivos *et al.* 2019). It was observed by microscopy that SSB_C forms tiny foci on replication forks of the chromosomic DNA whereas large foci are formed on single stranded forms of the F plasmid in the donor and the recipient cells. Mixing those two reporters, we are able to determine the timing of acquisition of the plasmid in the recipient cells. Moreover, we are also able to see aborted conjugative event. Using different mutations in the donor, in the recipient cells or on the conjugative plasmid, these abortive events can inform on the step of bacterial conjugation impacted by the mutation. These tools allow to synchronize the conjugation events and thus to understand the implication of the different genes in the chronology of the conjugation event. Moreover, these observations and related bacterial phenotypes can be quantified and thanks to the synchronization of the events and reveal implications of mutated or fused genes in the conjugation chronology. For instance, during my M2 internship, I revealed the expression profile of leading region genes regarding the conjugation event. I demonstrated that these genes are early produced even before the acquisition of the double stranded form of the F-Tn*10* plasmid. I also showed that YfjB and SSB proteins have a localisation pattern inside the recipient cell. Other studies in the laboratory using the same principle revealed the timing of expression of maintenance- and transfer-related genes of the F plasmid which constitute the expression profile of this plasmid in the transconjugant.

Using fluorescence reporters and real-time microscopy, it was also possible to characterize directly the pilus behaviour within the donor cell (Clarke *et al.* 2008). This was realized using a fluorescent R17 bacteriophage which binds the F pilus (Daehnel *et al.* 2005). Notably the F plasmid was shown to extent and retract and to bring closer potential recipient cells to the donor thanks to this extension-retractation ability. Moreover, previous observations of the acquisition of the F plasmid allowed to determine that conjugation process could occur between donor and recipient cells separated by 12µm distance (Babic *et al.* 2008). This microscopic observation thus questioned the paradigm stating that ssDNA is transferred only through the T4SS channel. Indeed, according to this observation, it is possible that the F pilus could transfer the plasmid into the recipient.

Establishment of the plasmid in the recipient strain and the conversion of the recipient into a transconjugant are major questions about the conjugation process. Fluorescence microscopy can be used to answer those questions. Notably a difficulty in this regard is to isolate new transconjugants which do not have fully expressed the plasmidic genes. A recent study showed that the acquisition of the conjugative plasmid in the new transconjugant decrease their fitness, even regarding new donor cells which have the plasmid and thus suffer metabolic burden due to its replication (Prensky *et al.* 2021). To select the newly acquired transconjugants, authors used the resistance carried by the conjugative plasmid. This cannot not be done with transconjugants that have not already expressed the plasmidic genes. However, it is possible to use fluorescence reporters to select those transconjugants. Notably the E5 mutant fluorescence reporter of the drFP583 red fluorescent protein (Terskikh *et al.*

2000). This reporter has the ability to change its fluorescence over time going from green to red fluorescence. Labeling leading region genes with this fluorescent marker would help to distinguish newly acquired transconjugants with old ones. Indeed, during the acquisition of the ssDNA, the leading genes would be expressed and green fluorescence will appear in the transconjugants. Next, the plasmid would be in double stranded form, which silence the expression of the leading genes and over time the produced labeled proteins would turn into red fluorescence. This technique associated with cell sorting in flux cytometry would allow to select new transconjugants without using antibiotic resistance provided by the conjugative plasmid.

Sometimes, adding fluorescent reporter on protein impairs its function. For instance, during my thesis it seemed to be the case for *ygeA-sfgfp* fusion and certainly *ygeB-sfgfp* fusions that was impossible to obtain. This could be due to the large size of the sfGFP. To reduce this size, it is possible to use the split GFP assays. In these assays, the protein of interest is fused to the β-strand 11 of GFP (GFP_{11}), whereas the 1-10 β-strand of the GFP (GFP_{1-10}) are expressed separately. When both fragments are found into the same cell, full GFP is formed and emits fluorescence (Cabantous, Terwilliger and Waldo 2005). Fusion of YgeA with the GFP_{11} could allow to restore conjugative efficiency and maybe a YgeB-GFP_{11} could be obtained. Moreover, expression GFP_{1-10} in the recipient strain would allow to see their early expression in the transconjugant with fluorescence microscopy.

A recent study used the Cre recombinase assay to prove that pED208 proteins produced by the leading genes were translocated from the donor into the recipient cells by the conjugative machinery (den Dulk-Ras, Vergunst and Hooykaas 2014; Al Mamun, Kishida and Christie 2021). In this system, proteins of interest are fused with the Cre recombinase and produced by an ectopic plasmid. The recipient cell contained a tetracycline resistance gene within an antibiotic cassette conferring resistance to chloramphenicol. In this construction, only tetracycline resistance was able to be expressed. The tetracycline resistance gene was flanked by lox sites. These lox sites can be recombined by the Cre recombinase and thus if the Cre recombinase enters the recipient cell, following the recombination, the tetracycline resistance gene would be lost and chloramphenicol gene is reconstructed. The resulting bacteria would lose their ability to resist to tetracycline and gain ability to resist to chloramphenicol. Using this assay, it was proved that pED208 leading genes product and partition proteins were translocated into the recipient (Al Mamun, Kishida and Christie 2021). To verify that this is also true for the F plasmid, it could be interesting to construct variants of the leading genes product fused with GFP_{11} on expression plasmids that cannot be transferred. Conjugation mixes should be performed with recipient bacteria expressing the GFP_{1-10} proteins. And next the visualization under the fluorescent microscope would allow to see if proteins are translocated via the F-Tn*10* conjugative machinery and it would also give an idea of the amount of translocated proteins and their localization just after the transfer. Moreover, monitoring those proteins with the ParB/*parS* reporter system indicating the acquisition of the double stranded form of the plasmid could be relevant to synchronize the events. We would then be able to compare the level of translocated proteins versus the level of proteins in the recipient that was monitored during my thesis. The split GFP system has also been used to see interactions between proteins. Indeed, if one protein is fused with the GFP_{11} and another with the GFP_{1-10}, when they are interacting, the GFP is able to reform and green fluorescence is observed (Blakeley, Chapman and McNaughton 2012). Again, in our settings, it could be an interesting tool to test interactions of proteins with others and see if proteins of the leading region interact with each other.

The strength of microscopy is the ability for the experimenter to directly see the observed phenomenon. A recent review reported the extent of the fluorescent tools and their ability to target the different components inside and outside the bacterial cell (Cambré and Aertsen 2020). Fluorescence reporters combined with microscopy are constantly evolving to answer questions regarding bacterial functions *in vivo*, in real time and from the single cell to the community level.

Materials and Methods

Bacterial strains, plasmids, primer and growth culture conditions

Bacterial strains, plasmids and primers are listed in Tables S1, S2 and S3 respectively. Plasmid cloning were done by Gibson Assembly and verified by Sanger sequencing (Eurofin Biotech). Chromosomal gene loci were transferred by phage P1 transduction to generate the final strains.

Unless otherwise noted, strains were grown at 37°C in Luria-Bertani (LB) broth, M9 medium supplemented with glucose (0.2%) and casamino acid (0.4%) (M9-CASA) or M63 medium supplemented with glucose (0.2%) and casamino acid (0.4%) (M63). When appropriate, the media were supplemented with the following antibiotics: 50 µg/ml kanamycin (Kan), 20 µg/ml chloramphenicol (Cm), 10 µg/ml tetracycline (Tc), 20 µg/ml nalidixic acid (Nal), 20 µg/ml streptomycin (St), 100 µg/ml ampicillin (Ap), 10 µg/ml gentamycin (Gm), 50 µg/ml rifampicin (Rif). When appropriate 40 µg/ml 5-bromo-4-chloro-3-indolyl-β-d-galactopyranoside (X-Ggal) and 40 µM isopropyl β-D-1-thiogalactopyranoside (IPTG) were added.

TAPs construction and one-step-cloning change of the spacer sequence on the TAPs

Plasmid construction was performed by IVA cloning (García-Nafría, Watson and Greger 2016), expect for changing the spacer sequence in the TAPs, which was performed by the replacement of the spacer in pEGL129 by a SapI-spacer-SapI DNA sequence. The nsp (non-specific) spacer sequence is flanked by two SapI restriction sites that allow for liberation of non-cohesive DNA ends upon SapI digestion. To replace the nsp spacer, a new spacer is constructed by annealing 2 oligonucleotides (listed in supplementary Table S3) with complementary sequences to the non-cohesive ends generated by SapI restriction of TAP-Cas9-nsp or TAP-dCas9-nsp plasmids. Ligation production between the new spacer fragment and the TAP backbone was transformed into DH5α or TB28 strains. Constructions were verified by PCR reaction and sequencing.

Strains construction

Isolation of streptomycin resistant strain

Equivalent of 1.10^8, 1.10^9, 1.10^{10} of the *E. coli* HS, Nissle and IAI1 from overnight cultures were plated on LB agar plates supplemented with 20 µg/ml 100 µg/ml streptomycin. Spontaneous clones obtained and base strains were streaked on LB agar plates supplemented with 20 µg/ml St to verify their streptomycin resistant phenotypes.

Modification of the F-Tn*10* plasmid

Modifications of the F plasmid were obtained by homologous recombination properties from the λred system (Yu *et al.* 2000). Briefly, Kanamycin gene resistance cassette with flanking Flipase Recognition Target (FRT) regions was PCR amplified from the pROD62 plasmid with primers containing 40 nt homologous to sequences flanking *Frpo*, *Fssb*, *ygeA* and *oriT* regions. Strains DY330 containing the F-Tn*10* or F-Tn*10 parS* plasmid were transformed with PCR product and then selected on LB agar plated supplemented with Kn and Tc (to select for the F-Tn*10* plasmid). Modified F plasmids were transferred by conjugation for *Frpo*, *Fssb* and *ygeA* deletions. As it is impossible for *oriT* deletion, it was transferred by phage P1 transduction.

Next, strains were transformed with the thermosensitive pCP20 plasmid carrying the flipase gene under the control of a thermoinducible promoter and then selected on LB agar plates supplemented with ampicillin. Flipase expression and cure of the thermosensitive plasmid are realized by incubation of the transformed clones at 42°C. Excision of the resistance gene and plasmid loss are verified by characterization of the resistance profile of the clone and then PCR confirmation and systematic sequencing.

Preparation of the P1 lysate

300 µl of donor strain overnight culture in LB supplemented with 5 mM $CaCl_2$ and appropriate antibiotic are distributed into 4 flasks, mixed with 0, 1, 10 and 100 µl of wild-type P1 lysate and incubated 20 min at 37°C. 5 ml of LB supplemented with 5 mM $CaCl_2$ are added and flasks are incubated at 37°C for around 4 to 6 hours. When the culture become clear, due to the lysis of cells, 1 ml of chloroform is added and culture is vortexed. Next culture is centrifugated 10 min at 4000 rpm, pellet is thrown and 200 µl of chloroform is added to the supernatant. P1 lysate are stocked at 4°C.

P1 transduction

500 µl of recipient strain overnight culture in LB supplemented with 5 mM $CaCl_2$ are distributed into 4 eppendorf tubes, mixed with 0, 1, 10 and 100 µl of prepared P1 lysate and incubated 20 min at 37°C. Cells are then pelleted, resuspended into 1 mL in LB supplemented with 7,5 mM citrate ad incubated 1h30 at 37°C. Finally cells are plated on LB agar plates supplemented with 7,5 mM citrate and appropriate antibiotic.

Conjugation assay

Overnight cultures in LB of donor and recipient strains were diluted to an A_{600} of 0.05 and grown until an A_{600} comprised between 0.7 and 0.9 was reached. 50 µl of donor and 150µl of recipient cultures were mixed into an Eppendorf tube. At time 0 min, 100 µl of the mix were diluted into 1 ml LB, serial diluted and plated on LB agar supplemented with antibiotics to select for donor, recipient and transconjugant. The remaining 100 µl were incubated for 90 min at 37°C. 1 ml of LB was added gently and the tubes were incubated again at 37°C for 90 min or 22h30. Conjugation mix were vortexed and treated the same as time 0 min.

Multispecies conjugation

Overnight cultures grown in LB of donor and recipient strains were diluted to an A_{600} of 0.05 and grown until an A_{600} comprised between 0.7 and 0.9 was reached. A recipient mix is prepared by mixing *C. rodentium*, *E. cloacae*, *E. coli* EPEC and *E. coli* HS recipients strains. This mix is serial diluted and plated on LB agar supplemented with antibiotics to select for each recipient. 100 µl of donor and 100 µl of the recipient mix were added to an Eppendorf tube to perform mating. At time 0 min, 100 µl of the mix were diluted into 1 ml LB, serial diluted and plated on LB agar supplemented with antibiotics to select for donor, recipients and transconjugants. The remaining 100 µl were incubated for 1h30 at 37°C. 1 ml of LB was gently added and the tubes were incubated for an additional 1h30 at 37°C. Conjugation mix were then vortexed, serial diluted and plated on LB agar supplemented with antibiotics to select for donor, recipients and transconjugants. In the figures, the efficiencies of conjugation are represented either as the final concentration of transconjugant cell (CFU/ml) or as the percentage of transconjugant cells calculated from the ratio (T/R+T).

Conjugation with RP4 conjugative machinery

Overnight cultures of donor and recipient strains were grown in LB and diluted to an A_{600} of 0.05 and grown until an A_{600} of 0.5. 750 µl of donor are mixed with 750 µl of recipient strain and centrifugated at 5,000 rpm during 10 min. 1450 µl of supernatant is removed and the pellet is resuspended into the remaining 50 µl and dropped on a 0.45 µm nitrocellulose filter already placed on LB agar media. Conjugation mixes are incubated for 2h at 37°C and then resuspended into 1mL of LB. Resuspended conjugation mixes are then serial diluted and plated on LB agar supplemented with antibiotics to select for donor, recipients and transconjugants. In the figures, the efficiencies of conjugation are represented either as the final concentration of transconjugant cell (CFU/ml) or as the percentage of transconjugant cells calculated from the ratio (T/R+T).

Long-term conjugation experiment

Conjugation mixes were prepared and incubated at 37°C without agitation. Every 24 h, 100 µl of the mix were diluted into 1 ml of LB and re-incubated at 37°C. The remaining of the mixes were vortexed, serial diluted and plated on LB agar supplemented with antibiotics selecting for donor, recipient and transconjugant cell.

In vivo experiments realized by Gregory Jubelin

C3H/HeOuJ mice purchased from Charles River lab and housed in cages of no more than five mice per cage. Mice experiments were performed with 5 mice per group. Each mouse was infected by oral gavage with 200µl of PBS containing 5.10^8 bacterial cells of *C. rodentium* ICC169 Nal^R grown in LB overnight. Uninfected mice were given PBS only. At day 1, 3, 5, 7 and 9, mice of infected groups "I – HS TAP-Cas9-nsp" and "I – HS TAP-Cas9-Cr22" were fed with 10^{10} of donor strain HS F-Tn*10* Tap-Cas9-nsp and TAP-cas9-Cr22, respectively. The mice group "I – HS TAP-Cas9-Cr22 gavage Day 1" was fed with the HS F-Tn*10* TAP-Cas9-Cr22 only at day 1. Each day, faecal samples were collected, homogenized in PBS and subsequently diluted before plating on LB agar plates supplemented with appropriate antibiotics to select for recipient and transconjugant cells. Body weight and clinical signs of mice were monitored daily to evaluate the severity of infection. Mice presenting a weight loss > 15 % compared to body weight at day 0 or presenting severe clinical symptoms were immediately euthanized.

Live-cell microscopy experiments

Snapshots experiments

Overnight cultures in M9-CASA of donor and recipient cells were diluted to an A_{600} of 0.05 and grown until an A_{600} comprised between 0.7 and 0.9. 25µl of donor and 75 µl of recipient were mixed into an Eppendorf tube, vortexed and incubated at 37°C. 1 mL of fresh M9-CASA was added after 1h30 incubation. At time 0, 1, 2, 6 and 9h after incubation, 10 µl of mix were dropped on a slide containing M9-CASA with 1% agar and directly observed under the microscope.

Time-lapse experiments

Overnight cultures in M9-CASA of donor and recipient cells were diluted to an A_{600} of 0.05 and grown until an A_{600} comprised between 0.7 and 0.9. 25µl of donor and 75 µl of recipient were mixed into an Eppendorf tube, vortexed and 50 µl of the mix was loaded into a B04A

microfluidic chamber (ONIX, CellASIC®). Nutrient supply was maintained at 1 psi and the temperature maintained at 37°C. Cells were imaged every 5 min for 90 minutes.

Image acquisition

Conventional wide-field fluorescence microscopy imaging was carried out on an Eclipse Ti-E microscope (Nikon), equipped with x100/1.45 oil Plan Apo Lambda phaseobjective, FLash4 V2 CMOS camera (Hamamatsu), and using NIS software for image acquisition. Acquisition settings were 100 ms for sfGFP, 100 ms for mCherry using 50% power of a Fluo LED Spectra X light source at 488 nm and 560 nm excitation wavelengths, respectively.

Image analysis

For the analysis of the length, detection of bacterial cells or foci was done manually using the Manual-editing interface of MicrobeJ plugin (Ducret, Quardokus and Brun 2016) of Fiji software. Mean intensity fluorescence and length were automatically extracted. Acquisition of the plasmid was determined when a ParB-mCherry foci is observed. Cells were synchronized using the acquisition of the plasmid as time 0 in Figures R12 and R14 to compare sfGFP fluorescence apparition.

Table M1 : Strains

Name	Genotype	Reference
TB28	*E. coli* K12 F- Lambda- *rph-1* DE*(lacIZYA)::FRT* (lac-)	Lab Collection
MS388	*E. coli* MG1655 *rpsL* (Str^R, lac+)	Gift from F. Cornet
LY720	*Citrobacter rodentium* ICC168 (Nal^R)	(Gueguen and Cascales 2013)
LY1410	*Enterobacter cloacae* ATCC 13047 (Ap^R, St^R)	Gift from P. Bogaerts
LY1615	EPEC E2348 (Rif^R)	(Reuter *et al.* 2021)
LY1667	*Escherichia coli* IAI1 (St^R)	Derivative from LY1506 with a spontaneous mutation leading to streptomycin resistance phenotype
LY1601	*Escherichia coli* HS (St^R)	This study
LY1666	*Escherichia coli* Nissle (St^R)	This study
LY1506	*E. coli* IAI1	Gift from E. Denamur
LY1563	*E. coli* HS GenBank: CP000802.1	Gift from G. Jubelin
LY1562	*E. coli* Nissle GenBank: CP007799.1	Gift from G. Jubelin
LY1907	*E. coli* IAI1 St^R / F-Tn*10* / TAP-Cas9-nsp (St^R, Tc^R, Kn^R)	This study
LY1675	*E. coli* HS St^R / F-Tn*10* / TAP-Cas9-nsp (St^R, Tc^R, Kn^R)	This study
LY1676	*E. coli* Nissle St^R / F-Tn*10* / TAP-Cas9-nsp (St^R, Tc^R, Kn^R)	This study
LY1908	*E. coli* IAI1 St^R / F-Tn*10* / TAP-Cas9-Cr1 (St^R, Tc^R, Kn^R)	This study
LY1909	*E. coli* IAI1 St^R / F-Tn*10* / TAP-Cas9-Cr22 (St^R, Tc^R, Kn^R)	This study
LY1723	*E. coli* HS St^R / F-Tn*10* / TAP-Cas9-Cr1 (St^R, Tc^R, Kn^R)	This study
LY1846	*E. coli* HS StR / F-Tn*10* / TAP-Cas9-Cr22 (St^R, Tc^R, Kn^R)	This study
LY1724	*E. coli* HS StR / F-Tn*10* / TAP-Cas9-EPEC (St^R, Tc^R, Kn^R)	This study
LY1369	LY636 / F-Tn*10* / TAP-Cas9-nsp (Cm^R, Tc^R, Kn^R)	(Reuter *et al.* 2021)
LY1244	MS388 / F-Tn*10* / TAP-Cas9-nsp (St^R, Tc^R, Kn^R)	(Reuter *et al.* 2021)
LY1618	LY636 / F-Tn*10* / TAP-Cas9-EPEC (Cm^R, Tc^R, Kn^R)	(Reuter *et al.* 2021)
LY1239	MS388 / F-Tn*10* / TAP-Cas9-Cr1 (St^R, Tc^R, Kn^R)	(Reuter *et al.* 2021)
LY1276	MS388 / F-Tn*10* / TAP-Cas9-Cr22 (St^R, Tc^R, Kn^R)	(Reuter *et al.* 2021)
LY1524	LY636 / F-Tn*10* / TAP-dCas9-nsp (St^R, Tc^R, Kn^R)	(Reuter *et al.* 2021)

LY1523	LY636 / F-Tn*10* / TAP-dCas9-OXA48 (St^R, Tc^R, Kn^R)	(Reuter *et al.* 2021)
LY1973	LY636 / F-Tn*10* Δ*oriT* / TAP-dCas9-nsp (St^R, Tc^R, Kn^R)	This study
LY1975	LY636 / F-Tn*10* Δ*oriT* / TAP-dCas9-OXA48 (St^R, Tc^R, Kn^R)	This study
LY1507	MS388 *ilvA::erm* / pOXA-48a (St^R, Erm^R, Ap^R, lac+)	(Reuter *et al.* 2021)
LY1932	LY636 / F-Tn*10* Δ*oriT* (Cm^R, Tc^R)	This study
DY330	W3110 Δ*lacU169, gal490,* λ*cI857* Δ*(cro-bioA)*, (lac-)	(Yu *et al.* 2000)
LY156	DY330 / F-Tn*10* (Tc^R, lac-)	Conjugation DY300 X LY5 to Tc^R, lac-
LY406	DY330 / F-Tn*10 parS* (Tc^R, lac-)	Conjugation DY300 X LY394 to Tc^R, lac-
LY820	DY330 / F-Tn*10* Δ*oriT* (Tc^R, lac-)	This study
LY1183	*Salmonella enterica* ser. Typhimurium LT2 (Genbank NC_003197.2)	Gift from E. Cascales
LY1977	*Salmonella enterica* ser. Typhimurium LT2 (St^R)	Derivative from LY1183 with a spontaneous mutation leading to streptomycin resistance phenotype
LY1708	*Vibrio cholerae* N16961 (St^R)	Gift from Z. Baharoglu
LY1182	*Klebsiella pneumoniae* LM21 (St^R)	Gift from E. Cascales
LY1981	LY636 / RP4 / TAP_{RK2}-Cas9-nsp (Cm^R, Tc^R, Ap^R, Kn^R, Gm^R)	This study
LY2013	LY636 / RP4 / TAP_{RK2}-Cas9-St (Cm^R, Tc^R, Ap^R, Kn^R, Gm^R)	This study
LY2012	LY636 / RP4 / TAP_{RK2}-Cas9-Vc (Cm^R, Tc^R, Ap^R, Kn^R, Gm^R)	This study
LY2052	LY636 / RP4 / TAP_{RK2}-Cas9-Kp (Cm^R, Tc^R, Ap^R, Kn^R, Gm^R)	This study
LY1746	LY636 / RP4 (Cm^R, Tc^R, Ap^R, Kn^R)	Lab collection
LY1628	BM21 / RP4 (Ap^R, Cm^R, Kn^R, Nal^R)	Gift from D. Mazel
LY636	TB28 *ilvA::IsceICS-frt-cat-frt* (Cm^R, lac-)	Lab collection
LY1361	LY636 / F-Tn*10* (St^R, Tc^R)	(Reuter *et al.* 2021)
LY1932	TB28 ilvA::Cm / F-Tn*10* Δ*oriT*-min-FRT	This study
LY1379	LY636 / F-Tn*10* / TAP-ΔCRISPR (St^R, Tc^R, Kn^R)	(Reuter *et al.* 2021)
LY1369	LY636 / F-Tn*10* / TAP-Cas9-nsp (St^R, Tc^R, Kn^R)	(Reuter *et al.* 2021)
LY1971	LY636 / F-Tn*10* Δ*oriT* / TAP-ΔCRISPR (St^R, Tc^R, Kn^R)	This study
LY1972	LY636 / F-Tn*10* Δ*oriT* / TAP-Cas9-nsp (St^R, Tc^R, Kn^R)	This study
MS428	MS388 Δ*lacZ ::gfp-parB*$_{P1}$ (St^R, lac-)	Lab collection
LY5	MS388 / F-Tn*10* (St^R, Tc^R)	(Nolivos *et al.* 2019)
LY875	MS388 / F-Tn*10 parS*	(Nolivos *et al.* 2019)
LY756	MS388 / F-Tn*10 parS ygeA-sfGFP*	Lab collection
LY791	MS388 / F-Tn*10 parS yfjA-sfGFP*	Lab collection
LY792	MS388 / F-Tn*10 parS yfjB-sfGFP*	Lab collection
LY270	MS388 / F-Tn*10 parS ssb-sfGFP*	Lab collection
LY754	MS388 / F-Tn*10 parS psiB-sfGFP*	Lab collection
LY162	DY330 / F-Tn*10 parS*	(Nolivos *et al.* 2019)
LY732	DY330 / F-Tn*10 parS ygeA-sfGFP-Kn*	Lab collection
LY733	DY330 / F-Tn*10 parS yfjA-sfGFP-Kn*	Lab collection
LY731	DY330 / F-Tn*10 parS yfjB-sfGFP-Kn*	Lab collection
LY225	DY330 / F-Tn*10 parS ssb-sfGFP-Kn*	Lab collection
LY734	DY330 / F-Tn*10 parS psiB-sfGFP-Kn*	Lab collection
LY318	MS388 / pSN70 *parB-mCherry*	(Nolivos *et al.* 2019)

Table M2 : Plasmids

Name	Construct and usage	Reference
TAP-ΔCRISPR (pBG6)	Carries F *oriT*, pBBR1 *oriV*, Kn^R	Replacement of RK2 *oriT* in pSEVA231 by F plasmid *oriT* (Reuter *et al.* 2021)
TAP-Cas9-nsp (pBG29)	Produces Cas9 and nsp spacer, Kn^R	Insertion of sgRNA scaffold region under the Bba_J23119 promoter from pgRNA-SapI plasmid in pBG28
TAP-Cas9-Cr1 (pAR4)	Produces Cas9 with Cr1 spacer targeting a single locus in *C. rodentium*, Kn^R	Replacement of nsp in pBG29 by Cr1 spacer
TAP-Cas9-Cr22 (pAR7)	Produces Cas9 with Cr22 spacer targeting 22 locus in *C. rodentium*, Kn^R	Replacement of nsp in pBG29 by Cr22 spacer
TAP-Cas9-EPEC (pAR28)	Produces Cas9 with EPEC spacer targeting a single locus in *E. coli* EPEC, Kn^R	Replacement of nsp in pBG29 by EPEC spacer
TAP-dCas9-nsp (pAR6)	Produces dCas9 and nsp spacer, Kn^R	Insertion of sgRNA scaffold region under the Bba_J23119 promoter into pBG31
TAP-dCas9-OXA48 (pBG51)	Produces dCas9 with OXA48 spacer targeting the promoter region of bla_{OXA48}, Kn^R	Replacement of nsp in pAR6 by OXA48 spacer
TAP_{RK2}-Cas9-nsp (pDJ14)	Produces Cas9 and nsp spacer, Gm^R	Replacement of *kan* in pBG29 by *acc3* from pSEVA631
TAP_{RK2}-Cas9-St (pAR30)	Produces Cas9 with St spacer targeting a single locus in *S. enterica* sv Typhimurium LT2, Gm^R	Replacement of nsp in pDJ14 by St spacer
TAP_{RK2}-Cas9-Vc (pAR31)	Produces Cas9 with Vc spacer targeting a single locus in *V. cholerae* N16961, GmR	Replacement of nsp in pDJ14 by Vc spacer
TAP_{RK2}-Cas9-Kp (pAR32)	Produces Cas9 with Kp spacer targeting a single locus in *K. pneumoniae* LM21, Gm^R	Replacement of nsp in pDJ14 by Kp spacer
F-Tn*10*	Carries Tn*10* transposon in the intergenic region *ybdB-ybfA* and the *tra* genes necessary to encode conjugation machinery	Accession: MK492260.1
F-Tn*10 parS*	Carries Tn*10* transposon in the intergenic region *ybdB-ybfA,* the *tra* genes necessary to encode conjugation machinery and $parS_{PMT1}$ inserted at the intergenic *ygeB-ygfA* locus	(Nolivos *et al.* 2019)
F-Tn*10 parS ssb-sfGFP*	Carries Tn*10* transposon in the intergenic region *ybdB-ybfA,* the *tra* genes necessary to encode conjugation machinery, $parS_{PMT1}$ inserted at the intergenic *ygeB-ygfA* locus and *ssb-sfGFP* fusion at the endogenous locus	Lab collection
F-Tn*10 parS yfjA-sfGFP*	Carries Tn*10* transposon in the intergenic region *ybdB-ybfA,* the *tra* genes necessary to encode conjugation machinery, $parS_{PMT1}$ inserted at the intergenic *ygeB-ygfA* locus and *yfjA-sfGFP* fusion at the endogenous locus	Lab collection
F-Tn*10 parS yfjB-sfGFP*	Carries Tn*10* transposon in the intergenic region *ybdB-ybfA,* the *tra* genes necessary to encode conjugation machinery, $parS_{PMT1}$ inserted at the intergenic *ygeB-ygfA* locus and *yfjB-sfGFP* fusion at the endogenous locus	Lab collection
F-Tn*10 parS psiB-sfGFP*	Carries Tn*10* transposon in the intergenic region *ybdB-ybfA,* the *tra* genes necessary to encode conjugation machinery, $parS_{PMT1}$ inserted at the intergenic *ygeB-ygfA* locus and *psiB-sfGFP* fusion at the endogenous locus	Lab collection

F-Tn*10 parS ygeA-sfGFP*	Carries Tn*10* transposon in the intergenic region *ybdB-ybfA,* the *tra* genes necessary to encode conjugation machinery, $parS_{PMT1}$ inserted at the intergenic *ygeB-ygfA* locus and *ygeA-sfGFP* fusion at the endogenous locus	Lab collection
RP4	Carries Amp^R, Kn^R, Tc^R and the *tra* and *trb* genes encoding of the RK2 conjugation machinery	Gift from D. Mazel
pOXA-48a	Carries the bla_{OXA-48} gene that encodes the OXA-48 carbapenemase	Gift from P. Bogaerts

Table M3 : Primers

Primer	**Sequence**	**Construct**
ol507	agatgatgggggctgaaaaccagagagaggagaaagcaggGTGTAGGCTGGAGCTGCTTC	deletion ygeA
ol508	caagattgcaacaatcaggagggatattcatcacatccggCATATGAATATCCTCCTTAG	
ol473	cttcctcttcttcctcttctttccgttcctctcctgcttaGTGTAGGCTGGAGCTGCTTC	deletion Fssb
ol474	taatgccacgaactgccatgatgtgtctccttctgttgatCATATGAATATCCTCCTTAG	
ol505	actccacaaaaaggctcaacaggttggtggttctcaccacGTGTAGGCTGGAGCTGCTTC	deletion oriT
ol506	cggcgcgttgttgtagccgcgccgacaccgctttttttaaaCATATGAATATCCTCCTTAG	
Primer	**Sequence (spacer in capitals)**	**Spacer name**
ol727	TAGTACATGCGCTTTTGTGTAG	St
ol728	AAACTACACAAAAGCGCATGTA	
ol729	tagtTAGTGTATCTATGCTCAg	Vc
ol730	aaacTGAGCATAGATACACTAa	
ol948	TAGTTGAACGAACCAGACGAGG	Kp
ol949	AAACCTCGTCTGGTTCGTTCAA	

Bibliography :

Abajy MY, Kopeć J, Schiwon K *et al.* A Type IV-Secretion-Like System Is Required for Conjugative DNA Transport of Broad-Host-Range Plasmid pIP501 in Gram-Positive Bacteria. *Journal of Bacteriology* 2007;**189**:2487–96.

Adachi S, Hori K, Hiraga S. Subcellular positioning of F plasmid mediated by dynamic localization of SopA and SopB. *J Mol Biol* 2006;**356**:850–63.

Akroyd J, Symonds N. Localization of the gam gene of bacteriophage Mu and characterisation of the gene product. *Gene* 1986;**49**:273–82.

Al Mamun AAM, Kishida K, Christie PJ. Protein Transfer through an F Plasmid-Encoded Type IV Secretion System Suppresses the Mating-Induced SOS Response. Zhulin IB (ed.). *mBio* 2021;**12**, DOI: 10.1128/mBio.01629-21.

Ali M, Nelson AR, Lopez AL *et al.* Updated Global Burden of Cholera in Endemic Countries. Remais JV (ed.). *PLOS Neglected Tropical Diseases* 2015;**9**:e0003832.

Althorpe NJ, Wilkins BM, Roscoe RA *et al.* Expression of leading region genes on IncI1 plasmid ColIb-P9: genetic evidence for single-stranded DNA transcription. *Microbiology* 1999;**145**:2655–62.

Álvarez-Rodríguez I, Ugarte-Uribe B, de la Arada I *et al.* Conjugative Coupling Proteins and the Role of Their Domains in Conjugation, Secondary Structure and in vivo Subcellular Location. *Front Mol Biosci* 2020;**7**:185.

Ambrose SJ, Harmer CJ, Hall RM. Compatibility and entry exclusion of IncA and IncC plasmids revisited: IncA and IncC plasmids are compatible. *Plasmid* 2018;**96–97**:7–12.

Anders C, Niewoehner O, Duerst A *et al.* Structural basis of PAM-dependent target DNA recognition by the Cas9 endonuclease. *Nature* 2014;**513**:569–73.

Anderson DG, Kowalczykowski SC. The Translocating RecBCD Enzyme Stimulates Recombination by Directing RecA Protein onto ssDNA in a -Regulated Manner. 1997:10.

Aniukwu J, Glickman MS, Shuman S. The pathways and outcomes of mycobacterial NHEJ depend on the structure of the broken DNA ends. *Genes Dev* 2008;**22**:512–27.

Anthony KG, Sherburne C, Sherburne R *et al.* The role of the pilus in recipient cell recognition during bacterial conjugation mediated by F-like plasmids. *Molecular Microbiology* 1994;**13**:939–53.

Arends K, Schiwon K, Sakinc T *et al.* Green Fluorescent Protein-Labeled Monitoring Tool To Quantify Conjugative Plasmid Transfer between Gram-Positive and Gram-Negative Bacteria. *Applied and Environmental Microbiology* 2012;**78**:895–9.

Aspray TJ, Hansen SK, Burns RG. A soil-based microbial biofilm exposed to 2,4-D: bacterial community development and establishment of conjugative plasmid pJP4. *FEMS Microbiol Ecol* 2005;**54**:317–27.

Astot C, Dolezal K, Nordstrom A *et al.* An alternative cytokinin biosynthesis pathway. *Proceedings of the National Academy of Sciences* 2000;**97**:14778–83.

Atmakuri K, Cascales E, Christie PJ. Energetic components VirD4, VirB11 and VirB4 mediate early DNA transfer reactions required for bacterial type IV secretion: ATP-binding proteins co-ordinate DNA transfer. *Molecular Microbiology* 2004;**54**:1199–211.

Audette GF, Manchak J, Beatty P *et al.* Entry exclusion in F-like plasmids requires intact TraG in the donor that recognizes its cognate TraS in the recipient. *Microbiology (Reading)* 2007;**153**:442–51.

Austin S, Nordström K. Partition-mediated incompatibility of bacterial plasmids. *Cell* 1990;**60**:351–4.

Aviv G, Rahav G, Gal-Mor O. Horizontal Transfer of the Salmonella enterica Serovar Infantis Resistance and Virulence Plasmid pESI to the Gut Microbiota of Warm-Blooded Hosts. Davies JE (ed.). *mBio* 2016;**7**, DOI: 10.1128/mBio.01395-16.

Babic A, Lindner AB, Vulic M *et al.* Direct visualization of horizontal gene transfer. *Science* 2008;**319**:1533–6.

Badran AH, Liu DR. Development of potent in vivo mutagenesis plasmids with broad mutational spectra. *Nat*

Commun 2015;**6**:8425.

Bagdasarian M, Bailone A, Angulo JF *et al.* PsiB, an anti-SOS protein, is transiently expressed by the F sex factor during its transmission to an Escherichia coli K-12 recipient. *Molecular Microbiology* 1992;**6**:885–93.

Baharoglu Z, Bikard D, Mazel D. Conjugative DNA Transfer Induces the Bacterial SOS Response and Promotes Antibiotic Resistance Development through Integron Activation. Matic I (ed.). *PLoS Genetics* 2010;**6**:e1001165.

Bakkeren E, Huisman JS, Fattinger SA *et al.* Salmonella persisters promote the spread of antibiotic resistance plasmids in the gut. *Nature* 2019;**573**:276–80.

Bañuelos-Vazquez LA, Cazares D, Rodríguez S *et al.* Transfer of the Symbiotic Plasmid of Rhizobium etli CFN42 to Endophytic Bacteria Inside Nodules. *Frontiers in Microbiology* 2020;**11**, DOI: 10.3389/fmicb.2020.01752.

Barlow M. What antimicrobial resistance has taught us about horizontal gene transfer. *Methods Mol Biol* 2009;**532**:397–411.

Barry GF, Rogers SG, Fraley RT *et al.* Identification of a cloned cytokinin biosynthetic gene. *Proceedings of the National Academy of Sciences* 1984;**81**:4776–80.

Batchelor RA, Pearson BM, Friis LM *et al.* Nucleotide sequences and comparison of two large conjugative plasmids from different Campylobacter species. *Microbiology (Reading)* 2004;**150**:3507–17.

Baxter JC, Funnell BE. Plasmid Partition Mechanisms. 2014:20.

Becker EC, Meyer R. Origin and Fate of the 3′ Ends of Single-Stranded DNA Generated by Conjugal Transfer of Plasmid R1162. *Journal of Bacteriology* 2012;**194**:5368–76.

Belogurov AA, Delver EP, Agafonova OV *et al.* Antirestriction protein ard (type C) encoded by IncW plasmid psa has a high similarity to the "protein transport" domain of TraC1 primase of promiscuous plasmid RP4 1 1Edited by M. Gottesman. *Journal of Molecular Biology* 2000;**296**:969–77.

Ben Maamar S, Glawe AJ, Brown TK *et al.* Mobilizable antibiotic resistance genes are present in dust microbial communities. van Schaik W (ed.). *PLOS Pathogens* 2020;**16**:e1008211.

Beranek A, Zettl M, Lorenzoni K *et al.* Thirty-Eight C-Terminal Amino Acids of the Coupling Protein TraD of the F-Like Conjugative Resistance Plasmid R1 Are Required and Sufficient To Confer Binding to the Substrate Selector Protein TraM. *Journal of Bacteriology* 2004;**186**:6999–7006.

Bertozzi Silva J, Storms Z, Sauvageau D. Host receptors for bacteriophage adsorption. Millard A (ed.). *FEMS Microbiology Letters* 2016;**363**:fnw002.

Bertrand C, Thibessard A, Bruand C *et al.* Bacterial NHEJ: a never ending story. *Molecular Microbiology* 2019;**111**:1139–51.

van Biesen T, Frost LS. Differential levels of fertility inhibition among F-like plasmids are related to the cellular concentration of finO mRNA. *Mol Microbiol* 1992;**6**:771–80.

van Biesen T, Frost LS. The FinO protein of IncF plasmids binds FinP antisense RNA and its target, traJ mRNA, and promotes duplex formation. *Mol Microbiol* 1994;**14**:427–36.

Bikard D, Euler CW, Jiang W *et al.* Exploiting CRISPR-Cas nucleases to produce sequence-specific antimicrobials. *Nature Biotechnology* 2014;**32**:1146–50.

Bikard D, Hatoum-Aslan A, Mucida D *et al.* CRISPR interference can prevent natural transformation and virulence acquisition during in vivo bacterial infection. *Cell Host Microbe* 2012;**12**:177–86.

Bikard D, Jiang W, Samai P *et al.* Programmable repression and activation of bacterial gene expression using an engineered CRISPR-Cas system. *Nucleic Acids Research* 2013;**41**:7429–37.

Bingle LE, Thomas CM. Regulatory circuits for plasmid survival. *Curr Opin Microbiol* 2001;**4**:194–200.

Blakeley BD, Chapman AM, McNaughton BR. Split-superpositive GFP reassembly is a fast, efficient, and robust method for detecting protein-protein interactions in vivo. *Mol Biosyst* 2012;**8**:2036–40.

Böldicke, Hillenbrand, Lanka *et al.* Rifampicin-resistant initiation of DNA synthesis on the isolated strands of ColE

plasmid DNA - PubMed. 1981.

Bradley DE. Morphological and serological relationships of conjugative pili. *Plasmid* 1980;**4**:155–69.

Bradley DE. Derepressed plasmids of incompatibility group I1 determine two different morphological forms of pilus. *Plasmid* 1983;**9**:331–4.

Bradley DE, Taylor DE, Cohen DR. Specification of surface mating systems among conjugative drug resistance plasmids in Escherichia coli K-12. *Journal of Bacteriology* 1980;**143**:1466–70.

Brantl S. Plasmid Replication Control by Antisense RNAs. *Microbiol Spectr* 2014;**2**:PLAS-0001-2013.

Brito IL. Examining horizontal gene transfer in microbial communities. *Nature Reviews Microbiology* 2021;**19**:442–53.

Brito IL, Yilmaz S, Huang K *et al.* Mobile genes in the human microbiome are structured from global to individual scales. *Nature* 2016;**535**:435–9.

Brolund A, Sandegren L. Characterization of ESBL disseminating plasmids. *Infectious Diseases* 2016;**48**:18–25.

Brooks AC, Hwang LC. Reconstitutions of plasmid partition systems and their mechanisms. *Plasmid* 2017;**91**:37–41.

Brooks JF, Behrendt CL, Ruhn KA *et al.* The microbiota coordinates diurnal rhythms in innate immunity with the circadian clock. *Cell* 2021;**184**:4154–4167.e12.

Bundock P, den Dulk-Ras A, Beijersbergen A *et al.* Trans-kingdom T-DNA transfer from Agrobacterium tumefaciens to Saccharomyces cerevisiae. *EMBO J* 1995;**14**:3206–14.

Bundock P, Hooykaas PJJ. Integration of Agrobacterium tumefaciens T-DNA in the Saccharomyces cerevisiae genome by illegitimate recombination. *Proceedings of the National Academy of Sciences* 1996;**93**:15272–5.

Cabantous S, Terwilliger TC, Waldo GS. Protein tagging and detection with engineered self-assembling fragments of green fluorescent protein. *Nat Biotechnol* 2005;**23**:102–7.

Cabezón E, Sastre JI, de la Cruz F. Genetic evidence of a coupling role for the TraG protein family in bacterial conjugation. *Molecular and General Genetics MGG* 1997;**254**:400–6.

Cambré A, Aertsen A. Bacterial Vivisection: How Fluorescence-Based Imaging Techniques Shed a Light on the Inner Workings of Bacteria. *Microbiol Mol Biol Rev* 2020;**84**:e00008-20.

Cantón R, Akóva M, Carmeli Y *et al.* Rapid evolution and spread of carbapenemases among Enterobacteriaceae in Europe. *Clinical Microbiology and Infection* 2012;**18**:413–31.

Carattoli A, Bertini A, Villa L *et al.* Identification of plasmids by PCR-based replicon typing. *Journal of Microbiological Methods* 2005;**63**:219–28.

Carattoli A, Seiffert SN, Schwendener S *et al.* Differentiation of IncL and IncM Plasmids Associated with the Spread of Clinically Relevant Antimicrobial Resistance. Janssen PJ (ed.). *PLOS ONE* 2015;**10**:e0123063.

Carmody RN, Gerber GK, Luevano JM *et al.* Diet dominates host genotype in shaping the murine gut microbiota. *Cell Host Microbe* 2015;**17**:72–84.

Carver PL ed. 1. METALS IN MEDICINE: THE THERAPEUTIC USE OF METAL IONS IN THE CLINIC. *Essential Metals in Medicine: Therapeutic Use and Toxicity of Metal Ions in the Clinic*. De Gruyter, 2019, 1–16.

Casadevall A, Pirofski L. Virulence factors and their mechanisms of action: the view from a damage–response framework. *Journal of Water and Health* 2009;**7**:S2–18.

Cascales E, Atmakuri K, Liu Z *et al.* Agrobacterium tumefaciens oncogenic suppressors inhibit T-DNA and VirE2 protein substrate binding to the VirD4 coupling protein. *Mol Microbiol* 2005;**58**:565–79.

Cascales E, Buchanan SK, Duché D *et al.* Colicin biology. *Microbiol Mol Biol Rev* 2007;**71**:158–229.

CDC. CDC: Salmonella Outbreak Linked to BrightFarms Packaged Salad Greens. *Centers for Disease Control and Prevention* 2021a.

CDC. CDC: Salmonella Outbreaks Linked to Italian-Style Meats. *Centers for Disease Control and Prevention* 2021b.

Chandler M, de la Cruz F, Dyda F *et al.* Breaking and joining single-stranded DNA: the HUH endonuclease superfamily. *Nature Reviews Microbiology* 2013;**11**:525–38.

Charpentier E, Richter H, van der Oost J *et al.* Biogenesis pathways of RNA guides in archaeal and bacterial CRISPR-Cas adaptive immunity. *FEMS Microbiology Reviews* 2015;**39**:428–41.

Chase JW, Williams KR. SINGLE-STRANDED DNA BINDING PROTEINS REQUIRED FOR DNA REPLICATION. 1986:37.

Chatfield LK, Wilkins BM. Conjugative transfer of IncI1 plasmid DNA primase. *Mol Gen Genet* 1984;**197**:461–6.

Chattoraj DK. Control of plasmid DNA replication by iterons: no longer paradoxical: Control of DNA replication by iterons. *Molecular Microbiology* 2002;**37**:467–76.

Chayot R, Montagne B, Mazel D *et al.* An end-joining repair mechanism in Escherichia coli. *Proceedings of the National Academy of Sciences* 2010;**107**:2141–6.

Chen CY, Kado CI. Inhibition of Agrobacterium tumefaciens oncogenicity by the osa gene of pSa. *Journal of Bacteriology* 1994;**176**:5697–703.

Chen C-Y, Kado CI. Osa protein encoded by plasmid pSa is located at the inner membrane but does not inhibit membrane association of VirB and VirD virulence proteins in *Agrobacterium tumefaciens*. *FEMS Microbiology Letters* 1996;**135**:85–92.

Chen J, Novick RP. Phage-mediated intergeneric transfer of toxin genes. *Science* 2009;**323**:139–41.

Chen JS, Dagdas YS, Kleinstiver BP *et al.* Enhanced proofreading governs CRISPR–Cas9 targeting accuracy. *Nature* 2017;**550**:407–10.

Chen W-M, Moulin L, Bontemps C *et al.* Legume Symbiotic Nitrogen Fixation byβ-Proteobacteria Is Widespread inNature. *Journal of Bacteriology* 2003;**185**:7266–72.

Choudhary E, Thakur P, Pareek M *et al.* Gene silencing by CRISPR interference in mycobacteria. *Nature Communications* 2015;**6**, DOI: 10.1038/ncomms7267.

Citorik RJ, Mimee M, Lu TK. Sequence-specific antimicrobials using efficiently delivered RNA-guided nucleases. *Nature Biotechnology* 2014;**32**:1141–5.

Clarke M, Maddera L, Harris RL *et al.* F-pili dynamics by live-cell imaging. *Proceedings of the National Academy of Sciences* 2008;**105**:17978–81.

Clemens JD, Nair GB, Ahmed T *et al.* Cholera. *The Lancet* 2017;**390**:1539–49.

Close SM, Kado CI. The osa gene of pSa encodes a 21.1-kilodalton protein that suppresses Agrobacterium tumefaciens oncogenicity. *Journal of Bacteriology* 1991;**173**:5449–56.

Coetzee JN, Datta N, Hedges RW. R Factors from Proteus rettgeri. *Journal of General Microbiology* 1972;**72**:543–52.

Collins LT, Otoupal PB, Campos JK *et al.* Design of a De Novo Aggregating Antimicrobial Peptide and a Bacterial Conjugation-Based Delivery System. *Biochemistry* 2019;**58**:1521–6.

Costa TRD, Ilangovan A, Ukleja M *et al.* Structure of the Bacterial Sex F Pilus Reveals an Assembly of a Stoichiometric Protein-Phospholipid Complex. *Cell* 2016;**166**:1436–1444.e10.

Courcelle J, Khodursky A, Peter B *et al.* Comparative Gene Expression Profiles Following UV Exposure in Wild-Type and SOS-Deficient *Escherichia coli*. *Genetics* 2001;**158**:41–64.

Couturier M, Bex F, Bergquist PL *et al.* Identification and Classification of Bacterial Plasmids. *MICROBIOL REV* 1988;**52**:21.

Crawford JA, Kaper JB, DiRita VJ. Analysis of ToxR-dependent transcription activation of ompU, the gene encoding a major envelope protein in Vibrio cholerae. *Mol Microbiol* 1998;**29**:235–46.

Critchlow SE, O'Dea MH, Howells AJ *et al.* The interaction of the F plasmid killer protein, CcdB, with DNA gyrase:

induction of DNA cleavage and blocking of transcription. *J Mol Biol* 1997;**273**:826–39.

Croucher NJ, Finkelstein JA, Pelton SI *et al.* Population genomics of post-vaccine changes in pneumococcal epidemiology. *Nature Genetics* 2013;**45**:656–63.

Cui L, Bikard D. Consequences of Cas9 cleavage in the chromosome of *Escherichia coli*. *Nucleic Acids Research* 2016;**44**:4243–51.

Cui L, Vigouroux A, Rousset F *et al.* A CRISPRi screen in E. coli reveals sequence-specific toxicity of dCas9. *Nature Communications* 2018;**9**, DOI: 10.1038/s41467-018-04209-5.

Curtiss R. BACTERIAL CONJUGATION. *BACTERIAL CONJUGATION* 1969:68.

Cuthbertson L, Nodwell JR. The TetR Family of Regulators. *Microbiology and Molecular Biology Reviews* 2013;**77**:440–75.

Daehnel K, Harris R, Maddera L *et al.* Fluorescence assays for F-pili and their application. *Microbiology (Reading)* 2005;**151**:3541–8.

Dahlberg C, Bergström M, Hermansson M. In Situ Detection of High Levels of Horizontal Plasmid Transfer in Marine Bacterial Communities. *Applied and Environmental Microbiology* 1998;**64**:2670–5.

Dao-Thi M-H, Van Melderen L, De Genst E *et al.* Molecular Basis of Gyrase Poisoning by the Addiction Toxin CcdB. *Journal of Molecular Biology* 2005;**348**:1091–102.

DasGupta S, Mukhopadhyay G, Papp PP *et al.* Activation of DNA binding by the monomeric form of the P1 replication initiator RepA by heat shock proteins DnaJ and DnaK. *J Mol Biol* 1993;**232**:23–34.

Datta N, Hedges RW. Host Ranges of R Factors. *Journal of General Microbiology* 1972;**70**:453–60.

Datta N, Hedges RW. R factors of compatibility group A. *J Gen Microbiol* 1973;**74**:335–7.

Datta N, Hedges RW, Shaw EJ *et al.* Properties of an R factor from Pseudomonas aeruginosa. *J Bacteriol* 1971;**108**:1244–9.

David LA, Maurice CF, Carmody RN *et al.* Diet rapidly and reproducibly alters the human gut microbiome. *Nature* 2014;**505**:559–63.

Davidson AR, Lu W-T, Stanley SY *et al.* Anti-CRISPRs: Protein Inhibitors of CRISPR-Cas Systems. *Annual Review of Biochemistry* 2020;**89**:309–32.

Davidson MS, Summers AO. Wide-host-range plasmids function in the genus thiobacillus. *Appl Environ Microbiol* 1983;**46**:565–72.

De Gelder L, Vandecasteele FPJ, Brown CJ *et al.* Plasmid donor affects host range of promiscuous IncP-1beta plasmid pB10 in an activated-sludge microbial community. *Appl Environ Microbiol* 2005;**71**:5309–17.

De Jonge N, Simic M, Buts L *et al.* Alternative interactions define gyrase specificity in the CcdB family. *Mol Microbiol* 2012;**84**:965–78.

De La Cochetière MF, Durand T, Lalande V *et al.* Effect of Antibiotic Therapy on Human Fecal Microbiota and the Relation to the Development of Clostridium difficile. *Microbial Ecology* 2008;**56**:395–402.

De Oliveira DMP, Forde BM, Kidd TJ *et al.* Antimicrobial Resistance in ESKAPE Pathogens. *Clinical Microbiology Reviews* 2020;**33**, DOI: 10.1128/CMR.00181-19.

Del Solar G, Espinosa M. Plasmid copy number control: an ever-growing story: Control of plasmid replication. *Molecular Microbiology* 2002;**37**:492–500.

Delcour AH. Outer membrane permeability and antibiotic resistance. *Biochim Biophys Acta* 2009;**1794**:808–16.

Deltcheva E, Chylinski K, Sharma CM *et al.* CRISPR RNA maturation by trans-encoded small RNA and host factor RNase III. *Nature* 2011;**471**:602–7.

Demarre G, Guérout A-M, Matsumoto-Mashimo C *et al.* A new family of mobilizable suicide plasmids based on broad host range R388 plasmid (IncW) and RP4 plasmid (IncPα) conjugative machineries and their cognate

Escherichia coli host strains. *Research in Microbiology* 2005;**156**:245–55.

Deshpande LM, Chopade BA. Plasmid mediated silver resistance in Acinetobacter baumannii. *Biometals* 1994;**7**:49–56.

Diaz R, Rech J, Bouet J-Y. Imaging centromere-based incompatibilities: Insights into the mechanism of incompatibility mediated by low-copy number plasmids. *Plasmid* 2015;**80**:54–62.

Diaz Ricci JC, Hernández ME. Plasmid effects on Escherichia coli metabolism. *Crit Rev Biotechnol* 2000;**20**:79–108.

Dixon DA, Kowalczykowski SC. The recombination hotspot chi is a regulatory sequence that acts by attenuating the nuclease activity of the E. coli RecBCD enzyme. *Cell* 1993;**73**:87–96.

Domingues S, Harms K, Fricke WF *et al.* Natural Transformation Facilitates Transfer of Transposons, Integrons and Gene Cassettes between Bacterial Species. Gilmore MS (ed.). *PLoS Pathogens* 2012;**8**:e1002837.

Dong H, Xiang H, Mu D *et al.* Exploiting a conjugative CRISPR/Cas9 system to eliminate plasmid harbouring the mcr-1 gene from Escherichia coli. *International Journal of Antimicrobial Agents* 2019;**53**:1–8.

Dostál L, Shao S, Schildbach JF. Tracking F plasmid TraI relaxase processing reactions provides insight into F plasmid transfer. *Nucleic Acids Research* 2011;**39**:2658–70.

Doumith M, Ellington MJ, Livermore DM *et al.* Molecular mechanisms disrupting porin expression in ertapenem-resistant Klebsiella and Enterobacter spp. clinical isolates from the UK. *J Antimicrob Chemother* 2009;**63**:659–67.

Doumith M, Findlay J, Hirani H *et al.* Major role of pKpQIL-like plasmids in the early dissemination of KPC-type carbapenemases in the UK. *J Antimicrob Chemother* 2017;**72**:2241–8.

Draper O, Cesar CE, Machon C *et al.* Site-specific recombinase and integrase activities of a conjugative relaxase in recipient cells. *Proceedings of the National Academy of Sciences* 2005;**102**:16385–90.

Dubuy HG, Dubuy HG, Riley F *et al.* TETRACYCLINE FLUORESCENCE IN PERMEABILITY STUDIES OF MEMBRANES AROUND INTRACELLULAR PARASITES. *Science* 1964;**145**:163–5.

Ducret A, Quardokus EM, Brun YV. MicrobeJ, a tool for high throughput bacterial cell detection and quantitative analysis. *Nat Microbiol* 2016;**1**:16077.

Dudley EG, Abe C, Ghigo J-M *et al.* An IncI1 Plasmid Contributes to the Adherence of the Atypical Enteroaggregative *Escherichia coli* Strain C1096 to Cultured Cells and Abiotic Surfaces. *Infection and Immunity* 2006;**74**:2102–14.

den Dulk-Ras A, Vergunst AC, Hooykaas PJJ. Cre Reporter Assay for Translocation (CRAfT): a tool for the study of protein translocation into host cells. *Methods Mol Biol* 2014;**1197**:103–21.

Dutreix M, Backman A, Celerier J *et al.* Identification of psiB genes of plasmids F and R6-5. Molecular basis for psiB enhanced expression in plasmid R6-5. *Nucleic Acids Research* 1988;**16**:10669–79.

Dutta D, Kaushik A, Kumar D *et al.* Foodborne Pathogenic Vibrios: Antimicrobial Resistance. *Front Microbiol* 2021;**12**:638331.

Ebersbach G, Gerdes K. Plasmid Segregation Mechanisms. *Annual Review of Genetics* 2005;**39**:453–79.

Eisenbrandt R, Kalkum M, Lai E-M *et al.* Conjugative Pili of IncP Plasmids, and the Ti Plasmid T Pilus Are Composed of Cyclic Subunits. *Journal of Biological Chemistry* 1999;**274**:22548–55.

Escobar MA, Dandekar AM. Agrobacterium tumefaciens as an agent of disease. *Trends in Plant Science* 2003;**8**:380–6.

Escudero J, Den Dulk-Ras A, Regensburg-Tuïnk TJG *et al.* VirD4-independent transformation by CloDF13 evidences an unknown factor required for the genetic colonization of plants via Agrobacterium: Trans -kingdom transfer of CloDF13. *Molecular Microbiology* 2003;**47**:891–901.

European Medicines Agency. Environmental risk assessments for medicinal products containing, or consisting of, genetically modified organisms (GMOs). *European Medicines Agency* 2018.

Fan Y, Pedersen O. Gut microbiota in human metabolic health and disease. *Nature Reviews Microbiology* 2020,

DOI: 10.1038/s41579-020-0433-9.

Fang L, Davey MJ, O'Donnell M. Replisome Assembly at oriC, the Replication Origin of E. coli, Reveals an Explanation for Initiation Sites outside an Origin. *Molecular Cell* 1999;**4**:541–53.

Faure G, Makarova KS, Koonin EV. CRISPR–Cas: Complex Functional Networks and Multiple Roles beyond Adaptive Immunity. *Journal of Molecular Biology* 2019;**431**:3–20.

Ferguson BJ, Indrasumunar A, Hayashi S *et al.* Molecular analysis of legume nodule development and autoregulation. *J Integr Plant Biol* 2010;**52**:61–76.

Filonov GS, Piatkevich KD, Ting L-M *et al.* Bright and stable near-infrared fluorescent protein for in vivo imaging. *Nat Biotechnol* 2011;**29**:757–61.

Finlay BB, Frost LS, Paranchych W *et al.* Major antigenic determinants of F and ColB2 pili. *J Bacteriol* 1985;**163**:331–5.

Fleming A. ON THE ANTIBACTERIAL ACTION OF CULTURES OF A PENICILLIUM, WITH SPECIAL REFERENCE TO THEIR USE IN THE ISOLATION OF B. INFLUENZ?1E. 1929:13.

Foley SL, Kaldhone PR, Ricke SC *et al.* Incompatibility Group I1 (IncI1) Plasmids: Their Genetics, Biology, and Public Health Relevance. *Microbiology and Molecular Biology Reviews* 2021;**85**, DOI: 10.1128/MMBR.00031-20.

Forsberg KJ, Reyes A, Wang B *et al.* The Shared Antibiotic Resistome of Soil Bacteria and Human Pathogens. *Science* 2012;**337**:1107–11.

Francia MV, Clewell DB, de la Cruz F *et al.* Catalytic domain of plasmid pAD1 relaxase TraX defines a group of relaxases related to restriction endonucleases. *Proceedings of the National Academy of Sciences* 2013;**110**:13606–11.

Francino MP. Antibiotics and the Human Gut Microbiome: Dysbioses and Accumulation of Resistances. *Frontiers in Microbiology* 2016;**6**, DOI: 10.3389/fmicb.2015.01543.

Frost L, Lee S, Yanchar N *et al.* finP and fisO mutations in FinP anti-sense RNA suggest a model for FinOP action in the repression of bacterial conjugation by the Flac plasmid JCFL0. *Mol Gen Genet* 1989;**218**:152–60.

Frost LS, Finlay BB, Opgenorth A *et al.* Characterization and sequence analysis of pilin from F-like plasmids. *J Bacteriol* 1985;**164**:1238–47.

Frost LS, Ippen-Ihler K, Skurray RA. Analysis of the Sequence and Gene Products of the Transfer Region of the F Sex Factor. *MICROBIOL REV* 1994;**58**:49.

Gaffney D, Skurray R, Willetts N *et al.* Regulation of the F conjugation genes studied by hybridization and tra-lacZ fusion. *Journal of Molecular Biology* 1983;**168**:103–22.

Garcia-Doval C, Jinek M. Molecular architectures and mechanisms of Class 2 CRISPR-associated nucleases. *Current Opinion in Structural Biology* 2017;**47**:157–66.

García-Nafría J, Watson JF, Greger IH. IVA cloning: A single-tube universal cloning system exploiting bacterial In Vivo Assembly. *Scientific Reports* 2016;**6**, DOI: 10.1038/srep27459.

García-Quintanilla M, Ramos-Morales F, Casadesús J. Conjugal Transfer of the *Salmonella enterica* Virulence Plasmid in the Mouse Intestine. *Journal of Bacteriology* 2008;**190**:1922–7.

Garcia-Vallve S. Horizontal Gene Transfer in Bacterial and Archaeal Complete Genomes. *Genome Research* 2000;**10**:1719–25.

Garcillán-Barcia MP, de la Cruz F. Why is entry exclusion an essential feature of conjugative plasmids? *Plasmid* 2008;**60**:1–18.

Garcillán-Barcia MP, Francia MV, de La Cruz F. The diversity of conjugative relaxases and its application in plasmid classification. *FEMS Microbiology Reviews* 2009;**33**:657–87.

Garcillán-Barcia MP, Jurado P, González-Pérez B *et al.* Conjugative transfer can be inhibited by blocking relaxase activity within recipient cells with intrabodies: Conjugation termination inhibitors. *Molecular Microbiology*

2007;**63**:404–16.

Garcillán-Barcia MP, Redondo-Salvo S, Vielva L *et al.* MOBscan: Automated Annotation of MOB Relaxases. *Methods Mol Biol* 2020;**2075**:295–308.

Gasson M, Willetts N. Transfer Gene Expression during Fertility Inhibition of the Escherichia coil K12 Sex Factor F by the I-like Plasmid R62. :5.

Gasson MJ, Willetts NS. Five control systems preventing transfer of Escherichia coli K-12 sex factor F. *Journal of Bacteriology* 1975;**122**:518–25.

Getino M, de la Cruz F. Natural and Artificial Strategies To Control the Conjugative Transmission of Plasmids. Baquero F, Bouza E, Gutiérrez-Fuentes JA, et al. (eds.). *Microbiology Spectrum* 2018;**6**, DOI: 10.1128/microbiolspec.MTBP-0015-2016.

Ghigo J-M. Natural conjugative plasmids induce bacterial bio®lm development. 2001;**412**:4.

Globyte V, Lee SH, Bae T *et al.* CRISPR /Cas9 searches for a protospacer adjacent motif by lateral diffusion. *The EMBO Journal* 2019;**38**, DOI: 10.15252/embj.201899466.

Goessweiner-Mohr N, Arends K, Keller W *et al.* Conjugation in Gram-Positive Bacteria. :19.

Golub E, Bailone A, Devoret R. A gene encoding an SOS inhibitor is present in different conjugative plasmids. *J Bacteriol* 1988;**170**:4392–4.

Golub EI, Low KB. Conjugative plasmids of enteric bacteria from many different incompatibility groups have similar genes for single-stranded DNA-binding proteins. *J Bacteriol* 1985;**162**:235–41.

Golub EI, Low KB. Derepression of single-stranded DNA-binding protein genes on plasmids derepressed for conjugation, and complementation of an E. coli ssb- mutation by these genes. *Mol Gen Genet* 1986;**204**:410–6.

Gong T, Zeng J, Tang B *et al.* CRISPR-Cas systems in oral microbiome: From immune defense to physiological regulation. *Molecular Oral Microbiology* 2020;**35**:41–8.

Gonzalez-Perez B, Lucas M, Cooke LA *et al.* Analysis of DNA processing reactions in bacterial conjugation by using suicide oligonucleotides. *The EMBO Journal* 2007;**26**:3847–57.

Goossens H. Antibiotic consumption and link to resistance. *Clinical Microbiology and Infection* 2009;**15**:12–5.

Griffith F. The Significance of Pneumococcal Types. *J Hyg (Lond)* 1928;**27**:113–59.

Grohmann E, Muth G, Espinosa M. Conjugative Plasmid Transfer in Gram-Positive Bacteria. *Microbiology and Molecular Biology Reviews* 2003;**67**:277–301.

de Groot MJ, Bundock P, Hooykaas PJ *et al.* Agrobacterium tumefaciens-mediated transformation of filamentous fungi. *Nat Biotechnol* 1998;**16**:839–42.

Guasch A, Lucas M, Moncalián G *et al.* Recognition and processing of the origin of transfer DNA by conjugative relaxase TrwC. *Nature Structural & Molecular Biology* 2003;**10**:1002–10.

Gueguen E, Cascales E. Promoter swapping unveils the role of the Citrobacter rodentium CTS1 type VI secretion system in interbacterial competition. *Appl Environ Microbiol* 2013;**79**:32–8.

Guérout A-M, Iqbal N, Mine N *et al.* Characterization of the phd-doc and ccd toxin-antitoxin cassettes from Vibrio superintegrons. *J Bacteriol* 2013;**195**:2270–83.

Guiney DG, Fierer J. The Role of the spv Genes in Salmonella Pathogenesis. *Frontiers in Microbiology* 2011;**2**, DOI: 10.3389/fmicb.2011.00129.

Gullberg E, Albrecht LM, Karlsson C *et al.* Selection of a multidrug resistance plasmid by sublethal levels of antibiotics and heavy metals. *mBio* 2014;**5**:e01918-01914.

Gullberg E, Cao S, Berg OG *et al.* Selection of resistant bacteria at very low antibiotic concentrations. *PLoS Pathog* 2011;**7**:e1002158.

Gunton JE, Gilmour MW, Alonso G *et al.* Subcellular localization and functional domains of the coupling protein,

TraG, from IncHI1 plasmid R27. *Microbiology* 2005;**151**:3549–61.

Guo M, Ren K, Zhu Y *et al.* Structural insights into a high fidelity variant of SpCas9. *Cell Research* 2019;**29**:183–92.

Guyer MS, Reed RR, Steitz JA *et al.* Identification of a sex-factor-affinity site in E. coli as gamma delta. *Cold Spring Harb Symp Quant Biol* 1981;**45 Pt 1**:135–40.

Gyohda A, Furuya N, Kogure N *et al.* Sequence-specific and Non-specific Binding of the Rci Protein to the Asymmetric Recombination Sites of the R64 Shufflon. *Journal of Molecular Biology* 2002;**318**:975–83.

Haase J, Kalkum M, Lanka E. TrbK, a Small Cytoplasmic Membrane Lipoprotein, Functions in Entry Exclusion of the IncP␣ Plasmid RP4. *J BACTERIOL* 1996;**178**:10.

Haase J, Lurz R, Grahn AM *et al.* Bacterial conjugation mediated by plasmid RP4: RSF1010 mobilization, donor-specific phage propagation, and pilus production require the same Tra2 core components of a proposed DNA transport complex. *J Bacteriol* 1995;**177**:4779–91.

Hamilton TA, Pellegrino GM, Therrien JA *et al.* Efficient inter-species conjugative transfer of a CRISPR nuclease for targeted bacterial killing. *Nature Communications* 2019;**10**, DOI: 10.1038/s41467-019-12448-3.

Hanlon GW. Bacteriophages: an appraisal of their role in the treatment of bacterial infections. *International Journal of Antimicrobial Agents* 2007;**30**:118–28.

Harmer CJ, Hall RM. The A to Z of A/C plasmids. *Plasmid* 2015;**80**:63–82.

Harrington LC, Rogerson AC. The F pilus of Escherichia coli appears to support stable DNA transfer in the absence of wall-to-wall contact between cells. *Journal of Bacteriology* 1990;**172**:7263–4.

Harrison E, Brockhurst MA. Ecological and Evolutionary Benefits of Temperate Phage: What Does or Doesn't Kill You Makes You Stronger. *Bioessays* 2017;**39**, DOI: 10.1002/bies.201700112.

Hasman H, Aarestrup FM. tcrB, a gene conferring transferable copper resistance in Enterococcus faecium: occurrence, transferability, and linkage to macrolide and glycopeptide resistance. *Antimicrob Agents Chemother* 2002;**46**:1410–6.

Haugan K, Karunakaran P, Tøndervik A *et al.* The host range of RK2 minimal replicon copy-up mutants is limited by species-specific differences in the maximum tolerable copy number. *Plasmid* 1995;**33**:27–39.

Head CG, Tardy A, Kenney LJ. Relative binding affinities of OmpR and OmpR-phosphate at the ompF and ompC regulatory sites. *J Mol Biol* 1998;**281**:857–70.

Hedges RW. R factors from Providence. *J Gen Microbiol* 1974;**81**:171–81.

Hehemann J-H, Correc G, Barbeyron T *et al.* Transfer of carbohydrate-active enzymes from marine bacteria to Japanese gut microbiota. *Nature* 2010;**464**:908–12.

Heinemann JA, Sprague GF. Bacterial conjugative plasmids mobilize DNA transfer between bacteria and yeast. *Nature* 1989;**340**:205–9.

Heler R, Samai P, Modell JW *et al.* Cas9 specifies functional viral targets during CRISPR–Cas adaptation. *Nature* 2015;**519**:199–202.

Helmuth R, Achtman M. Operon structure of DNA transfer cistrons on the F sex factor. *Nature* 1975;**257**:652–6.

Hernández-Ramírez KC, Reyes-Gallegos RI, Chávez-Jacobo VM *et al.* A plasmid-encoded mobile genetic element from Pseudomonas aeruginosa that confers heavy metal resistance and virulence. *Plasmid* 2018;**98**:15–21.

Herring CD, Blattner FR. Global transcriptional effects of a suppressor tRNA and the inactivation of the regulator frmR. *J Bacteriol* 2004;**186**:6714–20.

Hille F, Richter H, Wong SP *et al.* The Biology of CRISPR-Cas: Backward and Forward. *Cell* 2018;**172**:1239–59.

Hiraga S. Dynamic localization of bacterial and plasmid chromosomes. *Annu Rev Genet* 2000;**34**:21–59.

Honda Y, Akioka T, Takebe S *et al.* Mutational analysis of the specific priming signal essential for DNA replication

of the broad host-range plasmid RSF1010. *FEBS Letters* 1993;**324**:67–70.

Hooper LV, Littman DR, Macpherson AJ. Interactions Between the Microbiota and the Immune System. *Science* 2012;**336**:1268–73.

Hormaeche I, Alkorta I, Moro F *et al.* Purification and Properties of TrwB, a Hexameric, ATP-binding Integral Membrane Protein Essential for R388 Plasmid Conjugation. *Journal of Biological Chemistry* 2002;**277**:46456–62.

Hormaeche I, Segura RL, Vecino AJ *et al.* The transmembrane domain provides nucleotide binding specificity to the bacterial conjugation protein TrwB. *FEBS Letters* 2006;**580**:3075–82.

Hospenthal MK, Costa TRD, Waksman G. A comprehensive guide to pilus biogenesis in Gram-negative bacteria. *Nature Reviews Microbiology* 2017;**15**:365–79.

Howland CJ, Rees CE, Barth PT *et al.* The ssb gene of plasmid ColIb-P9. *J Bacteriol* 1989;**171**:2466–73.

Hsu PD, Scott DA, Weinstein JA *et al.* DNA targeting specificity of RNA-guided Cas9 nucleases. *Nat Biotechnol* 2013;**31**:827–32.

Hu B, Khara P, Christie PJ. Structural bases for F plasmid conjugation and F pilus biogenesis in *Escherichia coli*. *Proceedings of the National Academy of Sciences* 2019;**116**:14222–7.

Hu JH, Miller SM, Geurts MH *et al.* Evolved Cas9 variants with broad PAM compatibility and high DNA specificity. *Nature* 2018;**556**:57–63.

Humbert M, Huguet KT, Coulombe F *et al.* Entry Exclusion of Conjugative Plasmids of the IncA, IncC, and Related Untyped Incompatibility Groups. O'Toole G (ed.). *Journal of Bacteriology* 2019;**201**, DOI: 10.1128/JB.00731-18.

Hutchings MI, Truman AW, Wilkinson B. Antibiotics: past, present and future. *Current Opinion in Microbiology* 2019;**51**:72–80.

Ilangovan A, Connery S, Waksman G. Structural biology of the Gram-negative bacterial conjugation systems. *Trends in Microbiology* 2015;**23**:301–10.

Ilangovan A, Kay CWM, Roier S *et al.* Cryo-EM Structure of a Relaxase Reveals the Molecular Basis of DNA Unwinding during Bacterial Conjugation. *Cell* 2017;**169**:708–721.e12.

Ishiai M, Wada C, Kawasaki Y *et al.* Replication initiator protein RepE of mini-F plasmid: functional differentiation between monomers (initiator) and dimers (autogenous repressor). *Proceedings of the National Academy of Sciences* 1994;**91**:3839–43.

Ishino Y, Shinagawa H, Makino K *et al.* Nucleotide sequence of the iap gene, responsible for alkaline phosphatase isozyme conversion in Escherichia coli, and identification of the gene product. *Journal of Bacteriology* 1987;**169**:5429–33.

Ishiwa A, Komano T. The lipopolysaccharide of recipient cells is a specific receptor for PilV proteins, selected by shufflon DNA rearrangement, in liquid matings with donors bearing the R64 plasmid. *Mol Gen Genet* 2000;**263**:159–64.

Itoh Y, Wang X, Hinnebusch BJ *et al.* Depolymerization of beta-1,6-N-acetyl-D-glucosamine disrupts the integrity of diverse bacterial biofilms. *J Bacteriol* 2005;**187**:382–7.

Jajere SM. A review of Salmonella enterica with particular focus on the pathogenicity and virulence factors, host specificity and antimicrobial resistance including multidrug resistance. *Vet World* 2019;**12**:504–21.

Jakubowski SJ, Krishnamoorthy V, Cascales E *et al.* Agrobacterium tumefaciens VirB6 Domains Direct the Ordered Export of a DNA Substrate Through a Type IV Secretion System. *Journal of Molecular Biology* 2004;**341**:961–77.

Jansen R, Embden JDA van, Gaastra W *et al.* Identification of genes that are associated with DNA repeats in prokaryotes. *Molecular Microbiology* 2002;**43**:1565–75.

Jerome LJ, van Biesen T, Frost LS. Degradation of FinP antisense RNA from F-like plasmids: the RNA-binding protein, FinO, protects FinP from ribonuclease E. *J Mol Biol* 1999;**285**:1457–73.

Ji W, Lee D, Wong E *et al.* Specific Gene Repression by CRISPRi System Transferred through Bacterial Conjugation.

ACS Synthetic Biology 2014;**3**:929–31.

Jiang F, Taylor DW, Chen JS *et al.* Structures of a CRISPR-Cas9 R-loop complex primed for DNA cleavage. *Science* 2016;**351**:867–71.

Jinek M, Chylinski K, Fonfara I *et al.* A Programmable Dual-RNA-Guided DNA Endonuclease in Adaptive Bacterial Immunity. *Science* 2012;**337**:816–21.

João J, Lampreia J, Prazeres DMF *et al.* Manufacturing of bacteriophages for therapeutic applications. *Biotechnology Advances* 2021;**49**:107758.

Jones AL, Barth PT, Wilkins BM. Zygotic induction of plasmid ssb and psiB genes following conjugative transfer of Incl1 plasmid Collb-P9. *Molecular Microbiology* 1992;**6**:605–13.

Jones BV, Sun F, Marchesi JR. Comparative metagenomic analysis of plasmid encoded functions in the human gut microbiome. *BMC Genomics* 2010;**11**:46.

Jones DL, Leroy P, Unoson C *et al.* Kinetics of dCas9 target search in *Escherichia coli*. *Science* 2017;**357**:1420–4.

Kado CI. Agrobacterium-Mediated Horizontal Gene Transfer. In: Setlow JK (ed.). *Genetic Engineering*. Boston, MA: Springer US, 1998, 1–24.

Kalkum M. Tying rings for sex. *Trends in Microbiology* 2002;**10**:382–7.

Kang YK, Kwon K, Ryu JS *et al.* Nonviral Genome Editing Based on a Polymer-Derivatized CRISPR Nanocomplex for Targeting Bacterial Pathogens and Antibiotic Resistance. *Bioconjugate Chemistry* 2017;**28**:957–67.

Kav AB, Sasson G, Jami E *et al.* Insights into the bovine rumen plasmidome. *Proceedings of the National Academy of Sciences* 2012;**109**:5452–7.

Kholodii G, Mindlin S, Petrova M *et al.* Tn *5060* from the Siberian permafrost is most closely related to the ancestor of Tn *21* prior to integron acquisition. *FEMS Microbiology Letters* 2003;**226**:251–5.

Kiga K, Tan X-E, Ibarra-Chávez R *et al.* Development of CRISPR-Cas13a-based antimicrobials capable of sequence-specific killing of target bacteria. *Nature Communications* 2020;**11**, DOI: 10.1038/s41467-020-16731-6.

Kingsman A, Willetts N. The requirements for conjugal DNA synthesis in the donor strain during flac transfer. *J Mol Biol* 1978;**122**:287–300.

Klee H, Montoya A, Horodyski F *et al.* Nucleotide sequence of the tms genes of the pTiA6NC octopine Ti plasmid: two gene products involved in plant tumorigenesis. *Proceedings of the National Academy of Sciences* 1984;**81**:1728–32.

Kleinstiver BP, Pattanayak V, Prew MS *et al.* High-fidelity CRISPR–Cas9 nucleases with no detectable genome-wide off-target effects. *Nature* 2016;**529**:490–5.

Klimke WA, Rypien CD, Klinger B *et al.* The mating pair stabilization protein, TraN, of the F plasmid is an outer-membrane protein with two regions that are important for its function in conjugation. *Microbiology* 2005;**151**:3527–40.

Kohler V, Keller W, Grohmann E. Regulation of Gram-Positive Conjugation. *Frontiers in Microbiology* 2019;**10**, DOI: 10.3389/fmicb.2019.01134.

Komano T. Shufflons: Multiple Inversion Systems and Integrons. *Annual Review of Genetics* 1999;**33**:171–91.

Komano T, Kim S-R, Nisioka T. Transfer Region of Incll Plasmid R64 and Role of Shufflon in R64 Transfer. *J BACTERIOL* 1990;**172**:6.

Kong H-K, Pan Q, Lo W-U *et al.* Fine-tuning carbapenem resistance by reducing porin permeability of bacteria activated in the selection process of conjugation. *Sci Rep* 2018;**8**:15248.

Konieczny I, Bury K, Wawrzycka A *et al.* Iteron Plasmids. *Microbiol Spectr* 2014;**2**, DOI: 10.1128/microbiolspec.PLAS-0026-2014.

Koraimann G, Teferle K, Markolin G *et al.* The FinOP repressor system of plasmid R1: analysis of the antisense RNA control of traJ expression and conjugative DNA transfer. *Mol Microbiol* 1996;**21**:811–21.

Kubik S, Wegrzyn K, Pierechod M *et al.* Opposing effects of DNA on proteolysis of a replication initiator. *Nucleic Acids Research* 2012;**40**:1148–59.

Kumar RB, Das A. Polar location and functional domains of the Agrobacterium tumefaciens DNA transfer protein VirD4. *Mol Microbiol* 2002;**43**:1523–32.

Kunik T, Tzfira T, Kapulnik Y *et al.* Genetic transformation of HeLa cells by Agrobacterium. *Proc Natl Acad Sci U S A* 2001;**98**:1871–6.

Kutter E, De Vos D, Gvasalia G *et al.* Phage therapy in clinical practice: treatment of human infections. *Curr Pharm Biotechnol* 2010;**11**:69–86.

Lagares A, Sanjuán J, Pistorio M. The Plasmid Mobilome of the Model Plant-Symbiont Sinorhizobium meliloti: Coming up with New Questions and Answers. :14.

Lang S, Zechner EL. General requirements for protein secretion by the F-like conjugation system R1. *Plasmid* 2012;**67**:128–38.

Laskaris P, Tolba S, Calvo-Bado L *et al.* Coevolution of antibiotic production and counter-resistance in soil bacteria. *Environmental Microbiology* 2010;**12**:783–96.

Lawley T., Klimke W., Gubbins M. *et al.* F factor conjugation is a true type IV secretion system. *FEMS Microbiology Letters* 2003;**224**:1–15.

Lawley TD, Taylor DE. Characterization of the double-partitioning modules of R27: correlating plasmid stability with plasmid localization. *J Bacteriol* 2003;**185**:3060–7.

Lawrence JG, Ochman H. Molecular archaeology of the *Escherichia coli* genome. *Proceedings of the National Academy of Sciences* 1998;**95**:9413–7.

Le Rhun A, Escalera-Maurer A, Bratovič M *et al.* CRISPR-Cas in *Streptococcus pyogenes*. *RNA Biology* 2019;**16**:380–9.

Leatham MP, Banerjee S, Autieri SM *et al.* Precolonized human commensal Escherichia coli strains serve as a barrier to E. coli O157:H7 growth in the streptomycin-treated mouse intestine. *Infect Immun* 2009;**77**:2876–86.

Lederberg J, Tatum EL. Gene recombination in Escherichia coli. *Nature* 1946;**158**:558.

Lederberg J, Tatum EL. Sex in Bacteria: Genetic Studies, 1945-1952. *Science* 1953;**118**:169–75.

Lee K-H, Lee S-G, Eun Lee K *et al.* Identification, structural, and biochemical characterization of a group of large Csn2 proteins involved in CRISPR-mediated bacterial immunity. *Proteins* 2012;**80**:2573–82.

Lee L-Y, Gelvin SB. Osa Protein Constitutes a Strong Oncogenic Suppression System That Can Block *vir* -Dependent Transfer of IncQ Plasmids between *Agrobacterium* Cells and the Establishment of IncQ Plasmids in Plant Cells. *Journal of Bacteriology* 2004;**186**:7254–61.

Lesterlin C, Ball G, Schermelleh L *et al.* RecA bundles mediate homology pairing between distant sisters during DNA break repair. *Nature* 2014;**506**:249–53.

Liebert CA, Hall RM, Summers AO. Transposon Tn *21* , Flagship of the Floating Genome. *Microbiology and Molecular Biology Reviews* 1999;**63**:507–22.

Lilley AK, Fry JC, Day MJ *et al.* In situ transfer of an exogenously isolated plasmid between Pseudornonas spp. in sugar beet rhizosphere. 1994:7.

Lilly J, Camps M. Mechanisms of Theta Plasmid Replication. 2015:18.

Lindsay JA, Ruzin A, Ross HF *et al.* The gene for toxic shock toxin is carried by a family of mobile pathogenicity islands in *Staphylococcus aureus*. *Molecular Microbiology* 1998;**29**:527–43.

Lindström K, Mousavi SA. Effectiveness of nitrogen fixation in rhizobia. *Microbial Biotechnology* 2020;**13**:1314–35.

Ling J, Wang H, Wu P *et al.* Plant nodulation inducers enhance horizontal gene transfer of *Azorhizobium caulinodans* symbiosis island. *Proceedings of the National Academy of Sciences* 2016;**113**:13875–80.

Llosa M, Alkorta I. Coupling Proteins in Type IV Secretion. In: Backert S, Grohmann E (eds.). *Type IV Secretion in Gram-Negative and Gram-Positive Bacteria*. Vol 413. Cham: Springer International Publishing, 2017, 143–68.

Llosa M, Zunzunegui S, de la Cruz F. Conjugative coupling proteins interact with cognate and heterologous VirB10-like proteins while exhibiting specificity for cognate relaxosomes. *Proceedings of the National Academy of Sciences* 2003;**100**:10465–70.

Łobocka M, Dąbrowska K, Górski A. Engineered Bacteriophage Therapeutics: Rationale, Challenges and Future. *BioDrugs* 2021;**35**:255–80.

Loh S, Cram D, Skurray R. Nucleotide sequence of the leading region adjacent to the origin of transfer on plasmid F and its conservation among conjugative plasmids. *Molecular and General Genetics MGG* 1989;**219**:177–86.

Loper JE, Hassan KA, Mavrodi DV *et al.* Comparative Genomics of Plant-Associated Pseudomonas spp.: Insights into Diversity and Inheritance of Traits Involved in Multitrophic Interactions. Guttman DS (ed.). *PLoS Genetics* 2012;**8**:e1002784.

López-Igual R, Bernal-Bayard J, Rodríguez-Patón A *et al.* Engineered toxin–intein antimicrobials can selectively target and kill antibiotic-resistant bacteria in mixed populations. *Nature Biotechnology* 2019;**37**:755–60.

Lou H, Chen M, Black SS *et al.* Altered antibiotic transport in OmpC mutants isolated from a series of clinical strains of multi-drug resistant E. coli. *PLoS One* 2011;**6**:e25825.

Low HH, Gubellini F, Rivera-Calzada A *et al.* Structure of a type IV secretion system. *Nature* 2014;**508**:550–3.

Lu J, Frost LS. Mutations in the C-terminal region of TraM provide evidence for in vivo TraM-TraD interactions during F-plasmid conjugation. *J Bacteriol* 2005;**187**:4767–73.

Lu J, Wong JJW, Edwards RA *et al.* Structural basis of specific TraD-TraM recognition during F plasmid-mediated bacterial conjugation: Specific interactions between F plasmid TraD and TraM. *Molecular Microbiology* 2008;**70**:89–99.

Lu TK, Collins JJ. Dispersing biofilms with engineered enzymatic bacteriophage. *Proceedings of the National Academy of Sciences* 2007;**104**:11197–202.

Lucas M, González-Pérez B, Cabezas M *et al.* Relaxase DNA Binding and Cleavage Are Two Distinguishable Steps in Conjugative DNA Processing That Involve Different Sequence Elements of the nic Site. *Journal of Biological Chemistry* 2010;**285**:8918–26.

Maindola P, Raina R, Goyal P *et al.* Multiple enzymatic activities of ParB/Srx superfamily mediate sexual conflict among conjugative plasmids. *Nature Communications* 2014;**5**, DOI: 10.1038/ncomms6322.

Mąka Ł, Popowska M. Antimicrobial resistance of Salmonella spp. isolated from food. *Rocz Panstw Zakl Hig* 2016;**67**:343–58.

Makarova KS, Wolf YI, Iranzo J *et al.* Evolutionary classification of CRISPR–Cas systems: a burst of class 2 and derived variants. *Nature Reviews Microbiology* 2020;**18**:67–83.

Makino K, Yokoyama K, Kubota Y *et al.* Complete nucleotide sequence of the prophage VT2-Sakai carrying the verotoxin 2 genes of the enterohemorrhagic Escherichia coli O157:H7 derived from the Sakai outbreak. *Genes & Genetic Systems* 1999;**74**:227–39.

Marino ND, Pinilla-Redondo R, Csörgő B *et al.* Anti-CRISPR protein applications: natural brakes for CRISPR-Cas technologies. *Nature Methods* 2020;**17**:471–9.

Marraffini LA, Sontheimer EJ. CRISPR Interference Limits Horizontal Gene Transfer in Staphylococci by Targeting DNA. *Science* 2008;**322**:1843–5.

Masai H, Arai K. Frpo: A Novel Single-Stranded DNA Promoter for Transcription and for Primer RNA Synthesis of DNA Replication. *Cell* 1997;**89**:897–907.

Matic I, Rayssiguier C, Radman M. Interspecies gene exchange in bacteria: the role of SOS and mismatch repair systems in evolution of species. *Cell* 1995;**80**:507–15.

McHenry CS. DNA Replicases from a Bacterial Perspective. *Annual Review of Biochemistry* 2011;**80**:403–36.

McMahon SA, Roberts GA, Johnson KA *et al.* Extensive DNA mimicry by the ArdA anti-restriction protein and its role in the spread of antibiotic resistance. *Nucleic Acids Research* 2009;**37**:4887–97.

Meeske AJ, Nakandakari-Higa S, Marraffini LA. Cas13-induced cellular dormancy prevents the rise of CRISPR-resistant bacteriophage. *Nature* 2019;**570**:241–5.

Men C, Liu R, Wang Q *et al.* The impact of seasonal varied human activity on characteristics and sources of heavy metals in metropolitan road dusts. *Science of The Total Environment* 2018;**637**–**638**:844–54.

Merryweather A, Barth PT, Wilkins BM. Role and specificity of plasmid RP4-encoded DNA primase in bacterial conjugation. *Journal of Bacteriology* 1986;**167**:12–7.

Merryweather A, Rees CE, Smith NM *et al.* Role of sog polypeptides specified by plasmid ColIb-P9 and their transfer between conjugating bacteria. *The EMBO Journal* 1986;**5**:3007–12.

Miao D-M, Honda Y, Tanaka K *et al.* A base-paired hairpin structure essential for the functional priming signal for DNA replication of the broad host range plasmid RSF1010. *Nucleic Acids Research* 1993;**21**:4900–3.

Mierzejewska J, Jagura-Burdzy G. Prokaryotic ParA-ParB-parS system links bacterial chromosome segregation with the cell cycle. *Plasmid* 2012;**67**:1–14.

Miller JF, Lanka E, Malamy MH. F factor inhibition of conjugal transfer of broad-host-range plasmid RP4: requirement for the protein product of pif operon regulatory gene pifC. *Journal of Bacteriology* 1985;**163**:1067–73.

Mojica FJM, Díez-Villaseñor C, García-Martínez J *et al.* Short motif sequences determine the targets of the prokaryotic CRISPR defence system. *Microbiology* 2009;**155**:733–40.

Mojica FJM, Juez G, Rodriguez-Valera F. Transcription at different salinities of Haloferax mediterranei sequences adjacent to partially modified PstI sites. *Molecular Microbiology* 1993;**9**:613–21.

Moncalián G, Cabezón E, Alkorta I *et al.* Characterization of ATP and DNA Binding Activities of TrwB, the Coupling Protein Essential in Plasmid R388 Conjugation. *Journal of Biological Chemistry* 1999;**274**:36117–24.

Moreb EA, Hoover B, Yaseen A *et al.* Managing the SOS Response for Enhanced CRISPR-Cas-Based Recombineering in *E. coli* through Transient Inhibition of Host RecA Activity. *ACS Synthetic Biology* 2017;**6**:2209–18.

Moriguchi K, Zoolkefli FIRM, Abe M *et al.* Targeting Antibiotic Resistance Genes Is a Better Approach to Block Acquisition of Antibiotic Resistance Than Blocking Conjugal Transfer by Recipient Cells: A Genome-Wide Screening in Escherichia coli. *Frontiers in Microbiology* 2020;**10**, DOI: 10.3389/fmicb.2019.02939.

Munck C, Sheth RU, Freedberg DE *et al.* Recording mobile DNA in the gut microbiota using an Escherichia coli CRISPR-Cas spacer acquisition platform. *Nature Communications* 2020;**11**, DOI: 10.1038/s41467-019-14012-5.

Nakamura A, Wada C, Miki K. Structural basis for regulation of bifunctional roles in replication initiator protein. *Proceedings of the National Academy of Sciences* 2007;**104**:18484–9.

Nakata A, Amemura M, Makino K. Unusual nucleotide arrangement with repeated sequences in the Escherichia coli K-12 chromosome. *Journal of Bacteriology* 1989;**171**:3553–6.

Neil K, Allard N, Grenier F *et al.* Highly efficient gene transfer in the mouse gut microbiota is enabled by the Incl2 conjugative plasmid TP114. *Communications Biology* 2020;**3**, DOI: 10.1038/s42003-020-01253-0.

Neil K, Allard N, Rodrigue S. Molecular Mechanisms Influencing Bacterial Conjugation in the Intestinal Microbiota. *Frontiers in Microbiology* 2021;**12**, DOI: 10.3389/fmicb.2021.673260.

Newire E, Aydin A, Juma S *et al.* Identification of a Type IV-A CRISPR-Cas System Located Exclusively on IncHI1B/IncFIB Plasmids in Enterobacteriaceae. *Frontiers in Microbiology* 2020;**11**, DOI: 10.3389/fmicb.2020.01937.

Newsom S, Parameshwaran HP, Martin L *et al.* The CRISPR-Cas Mechanism for Adaptive Immunity and Alternate Bacterial Functions Fuels Diverse Biotechnologies. *Frontiers in Cellular and Infection Microbiology* 2021;**10**, DOI: 10.3389/fcimb.2020.619763.

Nguyen F, Starosta AL, Arenz S *et al.* Tetracycline antibiotics and resistance mechanisms. *Biological Chemistry* 2014;**395**:559–75.

Nicholson FA, Smith SR, Alloway BJ *et al.* An inventory of heavy metals inputs to agricultural soils in England and Wales. *Science of The Total Environment* 2003;**311**:205–19.

Nikaido H. Multidrug efflux pumps of gram-negative bacteria. *J Bacteriol* 1996;**178**:5853–9.

Nishimasu H, Ran FA, Hsu PD *et al.* Crystal Structure of Cas9 in Complex with Guide RNA and Target DNA. *Cell* 2014;**156**:935–49.

Nolivos S, Cayron J, Dedieu A *et al.* Role of AcrAB-TolC multidrug efflux pump in drug-resistance acquisition by plasmid transfer. *Science* 2019;**364**:778–82.

Nöllmann M, Crisona NJ, Arimondo PB. Thirty years of Escherichia coli DNA gyrase: from in vivo function to single-molecule mechanism. *Biochimie* 2007;**89**:490–9.

Nomura N, Masai H, Inuzuka M *et al.* Identification of eleven single-strand initiation sequences (ssi) for priming of DNA replication in the F, R6K, R100 and ColE2 plasmids. *Gene* 1991;**108**:15–22.

Nordström K, Molin S, Aagaard-Hansen H. Partitioning of plasmid R1 in Escherichia coli,: I. Kinetics of loss of plasmid derivatives deleted of the par region. *Plasmid* 1980;**4**:215–27.

Normander B, Christensen BB, Molin S *et al.* Effect of Bacterial Distribution and Activity on Conjugal Gene Transfer on the Phylloplane of the Bush Bean (*Phaseolus vulgaris*). *Applied and Environmental Microbiology* 1998;**64**:1902–9.

Novick RP, Hoppensteadt FC. On plasmid incompatibility. *Plasmid* 1978;**1**:421–34.

Novotny CP, Fives-Taylor P. Retraction of F Pili. *Journal of Bacteriology* 1974;**117**:1306–11.

O'Neill J. Tackling a crisis for the health and wealth of nations. 2014.

Ogura T, Hiraga S. Mini-F plasmid genes that couple host cell division to plasmid proliferation. *Proc Natl Acad Sci U S A* 1983;**80**:4784–8.

Oliveira PH, Touchon M, Rocha EPC. The interplay of restriction-modification systems with mobile genetic elements and their prokaryotic hosts. *Nucleic Acids Research* 2014;**42**:10618–31.

Olsen RH, Shipley PL. RP1 properties and fertility inhibition among P, N, W, and X incompatibility group plasmids. *Journal of Bacteriology* 1975;**123**:28–35.

O'Meara D, Nunney L. A phylogenetic test of the role of CRISPR-Cas in limiting plasmid acquisition and prophage integration in bacteria. *Plasmid* 2019;**104**:102418.

Ong C-LY, Beatson SA, McEwan AG *et al.* Conjugative plasmid transfer and adhesion dynamics in an Escherichia coli biofilm. *Appl Environ Microbiol* 2009;**75**:6783–91.

van Opijnen T, Bodi KL, Camilli A. Tn-seq: high-throughput parallel sequencing for fitness and genetic interaction studies in microorganisms. *Nat Methods* 2009;**6**:767–72.

Pal C, Bengtsson-Palme J, Kristiansson E *et al.* Co-occurrence of resistance genes to antibiotics, biocides and metals reveals novel insights into their co-selection potential. *BMC Genomics* 2015;**16**, DOI: 10.1186/s12864-015-2153-5.

Palermo G, Miao Y, Walker RC *et al.* Striking Plasticity of CRISPR-Cas9 and Key Role of Non-target DNA, as Revealed by Molecular Simulations. *ACS Central Science* 2016;**2**:756–63.

Pansegrau W, Lanka E. Enzymology of DNA transfer by conjugative mechanisms. *Prog Nucleic Acid Res Mol Biol* 1996;**54**:197–251.

Park J, Kim J-S, Bae S. Cas-Database: web-based genome-wide guide RNA library design for gene knockout screens using CRISPR-Cas9. *Bioinformatics* 2016;**32**:2017–23.

Park JY, Moon BY, Park JW *et al.* Genetic engineering of a temperate phage-based delivery system for CRISPR/Cas9 antimicrobials against Staphylococcus aureus. *Scientific Reports* 2017;**7**, DOI: 10.1038/srep44929.

Parsons JA, Bannam TL, Devenish RJ *et al.* TcpA, an FtsK/SpoIIIE Homolog, Is Essential for Transfer of the Conjugative Plasmid pCW3 in *Clostridium perfringens*. *Journal of Bacteriology* 2007;**189**:7782–90.

Pédelacq J-D, Cabantous S, Tran T *et al.* Engineering and characterization of a superfolder green fluorescent protein. *Nat Biotechnol* 2006;**24**:79–88.

Pei R, Lamas-Samanamud GR. Inhibition of biofilm formation by T7 bacteriophages producing quorum-quenching enzymes. *Appl Environ Microbiol* 2014;**80**:5340–8.

Peng Y, Rakowski SA, Filutowicz M. Small deletion variants of the replication protein, π, and their potential for over-replication-based antimicrobial activity. *FEMS Microbiology Letters* 2006;**261**:245–52.

Pérez-Mendoza D, de la Cruz F. Escherichia coli genes affecting recipient ability in plasmid conjugation: Are there any? *BMC Genomics* 2009;**10**:71.

Peters JE, Makarova KS, Shmakov S *et al.* Recruitment of CRISPR-Cas systems by Tn7-like transposons. *Proc Natl Acad Sci U S A* 2017;**114**:E7358–66.

Petrova V, Chitteni-Pattu S, Drees JC *et al.* An SOS Inhibitor that Binds to Free RecA Protein: The PsiB Protein. *Molecular Cell* 2009;**36**:121–30.

Pinilla-Redondo R, Mayo-Muñoz D, Russel J *et al.* Type IV CRISPR–Cas systems are highly diverse and involved in competition between plasmids. *Nucleic Acids Research* 2020a;**48**:2000–12.

Pinilla-Redondo R, Russel J, Mayo-Muñoz D *et al.* CRISPR-Cas systems are widespread accessory elements across bacterial and archaeal plasmids. *Nucleic Acids Res* 2021:gkab859.

Pinilla-Redondo R, Shehreen S, Marino ND *et al.* Discovery of multiple anti-CRISPRs highlights anti-defense gene clustering in mobile genetic elements. *Nat Commun* 2020b;**11**:5652.

Pinney RJ, Smith JT. Fertility inhibition of an N group R factor by a group X R factor, R6K. *J Gen Microbiol* 1974;**82**:415–8.

Pluta R, Boer DR, Lorenzo-Díaz F *et al.* Structural basis of a histidine-DNA nicking/joining mechanism for gene transfer and promiscuous spread of antibiotic resistance. *Proceedings of the National Academy of Sciences* 2017;**114**:E6526–35.

Ponticelli AS, Schultz DW, Taylor AF *et al.* Chi-dependent DNA strand cleavage by RecBC enzyme. *Cell* 1985;**41**:145–51.

Portes AB, Rodrigues G, Leitão MP *et al.* Global distribution of plasmid-mediated colistin resistance mcr gene in Salmonella: A systematic review. *J Appl Microbiol* 2021, DOI: 10.1111/jam.15282.

Pósfai G, Plunkett G, Fehér T *et al.* Emergent properties of reduced-genome Escherichia coli. *Science* 2006;**312**:1044–6.

Potron A, Poirel L, Nordmann P. Derepressed transfer properties leading to the efficient spread of the plasmid encoding carbapenemase OXA-48. *Antimicrob Agents Chemother* 2014;**58**:467–71.

Prensky H, Gomez-Simmonds A, Uhlemann A *et al.* Conjugation dynamics depend on both the plasmid acquisition cost and the fitness cost. *Molecular Systems Biology* 2021;**17**, DOI: 10.15252/msb.20209913.

Pui CF, Wong WC, Chai LC *et al.* Salmonella: A foodborne pathogen. *International Food Research Journal* 2011:465–73.

Qi LS, Larson MH, Gilbert LA *et al.* Repurposing CRISPR as an RNA-Guided Platform for Sequence-Specific Control of Gene Expression. *Cell* 2013;**152**:1173–83.

Qin J, Li Y, Cai Z *et al.* A metagenome-wide association study of gut microbiota in type 2 diabetes. *Nature* 2012;**490**:55–60.

Qu J, Prasad NK, Yu MA *et al.* Modulating Pathogenesis with Mobile-CRISPRi. *Journal of Bacteriology* 2019;**201**:9.

Ragonese H, Haisch D, Villareal E *et al.* The F plasmid-encoded TraM protein stimulates relaxosome-mediated cleavage at *oriT* through an interaction with TraI. *Molecular Microbiology* 2007;**63**:1173–84.

Ram G, Ross HF, Novick RP *et al.* Conversion of staphylococcal pathogenicity islands to CRISPR-carrying antibacterial agents that cure infections in mice. *Nature Biotechnology* 2018;**36**:971–6.

Randall-Hazelbauer L, Schwartz M. Isolation of the bacteriophage lambda receptor from Escherichia coli. *J Bacteriol* 1973;**116**:1436–46.

Rang CU, Kennan RM, Midtvedt T *et al.* Transfer of the plasmid RP1 in vivo in germ free mice and in vitro in gut extracts and laboratory media. *FEMS Microbiology Ecology* 1996;**19**:133–40.

Rasched I, Oberer E. Ff coliphages: structural and functional relationships. *Microbiol Rev* 1986;**50**:401–27.

Rawlings DE, Tietze E. Comparative Biology of IncQ and IncQ-Like Plasmids. *Microbiology and Molecular Biology Reviews* 2001;**65**:481–96.

Redmond JW, Batley M, Djordjevic MA *et al.* Flavones induce expression of nodulation genes in Rhizobium. *Nature* 1986;**323**:632–5.

Redzej A, Ukleja M, Connery S *et al.* Structure of a VirD4 coupling protein bound to a VirB type IV secretion machinery. *The EMBO Journal* 2017;**36**:3080–95.

Reece RJ, Maxwell A. DNA gyrase: structure and function. *Crit Rev Biochem Mol Biol* 1991;**26**:335–75.

Reisner A, Haagensen JAJ, Schembri MA *et al.* Development and maturation of Escherichia coli K-12 biofilms: IncF plasmid promoted E. coli biofilm maturation. *Molecular Microbiology* 2003;**48**:933–46.

Research C for BE and. Complementary and Alternative Medicine Products and their Regulation by the Food and Drug Administration. *US Food and Drug Administration* 2020.

Reuter A, Hilpert C, Dedieu-Berne A *et al.* Targeted-antibacterial-plasmids (TAPs) combining conjugation and CRISPR/Cas systems achieve strain-specific antibacterial activity. *Nucleic Acids Research* 2021, DOI: 10.1093/nar/gkab126.

Rice LB. Federal Funding for the Study of Antimicrobial Resistance in Nosocomial Pathogens: No ESKAPE. *The Journal of Infectious Diseases* 2008;**197**:1079–81.

Riede I, Eschbach ML. Evidence that TraT interacts with OmpA of Escherichia coli. *FEBS Lett* 1986;**205**:241–5.

Rivera-Urbalejo A, Pérez-Oseguera Á, Carreón-Rodríguez OE *et al.* Mutations in an antisense RNA, involved in the replication control of a repABC plasmid, that disrupt plasmid incompatibility and mediate plasmid speciation. *Plasmid* 2015;**78**:48–58.

Rock JM, Hopkins FF, Chavez A *et al.* Programmable transcriptional repression in mycobacteria using an orthogonal CRISPR interference platform. *Nat Microbiol* 2017;**2**:16274.

Rodrigues M, McBride SW, Hullahalli K *et al.* Conjugative Delivery of CRISPR-Cas9 for the Selective Depletion of Antibiotic-Resistant Enterococci. *Antimicrobial Agents and Chemotherapy* 2019;**63**, DOI: 10.1128/AAC.01454-19.

Rodríguez JM, Murphy K, Stanton C *et al.* The composition of the gut microbiota throughout life, with an emphasis on early life. *Microb Ecol Health Dis* 2015;**26**:26050.

Ronda C, Chen SP, Cabral V *et al.* Metagenomic engineering of the mammalian gut microbiome in situ. *Nat Methods* 2019;**16**:167–70.

Rozwandowicz M, Brouwer MSM, Fischer J *et al.* Plasmids carrying antimicrobial resistance genes in Enterobacteriaceae. *Journal of Antimicrobial Chemotherapy* 2018;**73**:1121–37.

Ruiz-Masó JA, MachóN C, Bordanaba-Ruiseco L *et al.* Plasmid Rolling-Circle Replication. *Microbiol Spectr* 2015;**3**:PLAS-0035-2014.

Ruotsalainen P, Penttinen R, Mattila S *et al.* Midbiotics: conjugative plasmids for genetic engineering of natural gut flora. *Gut Microbes* 2019;**10**:643–53.

Ruzin A, Lindsay J, Novick RP. Molecular genetics of SaPI1--a mobile pathogenicity island in Staphylococcus aureus. *Mol Microbiol* 2001;**41**:365–77.

Safari Sinegani AA, Younessi N. Antibiotic resistance of bacteria isolated from heavy metal-polluted soils with

different land uses. *Journal of Global Antimicrobial Resistance* 2017;**10**:247–55.

Salmonella Homepage | CDC. 2021.

Sampei G, Furuya N, Tachibana K *et al.* Complete genome sequence of the incompatibility group I1 plasmid R64. *Plasmid* 2010;**64**:92–103.

Samuels AL, Lanka E, Davies JE. Conjugative Junctions in RP4-Mediated Mating of *Escherichia coli*. *Journal of Bacteriology* 2000;**182**:2709–15.

Santini JM, Stanisich VA. Both the *fipA* Gene of pKM101 and the *pifC* Gene of F Inhibit Conjugal Transfer of RP1 by an Effect on *traG*. *Journal of Bacteriology* 1998;**180**:4093–101.

Saraswati S, Sitaraman R. Aging and the human gut microbiota-from correlation to causality. *Front Microbiol* 2014;**5**:764.

van Schaik W. The human gut resistome. *Philosophical Transactions of the Royal Society B: Biological Sciences* 2015;**370**:20140087.

Schröder G, Krause S, Zechner EL *et al.* TraG-Like Proteins of DNA Transfer Systems and of the *Helicobacter pylori* Type IV Secretion System: Inner Membrane Gate for Exported Substrates? *Journal of Bacteriology* 2002;**184**:2767–79.

Schröder G, Lanka E. TraG-Like Proteins of Type IV Secretion Systems: Functional Dissection of the Multiple Activities of TraG (RP4) and TrwB (R388). *Journal of Bacteriology* 2003;**185**:4371–81.

Scott JR. Regulation of plasmid replication. *Microbiol Rev* 1984;**48**:1–23.

Segura RL, Águila-Arcos S, Ugarte-Uribe B *et al.* Subcellular location of the coupling protein TrwB and the role of its transmembrane domain. *Biochimica et Biophysica Acta (BBA) - Biomembranes* 2014;**1838**:223–30.

Sekirov I, Russell SL, Antunes LCM *et al.* Gut Microbiota in Health and Disease. *Physiol Rev* 2010;**90**:46.

Selle K, Fletcher JR, Tuson H *et al. In Vivo* Targeting of Clostridioides difficile Using Phage-Delivered CRISPR-Cas3 Antimicrobials. Ballard JD (ed.). *mBio* 2020;**11**, DOI: 10.1128/mBio.00019-20.

Semenova E, Jore MM, Datsenko KA *et al.* Interference by clustered regularly interspaced short palindromic repeat (CRISPR) RNA is governed by a seed sequence. *Proceedings of the National Academy of Sciences* 2011;**108**:10098–103.

Shankar R, He L-K, Szilagyi A *et al.* A Novel Antibacterial Gene Transfer Treatment for Multidrug-Resistant Acinetobacter Baumannii-Induced Burn Sepsis: *Journal of Burn Care & Research* 2007;**28**:6–12.

Sharples GJ, Benson FE, Illing GT *et al.* Molecular and functional analysis of the ruv region of Escherichia coli K-12 reveals three genes involved in DNA repair and recombination. *Mol Gen Genet* 1990;**221**:219–26.

Shingler V, Thomas CM. Analysis of the trfA region of broad host-range plasmid RK2 by transposon mutagenesis and identification of polypeptide products. *Journal of Molecular Biology* 1984;**175**:229–49.

Shintani M, Sanchez ZK, Kimbara K. Genomics of microbial plasmids: classification and identification based on replication and transfer systems and host taxonomy. *Front Microbiol* 2015;**6**:242.

Singleton MR, Dillingham MS, Gaudier M *et al.* Crystal structure of RecBCD enzyme reveals a machine for processing DNA breaks. *Nature* 2004;**432**:187–93.

Sjlund M, Wreiber K, Andersson DI *et al.* Long-Term Persistence of Resistant *Enterococcus* Species after Antibiotics To Eradicate *Helicobacter pylori*. *Annals of Internal Medicine* 2003;**139**:483.

Skurray RA, Reeves P. F Factor-Mediated Immunity to Lethal Zygosis in *Escherichia coli* K-12. *Journal of Bacteriology* 1974;**117**:100–6.

Smillie C, Garcillán-Barcia MP, Francia MV *et al.* Mobility of Plasmids. *Microbiology and Molecular Biology Reviews* 2010;**74**:434–52.

Smith BT, Walker GC. Mutagenesis and More: umuDC and the Escherichia coli SOS Response. *Genetics* 1998;**148**:1599–610.

Smith GR. How RecBCD enzyme and Chi promote DNA break repair and recombination: a molecular biologist's view. *Microbiol Mol Biol Rev* 2012;**76**:217–28.

Soda S, Otsuki H, Inoue D *et al.* Transfer of antibiotic multiresistant plasmid RP4 from escherichia coli to activated sludge bacteria. *Journal of Bioscience and Bioengineering* 2008;**106**:292–6.

Sohlenkamp C, Geiger O. Bacterial membrane lipids: diversity in structures and pathways. *FEMS Microbiol Rev* 2016;**40**:133–59.

Sørensen SJ, Jensen LE. Transfer of plasmid RP4 in the spermosphere and rhizosphere of barley seedling. *Antonie Van Leeuwenhoek* 1998;**73**:69–77.

Sozhamannan S, Chattoraj DK. Heat shock proteins DnaJ, DnaK, and GrpE stimulate P1 plasmid replication by promoting initiator binding to the origin. *Journal of Bacteriology* 1993;**175**:3546–55.

Spies M, Kowalczykowski SC. The RecA Binding Locus of RecBCD Is a General Domain for Recruitment of DNA Strand Exchange Proteins. *Molecular Cell* 2006;**21**:573–80.

Spoto M, Guan C, Fleming E *et al.* A Universal, Genomewide GuideFinder for CRISPR/Cas9 Targeting in Microbial Genomes. Mitchell AP (ed.). *mSphere* 2020;**5**, DOI: 10.1128/mSphere.00086-20.

Starčič Erjavec M, Petkovšek Ž, Kuznetsova MV *et al.* Strain ŽP — the first bacterial conjugation-based "kill"–"anti-kill" antimicrobial system. *Plasmid* 2015;**82**:28–34.

Stecher B, Maier L, Hardt W-D. "Blooming" in the gut: how dysbiosis might contribute to pathogen evolution. *Nature Reviews Microbiology* 2013;**11**:277–84.

Stemmer M, Thumberger T, Del Sol Keyer M *et al.* CCTop: An Intuitive, Flexible and Reliable CRISPR/Cas9 Target Prediction Tool. *PLoS One* 2015;**10**:e0124633.

Sternberg SH, LaFrance B, Kaplan M *et al.* Conformational control of DNA target cleavage by CRISPR–Cas9. *Nature* 2015;**527**:110–3.

Sternberg SH, Redding S, Jinek M *et al.* DNA interrogation by the CRISPR RNA-guided endonuclease Cas9. *Nature* 2014;**507**:62–7.

Stubbendieck RM, Straight PD. Multifaceted Interfaces of Bacterial Competition. *J Bacteriol* 2016;**198**:2145–55.

Studier FW, Moffatt BA. Use of bacteriophage T7 RNA polymerase to direct selective high-level expression of cloned genes. *J Mol Biol* 1986;**189**:113–30.

Suzuki H, Yano H, Brown CJ *et al.* Predicting plasmid promiscuity based on genomic signature. *J Bacteriol* 2010;**192**:6045–55.

Tabor S, Richardson CC. A bacteriophage T7 RNA polymerase/promoter system for controlled exclusive expression of specific genes. *Proc Natl Acad Sci U S A* 1985;**82**:1074–8.

Tacconelli E. GLOBAL PRIORITY LIST OF ANTIBIOTIC-RESISTANT BACTERIA TO GUIDE RESEARCH, DISCOVERY, AND DEVELOPMENT OF NEW ANTIBIOTICS. 2017:7.

Takahagi M, Iwasaki H, Nakata A *et al.* Molecular analysis of the Escherichia coli ruvC gene, which encodes a Holliday junction-specific endonuclease. *J Bacteriol* 1991;**173**:5747–53.

Tallent SM, Langston TB, Moran RG *et al.* Transducing particles of Staphylococcus aureus pathogenicity island SaPI1 are comprised of helper phage-encoded proteins. *J Bacteriol* 2007;**189**:7520–4.

Tan SZ, Reisch CR, Prather KLJ. A Robust CRISPR Interference Gene Repression System in Pseudomonas. *J Bacteriol* 2018;**200**:e00575-17.

Tang M, Kong X, Hao J *et al.* Epidemiological Characteristics and Formation Mechanisms of Multidrug-Resistant Hypervirulent Klebsiella pneumoniae. *Front Microbiol* 2020;**11**:581543.

Tanner NA, Hamdan SM, Jergic S *et al.* Single-molecule studies of fork dynamics in Escherichia coli DNA replication. *Nature Structural & Molecular Biology* 2008;**15**:170–6.

Tedijanto C, Olesen SW, Grad YH *et al.* Estimating the proportion of bystander selection for antibiotic resistance

among potentially pathogenic bacterial flora. *Proceedings of the National Academy of Sciences* 2018;**115**:E11988–95.

Terskikh A, Fradkov A, Ermakova G *et al.* "Fluorescent timer": protein that changes color with time. *Science* 2000;**290**:1585–8.

Tetaz TJ, Luke RK. Plasmid-controlled resistance to copper in Escherichia coli. *J Bacteriol* 1983;**154**:1263–8.

Thoma L, Muth G. The conjugative DNA-transfer apparatus of Streptomyces. *International Journal of Medical Microbiology* 2015;**305**:224–9.

Thoma L, Vollmer B, Oesterhelt F *et al.* Live-cell imaging of Streptomyces conjugation. *International Journal of Medical Microbiology* 2019;**309**:338–43.

Tims S, Derom C, Jonkers DM *et al.* Microbiota conservation and BMI signatures in adult monozygotic twins. *ISME J* 2013;**7**:707–17.

Tong Y, Charusanti P, Zhang L *et al.* CRISPR-Cas9 Based Engineering of Actinomycetal Genomes. *ACS Synthetic Biology* 2015;**4**:1020–9.

Topilina NI, Mills KV. Recent advances in in vivo applications of intein-mediated protein splicing. *Mob DNA* 2014;**5**:5.

Torres-Perez, Garcia-Martin, Montoliu *et al.* WeReview: CRISPR Tools—Live Repository of Computational Tools for Assisting CRISPR/Cas Experiments. *Bioengineering* 2019;**6**:63.

Touchon M, Hoede C, Tenaillon O *et al.* Organised Genome Dynamics in the Escherichia coli Species Results in Highly Diverse Adaptive Paths. Casadesús J (ed.). *PLoS Genetics* 2009;**5**:e1000344.

Trokter M, Waksman G. Translocation through the Conjugative Type IV Secretion System Requires Unfolding of Its Protein Substrate. *J Bacteriol* 2018;**200**:e00615-17.

Turnbaugh PJ, Ley RE, Mahowald MA *et al.* An obesity-associated gut microbiome with increased capacity for energy harvest. *Nature* 2006;**444**:1027–31.

Turner TR, James EK, Poole PS. The plant microbiome. *Genome Biol* 2013;**14**:209.

UNEP. Lessons from Countries Phasing Down Dental Amalgam Use | Global Mercury Partnership. 2016.

USFDA. GRAS Notice (GRN) No. 198 http://www.fda.gov/Food/FoodIngredientsPackaging/GenerallyRecognizedasSafeGRAS/GRASListings/default.htm. 2006:48.

Vakulskas CA, Dever DP, Rettig GR *et al.* A high-fidelity Cas9 mutant delivered as a ribonucleoprotein complex enables efficient gene editing in human hematopoietic stem and progenitor cells. *Nature Medicine* 2018;**24**:1216–24.

Vecchiarelli AG, Hwang LC, Mizuuchi K. Cell-free study of F plasmid partition provides evidence for cargo transport by a diffusion-ratchet mechanism. *Proc Natl Acad Sci U S A* 2013;**110**:E1390-1397.

Vecchiarelli AG, Neuman KC, Mizuuchi K. A propagating ATPase gradient drives transport of surface-confined cellular cargo. *Proceedings of the National Academy of Sciences* 2014;**111**:4880–5.

Verma J, Bag S, Saha B *et al.* Genomic plasticity associated with antimicrobial resistance in *Vibrio cholerae*. *Proceedings of the National Academy of Sciences* 2019;**116**:6226–31.

Villa L, Carattoli A. Plasmid Typing and Classification. *Methods Mol Biol* 2020;**2075**:309–21.

Virolle C, Goldlust K, Djermoun S *et al.* Plasmid Transfer by Conjugation in Gram-Negative Bacteria: From the Cellular to the Community Level. *Genes* 2020;**11**:1239.

Waldor MK, Mekalanos JJ. Lysogenic Conversion by a Filamentous Phage Encoding Cholera Toxin. *Science* 1996;**272**:1910–4.

Walsh TR, Weeks J, Livermore DM *et al.* Dissemination of NDM-1 positive bacteria in the New Delhi environment and its implications for human health: an environmental point prevalence study. *Lancet Infect Dis* 2011;**11**:355–

62.

Wang G, Zhao G, Chao X *et al.* The Characteristic of Virulence, Biofilm and Antibiotic Resistance of Klebsiella pneumoniae. *International Journal of Environmental Research and Public Health* 2020;**17**:6278.

Wang L-H, Weng L-X, Dong Y-H *et al.* Specificity and enzyme kinetics of the quorum-quenching N-Acyl homoserine lactone lactonase (AHL-lactonase). *J Biol Chem* 2004;**279**:13645–51.

Waters CM, Bassler BL. Quorum sensing: cell-to-cell communication in bacteria. *Annu Rev Cell Dev Biol* 2005;**21**:319–46.

Wawrzyniak P, Płucienniczak G, Bartosik D. The Different Faces of Rolling-Circle Replication and Its Multifunctional Initiator Proteins. *Frontiers in Microbiology* 2017;**8**, DOI: 10.3389/fmicb.2017.02353.

Weingarten RA, Johnson RC, Conlan S *et al.* Genomic Analysis of Hospital Plumbing Reveals Diverse Reservoir of Bacterial Plasmids Conferring Carbapenem Resistance. Bonomo RA (ed.). *mBio* 2018;**9**, DOI: 10.1128/mBio.02011-17.

Weller GR. Identification of a DNA Nonhomologous End-Joining Complex in Bacteria. *Science* 2002;**297**:1686–9.

Westra ER, Levin BR. It is unclear how important CRISPR-Cas systems are for protecting natural populations of bacteria against infections by mobile genetic elements. *Proceedings of the National Academy of Sciences* 2020;**117**:27777–85.

Westra ER, Swarts DC, Staals RHJ *et al.* The CRISPRs, They Are A-Changin': How Prokaryotes Generate Adaptive Immunity. *Annual Review of Genetics* 2012;**46**:311–39.

Wheatley RM, MacLean RC. CRISPR-Cas systems restrict horizontal gene transfer in Pseudomonas aeruginosa. *ISME J* 2021;**15**:1420–33.

Whitaker N, Berry TM, Rosenthal N *et al.* Chimeric Coupling Proteins Mediate Transfer of Heterologous Type IV Effectors through the Escherichia coli pKM101-Encoded Conjugation Machine. *J Bacteriol* 2016;**198**:2701–18.

Whitaker N, Chen Y, Jakubowski SJ *et al.* The All-Alpha Domains of Coupling Proteins from the Agrobacterium tumefaciens VirB/VirD4 and Enterococcus faecalis pCF10-Encoded Type IV Secretion Systems Confer Specificity to Binding of Cognate DNA Substrates. Parkinson JS (ed.). *Journal of Bacteriology* 2015;**197**:2335–49.

Wilkins BM, Chilley PM, Thomas AT *et al.* Distribution of Restriction Enzyme Recognition Sequences on Broad Host Range Plasmid RP4: Molecular and Evolutionary Implications. *Journal of Molecular Biology* 1996;**258**:447–56.

Wilkins BM, Hollom SE. Conjugational synthesis of F lac+ and Col I DNA in the presence of rifampicin and in Escherichia coli K12 mutants defective in DNA synthesis. *Mol Gen Genet* 1974;**134**:143–56.

Willetts N. The transcriptional control of fertility in F-like plasmids. *J Mol Biol* 1977;**112**:141–8.

Willetts NS, Paranchych W. Inhibition of Flac transfer by the fin+ I-like plasmid R62. *J Bacteriol* 1974;**120**:101–5.

Winstel V, Liang C, Sanchez-Carballo P *et al.* Wall teichoic acid structure governs horizontal gene transfer between major bacterial pathogens. *Nat Commun* 2013;**4**:2345.

Wojkowska-Mach J, Godman B, Glassman A *et al.* Antibiotic consumption and antimicrobial resistance in Poland; findings and implications. *Antimicrobial Resistance & Infection Control* 2018;**7**, DOI: 10.1186/s13756-018-0428-8.

Wolrd Health Organization, Food and Agriculture Organization of the United Nations. Guidelines for the Evaluation of Probiotics in Food. 2002.

Wong JJW, Lu J, Glover JNM. Relaxosome function and conjugation regulation in F-like plasmids - a structural biology perspective: Regulation of conjugation in F-like plasmids. *Molecular Microbiology* 2012;**85**:602–17.

Wright LD, Grossman AD. Autonomous Replication of the Conjugative Transposon Tn *916*. Zhulin IB (ed.). *Journal of Bacteriology* 2016;**198**:3355–66.

Wright LD, Johnson CM, Grossman AD. Identification of a Single Strand Origin of Replication in the Integrative

and Conjugative Element ICEBs1 of Bacillus subtilis. Viollier PH (ed.). *PLOS Genetics* 2015;**11**:e1005556.

Wu CA, Zechner EL, Reems JA *et al.* Coordinated leading- and lagging-strand synthesis at the Escherichia coli DNA replication fork. V. Primase action regulates the cycle of Okazaki fragment synthesis. *Journal of Biological Chemistry* 1992;**267**:4074–83.

Wyatt HDM, West SC. Holliday junction resolvases. *Cold Spring Harb Perspect Biol* 2014;**6**:a023192.

Xu T, Li Y, Shi Z *et al.* Efficient Genome Editing in Clostridium cellulolyticum via CRISPR-Cas9 Nickase. Spormann AM (ed.). *Applied and Environmental Microbiology* 2015;**81**:4423–31.

Yakobson E, Deiss C, Hirata K *et al.* Initiation of DNA synthesis in the transfer origin region of RK2 by the plasmid-encoded primase: detection using defective M13 phage. *Plasmid* 1990;**23**:80–4.

Yano H, Shintani M, Tomita M *et al.* Reconsidering plasmid maintenance factors for computational plasmid design. *Comput Struct Biotechnol J* 2019;**17**:70–81.

Yehl K, Lemire S, Yang AC *et al.* Engineering Phage Host-Range and Suppressing Bacterial Resistance through Phage Tail Fiber Mutagenesis. *Cell* 2019;**179**:459–469.e9.

Yokoyama K, Makino K, Kubota Y *et al.* Complete nucleotide sequence of the prophage VT1-Sakai carrying the Shiga toxin 1 genes of the enterohemorrhagic Escherichia coli O157:H7 strain derived from the Sakai outbreak. *Gene* 2000;**258**:127–39.

Yoon YG, Koob MD. Transformation of isolated mammalian mitochondria by bacterial conjugation. *Nucleic Acids Res* 2005;**33**:e139.

York D, Filutowicz M. Autoregulation-deficient mutant of the plasmid R6K-encoded pi protein distinguishes between palindromic and nonpalindromic binding sites. *Journal of Biological Chemistry* 1993;**268**:21854–61.

Yosef I, Manor M, Kiro R *et al.* Temperate and lytic bacteriophages programmed to sensitize and kill antibiotic-resistant bacteria. *Proceedings of the National Academy of Sciences* 2015;**112**:7267–72.

Yoshida T, Kim S-R, Komano T. Twelve *pil* Genes Are Required for Biogenesis of the R64 Thin Pilus. *Journal of Bacteriology* 1999;**181**:2038–43.

Yu D, Ellis HM, Lee EC *et al.* An efficient recombination system for chromosome engineering in Escherichia coli. *Proc Natl Acad Sci U S A* 2000;**97**:5978–83.

Yusoff K, Stanisich VA. Location of a function on RP1 that fertility inhibits Inc W plasmids. *Plasmid* 1984;**11**:178–81.

Zatyka M, Bingle L, Jones AC *et al.* Cooperativity between KorB and TrbA repressors of broad-host-range plasmid RK2. *J Bacteriol* 2001;**183**:1022–31.

Zatyka M, Jagura-Burdzy G, Thomas CM. Transcriptional and translational control of the genes for the mating pair formation apparatus of promiscuous IncP plasmids. *J Bacteriol* 1997;**179**:7201–9.

Zhang H, Fouts DE, DePew J *et al.* Genetic modifications to temperate Enterococcus faecalis phage φEf11 that abolish the establishment of lysogeny and sensitivity to repressor, and increase host range and productivity of lytic infection. *Microbiology* 2013;**159**:1023–35.

Zhu LJ, Holmes BR, Aronin N *et al.* CRISPRseek: a bioconductor package to identify target-specific guide RNAs for CRISPR-Cas9 genome-editing systems. *PLoS One* 2014;**9**:e108424.

Zoolkefli FIRM, Moriguchi K, Cho Y *et al.* Isolation and Analysis of Donor Chromosomal Genes Whose Deficiency Is Responsible for Accelerating Bacterial and Trans-Kingdom Conjugations by IncP1 T4SS Machinery. *Front Microbiol* 2021;**12**:620535.

Zupan J, Hackworth CA, Aguilar J *et al.* VirB1* Promotes T-Pilus Formation in the *vir* -Type IV Secretion System of *Agrobacterium tumefaciens*. *Journal of Bacteriology* 2007;**189**:6551–63.

Zupan JR, Zambryski P. Transfer of T-DNA from Agrobacterium to the Plant Cell. *Plant Physiology* 1995;**107**:1041–7.

Zzaman S, Reddy JM, Bastia D. The DnaK-DnaJ-GrpE Chaperone System Activates Inert Wild Type π Initiator Protein of R6K into a Form Active in Replication Initiation. *Journal of Biological Chemistry* 2004;**279**:50886–94.

Study of bacterial conjugation from a practical and fundamental perspective

Microbial communities are composed of various bacterial species capable of exchanging genetic information through horizontal gene transfer mechanisms. Among these, bacterial conjugation allows the transfer of large DNA fragments, mostly plasmids, between a donor and a recipient bacterium in direct contact. The acquisition of the plasmid and the expression of the carried genes converts the recipient cell into a transconjugant cell. The product of the genes can confer a symbiotic lifestyle, virulence factors or resistance to heavy metals and antibiotics. It is estimated that conjugation is responsible for 80% of the acquisition of antibiotic resistance in bacteria, which is a major public health problem worldwide. In this context, two major objectives are to develop new antibacterial strategies alternative to antibiotics and to better understand the fundamental mechanism of dissemination of resistance by conjugation.

Our team combines microscopic and microbiological analyses at the single-cell and population scales to understand the process and dynamics of conjugation. My thesis project aimed at exploring practical and fundamental aspects of this mechanism.

First, I developed a novel antibacterial strategy based on conjugation-delivered plasmids carrying CRISPR-Cas (Clustered Regularly Interspaced Short Palindromic Repeats-CRISPR associated protein) systems. The CRISPR-Cas system is able to recognize and target specific DNA sequences, and introduce lethal double-strand breaks into the DNA of bacteria. We have therefore created plasmids mobilized by conjugation, called TAPs (Targeted-Antibacterial-Plasmids), able to specifically kill bacteria in a population. By platting assays, flow cytometry and fluorescence microscopy techniques, I was able to show the ability of TAPs to be transferred and to kill targeted strains. We also showed that TAPs can be used to re-sensitize a bacterial strain to an antibiotic.

In addition to this biotechnological application, I studied the dynamics of bacterial conjugation at the cellular level, using the F plasmid as a model. I explored the timing of expression of plasmid genes once transferred into the recipient bacterium as well as the establishment of antibiotic resistance after plasmid acquisition. I was interested in the genes located on the first part of the plasmid to enter in the recipient, called the "leading region". I was able to show that, unlike other plasmid genes, these are transiently expressed only in the transconjugant and not in the donor. This first result suggested an expression strategy that would first allow the establishment of the transferreplasmid, then its maintenance and eventually its transfer to another recipient cell.

I also studied the acquisition of tetracycline resistance conferred by the F plasmid encoding a specific TetA efflux pump that confers resistance to tetracycline. Using fluorescence microscopy, we were able to observe and analyze the dynamics of TetA production and tetracycline efflux in real-time. Our study shows that tetracycline resistance depends on a balance between TetA production and the ability of the tetracycline to block this production. Furthermore, we were able to correlate the increase in the intracellular amount of TetA with the ability of the cells to resist increasing amounts of tetracycline.